# Encapsulation of waste in cementitious systems for use in civil engineering applications

**Olalaken Ayoola Oladipo**

**A Submission presented in partial fulfilment of the requirement of the Glamorgan/Prifysgol De Cymru for the degree of Doctor of Philosophy**

**Work carried out in collaboration with Speedbuild UK Limited**

January 2018

# CERTIFICATE OF RESEARCH

This is to certify that, except where specific reference is made, the work described in this thesis is the result of work carried out by the candidate. Neither this thesis, nor any part of it, has been presented or is currently submitted in candidature for any other degree at any other university

…… Date

Olalekan Ayoola Oladipo
(Candidate)

…….. Date

Professor John Kinuthia
(Director of studies)

…… Date

Dr Jonathan E Oti
Supervisor

# ACKNOWLEDGEMENT

The author will like to thank Speedbuild UK Limited for the expertise and materials provided for the project and the Faculty of Computing, Engineering and Science of the university of South wales for the research and staffing resources provided. The author will also like to acknowledge here that, the preparation of this thesis was as a result of both direct investigations and wide range consultations involving a number of people, most importantly the supervisory team. The author will like to express his deepest gratitude and sincere appreciation to both Dr Jonathan Oti and Professor John Kinuthia, who I will expressly say that I have been lucky to work with as a team. Their extensive knowledge and guidance has enabled me to remain on the right track from the beginning to the end of this research work. Without their patience, constant support and timely interventions, this projected would have been difficult to accomplish.

In addition, the author will like to give specific thanks to Keith Milne, Steve Ngige, Clive Bennett, Darren Crocker, Paul Marshman, Huw Williams, Donna Philips Sibanda among others. Thank you all.

# ABSTRACT

The continuous proliferation of plastic materials in industries has led to the generation of huge volumes of waste plastics, which must be properly disposed of to prevent contamination of the natural environment. In line with current global efforts to tackle the enormity of plastic debris in the environment including ocean, this research evaluate the possibility of immobilising high volumes of waste plastics in cementitious systems using encapsulation technology. It also investigates the aptness of using the resulting encapsulated plastic waste forms in civil engineering applications. In order to evaluate the usability of the encapsulated waste form, material characterisation of the aggregates and binding materials were conducted along with the physical, mechanical and durability performances of the encapsulated plastic waste forms (concrete). The research work was also extended to provide an inferential statistical analysis of the physical and mechanical properties of the encapsulated plastic concrete relative to the control conventional concrete.

The overall results suggest that, it is possible to immobilise waste plastics in cementitious materials using encapsulation technology. The encapsulated plastic waste forms (encapsulated plastic concrete) have shown that high volumes of waste plastics can be mechanically bounded into solid monoliths, and based on the physical, mechanical and durability properties investigated as part of this work may be suitable for use in civil engineering applications. The encapsulated plastic waste-form demonstrated densities within the range 1400 – 1700kg/$m^3$, porosity within the range 8.9 – 21.2% and water absorption ranging between 3.7 – 15.4%. Furthermore, the unconfined compressive strength of the encapsulated plastic concrete ranged between 2.8 N/$mm^2$ – 17.4N/$mm^2$ after 28 days of water curing. Like concrete made from natural aggregates, the encapsulated plastic concrete also exhibited good resistance to frost action, sulphate attack and tolerated temperatures up to 150$^o$C.

On the possible applicability of the encapsulated plastic concrete in civil engineering applications, the lightweight property of the encapsulated plastic concrete makes it particularly suitable for off – site production and other lightweight applications such as concrete fills, landscaping and structural formworks, sandwich concrete with an outer load bearing leaf of precast concrete and, boundary and retention walling. The

encapsulated plastic concrete may be of particular benefit in low fire risk buildings such as sport centres and playgrounds, farmhouses, DIY outlets, outbuildings, storage units, garden centres among others. The high porosity of the encapsulated plastic concrete may also distinguish them as pervious concrete capable of applications in concrete flatwork applications such as driveways, sidewalks, parking lots, road drainage and flood defence applications. Other possible applications of the encapsulated plastic concrete include low-energy and low-carbon construction, speedy construction and extreme weather construction.

Fire safety measures such as safeguarding ignition sources, fire and smoke alarms, and sprinkler systems may have to be deployed due to the fire risk associated with the use of plastic materials in building construction. In addition, the low tensile strength of the encapsulated concrete implies that mesh or other reinforcements may be required, depending on the use of the concrete. The encapsulated plastic concrete also has low workability which may be mitigated through mechanical mixing, power vibration using poker vibrators, roller compactors, high-pressure concrete pumps and/or compacting in thin layers.

# ABBREVIATIONS AND SYMBOLS

| | |
|---|---|
| C1-3 | Conventional CEM IIB-concrete mix |
| CP1-3 | CEM IIB-encapsulated plastic concrete |
| CPP1-3 | CEM IIB-encapsulated plastic concrete with PFA used as mineral admixture |
| CPP1-$3_f$ | CEM IIB-encapsulated plastic concrete with PFA used as micro-filler |
| P1-3 | Conventional PG-concrete mix |
| PP1-3 | PG-encapsulated plastic concrete |
| PPP1-3 | PG-encapsulated plastic concrete with PFA used as mineral admixture |
| PPP1-$3_f$ | PG-encapsulated plastic concrete with PFA used as micro-filler |
| PG | Pozament ultra high strength grout |
| CEM IIB | Portland cement |
| J | Joules |
| G | Grams |
| $P_b$ | Bulk density |
| $P\rho$ | Particle density |
| $F$ | Flowability |
| V | Percentage void |
| $C_3A$ | Tri-Calcium Aluminate |
| $C_3S$ | Tri-Calcium Silicate (Alite) |
| $C_2S$ | Di-Calcium Silicate (Belite) |
| $C_4AF$ | Tetra-Calcium Alumino-Ferrite |
| C-S-H | Calcium-Silicate-Hydrate gel |
| $N$ | Porosity |
| WA | Water absorption |

## Table of Contents

## List of Figures

## List of Tables

# List of Equations

**Hydration reactions**



**Pozzolanic reaction:**



Phosphate ceramic



Acid attack on concrete:



**Alkali silica reaction:**



**Alkali carbonate reaction:**

# CHAPTER 1 – INTRODUCTION

*This Chapter discusses the background to the research, its aims and objectives, the key benefits, contribution to knowledge and a brief description of the structure of the entire thesis.*

## 1.1 BACKGROUND

Encapsulation is a waste immobilization technique where the waste is incorporated or surrounded by a solid matrix (Rao et al., 2007). It is already a common practice in the nuclear industry where encapsulation in cement or its composites has for many years being the preferred option for the treatment of intermediate and low level radioactive wastes (Swift, 2013). In medical sciences, encapsulation in polyethylene or metallic drums partially filled with inert fillers such as plastic foam, bituminous sand, lime, cement mortar, or clay is used to prevent humans and the environmental risk of contact with sharps (scalpel or hypodermic needle, breakable culture dish), chemicals or pharmaceutical residues, or incinerator ash before their final disposal in landfill/geological sites (Ferreira et al., 2012a).

Encapsulation technology is also becoming prevalent in civil engineering. Johnson et al., (2015) for example, encapsulated petroleum sludge waste in building blocks and concluded that the products met the minimum specification for construction blocks. In similar experiments, Kumari and Kanmani, (2011), successfully encapsulated textile sludge in polypropylene and Portland cements, while Patel and Pandey, (2012) encapsulated chemical sludge generated from textile wastewater treatment plants with Portland pozzolana cement. Although the investigations conducted by the researchers were limited to physical and mechanical properties, the studies recommended the resulting composite systems for use in civil engineering. Further works, including freeze-thaw, acid and alkaline resistance and carbonation among others may be necessary to verify the durability of the encapsulated waste forms.

This study will explore the possibility of immobilising high volumes of waste plastics in cement-based matrices using encapsulation technology. It will also experimentally investigate the aptness of the resulting composite systems as alternative to conventional construction materials.

## 1.2 STATEMENT OF PROBLEM

Most human advances over the last century have been facilitated by the use of plastic materials (North and Holden, 2013). In principle, plastics are extremely versatile materials ideal for a wide range of applications in healthcare, telecommunication, construction, aviation, automobile, textile and packaging, among many more applications. However, as with all consumer goods, the continuous proliferation of plastic materials have led to the generation of large volumes of waste plastics, which are becoming a threat to global ecosystem (North and Halden, 2013, UNEP, 2014, Webb et al., 2013, Thompson et al., 2009a, Koch and Calafat, 2009, and Hirai et al., 2011).

The same properties of plastic (low cost, lightweight and durability) that make it so valuable also make its disposal problematic. In many cases, plastics are thrown away after a single use, but because they are durable, they persist in the environment for several years. The accumulation of substantial quantities of plastic debris in the natural environment is the cause of many aesthetics, biodiversity, colonisation and often-fatal damaging effects on ecosystem (UNEP, 2014 and, Webb et al., 2013). There are reported incidences of sub-lethal or lethal effect of plastic debris on land and marine wildlife, potential changes in biodiversity of habitats due to the transportation of invasive species on plastic fragments and, general pollution, contamination and space uptake on terrestrial, marine and fresh waterways (UNEP, 2014. Mee et al., 2007, and Webb et al., 2009).

There are growing bodies of research works on the potential toxicity of chemical additives used in the manufacture of some plastic materials on mammals (Thompson et al., 2009a, Koch and Calafat, 2009, and Hirai et al., 2011). BPA, phthalates and brominated flame retardant used in the manufacture of some plastic materials (polycarbonate, PVC and epoxy resins) have generated considerable attention due to their possible endocrine disrupting effects (Koch and Calafat, 2009). Although, the extent and scale of health effects stemming from the pervasive human exposure to the chemical constituents of plastics are as of yet uncertain. Controlled laboratory exposure of animals to these chemicals has shown that, through bioaccumulation, BPA, phthalates and brominated flame retardant negatively affects thyroid hormones, pituitary function and reproduction in both male and female animals (Koch and Calafat, 2009, Andrady and

Neal, 2009, Halden, 2010 and, North and Halden, 2013). The exposure of female rodents to high levels of BPA during pregnancy and lactation had negative effects on survival rate, birth weight and growth of offspring in early life (Koch and Calafat, 2009). Brominated flame-retardants similarly have disrupting effects on oestrogen and thyroid hormones, and impaired development of the reproductive and nervous systems of rodents (Koch and Calafat, 2009).

In parallel with the health concerns, the current disposal routes for waste plastics, landfill and incinerating, are not the ideal solution (Hirai et al., 2011, Koch and Calafat, 2009, and Hopewell et al., 2009). Plastic materials are too valuable to end up in landfills. At the current rate of proliferation, production of plastic materials will consume around 20% of global oil production by 2050, and utilise about 15% of the annual global carbon budget during the same period (PlasticEurope, 2015). The economic value and the energy contained in waste plastics are typically lost through the current disposal routes (landfilling or incineration). Disposal of plastics in landfill sites also render land spaces, which may be suitable for other purposes with higher societal benefits redundant for several hundreds of years. Overtime, the liners separating landfills from underlying soil and water channels may also rupture or leak. The outflow of plastics' components and other contaminants contained in landfill leachates may constitute a long-term risk of pollution or contamination of soil and groundwater (Hopewell et al., 2009).

Incineration, another technique routinely used for the disposal of plastic wastes, is known to result in the production and release of greenhouse and toxic gases including, carbon dioxide, carcinogenic polycyclic aromatic hydrocarbons (PAH) and dioxins, and persistent organic pollutants such as polychlorinated biphenyl (PCB) into the environment (Hirai et al., 2011). As such, the environmental drawbacks of plastic waste disposal via both landfill and incineration makes plastic recycling possibly the only plausible route (Koch and Calafat, 2009). The recovery and subsequent re-use or recycling of post-consumer plastics offer economic and ecological advantages over the landfilling or incineration.

In line with the global drive to attain economic and environmental balance, the recycling of waste plastics as secondary raw materials comes into focus as an eco-efficient way to reintroduce valuable resources back into the economy (EU infographic on waste plastics,

2015). This approach will reduce the extraction of natural resources and the need for landfill or incineration practices. This study will explore the possibility of immobilising post-consumer plastics in cementitious matrices using encapsulation technology. The performance profiles of the resulting composite systems will be investigated experimentally to determine the aptness of encapsulated composites as alternative construction materials.

The design and development of low cost – low carbon construction materials from plastic waste and other industrial by-products and, the contribution of the resulting composites to sustainable construction, are the driving forces behind this current search for knowledge. Construction applications utilising waste plastics and industrial by-products, may also reduce the burden of post-consumer plastics on the environment and animal/human lives. In addition, utilising waste/by-products will also contribute towards the reduction of concrete's hefty carbon footprint and resource efficiency through smarter use of natural resources.

## 1.3 AIMS AND OBJECTIVES

The aim of this research can be summarised as follows:

- Theoretically provide an understanding of encapsulation technology and an intellectual context for applying such technology in immobilising waste for use in civil engineering construction works.
- Design and develop environmentally friendly composite systems from reclaimed (target) waste materials encapsulated in a cementitious matrix.
- Investigate the physical, mechanical, durability and environmental characteristics of the composite systems, and determine their possible application in building and civil engineering construction.

In order to achieve these aims the following objectives are undertaken:

a) A thorough literature review will be carried out to establish the currently available knowledge on encapsulation technology, its mechanisms, compatible waste materials and the various available matrices.
b) Establish the physical and chemical characteristics of the target wastes, using existing literatures and selected experimentations.

c) Establish the chemical characteristics and phase transition of the encapsulating matrix/solidifying reagents, using selected specialist tests such as calorimetry and thermogravimetric analysis.
d) Develop the target waste into environmentally friendly composites using cementitious binders and aggregate fillers.
e) Establish performance profiles for the composite systems based on density, porosity, moisture movement, unconfined compressive strength, tensile strength, resistance to frost action, chloride and sulphate attacks, leachability and thermal properties.
f) Interpret the performance and suggest the applicability of the composite systems in civil engineering.

## 1.4 KEY BENEFITS

The benefits likely to accrue from the current research include:

1. Environmental and economic benefits such as reduced land and marine pollution, resource conservation, environmental protection and job creation.
2. Affordable environmental friendly building products for 'low cost – low energy housing developments, particularly in developing countries.
3. Contributions towards government circular economic policies such as ambitious but realistic waste recycling targets (particularly, waste plastics), efficient energy recovery from waste policies and ultimately zero waste to landfill targets.
4. Contributions towards resource and economic efficiency, environmental performance and other social responsibilities by the construction industry.

## 1.5 CONTRIBUTION TO KNOWLEDGE

This research is anticipated to make the following contributions to knowledge;

i. Contribute to the existing knowledge on encapsulation technology, including its mechanisms, the compatible waste forms, the encapsulating matrices and the applicability of the technology to civil engineering works.
ii. Theoretically and experimentally, demonstrate the possibility of immobilising high volumes of waste plastics in cementitious systems using encapsulation technology.

iii. Identify the benefits likely to accrue from the use of the encapsulating matrices formulated in this study, for immobilising other waste materials requiring no stabilisation such as paper waste, construction and demolition wastes among others.

iv. Contribute to existing knowledge on the fluidity, standard consistency, setting times and degree of hydration of high carbon fly ash (one of the materials used in the encapsulation process in this study).

v. Contribute to sustainable construction particularly in the areas social, environment and economic sustainability including cost, materials and energy efficiency.

The design and development of encapsulated plastic systems for use in civil engineering works will further enhance the existing knowledge on the use of waste plastics in concrete formworks. Attempts at incorporating plastic as fine or coarse aggregate replacement have been explored with most researchers utilising up to 50% waste plastics (Agrawal et al., 2017, Gu and Ozbakkaloglu, 2016, and Ismail and Al-Hashmi 2008). This work however, is one of the earliest attempts at utilising 100% waste plastics as (coarse) aggregate replacement. Whilst also utilising Furnace bottom ash (FBA), and high carbon Pulverised fuel ash (PFA), materials which would have otherwise been disposed in landfills as aggregate and micro-fillers. Hence, the researcher considers this work to be not just an innovative approach for immobilising high volumes waste plastics (which would have been landfilled), but also an advancement on existing knowledge on utilization of waste/industrial by-products in construction. Additionally, the current research also maximises the use of waste materials, while minimising the use of cement. This makes the resulting composite systems capable of delivering low energy and low carbon construction solutions.

## 1.6 STRUCTURE OF THE THESIS

The structure of this thesis consists of seven chapters as follows:

**Chapter 1** provides the introduction of the research and the whole thesis report. It explains the background to the research, its aims and objectives, the key benefits, contribution to knowledge and a brief description of the structure of the entire thesis.

**Chapter 2** provides a brief literature review of the material (plastic), the enormity of the waste generated on the ecosystem, the current disposal routes, and the recycling technique proposed in the current work. The chapter also deeply explore the waste immobilisation technology known as encapsulation technology, its current application, the various mechanisms and the available encapsulating matrices. The chapter will conclude with the performance data required for the characterisation of the encapsulated plastic waste-form.

**Chapter 3** describes the details of the materials used in the current work including material sources, reasons for using each material and some material characterisation. For better presentation, the materials have been classified into three groups namely; binding materials, aggregates and micro-filler. The binding materials describe the Portland cement (CEM IIB) and Pozament ultra high strength grout (PG), while the aggregates sub-divided into fine and coarse aggregates include the recycled wastes (furnace bottom ash and (0-10 mm) plastic waste) and concrete fillers (river sand and (10 mm) limestone aggregates). Pulverised fuel ash is the only micro-filler considered for use in this work.

**Chapter 4** describes the details of the mix design, sample preparation, curing regime and experimental program/methods used in the current work. A flow table of the mix design is presented in Figure 1.1. The experimental program includes the preliminary tests used to evaluate some characteristics of the aggregate materials and the freshly mixed normal density concrete and encapsulated plastic systems (Encapsulated plastic systems). It also includes the analytical techniques used to investigate the engineering and durability performances of both systems.

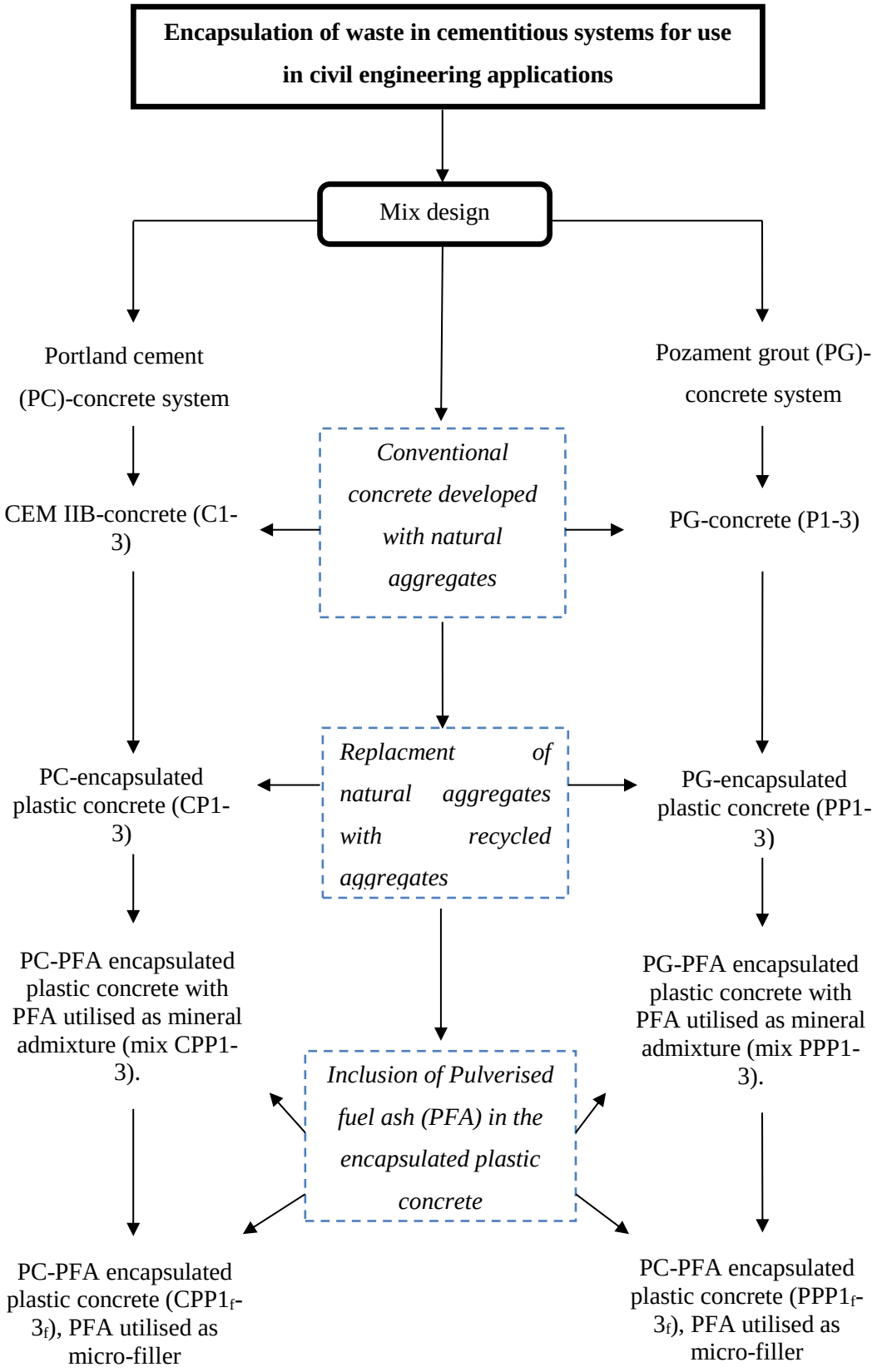


Figure 1.1: Flow-chart showing the mix design stages and different concrete mixtures

The designed mixtures were divided into two concrete systems based on the encapsulating matrix, namely; the Portland cement (CEM IIB)-concrete system and the Pozament (PG)-concrete system. The CEM IIB-concrete system consists of the conventional CEM IIB-concrete mixtures (C1-3) designed using the British method of mix design as stipulated in Neville (2012). These mixtures (C1-3) served as the reference concrete for all the concrete types developed. The three mixtures were selected based on variations in water/cement and aggregate/cement ratios. The first and second mixes (C1 and C2) utilised the same unit weight of cement and aggregate but different water/binder ratio. Mix C1 utilised a water/binder ratio of 0.5, while mix C2 utilised a water/binder ratio of 0.6. In line with the objective of the current work, the third mix (C3) utilised higher aggregate but lower cement contents relative to the preceding mixtures (C1 and C2). The water/binder ratio of mix C3 was maintained at 0.6.

Once the CEM IIB-concrete mixtures had been finalised, the natural aggregates (river sand and limestone aggregates) were replaced with reclaimed waste materials (furnace bottom ash and plastic aggregates respectively). The resulting composite mixtures were referenced CEM IIB-encapsulated plastic concrete mixtures (CP1-3). These mixtures (CP1-3) maintained the same mix proportion as the equivalent from the CEM IIB-concrete mixtures (C1-3). To improve the properties of the encapsulated concrete, Pulverised fuel ash (PFA) was included first as a mineral admixture (that is, it was considered as a binding material) and then later as a micro-filler (that is, it was considered as part of the aggregate materials). The mixtures with PFA utilised as a mineral admixture contain higher volumes of the reclaimed waste materials relative to the equivalent mixtures with PFA utilised as a micro-filler. The former set of mixtures were referenced CEM IIB-PFA encapsulated plastic concrete (CPP1-3), while the latter group of mixtures were referenced CEM IIB-PFA encapsulated plastic concrete ($CPP1_f$-$3_f$).

When the mix compositions from the CEM IIB–concrete system had been decided, the mixtures from each CEM IIB (conventional or encapsulated plastic) concrete type were duplicated for the PG-concrete system. The PG-concrete system thus comprises of the conventional PG-concrete mixtures (P1-3), PG-encapsulated plastic concrete (PP1-3), PG-PFA encapsulated plastic concrete (PPP1-3) and PG-PFA encapsulated plastic concrete ($PPP1_f$-$3_f$). These mixtures utilised PG-binder in the encapsulating matrix instead of PC-binder. The CEM IIB-concrete mix proportions were maintained in the

equivalent PG-concrete mixtures. PFA was similarly used either as a mineral admixture or as a micro-filler. The use of the PG- binder helped to identify the benefits likely to accrue from the use of a high fluidity cementitious grout on the encapsulated plastic concrete. A detailed discussion of the mix design stages is presented in Chapter 4, Section 4.1.

**Chapter 5** describes the detailed results of the various tests performed on the cementing matrices and the concrete systems.

**Chapter 6** discusses the overall results of the research, their interpretations and practical implications. For easier presentation, the chapter is divided into three sections. The first section discusses the workability, physio-mechanical and durability performance of the concrete mixtures (conventional or encapsulated plastic) from the CEM IIB-concrete system. The second section discuss the same parameters but for the equivalent mixtures from the PG-concrete system. The chapter concludes with a comparison of the two systems, and the analysis of the economic benefits and practical application of the encapsulated plastic concrete mixtures from both systems.

**Chapter 7** is the final chapter of the thesis. It summarises the main conclusions and identifies the areas for future research work.

# CHAPTER 2 – LITERATURE REVIEW

*This chapter will provide a brief literature review of the material (plastic), the enormity of the waste generated on the ecosystem, the current disposal routes, and the recycling technique proposed in the current work. It will also deeply explore the waste immobilisation technology known as encapsulation technology, its current application, the various mechanisms and the available encapsulating matrices. The chapter will conclude with the performance data required for the characterisation of the encapsulated plastic waste-form.*

## 2.1 PLASTIC AS A MATERIAL

Plastic is the general description given to a wide range of materials which at some point during their production are capable of flow and extrusion and can be moulded, cast, spun or applied as coating (Thompson et al., 2009b). It is a network of monomers chemically linked together to form macromolecules (North and Halden, 2013 and Thompson et al., 2009a). The monomers (base resins) are derived mostly from Naphtha, a highly flammable liquid hydrocarbon produced during the refining of crude oil (Thompson et al., 2009a). They typically include hydrogen and carbon molecules, although oxygen, nitrogen, sulphur, silicon, chlorine, fluorine or phosphorus are sometimes included to enhance the properties of the material.

The base resins are rarely used on their own. Instead, they are mixed with an array of additives, which may include reinforcing or non-reinforcing fillers, coupling agents, plasticizers, stabilisers, biocides, flame retardant, and optical effects among others (Subramanian, 2013, Thompson et al., 2009a and, Andrady and Neal, 2009). In order of use of the additives (types and volumes), the molecular structure of the monomers and the presence of impurities, the various diverse forms of plastics currently available are formed (Subramanian, 2013).

There are currently over 20 different synthesis and literally many thousands of grades and variations of globally available commercial plastics (Thompson et al., 2009a and Subramanian, 2013). However, based on chemical changes to their composition when heat is applied, they all fall into one of two categories of plastics namely: thermosets and thermoplastics (Subramanian, 2013 and Thompson et al., 2009a). When heated above the

melting temperature, thermosets melt but become permanently hard after cooling. The solidification of thermosets after cooling is irreversible, that is, they cannot be re-melted or reshaped. If further heat is applied, chemical decomposition of the material will occur (Subramanian, 2013). Thermoplastic however, are plastic materials that melt and become hard after cooling in a reversible reaction (Subramanian, 2013). They can be melted and reshaped as many times as required (Subramanian, 2013). Thermosets, such as polyurethane accounts for 10% of the global production of plastics, while thermoplastics, such as polyethylene (LDPE and HDPE), polypropylene (PP), polyvinyl chloride (PVC), polystyrene (PS and EPS), polyethylene terephthalate (PET) and polycarbonates accounts for the remaining 90% (PlasticsEurope, 2015).

Plastic materials are the most commonly used material since the beginning of the 20th century, and modern life is unthinkable without it (PlasticsEurope, 2015). Most human advances over the last century according to North and Halden, (2013) have been facilitated by the use of plastic materials. The low unit cost of plastics and the possibility of mass production, together with the lightweight, high versatility and durability properties of the materials, has made it the more desirable than competing materials (such as wood, glass and metal among others) in modern application (PlasticsEurope, 2015).

The high versatility and diverse properties of plastics make them ideal for usage in innumerable applications required to meet the demands of a modern society such as packaging, building and construction, medical and public health, agriculture, electronics, automobile, aircrafts, fabrics and many more (Andrady and Neal, 2009). In addition, the use of plastic materials also helps to improve resource efficiency with smarter, more efficient and sustainable use of natural resources (PlasticsEurope, 2015). Plastic materials play a key role in the eco-efficient manufacture of products including packaging and electronic devices, safety and resource efficient solutions in automobile and aircrafts, lower cost of building materials and low energy buildings (PlasticsEurope, 2015).

The most optimistic but accurate description of the influence of plastics on the modern society was given by chemists, Yarsley and Couzens, over 70 years ago. In their 1969 account on plastics in the modern world (reported by Thompson et al., 2009a), they spoke of a world free from moth and rust, and full of colour. A world largely built on synthetic materials made from the most universally distributed substances, a world where nations are

more dependent on localised resources, where man like a magician make what he wants for almost every need out of what is beneath and around him.

## 2.2 ACCUMULATION OF PLASTICS IN THE ENVIRONMENT

As a result, of the innumerable application of plastic materials, there has been a sharp increase in the global usage and consequently the demand and production of plastic materials. In 1950s, the global annual production of plastics was around 1.5 million tonnes/annum, this figure had increased to 311 million tonnes/annum by 2014 (PlasticsEurope, 2015). The 4-5% annual increase in production projected, suggest that around 400 million tonnes/annum of plastic materials will be consumed annually by 2020 (PlasticsEurope, 2015). The statistical data for the global production of plastic from 1950 – 2015 obtained from PlasticsEurope (2015) is shown in Figure 2.1**.**

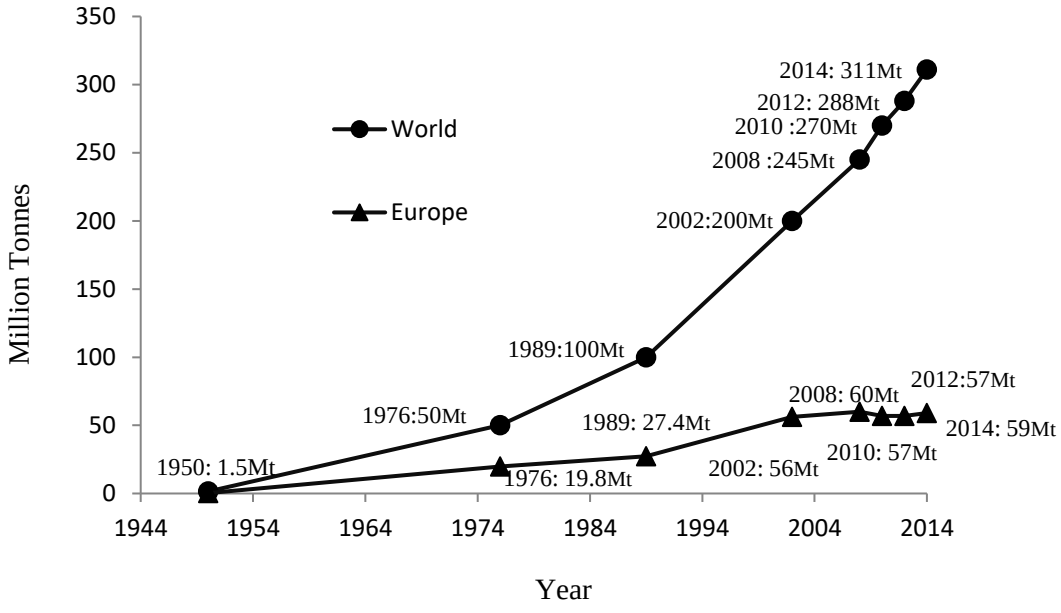


Figure 2.1: World plastics production 1950-2015.

The continuous proliferation of plastics in industries have led to the generation of large volumes of waste plastics, which are becoming a threat to global ecology and possibly human health (Koch and Calafat, 2009 and, Webb et al., 2013). Currently an annual estimated 10% of municipal solid waste is composed of plastic debris, another 10-20

million tonnes end up in world seas and oceans annually, and over 130 million tonnes are annually disposed in landfills (PlasticsEurope, 2015). A considerable volume of waste plastics also end up dispersed in the environment. Discarded plastics contaminate a wide range of terrestrial, freshwater and marine habitats (Thompson et al., 2009b). The foremost problem associated with the accumulation of substantial quantities of plastic debris in the natural environment is the aesthetic issue. Plastic waste can be unsightly as shown in Figure 2.2. In addition, there is also the lethal effects of plastic debris on land and marine wildlife (Figure 2.3a-d), potential changes in biodiversity of habitats due to the transportation of invasive species on plastic fragments and general pollution, contamination and space uptake on terrestrial, marine and fresh, waterways (UNEP, 2014. Mee et al., 2007 and Webb et al., 2009).

Figure 2.2: Aesthetic issues associated with dispersed post-consumer plastics

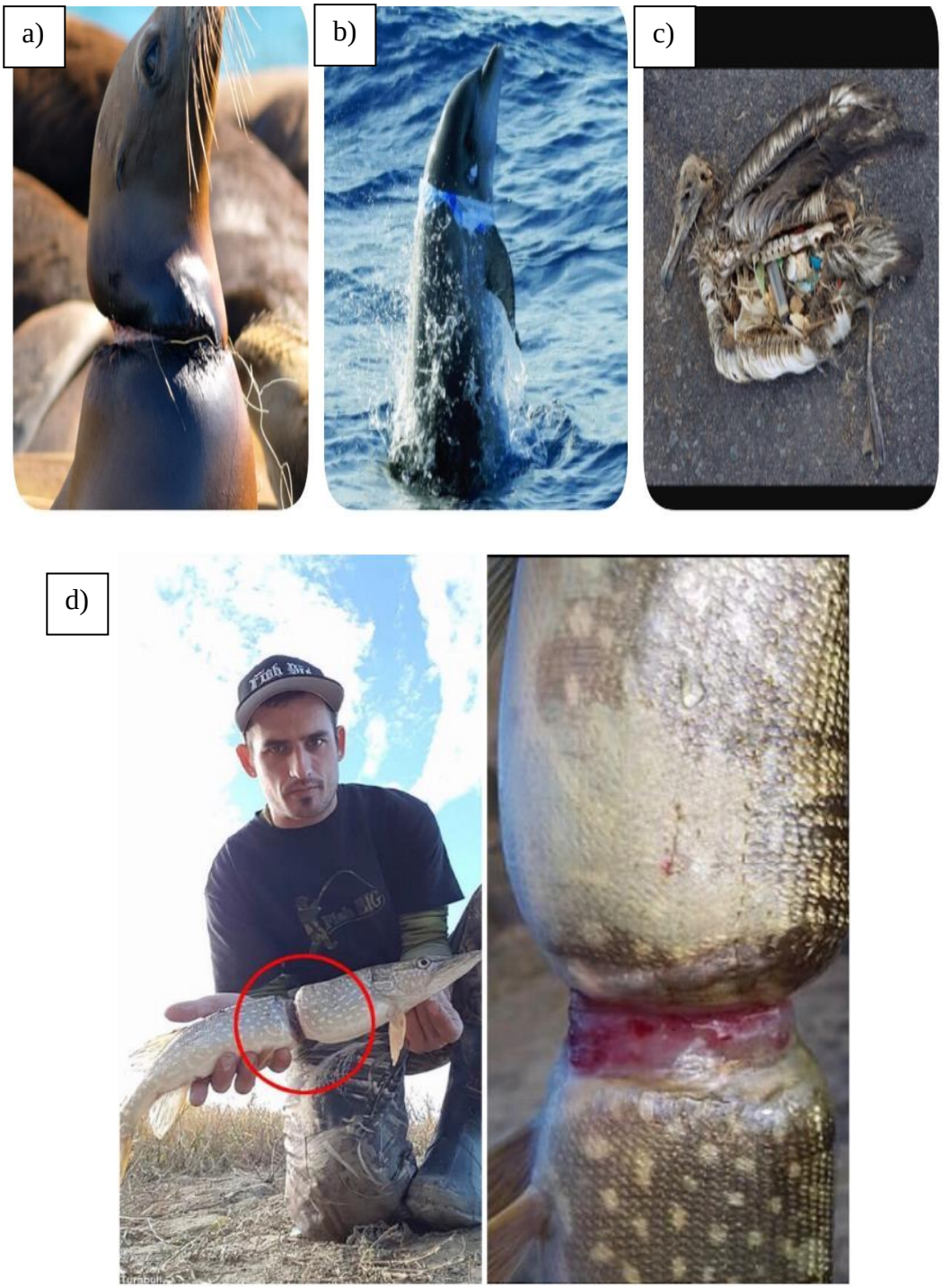


Figure 2.3(a-d): Some of the effect of plastic debris on land and marine wildlife. (Photos sourced from, Schallhorn, 2015, and Jordan, 2009),

In addition to reported incidences of mortality or sub-lethal effect of plastic debris on marine wildlife (Figure 2.2), there are also research works presenting evidence of potential toxicity of chemical additives used in the manufacture of some plastic materials on mammals (Thompson et al., 2009a, Thompson et al., 2009b, Koch and Calafat, 2009, and Hirai et al., 2011). Although, the extent and scale of health effects stemming from the pervasive human exposure to the chemical constituents of plastics are as of yet uncertain. Controlled exposure of laboratory animals to BPA used in polycarbonates plastics, epoxy resins, polyvinyl chloride (PVC) and protective coating in metal packaging negatively affects thyroid hormones, pituitary function and reproductive successes in both male and female animals (Koch and Calafat, 2009, Andrady and Neal, 2009 and, North and Halden, 2013). According to Koch and Calafat (2009), exposure of female rodents to high levels of BPA during pregnancy and lactation had negative developmental effects on survival rate, birth weight and growth of offspring in early life.

Phthalates a class of chemicals used to soften and increase the flexibility of plastics and vinyls consumer products such as flexible and vinyl toys, vinyl flooring, shower curtains plumbing pipes, food packaging, plastic wraps, medical tubing, fluid bags and many more are shown as the cause reproductive toxins in animal experiments (Koch and Calafat, 2009). Andrady and Neal (2009) reported that the male reproductive system is particularly sensitive to phthalates. Rats exposed to higher doses of phthalates than humans will commonly be exposed to have shown rapid and severe changes in the size and shapes of their testis, resulting in interference with the production of testicular testosterone among others. The two most used phthalate esters diethylhexylphthalate ($C_8H_4$ $(C_8H_{17}COO)_2$) and di-n-butylphthalate ($C_{16}H_{22}O_4$) are also known water and soil contaminants, and weak animal carcinogens (Koch and Calafat, 2009). Furthermore, detectable levels of BPA from plastics have been found in the urine of adults in the United States, while the U.S food and drug administration agency in 2011 amended its regulations to disallow the use of BPA in feeding bottles, Sippy cups and formula packages. (USFDA, 2011)

## 2.3 CURRENT WASTE MANAGEMENT SOLUTIONS

### 2.3.1 Disposal methods

There are currently three routes used for the disposal of plastic wastes namely; landfill, incineration and recycling (Web et al., 2013). Disposal of plastic debris in landfills are the most widely used but is highly regarded as unsustainable because it requires a lot of space and the energy contained in the waste is typically lost through this route (Halden, 2010, and North and Halden, 2013). Plastic debris in landfills also act as a source of secondary environmental pollutants. When landfill liners and textiles (Geomembranes) are compromised potential toxins including benzene, toluene, xylenes, ethyl benzenes, trimethyl benzenes and, endocrine disrupting compound are released as gases or in leachates (Svenson et al.,2009). Furthermore, BPA released from plastics in landfills have also been shown to lead to an increase in the production of hydrogen sulphide, a poisonous, corrosive and flammable gas with the characteristic rotten egg smell (Tsuchida et al., 2011). High concentration of hydrogen sulphides can be potentially lethal to living organisms (Tsuchida et al., 2011). In addition, both synthetic and naturally occurring polymers do not get the necessary exposure to ultraviolet (UV) rays and microbes needed to degrade, when immobilised in landfills (WRAP, 2014).

Incineration is another technique routinely used for the disposal of plastic wastes. It is however, known to result in the production and release of toxic gases, carcinogenic polycyclic aromatic hydrocarbons (PAHs and PCBs) and dioxins into the natural environment (Hirai et al., 2011). The environmental drawbacks of plastic waste disposal via both landfill and incineration leaves reusing or recycling plastic debris as possibly the only plausible disposal routes due to the economic and ecological advantages (Koch and Calafat, 2009). The main drawbacks of recycling are the technical issues relating to collection and sorting, and the fact that not all plastics are recyclable. Some plastics due to their previous use or chemical composition will still end up in landfills (North and Halden, 2013). These plastics are commonly referred to as end or life plastics.

In developed countries where waste management solutions including collection, sorting, material reduction, increased recycling capacity, facilities for end-of-life recyclability, application of product life cycle analysis and revised risk assessment approaches are practiced. Many innovative and pioneering works have led to the recovery and recycling of plastic wastes into either resins or plastic composites used in packaging, textile fibre,

landscaping, construction, development of bio-based feedstock among others (Thompson et al., 2009a). Although the technical issues of plastic recycling persist in developing countries, there are some reported uses of recycled plastics in India and Nigeria among others especially in concrete and bitumen applications (Swami et al., 2012 and Ede, 2015).

### 2.3.2 Valorisation and recycling of post-consumer plastic.

#### *2.3.2.1 Down gauging and re-use*

The principles of down-gauging entails reducing the amount of packaging used per item which in turn advance the reduction in the usage of raw materials (Thompson et al., 2009a). Economy however dictates that most manufacturers would have already used close to the minimal material necessary for a given application. Hence, down gauging may not necessarily relate to a reduction in the volume of waste plastics current produced annually. In general, re-using waste plastic is always the preferred choice, as it requires less energy, reduce cost and conserve resources (Thompson et al., 2009a, 2009b, WRAP, 2006 and WRAP, 2014).

Reusing means that the waste plastic can be used again for the original purpose, which it was designed without need for reprocessing. The most commonly reused waste plastics are Low-density polyethylene (LDPE) used in carrier bags and high-density polyethylene (HDPE) bottles used in plastic bottles. The reuse of carrier bags is currently boosted in the UK by legislation, the carrier bag charge, retailer responsibility enacted in the UK in 2015 (DEFRA, 2015). Similarly, the Waste & Resources Action Programme (WRAP) have carried out a successfully trial of large-scale reuse of HDPE plastics for the same purposes they were originally designed (WRAP, 2006 and WRAP, 2014). There is however, limited potential for wide scale re-use of waste plastics due to the wide array of plastic materials currently available, the logistics of returning post-consumer plastics to the supplier and the enhanced engineering properties of some of plastic materials (Thompson et al., 2009a). Some plastics are precisely engineered to serve a certain purpose, when they are no longer fit for purpose, reusing them for the same purpose may not be feasible (PlasticEurope, 2015).

#### *2.3.2.2 Primary recycling*

Primary recycling, also known as re-extrusion involves the reintroduction of waste plastics back into the extrusion cycles, to produce virgin resins for the production of materials with

similar properties as the waste material (Al-Salam, 2009). Plastics recycled through via this route can be used in as many applications and products as the prime-plastic (WRAP, 2014). Retailers and brand manufacturers for example, increasingly use recycled PET and HDPE in primary packaging such as trays and bottles, as it helps demonstrate their commitments to sustainable resource use. Household names such as Coca Cola, M&S, Boots, Halfords and Body shop among others all currently use recycled plastics in selected product lines (WRAP, 2014).

One of the major challenges of primary recycling according to Parfitt, (2000) is selective collection system required to maintain a contaminant free extrusion cycle. This recycling route is only applicable to decontaminated waste plastics. A single contaminated plastic can ruin the entire melt. Therefore, kerbside systems required to collect relatively small quantities of mixed waste plastics from a large number of sources and the high precision sorting required poses a resource drain and involves significant operating costs (Parfitt, 2000).

#### *2.3.2.3 Mechanical recycling*

Mechanical recycling is a secondary plastic recycling technique that refers to operations that aim to recover waste plastics via mechanical processes to produce recyclates that can be converted into new plastic materials (PlasticsEurope, 2008). The process typically involve grinding, washing, drying, granulating, re-granulating and compounding the waste materials into pellet sized resins which can be feed into new plastic production lines or used as aggregates in an entirely different production line. For mechanical recycling only thermoplastics are of interest, that is plastic materials that melts upon heating and becomes hard after cooling in a reversible reaction (PlasticsEurope, 2008 and 2015). Thermoplastic as previously mentioned previously, account for over 90% of the available plastic syntheses, as such this recycling technique is currently the most utilised.

A major limitation of mechanical recycling is that thermoplastics poses a wide range of engineering and durability properties, which may be non-compatible with one another (Kartalis, 2000). Combining these different properties will yield weaker recyclates compared to the scrap materials. Therefore, mechanical recycling can only be used for homogenous single-polymer plastics. The more complex and contaminated the waste the more difficult it is to recycle using this technique (Kartalis, 2000). Additionally, thermosets

cannot be reprocessed this way but can be chemically recycled back into feedstocks used in the production of new plastics (Al-Saleem, 2010).

#### *2.3.2.4 Chemical recycling*

Chemical recycling is a tertiary recycling technique, which refers to the operations that aim to chemically convert waste plastics back to monomers or other basic materials (Al-Saleem, 2010). The output may be suitable for use as feedstock in the polymerisation of new plastics/polymers or useful as alternative fuel (PlasticsEurope, 2008). The term chemical is used due to the alteration in the chemical structure of the polymer after recycling. The main advantage of chemical recycling is the possibility of treating heterogeneous and contaminated plastics with limited need for pre-treatment (Al-Saleem, 2010). Some energy can also be recovered from waste plastics through this recycling route (Thompson et al., 2009a). Several technologies including pyrolysis, gasification, liquid-gas hydrogenation, viscosity breakdown, steam or catalytic breakdown among others are chemical recycling techniques deployed as a means of producing various fuel fractions from waste plastics (Al-Saleem, 2009 and 2010). In general, investment levels and energy consumption of these technologies are such that only large-scale recycling plants are economically viable (PlasticsEurope, 2008). The major beneficiaries of this recycling technique are petrochemical companies, who utilise waste plastics as feedstock supplements in fuel production for the sustenance of their plants/factory (Al-Saleem, 2010).

#### *2.3.2.5 Recycling post-consumer plastic in concrete – an all-encompassing review*

As part of the sustained efforts to recycle post-consumer plastics into new production lines, several studies have been conducted on the recycling of post-consumer (waste) plastics in construction materials such as cement mortar and concrete (Bhogayata et al., 2017, Badache et al., 2018, Schaefer et al., 2018, Latroch et al., 2018, Khalid et al., 2018, Thorneycroft et al., 2018 and, Novak and Kohoutkova 2018, among others). Most of the previous works investigated the use of recovered waste plastics either as conventional aggregate replacements or as concrete reinforcements. Their findings indicated that recovered plastics can be used to produce good quality concrete and mortar blends. The performance profiles of the fresh and hardened cement mortar and concrete incorporating waste plastics reported in existing studies also indicated that the resulting composite materials might be suitable for use in structural precast or recast applications and/or other construction formworks requiring lightweight materials. Furthermore, the existing studies

exemplified the significant energy and cost reductions associated with the use of waste plastics in concrete and, the reduction in health and environmental burden associated with discarded plastics (Herki et al., 2013, Yang et al., 2015, Coppola et al., 2016, Colangelo et al., 2016, Nursyamsi et al., 2017 and Rumsys et al., 2017 among other). Some limitations observed in the existing studies such as the limited information on the durability behaviour of concrete incorporating plastics particularly in sulphate environment and the performance of concrete incorporating containing recycled plastic and supplementary cementitious materials such as PFA are addressed in this study.

*2.3.2.5.1 Physical and Mechanical properties of concrete containing waste plastics*

The physical and mechanical properties of fresh and hardened concrete were extensively evaluated in previous studies on the recycling of post-consumer plastics in concrete reviewed as part of this work. Some observations made on the physical and mechanical properties of concrete containing waste plastics reported in previous studies and the factors influencing them are shown in Table 2.1. In summary, majority of the existing studies recognised the percentage incorporation of recycled aggregate/fibre as one of the dominant factors influencing the physical and mechanical properties of concrete containing plastics. The combined effect of non-uniform shape and, low specific weight, absorption capacity and bonding capacity of recycled plastics decreases workability, increase porosity and decrease the mechanical properties of concrete. As such, when the percentage of plastic aggregates or fibres in concrete is increased, the deleterious effects of the physical and chemical properties of recycled plastics mentioned above become more pronounced.

In addition to the percentage of recycled aggregate/fibre incorporated in concrete, other factors such as water/cement ratio, aggregate/binder ratio, transition zone characteristics and curing conditions were also recognised in existing studies as having some influence on the physical and mechanical properties of concrete containing recycled plastics. These factors however, influence concrete containing recycled plastics, the same way they customarily affect conventional concrete. For example, an increase in water/cement ratio increase workability, increase porosity and, decrease density and mechanical properties of concrete containing recycled plastics. Likewise, the lack of chemical reactivity between recycled plastics and hydrated cement paste, increase the porosity at the interfacial zone and decrease the resistance of concrete to crack and fracture formation along the zone.

Table 2.1: Some of the factors influencing the physical and mechanical properties of concrete containing waste plastics

| *Test* | *Factors to be considered* | *Possible contribution to concrete properties* | *References* |
|---|---|---|---|
| Workability | ➢ Water/cement ratio.<br>➢ % of plastic aggregate or fibre.<br>➢ Properties of plastic aggregate (PA) or plastic fibre (PF).<br>➢ Aspect ratio of PF | ➢ Workability of cement mortar and concrete increased with increase in water/binder ratio.<br>➢ Increase in volume of PA/PF mostly reduce workability.<br>➢ The non-uniform shape of plastic aggregate increased segregation and decreased mobility of fresh concrete.<br>➢ The low water absorption % of plastic aggregates, increased free water content and, as such decreased workability of concrete.<br>➢ The higher the aspect ratio, the lower the workability. | Aldahdooh et al., (2017), Shamsaei et al., (2017), Mermerdas et al., (2017), Alqahtani et al., (2017), Zaleska et al., (2017), Bhogayata et al., (2017), Yang et al., (2015), Choi et al., (2009), Madandoust et al., (2011),Rai et al., (2012), Pelisser et al., (2012), Mazaheripour et al., (2011), karahan and Atis, (2011), Nili and Afroughsabet (2010), Kou et al., (2009), Ismail and Al-Hashmi, (2008) |
| Density | ➢ Percentage of plastic aggregate (PA) or plastic fibre (PF)<br>➢ Properties of PA and PF<br>➢ Water/cement ratio | ➢ The densities of concrete containing PA or PF were mostly lower than that of conventional concrete.<br>➢ Increase in the volume of PA cause a linear reduction in density.<br>➢ Little/no change in density was observed with the use of PF.<br>➢ Increase in water/cement ratio decreased porosity, while increase in fineness modulus increase density | Islam et al., (2015), Alfahdawi et al., (2016), Coppola et al., (2016), Badache et al., (2018) Shamsaei et al., (2017), Khalid et al., (2018), Lasco et al., (2017), Dalhat and Al-Abdul Wahhab, (2017), Ruiz-Herrero et al., (2016), Nursyamsi et al., (2017); Abd-Elaziz et al., (2017); Ghernouti et al., (2010) |
| Void ratio / absorption % | ➢ Shape of plastic aggregate/fibre<br>➢ % of plastic aggregates (PA) and fibre (PF)<br>➢ Water and Air contents | ➢ The low unit weight and high percentage of non-uniform shape of plastic aggregates increased the percentage void and absorption of hardened concrete containing PA/PF.<br>➢ Void ratio and absorption properties of polymer concrete increased with increase in PA/PF content.<br>➢ Increase in water and air content also increased void ratio and absorption capacity | Kumar et al., (2018); Ali et al., (2018); Latroch et al., (2018); Rumsys et al., (2017); Mermerdas et al., (2017); Ruiz-Herrero et al., (2016); Lo monte et al., (2014); Miranda et al., (2014) Correia et al., (2014); Safi et al., (2013); Pelisser et al., (2012); Wang and Meyer (2012); Karahan and Atis, (2011); Shaikh et al., (2015); Behfarnia K. and Rostami M. (2017): |

*Continued on page 23*

**Table 2.1: Some of the factors influencing the physical and mechanical properties of concrete containing waste plastics**

| *Test* | *Factors to be considered* | *Possible contribution to concrete properties* | *References* |
|---|---|---|---|
| *Compressive strength* | ➢ % of plastic aggregates (PA) and fibre (PF)<br>➢ Water/cement ratio<br>➢ Aggregate/binder ratio<br>➢ Physical properties of PA/PF<br>➢ Type of waste plastics<br>➢ Porosity of aggregates<br>➢ Transition zone characteristics<br>➢ Curing condition | ➢ Plastic aggregate alters the brittle behaviour of concrete to ductile behaviour.<br>➢ Compressive strength of concrete mostly decreased with increase in PA/PF content.<br>➢ The range of compressive strength observed in existing studies depends on the type and grading of plastic recycled.<br>➢ The higher the angularity, roughness and fineness modulus of aggregates, the higher the compressive strength.<br>➢ The high porosity of some plastic aggregate increased the adhesion of plastics to cement paste.<br>➢ Plastic fibres with high ultimate tensile strength fibre such as polypropylene may increase the compressive strength.<br>➢ The transition zones of concrete containing waste plastics are characterised by large capillary voids, which decreases compressive strength. | Latroch et al., (2018); Hannawi and Prince-Agbodjan (2014); Thorneycroft et al., (2018); Aldahdooh et al., (2018), Khalid et al., (2018); Senhadji et al., (2015); Malkapur et al., (2017); Islam et al., (2015); Choi et al., (2009); Galvao et al., (2011); Coppola et al., (2016); Arulrajah et al., (2017); Xuan et al., (2017); Purnomo et al., (2017); Azhdarpour et al., (2017); Bolat and Erkus (2014); Manjunath (2016); Azhdarpour et al., (2016); Bulut and Sahin (2017); Ruiz-Herrero et al., (2016); Nursyamsi et al., (2017); Ferreira et al., (2012b); Saikia and de Brito (2014); Hsie et al., (2008); Badache et al., (2017); Mermerdas et al., (2017); Pandya and Purohit (2014); Rahmani et al., (2013); Pelisser et al., (2012); Jiang et al., (2011); Park et al., (2008); Fraternaili et al., (2008 and 2014); Chaudry et al., (2014); De-Oliveira et al., (2011); Al-hadithi (2013); Bagherzadeh et al., (2011); Kakooei et al., (2012); Kumar and Baskar (2015a, b & c); |
| Tensile strength | ➢ % of PA or PF<br>➢ Physical properties of PA/PF<br>➢ Transition zone characteristics | ➢ Tensile strength decreased with increase in % of plastic aggregate, water/cement ratio and non-uniform shaped aggregates, but increased with reduction in elastic modulus.<br>➢ The tensile strength of concrete mostly increased upon the addition of PF. The longer the fibre the more positive its influence | Latroch et al., (2018), Thorneycroft et al., (2018) Bui et al., (2018), Shamsaei et al., (2017),Bhogayata et al., (2017), Mermerdas et al., (2017),Azhdarpour et al., (2017), Paliwal et al., (2017),Bulut and Sahin (2017), Mastali et al., (2016),Rahmani et al., (2013), Ruiz-Herrero et al., (2016). Ferreira et al., (2012b), Ramadevi and Manju, (2012), Nibudey et al., (2013) |

*Continued on page 24*

**Table 2.1: Some of the factors influencing the physical and mechanical properties of concrete containing waste plastics**

| *Test* | *Factors to be considered* | *Possible contribution to concrete properties* | *References* |
|---|---|---|---|
| Flexural strength | ➢ % of PA or PF<br>➢ Physical properties of PA/PF<br>➢ Transition zone characteristics | ➢ The flexural strength of concrete containing PA was observed to be generally lower than that of conventional concrete at the same water/cement ratio<br>➢ Increasing substitution level of plastic aggregate reduced flexural strength, while plastic fibres with high ultimate tensile strength may increase the flexural strength of concrete.<br>➢ Flexural strength improved only when the concrete had small fibre content. When the fibre content increase above a certain threshold, the flexural strength decrease. | Bulut and Sahin (2017); Rathod et al., (2017); Hannawi and Prince-Agbodjan (2014); Ismail and Al-Hashmi (2008); Nili and Afroughsabet (2010); Rahmani et al., (2013); Lucolano et al., (2013); Safi et al., (2013); Ruiz-Herrero et al., (2016); Chaudhary et al., (2014); Saikia and Brito (2014); Wang and Meyer (2012); Akcaozoglu and Ulu, (2014); Nibudey et al. (2013); Bagherzadeh et al., (2011); de Oliveira and Castro-Gomes, (2011); López-Buendía et al.,(2013); Mazaheripour et al., (2011); Mello et al., (2014) |
| Elastic modulus | ➢ Water/cement ratio.<br>➢ % of plastic aggregates (PA)<br>➢ Shape of PA/PF.<br>➢ Porosity of aggregates.<br>➢ Transition zone characteristics. | ➢ The inclusion of plastic aggregates decreased the elastic modulus relative to conventional concrete at the same water/cement ratio.<br>➢ Significantly, lower elastic modulus was observed when the shape of plastic aggregates is more irregular.<br>➢ Not much difference in elastic module was noticed with the inclusion of plastic fibre in concrete<br>➢ Increase in water/cement ratio and % of waste plastics mainly decrease elastic modulus of concrete | Latroch et al., (2018); Arulrajah et al., (2017); Xuan et al., (2017); Badache et al., (2018); Haghighatnejad et al., (2016); Irwan et al., (2013); Pelisser et al., (2012); Ferreira et al., (2012b); Bui et al., (2018); Ismail and Al-Hashmi (2008); Rahmani et al., (2013); Rai et al., (2012); Juki et al., (2013); Kumar and Baskar (2015a); Bulut and Şahin (2017); Abd-Elaziz et al., (2017); |

*Continued on page 25*

**Table 2.1: Some of the factors influencing the physical and mechanical properties of concrete containing waste plastics**

| *Test* | *Factors to be considered* | *Possible contribution to concrete properties* | *References* |
|---|---|---|---|
| Fracture toughness and Impact resistance | ➢ Compressive strength of concrete.<br>➢ % and physical properties of plastic aggregate and fibre<br>➢ Aspect ratio<br>➢ % of plastic | ➢ Due to the relatively high impact resistance of plastics, the abrasion resistance of concrete improve with the use of PA/PF.<br>➢ Abrasion resistance and toughness indices of concrete containing plastic fibre increased with increase in aspect ratio<br>➢ Directly linear correlations were observed between the ultimate impact resistance and compressive strength of concrete containing plastic fibres | Ferreira et al. (2012b); Saikia and Brito (2014); Prahallada and Prakash (2013a); Mastali et al., (2016); Nili and Afroughsabet (2010); Toutanji et al., (2010); Pacheco-Torgal et al., (2012); Hsie et al., (2008); Pelisser et al., (2012) |
| Ultra-sonic pulse velocity (UPV) | ➢ % of waste plastic<br>➢ Curing age<br>➢ Compressive strength<br>➢ Water/cement ratio | ➢ As the % of aggregate replaced with waste plastics increased, the speed registered by the ultra sound decrease.<br>➢ UPV values also decreased with increase in fibre content<br>➢ Increase in water/cement ratio decrease UPV<br>➢ There is a directly linear relationship between concrete's curing age and the ultra-sonic pulse velocity. Increase in curing age increased the UPV. Increase in compressive strength is also linear with increase in UPV | Azhdarpour et al., (2016); Badache et al., (2018); Al-Hadithi and Hilal (2016); Rahmani et al., (2013); Latroch et al., (2018); Senhadji et al., (2015): Kan and Demirboga (2009): Akcaozoglu et al., (2013); Lo Monte et al., (2014); Daud et al., (2013); Pastor et al., (2014); Park et al., (2008); Pacheco-Torgal et al., (2012) |
| Stress Vs Strain curve | ➢ % of waste plastic | ➢ When the % of plastic aggregates used in cement mortar or concrete increase, the initial slope of the stress V. stain curve and the maximum stress decreased, while the ultimate strain increased.<br>➢ At higher replacement percentage of conventional aggregate with plastic aggregates, the peak compressive strength was observed to be lower, while the strain and ultimate strength were observed to be higher than that of conventional concrete. | Ge et al., (2013) and Frigione (2010). |

*2.3.2.5.2 Durability properties of concrete containing recycled plastics*

Some observations made from the durability properties of concrete containing waste plastics reported in previous studies and the factors influencing them are described below;

A) Degradation of concrete containing recycled plastics in acidic and alkaline environments

The bulk plastics processed into plastic aggregates or plastic fibres, have high chemical stability, as such they remain stable in high alkaline environment such as concrete. The only exception was polyethylene terephthalate (PET), which as shown by Pelisser et al., (2012) demonstrated high degree of degradation in concrete air cured for 150 and 365 days. The high-level degradation observed from SEM micrographs was attributed to the easy disposition of PET fibres to damages by $Ca^{2+}$, $Na^{+}$, $K^{+}$ and $OH^{-}$ ions present in concrete. In addition, plastic fibres such as polypropylene, polyethylene terephthalate and polyester fibres experience superficial alterations when incorporated in alkaline media such as concrete (Won et al., 2010 and Pelisser et al., 2012). The fibres lost strength with increasing age due to their high hydrolysis and dissolution in alkaline media (Won et al., 2010).

Won et al., (2010) and Araghi et al., (2015), both reported slight reductions in physical and mechanical properties of concrete incorporating plastic aggregates subjected to sulphuric acid attack. Araghi et al., (2015), in their study on the effect of sulphuric acid on the weight, crushing load and ultrasonic wave of concrete containing 0, 5, 10 and 15% polyethylene terephthalate (PET) aggregates observed that, relative to conventional concrete, the concrete incorporating PET aggregates suffered higher reductions in weight, load bearing capacity and ultrasonic wave. The test specimens containing 15% PET demonstrated lower weight losses and better resistance against sulphuric acid attack, relative to the other specimens. In general, the researchers concluded that, concrete including PET aggregates could be used in environments prone to the accumulation of sulphuric acid.

With regards to concrete incorporating plastics fibres, Won et al., (2010) observed significant deterioration in long-term (120 days) performance of concrete containing 1% recycled PET fibre immersed in sulphuric acid. The deterioration in surface shape observed from SEM micrographs appeared to have progressed with increase in

immersion period. In the same study, Won et al., (2010) used SEM images to access the deterioration of the PET fibres incorporated in concrete cured in sodium sulphate and, salt and calcium rich environments. From observing the surface shape with increasing aging time, the researchers concluded that there was no apparent deterioration and almost no difference between the surface of the standard test specimens (with no fibre) and specimens with 1% PET fibres

B) Chloride ion penetration

As with conventional concrete, the migration of chloride ions in concrete containing plastic aggregates is influenced by water absorption, porosity, water permeability and curing conditions (Senhadji et al., 2015 and Silva et al. 2013). In their separate works, Senhadji et al., (2015), Silva et al., (2013) and Fraj et al., (2010) all reported that the chloride ion penetration of concrete containing waste plastics (PVC, PET and polyurethane respectively) was higher than that of conventional concrete. The results of the water absorption capacity, porosity and water permeability investigations reported in the studies were also observed to be higher in concrete containing the recycled plastics than the conventional concrete. Meanwhile, due to the impervious high-density polyethylene granules blocking the passage of chloride ions into concrete, Shanmugapriya and Santhi (2017) observed a reduction in chloride ion penetration of concrete containing HDPE, relative to conventional concrete. The chloride ion penetration result presented in the study however, increased with increase in HDPE content. Furthermore, Silva et al., (2013) observed that the chloride permeability of concrete containing waste plastics was highest in test specimens cured under laboratory conditions, followed by test specimens cured outdoors and, finally test specimens cured in a wet chamber.

C) Carbonation

As with chloride ion penetration, the carbonation of concrete containing plastic aggregates as reported in existing studies was mostly influenced by water absorption, porosity and water permeability. Ruiz-Herrero et al., (2016) and Silva et al., (2013) all reported that relative to conventional concrete, concrete containing plastic aggregates recorded higher carbonation depths. Silva et al., (2013), attributed the observed increase in carbonation depth to the high porosity of the concrete utilising polyethylene terephthalate (PET) as aggregate replacement. Similarly, in their studies of the

mechanical and thermal performance of concrete and mortar cellular materials containing waste plastics, Ruiz-Herrero et al., (2016), reported that the carbonation depth of cement mortar containing (0, 5, 10 and 20%) polyethylene (PE), polyvinyl chloride (PVC) or PE + PVC increased with increase in replacement percentage of waste plastics. The researchers also reported that, higher carbonation depth was observed for concrete containing PVC plastics alone, followed by PVC + PE and finally PE alone. They related the high carbonation of the PVC concrete firstly to the presence of chlorine in the PVC and secondly the high porosity of the concrete which enhances carbon dioxide diffusion. In contrast, Gavela et al., (2013), in their work on the corrosion behaviour of steel rebars in reinforced concrete containing wastes thermoplastic aggregates, reported no carbonation in all the test specimens.

Regarding the carbonation of concrete reinforced with waste plastic fibres, Verdolotti et al., (2014) reported a decrease in carbonation with increase in polymeric polyethylene (PE), polypropylene (PP) and polyethylene terephthalate (PET) fibre content. The researchers attributed this to the reduced diffusion of $CO_2$ in the composite. Verdolotti et al., (2014), also reported that, relative to the concrete mortar with 0% recycled plastic fibres, high degree of carbonation was observed in the composites incorporating plastic fibres.

D) Creep and shrinkage

Shrinkage and creep of concrete are not independent and an increase in shrinkage would mostly increase the magnitude of creep (Neville, 2012). The two phenomenon can generate early age or long-term cracking, and as such, a loss of durability of concrete structure. According to Neville (2012), modulus of elasticity of aggregates is probably the most important physical property of aggregate influencing creep and drying shrinkage. The higher the modulus of elasticity of aggregates, the higher the restraint offered by the aggregates to the potential creep and shrinkage of hydrated cement paste (Neville (2012). Lightweight aggregates such as recycled plastics typically exhibit low elastic modulus, thus offer low resistance to creep or shrinkage. Similarly, aggregate with high porosity generally have a lower modulus of elasticity, as such exhibit lower resistance to creep or shrinkage of the hydrated cement (Neville, 2012).

In agreement with Neville (2012), most of the existing reports on the recycling of post-consumer plastics in cement mortar or concrete, highlighted elastic modulus as the prime factor influencing the creep and drying shrinkage of cement composites incorporating recycled plastics. Hence as observed by Kou et al., (2009) and Fraj et al., (2010) concrete containing lightweight aggregates polyvinyl chloride (PVC) and Polyurethane (PUR) foam, due to their lower elastic modulus demonstrated higher shrinkage relative to concrete made using conventional materials with higher elastic modulus. Likewise, in their work on the valorisation of coarse rigid PUR foam waste in lightweight concrete, Fraj et al., (2010) observed that relative to conventional foamed concrete, PUR foam concrete demonstrated higher degree of shrinkage. The shrinkage was also observed to increase when the waste plastic was saturated with water before mixing. In addition to its lightweight property, the PUR foam waste was also highly porous and absorbed a considerable amount of water. In contrast, the drying shrinkage of concrete incorporating polyethylene terephthalate (PET) as fine and coarse aggregates was observed to be lower than those of conventional concrete due to lower porosity of the waste plastics (Silva et al., (2013). Kou et al., (2009), made similar observations, when the substitution level of polyvinyl chloride (PVC) in lightweight expanding clay aggregate concrete increased. The impervious nature of PVC, made more free water available for cement hydration, resulting in lower shrinkage values.

Kim et al., (2010) and, Karahan and Atis (2011) observed that drying shrinkage of concrete reduced with the incorporation of low volumes of PET and PP fibres (up to 0.2%). According to the researchers, the reduction in drying shrinkage upon the addition of plastic fibres may be attributed to the shear stress along the fibre/matrix interface. When the substitution level of PET and PP increased to 1%, Kim et al., (2010) observed that, the shrinkage of concrete increased relative to conventional concrete with no fibre. This was attributed to the large volume of air voids resulting from the presence of large percentage of plastic fibres.

E) Freeze and thaw resistance

As with conventional concrete, the freeze-thaw resistance of concrete incorporating plastic aggregates are also influenced by water absorption capacity, percentage void and water permeability (Karahan and Atis, 2011, Kan and Demirboga, 2009 and Wang and Meyer 2012). As observed in the report on the durability properties of polypropylene

fibre reinforced concrete by Karahan and Atis (2011), all the test specimens containing the synthetic fibre demonstrated weight and mechanical property losses after 50 freeze-thaw cycles. The observed losses Increased with increase in porosity and water absorption capacity of the test specimens. Kan and Demirboga (2009) made similar observations when substituted coarse aggregates and fine aggregates with modified expanding polystyrene aggregate (MEPS), the high porosity of resulted in significant losses in dynamic elastic modulus after 300 freeze-thaw cycles. Furthermore, the results presented by the researchers showed that, the coarse MEPS aggregates were more susceptible than fine MEPS aggregates to the freeze-thaw cycles.

Wang and Meyer (2012), in their evaluation of the performance of cement mortar made with (0, 10, 20 and 50%) recycled high impact polystyrene (HIPS), observed that the mechanical properties of all the mortar specimens remain constant after 300 freeze-thaw cycles, regardless of the HIPS replacement ratio. This according to the researchers may be attributed to the water permeability of the test specimens, which decreased, with the increase in substitution level of sand with HIPS aggregates. Similar results were obtained by Hannawi and Prince-Agbodjan (2014), in their work on the transfer behaviour and durability of cementitious mortars containing polycarbonate plastic wastes for example, indicated that while using recycled polycarbonate plastic particles as sand substitute in mortar, freeze/thaw cycles induced a mechanical property loss in all the concrete developed with plastic aggregate. The loss in mechanical property increased with increase in substitution percentage.

F) Thermal properties

In existing studies on the recycling of post-consumer plastics in concrete, the thermal conductivity of concrete were observed to decrease with the inclusion of waste plastics (Latroch et al., 2018, Zaleska et al., 2017, Yesilata et al., 2009, Pacheco-Torgal et al., 2012, Abd-Elaziz et al., 2017, Corinaldesi et al., 2015, Corinaldesi et al., 2011 and Akcaozoglu et al., 2013 and Fraternalli et al., 2011). Lo monte (2014), also observed that the thermal diffusivity of concrete containing expanding polystyrene (EPS) measured at temperatures 20$^{o}$C, 150$^{o}$C, 300$^{o}$C, 500$^{o}$C and 700$^{o}$C were lower than those of conventional concrete (Lo Monte et al., 2014)

In their investigation of the physico-mechanical and thermal properties of composite mortar containing expanded polyvinyl chloride aggregate (EPVC), Latroch et al., (2018) observed thermal conductivity of mortar decreased by about 60%, when the fine aggregates (sand) was replaced with 75% EPVC. The relatively huge difference between the thermal conductivity of the control mortar and the EPVC mortar was attributed to the much lower thermal conductivity of EPVC aggregates. The decrease in thermal conductivity was also observed to correlate with the increase in porosity of the EPVC mortar. In similar studies, the low thermal conductivity properties of recycled plastic aggregates such as polyethylene terephthalate (Corinaldesi et al., 2015, Akcaozoglu et al., 2013, Yesilata et al., 2009 and Pacheco-Torgal et al., 2012 ), high impact polystyrene (Wang and Meyer, 2012), expanded polystyrene (Abd-Elaziz et a., 2017 and Savadi et al., 2016), glass-fibre reinforced polystyrene aggregates from polypropylene tubes (Zaleska et al., 2017 and Corinaldesi et al., 2015), high-density polyethylene (Badache et al., 2018) and polyurethane foam (Corinaldesi et al., 2011), decreased the thermal conductivity of concrete (or mortar) incorporating them. Directly linear relationships were observed between the density and thermal conductivity of concrete incorporating plastics. The decrease in density of concrete containing recycled plastics was closely associated with decrease in thermal conductivity (Zaleska et al., 2017, Savadi et al., 2016 and, Akcaozoglu et al., 2013).

On the effect of plastic fibres, Fraternali et al. (2011) observed that relative to conventional concrete, the thermal conductivity of concrete reinforced with 1% volume fraction of polyethylene terephthalate or polypropylene fibres decreased by 18% and 21.8% respectively. In general, the decrease in thermal conductivity observed in the existing studies suggest that the composites containing recycled plastics have much better insulating properties than those of unmodified concrete (or mortar). These composites may be suitable for applications requiring good insulating properties and can therefore reduce energy consumption.

G) Fire resistance

In existing studies, the fire resisting properties of concrete incorporating post-consumer plastics were mostly considered a function of concrete porosity and the exothermic properties of plastics. The high porosity of concrete incorporating plastic aggregates facilitates heat propagation, while the exothermic thermal properties of waste plastics

generate additional heat (Novak and Kohoutkova, 2018 and Correia et al., 2014). For example, whilst exposing concrete test specimens containing polyethylene terephthalate to elevated temperature ranges (20$^{o}$C, 600$^{o}$C and 800$^{o}$C), Correia et al.,(2014) reported that, the additional heat generated by PET aggregates (at the temperature ranges investigated) increased the internal temperatures of concrete test specimens containing the recycled plastics relative to those of the control specimens. The difference in maximum temperature was observed to increase with increase in replacement percentages. The researchers also observed that the development of high internal temperatures and the high porosities of the test specimens containing PET aggregates increased the deterioration in compressive strength and young modulus of the concrete. No changes in splitting tensile strength was observed by the researchers, but localised spalling and colour changes due to the various physico-chemical changes of the concrete constituent were observed at high temperature. Albano et al., 2009 made similar observations, when they experimentally investigated the flexural strength of (0%, 10% and 20% recycled PET) concrete exposed to elevated temperatures, 200oC, 400oC and 600oC. The researchers reported no noticeable changes in flexural strength up to 200oC, but at 400oC and 600oC, the degradation of PET resulted in the formation of gas holes in the test specimens, which led to decrease in flexural strength.

For plastic reinforced concrete, Novak and Kohoutkova (2018) reported no spalling, when concrete reinforced with (0.2%) polypropylene fibres was subjected to elevated temperatures within the range 20oC/h - 1000oC/h. The presence of polypropylene fibres however, decreased the volumetric mass, peak compressive strength and the tensile strength of the concrete due to the high porosity of the test specimens, which resulted from the melting fibres.

H) Leachate and radiation assessment of concrete containing E-waste plastics

Over the last decade, many research works has been conducted on the use of E-waste plastics such as high-impact polystyrene (HIPS), acrylonitrile butadiene styrene (ABS) and printed circuit boards (PCBS) as partial aggregate replacement in cement concrete and mortar. As with the engineering properties of concrete incorporating other plastic types, the engineering properties of concrete mainly decreased with the incorporation of E-waste plastics in concrete (Wang and Meyer, 2012, Kumar and Baskar, 2015a,b and c, Kumar et al., 2018, Malkapur et al., 2017, Baron Colbert and You, 2012 and, Lakshmi

and Nagan, 2011). The difference in performance also appears to increase with increase in E-waste plastic content. E-wastes however, has a radioactive profile which include different concentrations of heavy metals (Cd, Cu, Zn and Pb) and, Uranium (238U), Thorium (232Th) and Potassium (40K) that may radiate from concrete into the natural environment contributing to rise in illness such as cancer, birth defects and cognitive disabilities.

In their assessment of the leachate characteristics of concrete containing (0%, 10%, 20%, 30%, 40% and 50%) high impact polystyrene (HIPS), Kumar et al., (2016) reported that the concentration of cadmium (Cd) and lead (Pb) measured after 28, 60 and 90 days were lower than the regulatory level of 1mg/l and 5mg/l respectively. The copper (Cu) and Zinc (Zn) in the leachate extracts were also found to be below the prescribed level of 100mg/l and 500mg/l respectively. All the results were also within the 0.5mg/l, 130mg/l, 500mgl and 1.5mg/l limits specified for Cd, Cu, Zn and Pb respectively, in the Resource Conservation and Recovery Act (RCRA). Similarly, Kumar et al., (2018), carried out an assessment of radioactivity of concrete containing HIPS using gamma-ray spectrometer and rand activity by solid-state nuclear track detector (SSNTD) technique. The result presented indicate that the gamma radiation and radon activity of concrete containing HIPS were well within the permissible limits. The radiation levels were also observed to decrease with increase in HIPS content of the concrete. In essence, concrete-containing HIPS does not pose any radiation hazards, nor does the leachate contain heavy metals above the specified standards. Hence, concrete-containing HIPS can be suitable for use in construction.

*2.3.2.5.3 Emerging trends and future prospects*

I. Use of supplementary cementitious materials

In recent years, many studies have been conducted to evaluate the effects of superplasticiser or supplementary cementitious materials (particularly fly ash and silica fumes) on the mechanical and durability properties of concrete containing recycled plastics (Paliwal et al., 2017, Shaikh et al., 2015, Awang et al., 2015, Herki et al., 2013, Pandya and Purohit, 2014 and, Schaefer et al., 2018). The results obtained in these studies show that the addition or partial replacement of hydraulic cement with (up to 10%) fly ash or silica fumes brought about an improvement in the properties of fresh and hardened properties of concrete containing recycled plastics. Herki et al., (2013) did report a

decrease in workability with increase in replacement level of fly ash, but this was solely due increase in water demand of the high carbon content of the fly ash utilised in the study. Furthermore, the inclusion of superplasticiser in the mix design of concrete containing recycled plastic aggregates showed improvement in workability, compressive, flexural and tensile strengths. In their experimental study on the use of waste plastics as coarse aggregates in concrete with superplasticiser admixture, Pirzada et al., (2018) reported that the strength of concrete increased with the addition of polycarbonate ether superplasticiser. The physical property of the fresh concrete was also observed to increase with increase in the percentage of superplasticiser.

II. Use of alternative filler aggregates

Arulrajah et al., (2017) and Rumsys et al., (2017) considered the influence of construction demolition waste and expanded clay soil respectively on the properties of fresh and hardened concrete containing recycled plastics. In their evaluation of the unconfined compressive strength, stiffness and resilient moduli of concrete containing three types of plastics (linear low density polyethylene filled with calcium carbonate, high density polyethylene and low density polyethylene) blended with either crushed brick (CB) or reclaimed asphaltic pavement(RAP), Arulrajah et al., (2017) concluded that relative to the control concrete, the UCS, stiffness and resilient moduli all decreased with the inclusion of recycled plastics. In spite of this, the concrete blend with recycled plastics and CB/RAP showed sufficient engineering characteristics as civil engineering construction material. For example, the addition of 3-5% plastic granules to CB and RAP resulted in resilient moduli sufficient for road construction applications. Rumsys et al., (2017), made similar observations when they immobilized waste plastics (HDPE and LDPE) with expanded soil stabilized with either silica fumes or ground quartz sand. Relative to the control without plastics, the waste plastic/expanded clay blends demonstrated higher density and water absorption capacities but lower compressive and tensile strengths. Despite the relatively lower strength, the compressive strength values recorded by the waste plastics/expanded clay blends at 28 days were in excess of 40 N/mm2, which are definitely good enough for consideration in many construction applications.

III. Use of waste plastics in self-compacting concrete

Self-compacting concrete (SCC) refers to the highly flowable concrete with excellent deformability and segregation resistance. This high performance concrete can flow through and fill gaps of reinforcement and corners of moulds without the need for vibration and compaction during placing (okamura and Oluchi (2003). The non-uniform shape of recycled plastic aggregates, which increase segregation and decrease mobility of fresh conventional concrete, would suggest that it is impractical to incorporate plastics without diminishing the characteristics of SCC. However, as shown in recent studies, although the inclusion of recycled plastics reduced the properties of SCC, the concrete produced demonstrated better performance in comparison to conventional concrete (Mermerdas et al., 2017 and Ibrahim 2017).

The use of recycled high-density polyethylene (Khalid et al., 2018 and Makapur et al., 2017), polyethylene terephthalate (Safi et al., 2013), polypropylene aggregates (Yang et al., 2015) and expanded polystyrene (Madandoust et al., 2011) as fine or coarse aggregate replacement in SCC generally resulted in decrease in density, compressive, flexural and tensile strength and modulus of elasticity of the concrete. However, the fluidity of SCC was observed to significantly improve by the presence of these wastes. Meanwhile, the addition of recycled plastics fibers, (polypropylene, glass-reinforced polymer and polyethylene terephthalate) decreased the workability but increased the mechanical properties and impact resistance of self-compacting concrete (Mastali et al., 2016, Ibrahim 2017, Mazaheripour et al., 2011 and, Al-Hadithi and Hilal 2016),

IV. Use of waste plastics in alkali-activated concrete

Recent developments has seen researchers utilize recycled plastics in alkali-activated concrete. This combination definitely possess much lower carbon footprint than conventional concrete. Behfarnia and Rostami (2017) investigated the mechanical and durability properties of fibre reinforced alkali-activated slag (AAS) concrete, and reported 0.24% by volume is the optimal quantity of polypropylene required to improve the mechanical and permeability properties of AAS concrete. Likewise, in their work on recycling waste PET aggregates in alkali-activated blast furnace slag and metakaolin blends, Akcaozoglu and Ulu, (2012), concluded AAS mortar containing up to 80% PET aggregates can be suitable for use in structural lightweight concrete.

V. Use of waste plastics in bituminous or asphaltic blends

Recent studies have also suggested the possible immobilisation of plastic aggregates in bituminous or asphaltic blends for road construction (Baron Colbert and You, 2012, Swami et al., 2012 and Vasudevan et al., 2011). Swami et al., (2012) in their work on the use of waste plastics for road works, reported that the polymer modified bituminous blend with optimum contents of 5-10% recycled plastic aggregates show reduction in cost, increased strength, reduced bleeding in hot temperatures and resistance to water penetration, when compared to standard bituminous blends, Vasudevan et al., (2011) also reported that polymer bituminous blends containing molten plastics are better binders than standard bituminous blends. Gawandea et al., (2012), gave a review of the techniques for using plastic waste in road and flexible concrete construction. They reported that polymer modified bituminous concrete demonstrated increased tensile strength, improved fatigue and increased durability in comparison to plain bituminous concrete.

Vi. Future prospect

Many studies reported in recent years on these materials indicate that the use of recycled plastic aggregates and fibres as partial aggregate replacement is gaining significant interests from many researchers. The research findings have shown that the use of these materials can improve concrete properties under appropriate conditions. The use of these materials can always contribute to the reduction of the hefty carbon-foot print of the construction industry. However, the motivating factor is to find an alternative disposal route better than the current practice (landfilling or incineration) for the high volume of the waste plastics generated annually. According to Kamaruddin et al., (2017), the realisation of an optimum disposal solution for waste plastics, can reduce the volume of solid wastes disposed in landfills by about 30%. Hence researchers continued exploration of the material in concrete.

Meanwhile, to turn a material defined as waste into a product is time consuming and requires a great deal of expertise and resources. In addition to legislative hurdles, the psychological barrier and human intrinsic resistance to change are major obstacles to a desire for large scale application of recycled plastics in concrete or mortar. The simple fear of the unknown can make it difficult for concrete producers and users to buy into the idea of using recycled plastics in concrete form works, especially given the perceived low

melting point of plastics and, the decrease in mechanical properties of recycled plastic concrete, no matter how modest, is prevalent. Although different researchers have propagated ways of mitigating these barriers and discussed alternative use of recycled plastics concrete other than structural applications, the forecast on the service life of concrete forms containing waste plastics remain relatively unknown. As such, a holistic approach including discussions around the psychological barrier, long-term performance, life cycle assessment and accrued environmental benefits of using this vibrant material in concrete is important for its large-scale application in concrete.

### 2.3.3 Recycling waste plastics in the current study

In this study, attempts at recycling high volume post-consumer (waste) plastics into concrete composites will be made using encapsulation technology. Encapsulation technology is a waste immobilisation technique used to prevent the free movement of contaminants from waste materials or by-products into the environment (Meegoda et al., 2003). It is already a common practice in the nuclear industry, where encapsulation in cement or its composites has been for many years the preferred option for the management of intermediate and low level radioactive wastes (Sharp et al., 2003 and Swift, 2013). The technology involves either the immobilisation of dispersed solids by mixing with a solidifying reagent to produce solid waste forms, or the complete emplacement of a solid waste in a matrix of high structural integrity (Glasser, 1997 and IAEA, 2003).

The waste plastics comprising of rigid thermoplastics will be encapsulated by mixing the waste material together with solidifying reagents (Portland cement or Pozament grout) and aggregate filler (Furnace Bottom ash). The use of waste/by products will be maximised at the expense of conventional construction materials (solidifying reagent). The resulting composites will be examined under laboratory conditions for physical, mechanical, durability properties, to determine their applicability in construction works.

## 2.4 WASTE IMMOBILISATION AND ENCAPSULATION TECHNOLOGY

Industrial activities globally generate large volumes of waste and by-products, which must be safely disposed in order to prevent migration of contaminants into the ecosystem. A modern technique used to prevent the free movement of the contaminants from wastes or by- products into the environment is commonly referred to as waste immobilisation

(Meegoda et al. 2003). Waste immobilisation can be temporary as in containment, cost effective as in solidification/stabilisation or almost permanent as in vitrification, (Meegoda et al., 2003 and, Plecas, and Dimovic, 2004). Vitrification is the safest and only permanent waste immobilisation technique. It involves the inertization of waste in a stable and heterogenous (silicate) glass through high temperature fusion which may involve the use of high temperature plasma touches operating at temperatures range 6000 – 20 000$^{o}$C, and glass forming additives (Meegoda et al., 2003 and Colombo et al., 2003). Containment meanwhile involves the temporary storage waste products (mostly hazardous waste) in concrete barriers or metallic drums among others, in readiness for geological disposal (NDA, 2009).

Atkins and Glasser, (1992), Glasser, (1997) and Swift, (2013) also considered waste immobilisation techniques to occur either through physical (solidification) or chemical mechanism (stabilisation) or sometimes a combination of both (solidification/stabilisation). Physical immobilisation mechanism is associated with entrapping the contaminant within a solid matrix, thereby rendering potential nuclides immobile, while chemical immobilisation mechanism involves treating the waste in such a way that it becomes chemically inert before incorporating into the structure of a matrix. When the physical entrapment (solidification) is combined with the chemical treatment of waste (stabilisation) the approach is commonly referred to as solidification/stabilisation (Randall et al., 2002). The principle of solidification/stabilisation is based on mixing wastes with suitable bonding and filling agents in order to alter their physical properties to a desirable form.

Encapsulation technology is based primarily on solidification, a clean-up method that acts to prevent hazardous waste from coming into contact with potential leaching agents by entrapping the waste in a monolithic mass of high structural integrity (Randall et al., 2002 and Swift, 2013). It does not necessarily involve a chemical interaction between the waste and the bonding/solidifying agents but include mechanically binding the solid waste into a single monolith (Glasser, 1997). In nuclear waste management, encapsulation is considered an alternative treatment method that relies of immobilizing radionuclides by isolating them in a protective matrix rather than dissolving them directly into glass (Boccaccini et al., 2007).

Independent of the mechanisms, encapsulation can be categorised into two types based on the size of the encapsulated waste materials, micro or macro-encapsulation (Randall et al., 2002). Micro-encapsulation involves mixing the waste together with the encasing material to achieve solidification, while macro-encapsulation involves pouring the encasing material over and around a larger mass of waste, thereby enclosing it in a solidified block (Poshadri and Aparna, 2010 and, Randal et al., 2002). Micro-encapsulation is the more common of the two. It is typically limited to inorganic wastes with simple geometry such as metals, glass, ceramics and concrete/construction rubbles and it relates (. It mostly relates) to waste materials that are smaller than 3'×3'×3' or 3000 pounds, and is generally easier to manage (Randall et al., 2002 and Poshadri and Aparna, 2010). In macro-encapsulation, the encasing shell is often filled with solid/filler materials such as cement kiln dust, fly ash, furnace bottom ash, silt, clay, metals, glass and asphalt to reduce the void volume and ensure that the encapsulating matrix is durable (Poshadri and Aparna, 2010).

### 2.4.1 Current applications

Encapsulation technology is invaluable in the immobilisation of high-level radioactive waste (HLW), but is also widely adopted in the immobilisation of low level (LLW) – intermediate level (ILW) radioactive wastes (Swift et al., 2013 and Sharp et al., 2003). According to the UK LLW-ILW inventory (UK National Planning Policy Framework and relevant practice guidance, 2016), encapsulation technology can be applied to a wide range of waste products ranging from liquid concentrates to solid wastes. Liquid concentrates, slurry or sludge typically requires some form of conditioning (physical or chemical) before encapsulation. Sugaya et al., (2011), for example, encapsulated two liquid concentrates containing sodium nitrates and monosodium phosphate in cement based matrices. The two effluents were conditioned using chemical treatment and cement immobilisation prior to encapsulation. In addition, Johnson et al., (2015) pre-treated petroleum waste sludge with vegetable oil before solidifying with fine aggregates. The vegetable oil also acted as the bonding agent in this case. Other works on waste slurry/sludge include those conducted by Raji and Kanmani (2008), and Kumari and Kanmani (2011).

Solid waste forms such as metals, Organic wastes (paper, plastics and organic ion exchanging resins), glass, ceramics, graphite, concrete, healthcare and medical related

wastes, agricultural wastes and other solid waste products are also included in the inventory of waste suitable for immobilisation using encapsulation technology. These waste-forms depending on the size can be micro or macro- encapsulated as previously described. Al-Barakah et al., (2013), Bai et al (2011), Zhou et al., (2006), Ferreira et al., (2012b) and Kupwade-patil et al., (2014) in separate works successfully demonstrated the encapsulation of agricultural wastes, medical wastes, wastes containing reactive metals (such as aluminium) and incinerator fly ash. The challenges of immobilising solid waste materials using encapsulation technology mostly include, minimising the waste to a manageable volume and the development of a robust encapsulation matrix.

In general, for a waste to be deemed suitable for conditioning procedures that would result in the formation of an encapsulated waste-form there are a few basic principles it must satisfy, (Radioactive waste management, 2015)

- Radionuclides in the waste should be immobilised prior to encapsulation.
- Loose particulates materials need to be minimised during waste conditioning.
- Toxic materials are minimised during waste conditioning.
- Free liquids (paints) are excluded.
- Hazardous materials are excluded or made safe prior to encapsulation.
- Gases generated do not result in the pressurisation of the waste-forms
- The presence and volume of voids is minimised

A waste form will only be able to satisfy these requirements, if characteristics such as fluidity, dispersability and mobility of nuclides within the waste forms are eliminated. The measures taken however need to ensure that potentially mobile nuclides are physically or chemically bonded within a reliable encapsulating matrix, and take into consideration the effect of ageing on the performance of the encapsulated waste forms.

## 2.5 ENCAPSULATING MATRIX

Encapsulation technology ultimately involves incorporating or surrounding a waste form with a solid matrix (Rao et al., 2007). The encapsulation matrix such as cementitious systems, bitumen, organic polymers, phosphate ceramic and inorganic polymers must be of high structural integrity capable of preventing the migration of contaminants from the waste into the ecosystem (Glasser, 1997 and IAEA, 2003). In line with the objective of

the current work, cementitious systems utilising Portland cement and its composite incorporating SCMs are the preferred encapsulating matrices.

### 2.5.1 Cementitious systems

In waste management, cement-based processes are widely used for both immobilisation of low-intermediate level waste materials (Sharp et al., 2003, Milestone, 2006, and Swift 2013). According to Sharp et al., (2003) cement offer several attributes that make it suitable for encapsulation notably:

- They are moderately inexpensive and readily available
- They can be easily prepared and used in remote operations
- They can be produced in form of a fluid grout capable of penetrating complex waste shapes.
- They assist the immobilisation of radionuclides by acting as a diffusion barrier, providing sorption and reaction sites.
- They maintain a high pH, which decrease the solubility of radionuclides.
- They also provide radiation stability, controllable permeation and diffusion characteristics, and have known properties including, physical, mechanical and durability properties.

Most cement-based systems usually include substantial amounts of Portland cement (PC) in their formulation. It is also common to use composite cements incorporating Portland cement blended with ground granulated blast-furnace slag or pulverised fuel ash (Sharp et al., 2003). An advantage of using Portland cement composite cements incorporating these mineral additives over Portland cement alone, reported by Sharp et al., (2003) and Swift, (2013) is the reduced heat of evolution. The optimisation of cementing systems, particularly the deliberate increase of alite at the expense of belite to meet the ever-increasing demands for rapid strength development in construction, is a disadvantage in the encapsulation of some waste forms due to the highly exothermic hydration of alite (Sharp et al., 2003). Large monoliths based on PC alone will have a large heat of hydration, which may alter the mineralogy, microstructure and associated porosity of the encapsulating matrix. This can also cause evaporation of mix water and thermal expansion, resulting in internal stresses and potential formation of cracks, which may compromise the integrity of the resulting system (Swift, 2013 and Sharp et al., 2003).

Cementitious materials therefore have a wide range of composition but essentially consist of Portland cement (itself a combination of silicate, aluminate, ferrite and gypsum) used on its own or cement mixed with supplementary cementitious materials (SCMs) and/or granular materials (aggregates) for flowable consistency (Sharp et al., 2003). A comprehensive review of the choice and use of cementitious materials for waste immobilisation is given by the International Atomic Energy Agency (IAEA, 1993a).

#### *2.5.1.1 Immobilisation mechanism of cement*

Cementitious materials used in encapsulation technology can be cement paste (cement and water only), cement grout (cement and very fine aggregate), mortar or concrete (Ojovan, 2011). In the immobilisation process, cements can partake in both physical and chemical mechanisms. Physical immobilisation is mainly realized by surface sorption, while the chemical mechanism may include, surface and bulk sorption, ion exchange, oxy/hydroxyl precipitation, characteristic phase formation or a combination of all these actions (Kotatkova et al., 2017) and Ojovan, 2011). The prevailing mechanism depends on the concentration of the reactive nuclides, while the capacity of retention in dependent on the mechanism (Kotatkova et al., 2017). Sorption usually presents lower immobilisation capacity compared to ion exchange or phase transformation (Ojovan, 2011).

The immobilisation procedures are controlled mainly by the formation of hydration products (C-S-H gel, Portlandite, AFm and AFt). Sorption for example is controlled mostly by the formation of C-S-H gel. The nanostructure of C-S-H gel, composed of small platelets and fibres, offers various precipitation sites for sorption of cations and anions (Ochs et al., 2016, and Kotatkova et al., 2017). Portlandite ($Ca(OH)_2$) does not exhibit high sorption, nor offer ion exchange due to the high energy required to introduce ions into the layered structure (Kotatkova et al., 2017). AFm (aluminate and ferric-oxide mono-sulphates) phases meanwhile, offer possibilities for ion exchange but sorption sites, even though they have the same layered structures as Portlandite. The layers of AFm created by the presence of trivalent ions ($AL^{3+}$ and $Fe^{3+}$) also contains anions within the interlayer spaces (Cornelis et al., 2008, and Kotatkova, 2017). Ion exchange occur through the substitution of the anions and cations ($Al^{3+}$ and $Fe^{3+}$) from the AFm phases with anions and trivalent cations from the encapsulated waste forms respectively (Kotatkova et al., 2017). Ettringite/AFt (alumina and ferric oxide tri-sulphates) phases

have very open elongated columns of alternating calcium and aluminium polyhedral, which provides substantial capacity for the substitution of its main ionic components (calcium, aluminium, iron and sulphates) by reactive metals from the waste materials (Kotatkova et al., 2017).

In case of blended cement containing pozzolans and latent hydraulic materials, the hydration reactions consume Portlandite produce C-S-H and C-A-H, which offer higher surface area for sorption and higher capacity for ion exchange (Kotatkova et al., 2017).

#### *2.5.1.2 Cement-waste interactions*

Some potential compatibility issues with the use of cementitious materials for the encapsulation of certain types of waste materials as identified in previous works (Bennett et al., 2001, Albano et al., 2009, Kotatkova et al., 2017, Gu and Ozbakkaloglu, 2016, Manjunath, 2016, and CEA, 2009) are summarised below:

- The solubility of some waste may affect the hydration and setting of the cementitious material. Acidic waste for example, tends to neutralise the alkalinity of cements when it dissolves. This may inhibit the formation of hydration products, delay setting times and strength development of the hydrated cement (Bennett et al., 2001). To mitigate this effect, soluble waste materials may be pre-treated with either hydroxides such as NaOH or $Ca(OH)_2$ (Bennett et al., 2001).
- The water absorption capacity of the waste material may impact the workability of the encapsulated waste form. If the water absorption capacity of the waste materials is low, the unabsorbed water retained in the matrix, may decrease the workability of the matrix. Similarly, if the water absorption capacity of the waste particles is high, the retention of water in the matrix may negatively influence the durability of the encapsulated plastic concrete form (Albano et al., 2009 and Kotatkova et al., 2017). The problem associated with high water retention according to Kotatkova et al., (2017) can be mitigated with the use of superplasticiser.
- The constituent of some solid waste materials according to Bennett et al., (2001) may influence the properties of the freshly mixed cement and the degree of hydration matrix. Metals embedded in cementitious materials for example, may corrode due to the formation of oxidation products. The oxidation products

occupy greater specific volume relative to the metals they replaced. The increased volume may lead internal stress and cracking of the matrix (Bennett et al., 2001).

- The miscibility and fluidity of cement pastes may also be influenced by the particle size, shape and texture of aggregate wastes, and the presence of compounds such as magnesium (Gu and Ozbakkaloglu, 2016, Manjunath, 2016, and CEA, 2009). The problems of miscibility may result in insufficient homogeneity of the matrix (Manjunath, 2016). This can be resolved by formulating a high viscosity cement paste or by adding surface-active agents such as plasticisers (CEA, 2009).
- Cellulose waste undergoes microbial degradation, which lead to the formation of carbon dioxide ($CO_2$). Over a period, the $CO_2$ reacts with atmospheric air causing carbonation, which has the tendency to reduce the pH of the cured cementitious matrix. Aside the corrosion of reinforcements (if any), reducing the pH of the matrix may increase the solubility of the radionuclides which may prompt leaching and compromise the integrity of the encapsulated system (Swift, 2013).
- The adsorption of solutes on the cement particles may also slow the setting times of the cement paste by blocking the dissolution of calcium sulphate (Kotatkova et al., 2017). Phosphates and carbon particles usually present in evaporator concentrates of effluent treatment plants and coal combustion regimes respectively, are known to retard the setting of cement paste and adversely affect its mechanical and durability properties (Benard et al., 2005, Wu, 2002 and Naik et al., 2006). Reduction of water content, addition of superplasticiser or hydroxyapatite (phosphate mineral) to the binder are some of the proposed solutions for undesirable performance caused by the adsorption of solutes on cements (Benard et al., 2005, Wu, 2002 and Naik et al., 2006).
- Additives may also be required to neutralise the effect of high salinity or sulphate-rich waste materials on the encapsulating matrix.

## 2.6 PORTLAND CEMENT

Portland cement is made by high temperature calcination of limestone (or chalk) and clay (or shale) in a rotary kiln. The maximum kiln temperature ranges between 1400- 1600$^{o}$C (Neville, 2012). Portland cement is commonly considered to consist of four main phase assemblages, alite ($Ca_3SiO_5$), belite ($Ca_2SiO_4$), tricalcium aluminate ($Ca_3AL_2O_6$) and ferrite phase ($Ca_2Fe_2O_5$), but a small percentage of gypsum ($CaSO_4.2H_2O$) is added during the milling process to regulate the hydration of the aluminate phase (Neville, 2012). None of these four phases however has its ideal composition, due to impurities present in the raw materials and those introduced by the fuel used in the calcining process, (Sharp et al., 2003). The actual composition according to Sharp et al., (2003), includes:

- Alite with 3-4% of other (Mg, Al and Fe) oxides
- Belite with 4-6% of other oxides, including Al, Fe, K, Mg and $SO_3$
- aluminate with up to 20% other oxides including Fe, Si, Mg, Na, K and Ti
- ferrite – part of a series varying between $Ca_2Fe_2O_5$ and $Ca_2A_{11}.FeO.6O_5$. Fe(III) is replaced by approximately equal content of Mg and Si (sometime Ti) to maintain charge neutrality.

Portland cement is therefore a complex mixture of several phases that can vary appreciably in composition and reactivity. The reactions by virtue of which Portland composite cement become a bonding agent takes place in the presence of water. When water is added to the cement hydration reactions takes place. The reactions involve alite ($C_3S$) and belite ($C_2S$) reacting readily with water to form calcium silicate hydrate (C-S-H) gel and portlandite ($Ca(OH)_2$). C-S-H gel is largely responsible for strength development. Its formation is generally controlled by alite ($C_3S$) in the first 28 days following hydrolysis and, belite ($C_2S$), the less abundant of the calcium silicates at later ages (Neville, 2012).

The hydration of $C_3S$ and $C_2S$ according to Neville (2012) can be written as:

$2C_3S + 6H = C_3S_2H_3 + 3Ca(OH)_2$ ..... Equation 2.1

$2\ C_2S + 4H = C_3S_2H_3 + Ca(OH)_2$ ..... Equation 2.2

The aluminate ($C_3A$) phase is the most reactive of the four phases but contributes little to strength development (Bye, 1999). Soon after mixing, the $C_3A$ reacts with water to form

aluminate rich gel which in turn reacts with the sulphate (gypsum) in the solution to produce ettringite (rod like crystals) and heat energy (Equation 2.3). Furthermore, once the sulphates have been completely consumed by the hydration reaction of $C_3A$, the ettringite becomes unstable, reacts with the excess $C_3A$ in solution and convert to a different solid phase with fewer sulphates known as mono-sulfoaluminates (Equation 2.4). However, if a new source of sulphate ions becomes available in the pore solution of hydrated cement, the low energy state of the mono-sulfoaluminates promotes the formation of ettringite (Equation 2.5). The reactivity of ferrite is variable but its hydration products (Equation 2.6 and 2.7) are similar to those of the aluminate (Bye, 1999).

$C_3A + 3C\underline{S}H_2 + 26H = C_6AS_3H_{32} + \text{Heat (207 cal/g)}$..... .....Equation 2.3

$C_3A + C_6AS_3H_{32} + 4H = 3C_4ASH_{12}$..... ..... Equation 2.4

$C_4ASH_{12} + 2SH_2 + 16H = C_6AS_3H_{32}$..... .....Equation 2.5

$C_4AF + 3SH_2 + 21H = C_6(A.F)S_3H_{32} + (F.A)H_3$..... .....Equation 2.6

$C_4AF + C_6(A.F)S_3H_{32} + 7H = 3_4(A.F)SH_{12} + (F.A)H_3$.....Equation 2.7

The hydration of Portland cement is highly exothermic. It generates large heat of hydration, which may alter the mineralogy, microstructure and associated porosity of the encapsulating matrix. This can also cause the evaporation of mix water and thermal expansion, resulting in internal stresses and potential formation of cracks in the encapsulating matrix (Swift, 2013, swift et al., 2013 and Sharp et al., 2003). Additionally, Portland cement yields a porous system, which allows the penetration of water, and enhances the leaching of ions from the waste materials (Swift, 2013). It is also not compatible with certain waste forms, (particularly wastes containing aluminium), resins capable of ion exchange and some radioactive wastes (Sharp et al., 2003). According to Sharp et al., (2003), the major problems associated with the use of Portland cement matrix for encapsulation of waste can be mitigated by the use of blended cement (Portland cement blended with pozzolans or latent hydraulic materials) and/or the incorporation of filler materials. An advantage of using blended cements over inert fillers is that the added/replacement materials also contribute to the strength development of the cement and significantly improve the microstructure of the resulting encapsulated composite (Sharp et al., 2003).

## 2.7 BLENDED CEMENT

In the UK blended cements consisting predominantly of Portland cement and either PFA or GGBS many years have been the preferred option for the encapsulation of Low and intermediate radioactive wastes (Sharp et al., 2003 and, Collier et al., 2014). In recent years alkaline-activated metakaolin have also been employed by some researchers for the encapsulation of reactive metals (Rooses et al., 2013 and Kuenzel et al., 2014). Blended cement offers several advantages over Ordinary Portland cement, which according to Sharp et al., (2003) includes:

- Long period of workability
- Low heat of hydration.
- Reduced bleeding and segregation.
- Low early age temperature rise, reducing the risk of thermal cracking in large monoliths.
- Reduced carbonation due to lower CaO content
- Increased precipitation sites for sorption of cations and anions due to the formation of more hydration product (C-S-H)
- High pH pore water, which reduce the solubility and migration of many heavy metal oxides, carbonates and hydroxides.
- High resistance to chloride ingress, reducing the risk of corrosion in reinforcement.
- High resistance to sulfate and chemical attacks.
- Considerable sustainability benefits.

### 2.7.1 Pulverised fuel ash

Pulverised fly ash (PFA) is a fine powder derived from the combustion of coal at power stations. It is primarily composed of spherical non-crystalline silicate, aluminium and iron oxide with some microcrystalline materials (Prakash and Sridharan, 2009 and Wu, 2002). The spherical geometry of the glassy component acts as a lubricating agent and helps improve the rheological properties of fresh concrete (Neville, 2012 and Aikawa et al., 2015). Most PFAs also contain up to 10% unburned carbon, generally present in the form of cellular particles larger than 45μm (Wu, 2002 and Naik et al., 2006). Larger amounts of carbon in PFA are considered harmful, as the cellular particles of carbon tend

to increase the water demand for a given consistency and increase admixture requirement (Naik et al., 2006).

PFA produce more C-S-H gel through pozzolanic reaction with the $Ca(OH)_2$ released during hydration of alite and belite. This reaction is much slower than the hydration reaction and mostly controlled by the alkaline silicate glass components of the fly ash (Aikawa et al., 2015). The pozzolanic reaction consumes the Portlandite ($Ca(OH)_2$) and fill the pore structure already formed by the hydration products with its own hydrates (secondary C-S- H gel). The consumption of Portlandite also helps increase the effective diffusivity of PC clinker, which maintains the stability of the alkaline saturation ratio of the paste (Aikawa et al., 2015). The latter is particularly important for the continuous severance of the Si - O – Si bonds required for the pozzolanic reaction with the $Ca(OH)_2$ ions (Aikawa et al., 2015). The pozzolanic reaction can be simply written as;

$Ca(OH)_2 + H_4SiO_4 = CSH$ .....Equation 2.8

The characterisation of PFA used for encapsulating LLW and ILW hazardous wastes typically include the current supply, the quality of the fly ash such as particle size distribution and carbon content, and the potential for future supply (Rice et al. 2014). The quality of the PFA used in composite cement is of great importance as they influence the final performance of the product (Rice et al. 2014, Snelson et al., 2009). To reduce the inconsistency of parameters such as carbon and particle size in PFA quality, BS EN 450 (Specification for use of pulverised fuel ash with Portland cement) provided a standard for PFA industrial use. Additionally, over 10000 tonnes/annum of PFA are currently used for encapsulated processes due to its durability enhancing characteristics, as such continued supply of the material that meets the performance requirements is therefore crucial for future operations.

### 2.7.2 Ground granulated blast furnace slags (GGBS)

GGBS is a by-product of iron manufacturing process (Richardson and Taylor, 2017). The furnace operating at a temperature of 1500$^{o}$C is carefully fed with a mixture of iron ore, coke and limestone (Divsholi et al., 2014). The iron ore is reduced to iron, while the slag, which floats to the top of the iron, is tapped from the furnace as a molten liquid. If allowed to cool slowly it has no cementitious properties but if rapidly quenched with water (granulated) to temperatures below 800$^{o}$C, it remains in a glassy, non-crystalline state

and is a latent hydraulic binder (Divsholi et al., 2014, and Richardson and Taylor, 2017). GGBS is usually activated with PC or lime but can also be activated by alkali-silicate or alkali-hydroxide (Sharp et al., 2003 and Bai et al., 2011).

GGBS contains more Si, Al and Mg but lower amount of CaO relative to OPC. In addition, it also contains sulphur impurities inform of sulphide ions (Sharp et al., 2003). The glassy silica content of GGBS significantly influences its usage and dictates its hydraulic properties (Sharp et al., 2003). The initial strength of PC/GGBS composite are usually lower than that of equivalents PC cement, although ultimately the strength can exceed that of Portland cement used on its own (Sharp et al., 2003). The higher the replacement level of PC with GGBS the lower the early age strength. A replacement level of up to 50% is commonly utilised in construction works (Higgins, 2006 and Collier et al., 2014).

GGBS like PFA is a well-established supplementary binder used in many cement applications. Soils stabilised with PC-GGBS blends are widely used in brick/block, road, pavement and foundation construction (Oti et al., 2010 and Pathak et al., 2014). In blended cement used as encapsulation pastes, high replacement levels of Portland cement with GGBS (up to 90%) are current employed (Collier et al., 2014). These high percentages are deployed to help reduce the heat of evolution and avoid problems associated with thermal cracking and loss of durability, while ensuring the pastes is sufficiently fluid for mixing or pouring around the waste form (Sharp et al., 2003 and collier et al., 2014). The use of high replacement ratios however meant that the reaction of the SCMs is limited due to the smaller amount of Portland cement present (relative to the SCMs). As a result, a considerable amount of alkaline pore solution remain which may cause the corrosion of reactive metals and compromise the integrity of the matrix (Collier et al., 2014).

## 2.8 ALTERNATIVE CEMENTS

Special cements such as calcium aluminate cement (CAC), calcium sulfoaluminate cement (CSA), Phosphate modified calcium aluminate cement, and magnesia-based cement, which provide a different hydration chemistry to Portland cement have been formulated by researchers for the encapsulation of waste materials not compatible with PC or any of its composites (including Zhou et al., 2006, Swift, 2013, Swift et al., 2003

and Collier et al., 2014). These cementitious systems generally combine lower heat of hydration, economy of cost, ready availability and low carbon footprint with rapid strength gain and fast setting (Swift et al., 2013). Their hydration also provides an internal pore solution where the pH is considerably lower than that of Portland cement, hence a reduction of expansive corrosion of metals and hydrogen generation (Sharp et al, 2003, Milestone, 2006, Zhou et al., 2006 and Bai et al., 2011).

Calcium aluminate cement is predominantly hydraulic calcium aluminates derived from the fusion of limestone and bauxite or other calcium rich materials (Richardson and Taylor, 2017). It mainly contains monocalcium aluminate ($CaO.Al_2O_4$ or $CaAl_2O_4$ or CA), but other calcium aluminates and less reactive phases from the impurities in the raw material may also be present (Richardson and Taylor, 2017). The strength development of calcium aluminate cement is primarily due to the hydration of CA, although other compounds may also participate in the long-term strength development (Bensted, 2002). The hydration reaction of CA is temperature dependent, yielding $CaO.Al_2O_3.\ 10H_2O$ at 20$^oC$, $2CaO.Al_2O_3.\ 8H_2O$ at 30$^oC$ and $3CaO.Al_2O_3.\ 6H_2O$ and $Al(OH)_3$ gel at 55$^oC$ (Matusinovic, 2005). At ambient temperature, $CaO.Al_2O_3.10H_2O$ and $2CaO.Al_2O_3.8H_2O$ are metastable and decompose to form $3CaO.Al_2O_3.\ 6H_2O$ and $Al(OH)_3$ gel. (Matusinovic, 2005). The loss of water during the decomposition process consequently increases porosity, which may be accompanied by a loss in strength (Matusinovic, 2005).

Calcium aluminate cement and its derivatives incorporating sulfates or phosphates have been used to efficiently encapsulate hazardous wastes. Navrro-Blasco et al., (2015) at the 14$^{th}$ international congress on the chemistry of cement demonstrated the effectiveness of calcium aluminate cement as an encapsulating matrix. They encapsulated sludge from the automotive industry using calcium aluminate cement. Similarly, calcium sulfoaluminates cement (CSA) was used for the encapsulation of waste materials containing the reactive metal by Zhou et al., (2006). The researchers observed that the high ettringite content of CSA significantly lowered the pH of the matrix, while the corrosion of aluminium in the matrix was observed to be limited.

### 2.8.1 Alkaline-activate cements

The use of alkaline - activated cementitious materials as has also been shown as a viable alternative Portland cement and its composites. Alkaline - activated cementitious

materials does not utilise PC or any of its clinkers (Thokchom e al., 2009). It instead contain very finely divided supplementary cementitious materials (GGBS, PFA and metakaolin) and a highly alkaline liquid which may include caustic alkalis (MOH), alkali silicates ($M_2O$. $nSIO_2$), aluminates ($M_2O.nAL_2O_3$), aluminate silicates ($M_2O.AL_2O_3.(2-6)SiO_2$), non-silicate weak acid ($M_2CO_3$, $M_2SO_3$, $M_3PO_3$) and non-silicate acid salt ($M_2SO_4$) among others (Bai et al., 2011). The liquid and powder combine to produce a mixture with low – viscosity fluid that can be reacted with the waste materials to form a solid matrix (Thokchom e al., 2009). The advantages of geopolymers over Portland cement or its composites utilising SCMs according to Bai et al., (2011) includes:

- High early age and long-term strength and rapid hardening: alkaline - activated cementitious materials can attain between 60 – 150 $N/mm^2$ compressive strength without the use of additives, shorter setting times and enhanced workability.
- Reduced water demand: The surface – active effect of alkaline components reduces the water demand of geopolymer matrix. The standard consistency of alkaline activated slags approximately 0.17 – 0.22 compared with up to 0.31 for Portland cement.
- Low heat of hydration: The energy released during the hydration of alkaline - activated cementitious materials is significantly lower than those of PC and PC composites. This is because the hydration products formed by alkaline activated systems have lower Ca/Si ratio than PC.
- Good resistance to chemical attack: The actions of $MgSO_4$, NaCl, $Na_2SO_4$, HCl and $H_2SO_4$ are higher on PC matrices than on alkaline - activated cementitious materials.
- Good resistance of freeze- thaw: due the lower water demand and high electrolyte concentration in the pore solution, alkaline - activated cementitious materials can withstand up to 1500 successive freeze-thaw cycles
- Refractory performance: Geopolymer matrices retain their structural performance at temperature up to $700^0C$, which is remarkably higher than that of PC matrix (up to $500^oC$).

Bai et al., (2011) utilised GGBS/slags activated with near neutral salts as encapsulating matrix for radioactive waste containing reactive aluminium. There results indicated that,

apart from C-S-H gel formed, a significant amount of ettringite was also formed by the matrix by the alkaline reaction (Bai et al., 2011). The C-S-H gel enhanced surface retention/sorptivity, while the high-water content of ettringite significantly lowered the pH of the encapsulated matrix and limit the corrosion of the aluminium in the matrix. In a separate work, Kupwade-patil et al., (2014) encapsulated solid waste incinerator ash in geopolymer concrete developed with alkaline-activated pulverised fly ash. There result indicates the concrete mixtures were workable, demonstrated compressive strength up to 41N/mm$^2$ and there was a reduction in the leaching of heavy metals. Other works such as those by Rooses et al., (2013) and Kuenzel et al., (2014) have also demonstrated that alkaline activated metakaolin systems may be effectively used for encapsulating waste. Their separate works employed metakaolin-based geopolymers in the encapsulation of aluminium and Magnesium-zirconium alloys respectively.

## 2.9 FILLER MATERIALS

Several cementitious and non-cementitious materials such as polyester and epoxy resins, synthetic elastomers, polysiloxane, sol-gels (e.g., polycerams), PFA, silt, clay, low melting point metals, glass, asphalt, Sulfur polymer stabilization/solidification (SPSS), chemically bonded phosphate ceramic (CBPC), and polyethylene can be used to mitigate the compatibility issues observed with Portland cement. Milestone, (2006) gave a comprehensive review of some of these materials and their application in waste immobilisation. Filler materials are typically used in macro encapsulation where the encasing shell is often filled with solid/filler materials to reduce the void volume and ensure that the encapsulating matrix is durable (Poshadri and Aparna, 2010). In micro-encapsulation, filler materials mostly micro-fillers PFA, silt or clay are often added to the encapsulating matrix, where they contribute strength development by improving the microstructure of the encapsulated waste form.

### 2.9.1 Furnace bottom ash (FBA)

The only filler material considered in the current work is Furnace bottom ash (FBA). FBA is derived from the same combustion process that produce Pulverised fuel ash (PFA). It is the coarse fraction of the ash produced in coal-fired power stations when pulverised fuel (coal) is fed into the boilers and burnt at high temperatures and pressures. FBA has similar chemical properties to PFA. Silica ($SiO_2$) with minor amount of mullite ($Al_6Si_2O_{13}$) dominates the mineralogy of both FBA (Kou and Poon, 2009). Minor

percentages of haematite ($Fe_2O_3$), magnetite ($Fe_3O_4$), Spinel ($MgAlO_4$) and fairchildite ($K_2(CO_3)_2$) were also identified under XRD by Glasser (2004). Unlike PFA, the material is still classified as an industrial waste material and often disposed in landfill sites.

Over the last decade, the continuous drive to achieve concrete sustainability has led to many researches works on the use of FBA as natural aggregate replacement in concrete. Research studies, such as those conducted by Jamshidi et al., (2014), Kou et al., (2009), Kou and Poon (2009) and Mounanga et al., (2008), indicated that, the use of FBA not only benefited sustainable development from waste reduction perspective, but also improved the physical and mechanical performance of concrete form works. Kou et al., (2009), showed that at a w/c of 0.53, concrete mixtures replacing natural fine aggregate (sand) with 100% FBA, attained similar compressive strength to the control concrete with natural fine aggregate at 90 days. When the water/cement ratios of both concrete types were reduced from 0.53 to 0.49 (in the same work), the FBA mix yielded higher mechanical performance for the same curing age relative to the control concrete. In addition, the slow release of moisture from the saturated pores of FBA particles were shown by Jamshidi et al., (2014) improve permeation properties and reduced the shrinkage of FBA - concrete due to the internal curing effect of FBA.

## 2.10 ALTERNATIVE MATERIALS USED FOR ENCAPSULATION

Alternative materials (other than cementitious systems) suitable for the immobilisation of low – intermediate level hazardous wastes include:

### 2.10.1 Bitumen

Bitumen is a complex mixture of heavy aliphatic and aromatic hydrocarbons, generally obtained from crude oil after the separation of the light fractions (IAEA, 1993b). The components of commercially available bitumen are mainly asphaltenes and maltenes, They are mostly hydrocarbons with minor fractions of sulphur, nitrogen and oxygen (Bennett et al., 2001). The rationale for using bitumen for immobilisation/encapsulation of waste according to Bennett et al., (2001) is to provide a solid waste form of low permeability that can be more easily stored and disposed compared to unconditioned wastes. The main advantages of bitumen include (Bennett et al., 2001):

- Bitumen is relatively cheap and readily available

- Bituminised waste-forms are virtually impermeable to water and are able to flow in response to applied stress so that they can be self-healing.
- Bituminised waste-forms have very low solubility and are compatible with most environmental conditions.
- Bituminised waste-forms have a high waste-loading capacity for liquid wastes and sludge.

### 2.10.2 Organic Polymers

Thermosetting resins and thermoplastic polymers (comprising of a range of different materials) are the two classes of organic polymers used as encapsulating matrices for mixed or radioactive waste (Bennett et al., 2001). Unlike cementitious or bituminous systems, organic polymers involve physically surrounding the active nuclides with the matrix rather than incorporating them in the immobilisation matrix. The rationale for using organic polymers for immobilisation/encapsulation of waste according to Bennett et al., (2001) is to provide a solid unreactive waste-form of low permeability that can be easily transported, stored and disposed than unconditioned waste. The main advantages of organic polymers include (Bennett et al., 2001):

- Depending on their formulation and the conditioning of waste prior to encapsulation, they can used to immobilise a wide variety of waste materials from liquid to solids including those containing high levels of salts
- Waste-forms encapsulated with organic polymer have higher waste loading capacity and compressive strength relative to equivalents encapsulated with cementitious materials. The US DOE for example suggested that polyester resins can consistently and reliably maintain a 50% by weight loading of dry mixed waste (Bennett et al., 2001).
- Waste-forms encapsulated with organic polymers have low density, which makes them easy to handle and transport.
- Organic polymers can be cheaper than cementitious matrices for large volumes of waste because of their higher waste loading capacity.

### 2.10.3 High temperature incineration and melting

A range of organic and inorganic wastes including, plastics, drums, concrete and metal fragments) can be incinerated and melted with high temperature plasma torches,

operating at temperatures ranging between 6000 and 20 000$^{o}$C (Bennett et al., 2001). The product, a relatively homogenous glassy slag provides a solid that is durable and resistance to leaching. High-temperature incineration and melting is a relatively new technique and there are only a few operating examples worldwide (mostly in Europe and the America). One of such is the Ellesmere Port rotary kiln incinerator operated by Veolia UK, which is the largest in the UK and the most advanced of such technology in Europe. High temperature incineration and melting facilities however are very expensive to install and operate due to their high-energy consumption.

The main advantages of high temperature incineration and melting include (Bennett et al., 2001):

- Virtually all solid waste types can be treated.
- High temperature incineration and melting averts the need to sort or remove non-combustible items as would be done with conventional lower temperature incinerators.
- High-temperature incineration and melting significantly reduce the waste volume.
- The solidified melts are compatible with standard waste packages.

### 2.10.4 Phosphate ceramics

Phosphate ceramics are dense rigid solids with crystalline structure composed mainly of magnesium potassium hydrates similar to apatite (Bennett et al., 2001). Apatite is a group of naturally occurring phosphate minerals including hydroxylapatite, fluroapatite and chlorapatite with high concentrations of $HO^{-}$, $F^{-}$ and $Cl^{-}$ in their crystalline structures. Apatite according to Arun, (2004) remains stable over several millions of years and has the capacity to incorporate compatible elements such as rare earth metals, caesium (Cs), strontium (Sr) and Uranium (U). Phosphate ceramics are formed by an exothermic reaction between phosphate anions and the metal cations (Bennett et al., 2001).

$MgO + KH_2PO_4 + 5H_2O = MgKPO_{4.6}.H_2O$ ……. Equation 2.9

During the reaction, radionuclides also react with $KH_2PO_4$ to form highly insoluble phosphates, while the bulk ceramic encapsulates the radionuclide phosphates in a dense solid matrix (Bennett et al., 2001). The first chemically bonded phosphate ceramics, zinc phosphate dental cements were developed over a century ago (Arun, 2004). The rationale

for using phosphate ceramic as an encapsulating matrix is that it provides a relatively cheap, solid, stable, insoluble material of high structural integrity (Bennett et al., 2001). The main advantages of this encapsulating matrix according to Bennett et al., (2001) include:

- Phosphate ceramic encapsulated waste-forms are cheap and easy to produce.
- Phosphate ceramic encapsulated waste-forms are insoluble and exhibit high resistance to radiation and chemical corrosion in alkaline environment.
- The matrix have high capacities for incorporating radionuclides and can be used to stabilise hazardous waste-forms such as Mecury (Hg), lead (Pb), Chromium (Cr), Nickel (Ni) and Technetium (Tc).

### 2.10.5 Inorganic polymer/synthetic Zeolites

Inorganic polymers are polymers composed of repeating monomer units connected by covalent bonds but with a skeletal structure lacking carbon atoms in the backbone (Naka, 2015). They are composed of polymeric silicon-oxygen-aluminium frameworks with alternating silicon and aluminium tetrahedra joined by oxygen sharing atoms (Bennett et al., 2001). The aluminium tetrahedron is balance by the presence of cations such as $K^+$ and $Na^+$ (Bennett et al., 2001). The amorphous polymer has a similar composition with Zeolite, another alumina silicate mineral. The amorphous polymer however lacks the micro porous structure of Zeolite (Bennett et al., 2001). The most commonly available inorganic polymer and synthetic Zeolites are (Naka, 2015 and Bennett et al., 2001);

1. Pyrament cement: low cost geopolymer cement with very high durability used for airport runways and taxiways. It is typically made up of up to 80% Portland cement and 20% polymeric materials activated by potassium carbonate and retarded with citric acid.
2. EKOR: Eurotech's proprietary radiation resistant product for nuclear waste encapsulation.
3. Geopolymere and the associated optimised two-step technology patented by Geopolytec

The rationale for using inorganic polymer or synthetic Zeolites includes the provision of a solid material for the stabilisation of mixed large-volume, loose wastes such as

contaminated rubble (Bennett et al., 2001). The advantages of this encapsulating matrix according to Bennett et al., (2001) include:

- Inorganic polymer and synthetic Zeolites are suitable for long-term containment of surface disposal facilities and remediation of contaminated sites.
- Inorganic polymer and synthetic Zeolites are effective in penetrating fine-grained materials such as dust, slurries, ashes and salts. They encapsulated waste forms typically possess relatively low-density and are easily transported.
- Inorganic polymer and synthetic Zeolites bond effectively with construction materials such as concrete, steel and glass in wet environment or underwater
- Inorganic polymer and synthetic Zeolites provide high strength, low shrinkage, freeze-thaw, and sulphate and corrosion resistance.

### 2.10.6 Glass

Glass is a rigid non-crystalline amorphous material, often transparent with relatively low porosity and widespread practical application. Many different types of glass composed of silicon, boron, aluminium and alkali or alkaline earth metals have been investigated as candidate materials for the encapsulation of high-level radioactive waste (Bennett et al., 2001, Ojovan, 2011, Donald, 2010 among others). Sodium borosilicate glasses according Ojovan, (2011), Donald, (2010) and Bennett et al, (2001) is the glass of choice used in encapsulation technology due to its relatively high durability, processing ability, cost and slightly lower melting temperature (1200$^{o}$C), compared to aluminosilicate glasses (≥1400$^{o}$C). Lead-iron-phosphate glasses can be prepared at lower temperatures and can be used to immobilise higher concentration of actinides that the borosilicate glasses, but they are thermally unstable at temperatures and their durability decreased at temperatures above 100$^{o}$C (Bennett et al, 2001). Donald, (2010) provided a detailed review of the processing characteristics, durability, corrosion behaviour, mechanical and thermal performance as well as radiation stability of sodium borosilicate system. Likewise, Ojovan and Batyukhnova, (2007) gave a review glasses for Nuclear waste immobilisation.

The rationale for using glass as an encapsulating matrix according to Bennett et al, (2001), is to provide a solid, stable and durable material that can be easily stored. Glass can also incorporate high concentration of hazardous wastes. It is tolerant to variation in

composition, exhibits chemical durability depending on its composition and environmental conditions to which it is exposed. In addition, glass is radiation stable and can accommodate changes during radioactive decay of high-level radioactive waste component (Ojovan, 2011, Donald, 2010 and Bennett et al, 2001).

### 2.10.7 Glass ceramics

Glass ceramics were first developed at the Corning glass works, a company founded in 1851 by Amory Houghton. They are prepared by subjecting conventional vitrified glass waste-forms to an addition phase of heating. This additional heating causes some of the glass to crystalline into ceramic. Hence, they share properties of both the parent glass materials and polycrystalline materials (Bennett et al., 2001, Ojovan and Batyukhnova 2007, and Donald, 2010). A review of a number of different glass-ceramic families proposed for the encapsulation of high level radioactive wastes are discussed by Donald, (2010).

The rationale for using glass-ceramic as an encapsulating matrix include (Bennett et al., 2001 and Donald, 2010)

- The provision of a solid, stable and durable material that can be easily stored, transported and disposed off.
- Glass-ceramic has better thermal, mechanical and durability properties than borosilicate glass and other glass forms used in waste immobilisation.
- Glass ceramics can incorporate higher waste loadings than borosilicate glass.

### 2.10.8 SYNROC

SYNROC is a particular kind of synthetic rock, invented in 1978 by Prof. Ted Ringwood (deceased) of the Australian national university. It has since been diversified but generally speaking, it is a combination of technologies, which provide the most effective, and durable means of immobilising a wide range of intermediate – high level hazardous waste (Radioactive waste management appendix, 2015). It is a ceramic made from several naturally occurring minerals, which together are able to incorporate nearly all the elements present in ILW – HLW into their crystal structure (Bennett et al., 2001). The main minerals of SYNROC are hollandite ($BaAl_2Ti_2O_7$), perovskite ($CaTiO_3$), zirconolite

($CaZrTiO_7$) and rutile ($TiO_2$). Actinides such as plutonium (Pu) are incorporated in the zirconolite phase, while sodium and barium are incorporated in perovskite. Hollandite principally immobilises caesium (Cs), potassium (K), rubidium (Rb) and barium (Radioactive waste management appendix, 2015, and Bennett et al., 2001). Each SYNROC crystal can hold up to 30% weight of HLW oxide in the crystalline phases (Radioactive waste management appendix, 2015, and Bennett et al., 2001).

The rationale for the immobilisation of radioactive waste in SYNROC is to provide a solid, stable and durable material that can be used to immobilise HLW, has better properties than borosilicate and can be easily stored and disposed of (Bennett et al., 2001)

The main advantages of SYNROC are that (Bennett et al., 2001):

- A wide range of radionuclide can be incorporated into the crystalline lattices of the SYNROC crystals.
- SYNROC is more stable, thus likely to be more durable than amorphous solids such as glass
- Depending on the nature of the waste material, it is possible to incorporate high unit weight of radionuclide in SYNROC than borosilicate glass
- SYNROC is relatively more resistance to acid attack than borosilicate

## 2.11 CHARACTERISATION OF THE ENCAPSULATED PLASTIC WASTE FORMS

The performance data for encapsulated waste-forms according to Randall et al., (2002) typically includes physical properties (density, porosity and permeability), mechanical property (compressive strength) and chemical properties (leachability). For macro-encapsulated waste, the most important performance evaluation criteria are the compressive strength, the waste form density, the presence of void spaces, and the barrier thickness (Randall et al., 2002). For micro-encapsulation, in addition to the evaluation criteria mentioned above, the toxicity characteristic of the leachate also plays an important role in determining whether the encapsulated waste form if suitable for use in other application or can be accepted by a landfill (Randall et al., 2002). Macro-encapsulated materials are typically subjected to leachate tests, because the inert encapsulating matrices substantially reduce the potential exposure of the waste material to leaching media (Randall, 2002).

In general, the physical, mechanical, biological and chemical properties of the waste form should make adequate contribution to the overall performance of the encapsulated waster forms and have no significant damaging effect on the performance of the encapsulating matrix (radioactive waste management appendix, 2015). In order to ensure good performance, the waste materials and the encapsulated matrix should contribute sufficient mechanical strength to encapsulated waste-forms and neither of them rely unduly on the other (NDA, 2009). The encapsulated waste form must retain sufficient mechanical strength for transportation and handling without compromising its integrity (Randall, 2002).

As previously, mentioned, cementitious systems utilising Portland cement and its composite incorporating SCMs are the preferred encapsulating matrix. The applicability of the encapsulated plastic waste form (henceforth referred to as the encapsulated plastic concrete) were determined by comparing their physical, mechanical and durability performance to those of conventional concrete developed with natural aggregates (river sand and 10 mm limestone aggregates). Concrete is available in various forms and it is often categorised based on its weight as normal weight ($\geq$ 2400 kg/m$^3$) or lightweight concrete (800-2000kg/m$^3$), based on its strength as normal strength (8.0 – 50/mm$^2$), high strength (50-200N/mm$^2$) and ultra-high strength concrete (up to 500N/mm$^2$), based on the presence of fibre as plain and fibre reinforced concrete, and based on performance as conventional and high-performance concrete.

The compressive strength of concrete is an important performance evaluation criterion for the grading of concrete, quality control and acceptance of concrete, scheduling of construction operations or protection afforded to the structure. It is usually regarded as the ability of concrete to resist load that tend to fracture it and often directly related to the porosity and durability of the concrete (Metha and Monteiro, 2006, Neville, 2012, Barbhuiya and Kumala, 2017, and Shi and Stegemann, 2000). The compressive strength conventional concrete usually varies between 8N/mm$^2$- $\geq$100N/mm$^2$, while the compressive strength of lightweight concrete varies between 8N/mm$^2$-88N/mm$^2$ (BS EN 206:2013+A1:2016). High strength and ultra-high strength concrete according to ACI 318 are used for engineering projects where the concrete must resist high compression load. They are commonly used in the erection of high-rise structures, columns, shear walls, foundation and in bridge applications. Normal strength concrete meanwhile, are

used for less critical applications such as sidewalks, pavements and slabs, low- mid-rise buildings and other structural applications requiring less critical load bearing.

### 2.11.1 Factors affecting the compressive strength of concrete

Some of the many factors, which may affect the strength development in concrete as, discussed below:

#### *2.11.1.1 Porosity*

Porosity (volumetric proportion of voids) of concrete has been extensively used for the prediction of the properties of concrete (Neville, 2012 and Naik et al., 2006). According to Neville, (2012) there's no doubt that the porosity of concrete defined as the total volume of the overall pores larger than the gel pores, expressed as a percentage of the overall volume of the hydrated cement paste, is the primary factor influencing the strength of the cement paste. As such, directly linear relationships can be said to exist between porosity and compressive strength of concrete.

During mixing, air and/or mix water can be entrapped or entrained within the matrix. The water typically evaporates leaving behind capillary void and gel pore. The gel pore relates to the void spaces between the cement paste and fine aggregates. They are usually microscopic with low interconnectivity and relatively impermeable to water (Naik et al., 2006). The capillary voids however, relates to the voids created by water particles movement and the space between the coarse aggregates and the mortar (Neville, 2012 and Naik et al., 2006). Capillary voids and entrained/entrapped air voids are mostly responsible for the porosity of concrete (Neville, 2012). The higher the size and volume of the voids, the lower the compressive strength of concrete (Neville, 2012).

The porosity of concrete is mostly influenced by the water/cement ratio (Neville, 2012). The increase in water content above the water absorption capacity of the aggregate materials and the water required for the complete hydration of the cement powder usually increase the porosity of concrete (Lamond and Pielert, 2006 and Neville, 2012). Water content below the standard consistency may also negatively affect the workability of the concrete (Lamond and Pielert, 2006). Other factors such as the quantity and physical properties of the aggregates (fine and coarse) including, particle size distribution, shape and texture, water absorption percentage, bulk density and specific gravity may also contribute to the size and volume of voids in concrete (Neville, 2012). Angular, flaky and

elongated particles increase segregation, and thus increase porosity in comparison to smooth, round or equidimensional particles. Similarly, aggregates with low water absorption capacity typically increase the excess water in the fresh mix, and as such increases segregation and porosity (Neville, 2012, Lamond and Pielert, 2006 and, Mindess et al., 2003).

The use of high substitution percentages of waste plastic in polymer concrete as either fine or coarse aggregate replacements have also been shown to increase porosity (Ismail and Al-Hashmi, 2008, Gu and Ozbakkaloglu, 2016, Manjunath 2016 and Albano et al., 2009). In a critical review on the use of plastic aggregates in carried out by Gu and Ozbakkaloglu (2016), the researchers reported an increase in porosity by almost 30% when the percentage of polypropylene fibre in concrete was increased by 0.15%. Additionally, concrete utilising 100% PUR foam reported increases in porosity of 60 - 159% (Gu and Ozbakkaloglu, 2016). This was mostly attributed to the poor miscibility of plastic (due to particle size distribution, shape and texture, water absorption percentage and specific bulk density of plastic aggregates) resulting in high air content and porosity (Gu and Ozbakkaloglu, 2016).

#### *2.11.1.2 Soundness of aggregates*

In concrete technology, soundness of aggregates typically refers to the ability of the aggregates to resist change in volume due to change in physical conditions (Neville, 2012). These physical conditions include freezing and thaw, temperature change, drying and wetting (in normal or salt-water condition). Aggregates are said to be unsound when volume changes are induced by these conditions. Weak rocks including cherts (hard, dark, opaque rock composed of silica) and flints (hard, sedimentary cryptocrystalline form of the mineral quartz), particularly the lightweight ones with fine – textured pore structure, limestone with laminae of expansive stone, shale and other particles containing clay minerals inherently exhibits concrete with weak compressive strength (Neville, 2012)

#### *2.10.1.3 Aggregate – paste bonding*

The integrity of the bond between the hydrated cement paste and the aggregate plays a crucial role in the overall compressive strength of concrete. If there is no bond, the space between the coarse aggregates and the mortar (that is, the interfacial zone) will be

occupied by a capillary void, which as previously mentioned induce porous and decrease compressive strength. The microstructure at the interfacial zone according to Neville (2012) includes a 10µm duplex film (0.5µm crystalline $Ca(OH)_2$ behind a 0.5µm C-S-H) and 50µm larger crystal of $Ca(OH)_2$. In concrete containing natural aggregates such as (10 mm) limestone aggregate, the large crystals of calcium hydroxide may react with the calcium carbonate from the limestone aggregates to form calcium carbonate – calcium hydroxide complexes which improves the microstructure at the interface zone (Neville, 2012 and, Metha and Monteiro, 2006). Metha and Monteiro (2006) also suggested a reaction might also occur between any calcium aluminate ($C_3A$) and calcium carbonates to form carboaluminate hydrates. These reactions reduce the porosity at the interface zones and increase the resistance of concrete to cracks and fractures along these zones.

#### *2.10.1.4 Cement – related parameters*

The particle size, spatial distribution and composition of Portland cement phases have a large influence on the hydration, microstructure development and ultimate compressive strength of cement-based materials. Alite ($C_3S$) for example, is the most reactive cement phase and it is largely responsible for the early age development of concrete. Hence, higher proportion of alite in cement, should give better early age strength. similarly works with high belite content have shown lower early age strength but higher later age (91 days) strength compared to the strength development of ordinary Portland cement (Chen et al., 2017 and Guo et al., 2016). Additionally, gypsum typically added during milling retards the hydration of the aluminate phase. If there is insufficient sulphate, a flash set may occur, and conversely if the sulphate is too much false setting can occur (Neville, 2012). A balance therefore is required between the ability of the main clinker phases, particularly the aluminate phase to react with the sulphates in the early stages of hydration and the ability of the cement to supply the sulphate. For particular cement, the optimum sulphate/gypsum content is commonly set at about 6% (BS EN 206:2013+A1:2016).

In addition to the compositional parameters considered above, physical parameters particularly cement surface area and particle size distribution play important roles in the strength development of concrete (Neville, 2012). According to Neville (2012), the total surface area of the cement, that represents the materials available for hydration. Thus, the rate of hydration depends on the fineness of the cement particles, the finer the cement, the quicker the rate of hydration (Neville, 2012). Finer cement particles will react much

more quickly than a large particle because, as cement reacts, a layer of hydration product forms around the individual particles, separating the unreacted core of the particle from the surrounding water. The thicker the layer grows the slower the rate of hydration and early age strength development of the cement (Richardson and Taylor, 2017).

From durability perspective, coarser cement often offers better durability relative to finer cement (Metha and Monteiro 2006). Very fine cement according to Neville, (2012), and Metha and Monteiro (2006) typically contain high aluminate content, which will require a high sulphate content to retard (during hydration). The higher sulphate content of finely ground cement may result in increased AFt and AFm phases in the hydrated concrete. If a new source of sulphate ions becomes available to the hydrated cement, the low energy state of the AFm phase may promote the formation of ettringite which may lead to the expansion of the concrete (Neville, 2012 and, Sharp et al., 2003).

A better parameter for describing the fineness of the cement is the specific surface area. The specific surface area is however a notoriously difficult parameter to pin down because most materials have features at many different length scale (Richardson and Taylor, 2017). As a result relying simply on surface area measurements can be misleading. Gypsum for example, can grind preferentially producing cement with a high surface area, which may also contain coarse cement phases resulting in slower hydration (Neville, 2012).

### 2.11.2 Concrete durability

Some of the relevant factors influencing the durability of concrete are discussed below:

#### *2.11.2.1 Freeze-thaw deterioration*

In freeze-thaw conditions, the moisture held in the cavities in the concrete freezes and exerts (ice) capillary pressure, which may cause the concrete to expand. Continuous cycles of freezing and thawing produces capillary and pore pressure, which may exceed the tensile strength of the concrete and may eventually result in scaling, chipping or the eventual cracking of the concrete/mortar (Oti et al., 2010, and Wang et al., 2014). Deterioration of concrete due to frost action is fundamentally a function of the porosity of the concrete. The ability of concrete to absorb and retain water in the capillary voids is a major cause of concrete deterioration (Neville, 2012). Concrete with low permeability are able to better resist the penetration of water and as a result performs better in freeze

– thaw condition. The permeability of concrete is directly related to the water/cement ratio, the lower the water/cement ratio the lower the permeability (Metha and Monteiro, 2006).

Sodium chloride and other deicing salts used for snow and ice removals can aggravate freeze-thaw deterioration (Skripkiunas et al., 2013). Deicers may also cause a build-up of osmotic and hydraulic pressure in excess of the hydraulic pressure produced when water held in concrete freezes. In addition, Skripkiunas et al., (2013), also noted that sodium chloride and other salts in concrete might absorb water, increasing the potential freeze-thaw deterioration. Furthermore, some aggregates and cementitious materials particularly those with high carbon content (high carbon PFA, for example) may absorb and retain water which may result in expansion and possibly disintegration of concrete if preent in high enough quantity (Wu, 2002 and Naik et al., 2006).

The resistance of concrete to freeze-and thaw in wet conditions is significantly improved by the use of air entraining agents (for example, Eucon Air Mix 250, Eucon AEA-92 and Eucon AEA-92s). Entrained voids prevent deterioration to concrete during freeze-thaw cycles by acting as empty chambers in the paste for the freezing or migrating water, thus reliving the capillary and pore pressures.

#### *2.11.2.2 Chemical attacks*

Concrete generally performs well when exposed to various atmospheric conditions including water, soil and many other chemicals exposures. However, ingress of certain acids, alkalis and dissolved salts can deteriorate concrete.

##### *2.11.2.2.1 Acids*

In general concrete is susceptible to acid attack because the components of cement pastes break down during contact with acids. While some weaker acids can be tolerated if exposed occasionally, Portland cement is known to be unable to hold up against any solution with a pH 3 or lower (Shi and Stegemann, 2000). The decomposition of concrete due to acid attack mostly depends on the porosity of the concrete, the concentration of the acid, the solubility of the calcium salts ($CaX_2$) and on the permeability of the concrete (Barbhuiya and Kumala, 2017). Acids such as nitric acid (from artificial manures), hydrochloric acid, acetic acid and sulphuric acid (from combustion fuel and sewage) are very aggressive. They react with calcium hydroxide produced by the hydration of alite

($C_3S$) and belite ($C_2S$) along with the C-S-H gel. In most cases, the chemical reaction (shown in equation 2.9) forms weak and water soluble calcium compounds, which are then leached away by the aqueous solutions, resulting in the disintegration of the concrete (Barbhuiya and Kumala, 2017 and, ACI 201, 1991). Other acids such as phosphoric acid and humic acid (from soil, humus peat and coal) are less harmful as their calcium salt, due to low solubility inhibits the attack by blocking the voids within the concrete (Shi and Stegemann, 2000).

$2HX + Ca(OH)_2 = CaX_2 + 2H_2O$ .....Equation 2.10

Expansion due to sulphuric acid attack is very damaging to concrete as it combines acid attack and sulphate attack. Sulphuric acid attack in concrete sewer pipes according to Barbhuiya and Kumala, (2017) is a global problem. Sulphuric acid reacts with calcium hydroxide in concrete to produce gypsum. The creation of gypsum in concrete causes volume increase. The gypsum also readily reacts with calcium aluminate to form ettringite. Ettringite occur seven times more space than the initial compounds. Ettringite exerts internal pressure, which may lead to the formation of cracks and eventual result in the deterioration of the concrete.

*2.11.2.2.2 Sulfate attack*

Sulphate attack is a chemical breakdown mechanism, where sulphate ions from an external source attack the components of hydrated cement paste. The decomposition of concrete due to sulphate attack mostly depends on the porosity and permeability of the concrete, and the concentration of sulphates in the environment (Zhang and Zong, 2014). When concrete is in contact with soil or sulphate containing water such as seawater, groundwater, swamp water or sewage water, the often massive formation of gypsum and ettringite may result in the loss of cohesion and strength by the concrete (Monteiro, 2006). Such sulphates include gypsum (calcium sulphate, $CaSO_4$), epsomite (magnesium sulphate, $MgSO_4$), and sodium sulphate ($Na_2SO_4$).

According to Neville (2012), sulphates of sodium ($Na_2SO_4$) attack calcium aluminate hydrates and calcium hydroxide to form ettringite and gypsum, while calcium sulphate ($CaSO_4$) attack calcium aluminate hydrates to form ettringite. Similarly, magnesium ($MgSO_4$), another sulphate found in soil or water, attack in a similar way similar to sodium sulphate and forms ettringite, gypsum and brucite (magnesium hydroxide).

Brucite forms primarily on the concrete surface, consumes calcium hydroxide, lower the pH of the pore solution and then decompose the calcium silicate hydrate, resulting in the loss of cohesion and strength.

Environment conditions have a great influence on sulphate attack. The attack is greater in concrete exposed to wet/dry cycles. It is a particular problem in marine and arid environment. In moist sulphate rich environments, Thaumasite ($Ca_3SiOH \cdot 12H_2O$) resulting from the reaction of calcium silicate hydrates with sulphate, calcium carbonate and water may for at very low temperatures (0-10$^oC$). In concrete undergoing excessive thaumasite formation, cement paste may be completely replaced by the sulphate, resulting in crack formation and scaling (Nielsen et al., 2014). When water evaporates, sulphate can accumulate on the concrete, increasing the concentration of sulphates at the surface and their potential for causing deterioration. In addition, salt solutions can also rise to the top via capillary action, when the concrete is dry, salt crystallisation occurs, sometimes generating enough capillary pressure to cause cracking and scaling (Monteiro, 2006).

Resistance to sulphate attack in concrete can be achieved by using low water/cement ratio, low calcium aluminate cement and sulphate resistant cements such as cements containing pozzolans (all pozzolans except class C fly ash) and ground granulated blast furnace slag (Nielsen et al., 2014).

*2.11.2.2.3 Salts and Alkalis*

Aluminium, magnesium, aluminium and iron chloride and nitrates causes deterioration to concrete (Yilmaz et al., 2002, Wong et al., 2013 and Verma et al., 2013). The ammonium salts are the most destructive. In alkaline environment, they release ammonium gas and hydrogen ions, which dissolve calcium hydroxide in concrete resulting in leaching and eventual weakening of the concrete (Wong et al., 2013).

***2.11.2.3 Alkaline aggregate reactivity***

Aggregate containing certain constituents can react with alkali hydroxides in concrete (sodium hydroxide, calcium hydroxide and potassium hydroxide). The reactivity is potentially harmful in concrete because it produces significant expansion and cracking over a long a period. This alkali aggregate reactivity (AAR) has two main forms namely, alkaline-silica reaction (ASR) and alkali-carbonate (ACR. Due to the prominence of

aggregates, containing reactive silica in concrete, alkaline-silica reaction (ASR) is more common (Helene, 2017 and Sanchez, 2017).

*2.11.2.3.1 Alkaline-silica reaction (ASR)*

Aggregates containing certain forms of silica will react with alkaline hydroxide in the presence of water to form gels that swells in the interconnected capillary pores in concrete (Sanchez, 2017). The gels have great affinity for moisture. When they absorb water, they swell and induce expansive pressure capable of causing cracks in hydrated cement paste and aggregates (Helene, 2017 and Sanchez, 2017). The reaction according to Sanchez, (2017) can be explained as a two-step process:

1. Alkali + reactive silica $\rightarrow$ alkali–silica gel. .....Equation 2.11

2. Alkali-silica gel + moisture $\rightarrow$ expansion .....Equation 2.12

The presence of gel does not necessarily imply destructive ASR. According to Helene, (2017), the expansion of some gel are limited, while slow swelling gel do not create problems. If the gel is high swelling however, it may cause pressure exceeding the tensile strength of concrete, which may result in cracking, or in advance cases closed joints and spalling concrete surfaces (Helene, 2017). Cracking is mostly consistent with areas of frequent moisture supply and low temperature, such as areas near waterline in piers, ground behind retaining wall among others (Helene, 2017 and Sanchez, 2017).

As with the other durability factors examined so far, decomposition of concrete due to ASR also depend predominantly on the porosity, reactive forms of silica present in the aggregates and frequent supply of moisture (Sanchez, 2017). ASR can be controlled by using certain mineral admixtures, such as silica fumes, fly ash and GGBS (Sanchez, 2017). Class F fly ash has been shown to reduce reactivity expansion by up to 70% (McCarthy et al., 2006). In addition, lithium compounds (chloride, carbonate, fluoride, nitrate and sulfate) have also been shown to effectively reduce ASR (Thomas and Folliard, 2007 and, Wang, 2014).

*2.11.2.3.1 alkali-carbonate reaction*

Alkali-carbonate reactions are commonly associated with the delomitization (that is the breakdown of dolomite) of reactive rocks with crystals of dolomite scattered in and

surrounded by a fine-grained matrix of calcite and clay (Stukovnik et al., 2015 and Katayama, 2010). The delomitization reaction can be written:

Dolomite ($CaMg(CO_3)_2$) + alkaline hydroxide = Brucite ($Mg(OH)_2$) + calcium carbonate + alkali carbonate ($M_2CO_3$).....Equation 2.13

This reaction and subsequent crystallization of brucite are the cause of considerable expansion in concrete (Stukovnik et al., 2015 and Katayama, 2010). Deterioration due to ACR are quite similar to deterioration as a result of ASR, ACR are however very rare as the aggregate susceptible to this reaction are less common and usually unsuitable for use in concrete for other reasons (Stukovnik et al., 2015).

#### *2.11.2.4 Abrasion/Erosion*

The wear and tear of concrete due to rubbing and friction is commonly referred to as abrasion damage. The two most common damaging forms abrasion occur on vehicular traffic surfaces and in hydraulic structures. Abrasion damages due to wind-bourne particles, although this is slightly rare (Liu et al., 2006). Damages due to abrasion occur when the outer paste wear out exposing the fine and coarse aggregates. Abrasion and impact to the already exposed aggregates may cause the degradation to the aggregate/paste bonding resulting in the formation of cracks.

#### *2.11.2.5 Elevated temperature*

Concrete exhibits good thermal performance at elevated temperatures of up to 300$^{o}$C. It is only beyond these temperatures that significant physiochemical changes leading to the degradation (loss in strength and stiffness) of the hydrate structure occur (Bailey and Khoury, 2011). The response of concrete (including reinforced concrete) to elevated temperature is influenced by the characteristics of the constituent materials of the concrete and the reinforcing steel (Bailey and Khoury, 2011 and Kodur, 2014). These characteristics according to Kudur (2014) include thermal, mechanical, deformation properties and material specific characteristics such as spalling in concrete. Thermal properties determine the extent of heat transfer to the structural members, while the mechanical properties determine the extent of strength loss and stiffness deterioration of the concrete (Kodur, 2014). In addition to the mechanical properties, the deformation property determines the extent of deformation and strains in the structural member (Kodur, 2014). All these properties vary as a function of temperature and depend on the

composition and characteristics of concrete as well as those of the reinforcing steel (Dwaikat and Kodur, 2010).

*2.11.2.5.1 Thermal properties*

Thermal properties including thermal conductivity, specific heat, thermal diffusivity and mass loss, are properties that influence the temperature rise and heat transfer within concrete. Thermal conductivity relates to the ability of a material to conduct heat. It is measured in joules per second per square meter area using the steady state or transient test methods. Thermal conductivity is mainly influenced by the degree of saturation of the concrete and is mostly unaffected by low temperatures (Neville, 2012 and Kodur, 2014). It however increases with high temperature up to about 50-60$^{o}$C, but due to the loss of moisture it decreases sharply at around 120$^{o}$C (Neville, 2012). When concrete is fully saturated, the conductivity ranges generally between 1.4-3.6 J/m$^{2}$s$^{o}$C/m (Neville, 2012).

Specific heat capacity is the amount of heat energy required to change the temperature of a unit mass by one degree Celsius, and can be expressed using the formula shown in Equation 2.14 (Kodur, 2014)

$E = m \times c \times \Delta T$ ……Equation 2.14

Where E is the heat energy, m is the mass of the material, c is the specific heat capacity and ΔT is the change in temperature

According to Kodur, (2014) specific heat is also mainly influenced by increase in moisture content, although the mineralogical characteristics of the aggregate may also play an important role. The variation in specific heat with temperature is commonly evaluated using differential scanning calorimetry (DSC) for temperatures up to 600$^{o}$C and differential thermal analyser for temperatures above 600$^{o}$C.

Thermal diffusivity of a material represents the rate at which temperature changes within a mass can take place. It is defined as the ratio of thermal conductivity to the volumetric specific heat of the materials and represented by equation 2.14.

$\alpha = \frac{K}{cp}$..... Equation 2.15

Where α is the diffusivity, k is the conductivity, c is the specific heat and p is the density.

From the equation, it can be seen that conductivity and diffusivity are directly proportional. Hence as with conductivity, diffusivity is influenced by the moisture content, which is dependent on the mix water, degree of hydration of cement and the exposure of the cement to drying condition (Neville, 2012).

*2.11.2.5.2 Deformation properties*

Thermal expansion, creep and transient strain are the three deformation properties that determine the performance of concrete at elevated temperature (Kodur, 2014). It is defined as the change in unit length of a material, when the temperature of concrete is raised by one degree. Thermal expansion of a material is generally dependent on temperature and usually evaluated through the dilatometric curve, which according to Kodur, (2014) is a record of the fractional change of a linear dimension of a solid at steadily increasing or decreasing temperature. It is considered to be positive (expansion) when the material elongates and negative (shrinkage) when the material shortens. The percentage change in length of a concrete specimen per degree temperature rise is known as the coefficient of thermal expansion of the concrete. Like most engineering materials, concrete has a positive coefficient of thermal expansion, but its value depends on the mix composition and its hygral state at the time of the temperature change (Neville, 2012). Thermal expansion is an important property used for predicting the thermal stresses of concrete under elevated condition, and is generally influenced by the cement type, water content, aggregate type, temperature and age. A comprehensive evaluation of the influence of each of this parameter on the expansion of concrete is given by Neville, (2012).

The time dependent plastic deformation of concrete at elevated temperature is commonly referred to as creep or creep strain. There is currently no satisfactory explanation for creep at elevated temperatures, but based on findings by Kodur, (2014), creep is mainly influenced by moisture, temperature, stress level and their duration. Deformation due to creep at normal stresses and ambient temperature are limited and considered insignificant (Kodur, 2014). Transient strain occurs during the first time of heating concrete and is influenced by factors such as temperature, strength, loading, moisture content and mix proportion (Kodur, 2014). It is apparently caused by the thermal incompatibility between the aggregate and cement paste, and as with creep strain deformation due to transient strain is significant only at high temperature (Kodur, 2014).

*2.11.2.5.3 Mechanical properties*

The mechanical properties that determine the performance of concrete at elevated temperature are compressive and tensile strength, modulus of elasticity, and stress-strain response of concrete constituent materials. Concrete exposed to temperature up to about 80$^{o}$C commonly do not experience any physical and chemical changes. However, once the temperature exceeds 100$^{o}$C, significant changes in concrete matrix occur, starting with the evaporation of bound and free water, inducing micro-cracking and slight reduction in compressive strength (Kudur, 2014). Between 100 – 200$^{o}$C, concrete experience further loss of water from the hydration product (C-S-H gel and calcium hydroxide), resulting in the further stiffening of the C-S-H gel (Cheng et al., 2004). Above 300$^{o}$C, the loss of bound water becomes more prominent, resulting in further loss of strength and the cracking due to the loss of adhesion and cohesion between the aggregate and hydrated cement paste (Newman & Choo, 2003, Kodur and Franssen, 2010, and Bailey and Khoury, 2011).

One of the chemical changes which occurs as the temperature rises above 400$^{o}$C, is the decomposition of calcium hydroxide leaving behind lime in the dehydrated concrete (Neville, 2012). Gel-like hydration products are also decomposed at this temperature according to Cheng et al., (2004). The recrystallization of lime due to the ingress of water can be disruptive and may lead to spalling and other post fire damages (Neville, 2012). This disruptive process is followed by considerable reduction in compressive strength and noticeable expansion between temperature range 500 – 780$^{O}$C due to the continued dehydroxylation of calcium hydroxide and dissociation of calcium carbonate into CaO and $CO^2$, in addition to recrystallisation of non-binding phases from the hydrated cement under re-combustion (Bailey and Khoury, 2011 and Cheng et al., 2004). The compressive strength reduction recorded by concrete at this temperature is usually between 50 - 70% of the original concrete strength (Neville, 2012). In addition, temperatures in the range 550-600$^{o}$C are generally recognised as the upper limit for the retention of any useful strength of concrete (Newman and Choo, 2003). Above this temperature range concrete is considered structurally useless. The complete degradation and the eventually melting of concrete occur at temperatures in excess of 1100$^{o}$C. An illustration of the physiochemical changes of concrete obtained from Bailey and Khoury, (2011) is presented in Table 2.2.

Table 2.2: The physiochemical changes of concrete (Bailey and Khoury, 2011)

| *Temperature* | *Change in prohormone of concrete structure* |
|---|---|
| 20-100ºC | Evaporation of physically bounded free water |
| 120-150 ºC | Decomposition of the calcium silicate hydrates |
| 150 ºC | Calcium- hydrate-silicate attains its first highest peak |
| 300 ºC | Appearance of micro-cracking and increased porosity |
| 400-600 ºC | Dehydration of calcium hydroxide and formation of calcium oxide |
| 535 ºC | Expansion due to inversion of α to β quartz |
| ≥ 700ºC | De-carbonation of $CaCO_3$ to $CaO + CO_2$ |
| ≥ 800 ºC | Complete evaporation of chemically bound water |
| 1200 ºC | Start of melting of concrete |
| 1400 ºC | Melting of concrete |

Generally, the reaction of concrete materials to heating is complex and various researchers have given different temperatures within the ranges specified above. According to Masaki and Maki, (2002) and Neville, (2012), the physical degradation of concrete strongly depends on the concrete matrix. In a work carried out by Oti et al., (2015) on the heating and cooling scenario of blended cement subjected to temperature of 180, 480 and 780ºC, control concrete mix composed of Portland cement, limestone aggregates and sea dredged sand were observed to demonstrate lower strength losses after the heat treatment relative to concrete mix with 20% GGBS, PFA, rice husk ash and waste glass powder. All the concrete types investigated recorded compressive strength losses for temperatures investigated. The concrete utilising the latent hydraulic material (GGBS) as Portland cement similarly demonstrated lower strength losses relative to the concrete utilising the pozzolans (PFA, RHA and WGP) for all temperatures investigated. The concrete with 20% RHA replacement of PC demonstrated the most compressive strength losses.

*2.11.2.5.4 Spalling*

In addition to thermal, mechanical and deformation properties, another property that has significantly impact the performance of concrete is spalling. Spalling is defined as the breaking up of the surface layer of concrete exposed to high and rapidly rising temperatures such as those encountered in fire incidents (Kodur and Phan, 2007). It is caused by the rehydration of lime released during the decomposition of calcium hydroxide and can be accompanied by violent explosions (Neville, 2012). The consequence of spalling according to Kodur, (2014) are limited as long as the extent of the damage is small. Extensive spalling may lead to loss in stability and integrity of the concrete. Further spalling exposes deeper layers of the concrete to extensive heating, thereby increasing heat transmission to the core of the concrete (Kodur, 2014).

# CHAPTER 3 – MATERIALS AND MIX DESIGN

*This Chapter describes the details of the materials used in the current work including material sources, reasons for using each material and some material characterisation. For better presentation, the materials have been classified into three groups namely; binding materials, aggregates and micro-filler. The binding materials describe the Portland cement (CEM IIB) and Pozament ultra high strength grout (PG), while the aggregates sub-divided into fine and coarse aggregates include the recycled wastes (furnace bottom ash and (0-10 mm) plastic waste) and concrete fillers (river sand and (10 mm) limestone aggregates). Pulverised fuel ash is the only micro-filler considered for use in this work.*

## 3.1 BINDING MATERIALS

### 3.1.1 Portland cement

A commercially available Portland cement (Blue Circle CEM II/B-V 32.5 R) conforming to BS EN 197 – 1 – 2000, supplied by Lafarge cement U.K Limited was used in the current work. The cement was sourced from Jewson UK Limited, a supplier of building materials and equipment based in the local area (Caerphilly, South Wales UK). The same supplier was maintained for the CEM IIB Portland cement throughout the research programme. The material is a Portland composite cement blend consisting of finely ground Portland cement clinker and low calcium fly ash (pulverised fuel ash). The standardised percentage composition of CEM II/B-V 32.5 R, by mass contains up to a maximum of 7% PFA (Elbusaefi, 2012). The siliceous Portland cement was preferred to Ordinary Portland cement due to the associated low environmental impact, higher fluidity, suppression of sulfate attack and alkali/silica reactions, and lower exothermal heat of hydration. It has similar elemental composition as OPC but slightly different oxide composition. In comparison to OPC, the percentages of CaO and MgO in the CEM IIB-V Portland cement are slightly lower in the composite cement, while the percentages of $SiO_2$, $Fe_2O_3$ and $Al_2O_3$ are slightly higher. The oxide composition of the cement obtained using XRD analysis by Elbusaefi, (2012) is presented in Table 3.1.

Table 3.1: Chemical composition of the CEM IIB Portland cement used in the current work

| *Component oxide* | CaO | $SiO_2$ | $A1_2O_3$ | $Fe_2O_3$ | MgO | $K_2O$ | $Na_2O$ |
|---|---|---|---|---|---|---|---|
| *% composition* | 45.00 | 29.91 | 11.18 | 4.13 | 2.43 | 1.45 | 0.38 |

PC clinker is widely recognised as a phase assemblage of alite ($C_3S$), belite ($C_2S$), aluminate ($C_3A$) and ferrite ($C_3AF$) with negligible proportion of minor compounds (lime, alkali and sulphates). The clinker was produced by calcining a mixture of finely ground limestone and clay or shale in a rotary kiln of up to about 1450$^oC$. After cooling, the sinter and partially fused clinker is ground with up to 5% gypsum into the fine powder, which is then blended with the fly ash electrostatically or mechanically precipitated from the exhaust gases of coal-fired stations to produce the Portland composite cement. Thermogravimetric and Derivative Thermogravimetric analyses were carried out on the binding materials used in the current research. The phase characterisation of the unhydrated CEM IIB Portland cement is shown in Figure 3.1. The identified phases, peak temperatures and the accompanying weight losses are shown in Table 3.2

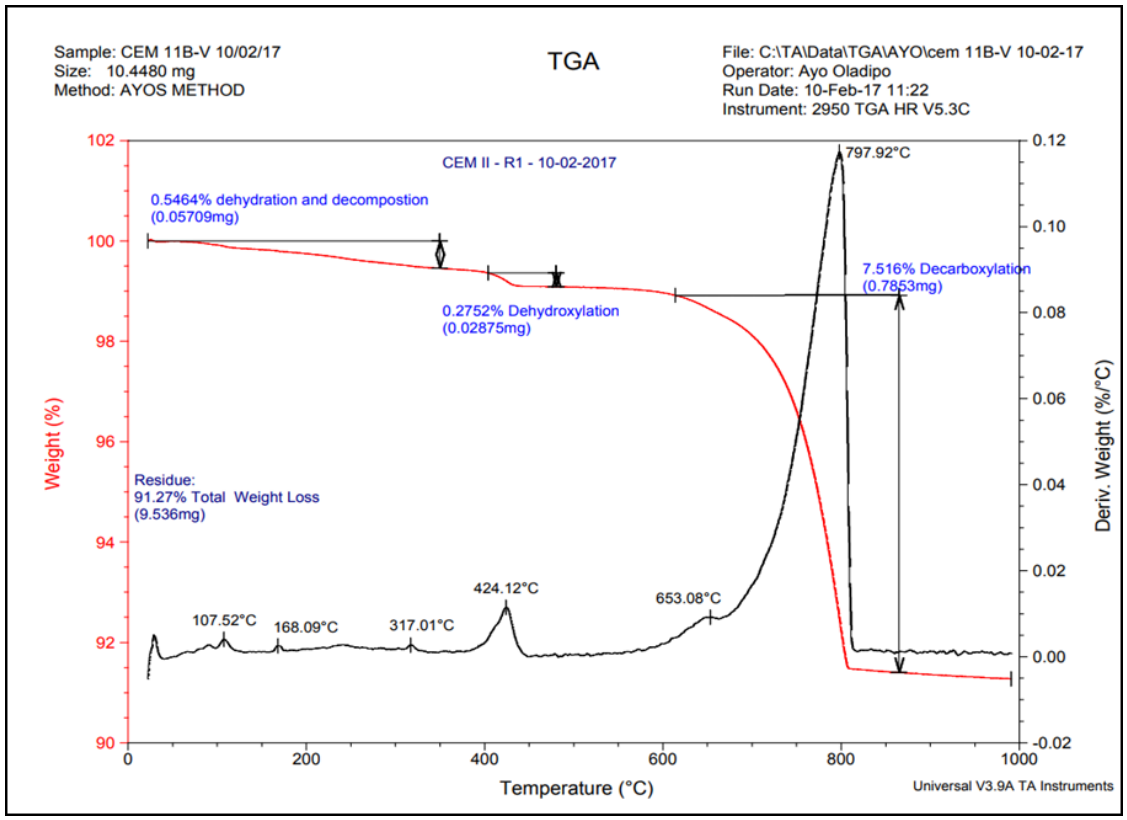


Figure 3.1: TG/DTG curves of unhydrated CEM IIB Portland cement

Table 3.2: Phase characterisation of the unhydrated CEM IIB-binder

| *Binding materials* | *Phase* | *Temperature range (°C)* | *Peak temperature (°C)* | *Weight loss (%)* | *Phase changes* |
|---|---|---|---|---|---|
| CEM II B Portland cement | Phase 1 | 25 - 350 | 107.52 | 0.55 | Loss of surface absorbed water and dehydration of ettringite ($C_6AS_3H_{32}$) |
| | | | 168.09 | | Dehydration of gypsum ($CaSO_4.2H_2O$ and $CaSO_4.0.5H_2O$) |
| | | | 317.01 | | Dehydration of calcium aluminate hydrates |
| | Phase 2 | 350 -450 | 424.12 | 0.28 | Dehydroxylation of $Ca(OH)_2$ |
| | Phase 3 | 600 – 850 | 653.08<br>797.92 | 7.52 | Decarboxylation of $CaCO_3$, |

The phase identification and characterisation of the unhydrated CEM II B Portland cement carried out using TG/DTG analysis indicated that when subjected to temperature increments up to 1000$^{o}$C, the unhydrated CEM IIB Portland cement undergo three major phase changes accompanied by weight loss. The first phase change observed between temperature range 25 – 350$^{o}$C correspond with the loss of surface absorbed water and the dehydration of the cement components including ettringite, gypsum and aluminate hydrates. During this phase, the CEM IIB cement, recorded endothermic peaks between temperature ranges, 100-110$^{o}$C, 160-170$^{o}$C and 310-320$^{o}$C. The total weight loss by the cement during this phase was approximately 0.55%.

The second and third phases include temperature peaks observed between temperatures ranging from 350 - 450 $^{o}$C and 600 – 850 $^{o}$C respectively. These phases coincide with the dehydroxylation of calcium hydroxide and the decarboxylation of the calcium carbonates respectively. During the second and third phases, a temperature peak corresponding to the dehydroxylation phase was observed between 420-430$^{o}$C, while temperatures peaks coinciding with the decarboxylation phase were observed at temperatures ranging from 650-660$^{o}$C and 790-780$^{o}$C. The presence of hydrated products (calcium hydrates and calcium hydroxide) suggests there has been slight hydration of the cement by the atmospheric absorbed water. The total weight loss by the Portland cement during the temperature treatment was 8.38%, most of which was observed during the third phase.

### 3.1.2 Pozament ultra high strength grout

The second binding material considered in the current work was Pozament ultra high strength grout (PG). The associated collaborating company, Speedbuild (UK) Limited, recommended the material. Their recommendation was based on observed fluidity, ease of placement, rapid setting time and high strength of the grout stemming from previous usage. Pozament grout is not cement *per se*, rather it is a high – performance repair mortar containing finely inter-ground cementitious materials blended with very fine crystalline aggregates ($CaCO_3$) and water reducers. It conforms to the standards specified in BS EN 1504- 3:2005, for the products and systems for the protection and repair of concrete. According to the manufacturer (Tarmac, UK Limited), Pozament (PG) comprises of low alkali and high specific surface area Portland cement fines inter-ground with other cementitious materials (PFA and silica fumes), high purity crystalline aggregates and some other compatible admixtures. It has no chloride, contains less than 2% $Na_2O$ and up to 4% sulphates ($SO_3$). The grout does not bleed or segregate at water/binder ratio up to 0.22. The material was designed for specialised applications such as filling ducts in post tensioned or pre-stressed structures, parapet rails, stanchion plates and machine-based plates.

The thermogravimetric analysis carried out on the grout (Table 3.2) indicated that, like the CEM 11 B Portland cement, the unhydrated PG powder showed three major component decomposition phases. A fourth phase relating to the fusion of the grout components at high temperature was also observed. Similar to the CEM IIB cement, loss of surface absorbed water and dehydration of ettringite ($C_6AS_3H_{32}$) was observed at a temperature peak of 70-100$^oC$. The dehydration of ettringite occurs slightly earlier than observed with the CEM II B cement. According to Ma et al., (2014), the addition gypsum to high aluminium containing mineral such as bauxite ($Al_2O_3.6H_2O$) and alunite ($KAl_3(SO_4)_2(OH)_6$) may cause the rapid generation of ettringite and improve the setting time of grout mortars. Furthermore, it is also typical of very fine cement to include high fractions of gypsum for proper retardation of the aluminate ($C_3A$) phase. According to Neville (2015), the finer the cement, the higher the aluminate phase available for early hydration. In essence, the Pozament grout based on the TG analysis appears to contain higher proportion of aluminate phase relative to the PC.

The decomposition of calcium aluminate hydrates were observed at 320-330$^{o}$C. The second and third phases observed between temperatures ranging from 350-450$^{o}$C and 600 – 850$^{o}$C respectively, similarly corresponds with the dehydroxylation of calcium hydroxide ($Ca(OH)_2$) and decarbonation of calcium carbonates ($CaCO_3$). An exothermic peak was observed at 690-700$^{o}$C. The fusion/exothermic reaction could also imply carbonation of the PG components. This may be related to the carbonation of the metastable aragonite or vaterite to form the more stable calcite.

The phase characterisation of the unhydrated PG-binder is shown in Figure 3.2. The identified phases, peak temperatures and the accompanying weight losses are shown in Table 3.3

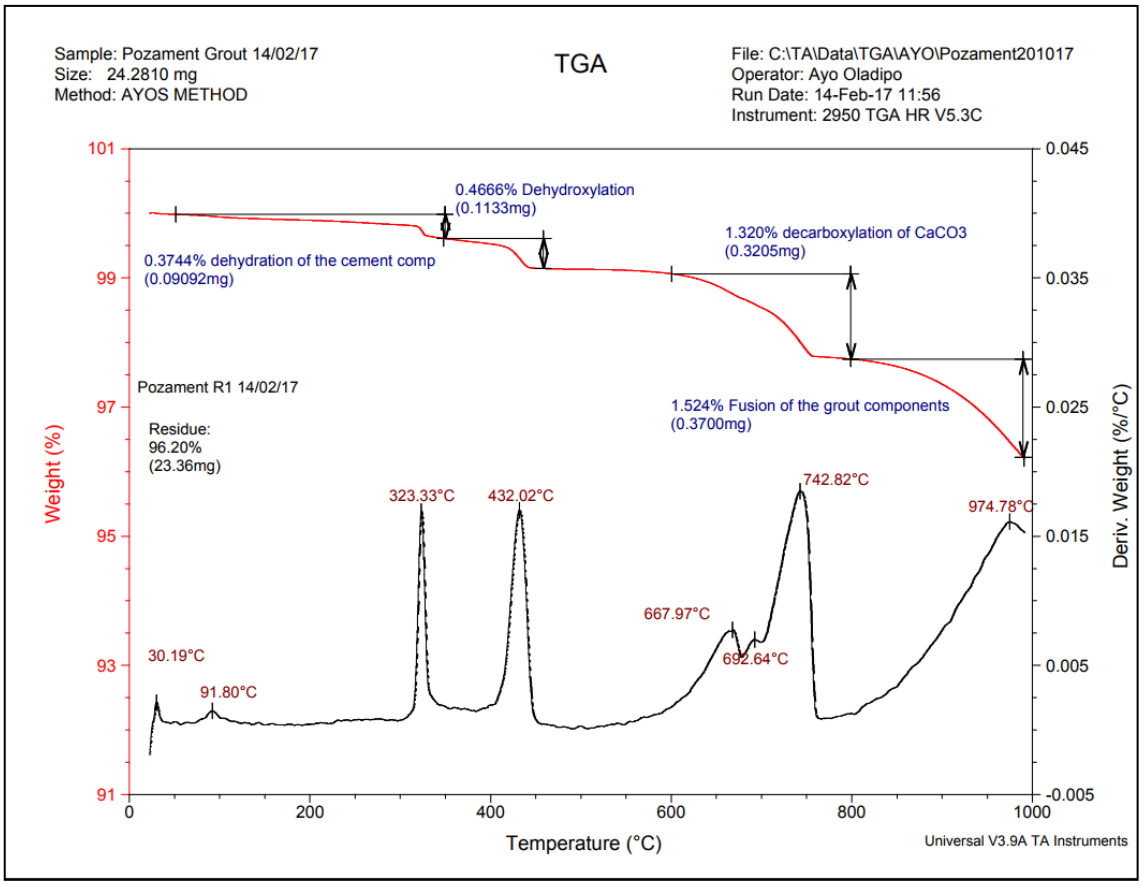


Figure 3.2: TG/DTG curves of unhydrated Pozament ultra high strength grout.

Table 3.3: Phase characterisation of the unhydrated PG-binder

| *Binding materials* | *Phase* | *Temperature range ($^oC$)* | *Peak temperature ($^oC$)* | *Weight loss (%)* | *Phase changes* |
|---|---|---|---|---|---|
| Pozament Grout | Phase 1 | 25- 350 | 91.80 | 0.37 | Loss of surface absorbed water and dehydration of ettringite ($C_6AS_3H_{32}$) |
| | | | 323.33 | | Dehydration of calcium aluminate hydrates |
| | Phase 2 | 350 -450 | 432.02 | 0.44 | Dehydroxylation of $Ca(OH)_2$ |
| | Phase 3 | 600 - 850 | 667.7<br>742.82 | 1.32 | Decarboxylation of $CaCO_3$, possibly vaterite or aragonite<br>Decarboxylation of $CaCO_3$, possibly calcite |
| | Phase4 | ≥ 850 | 974.78 | 1.52 | Fusion of the Pozament components at high temperature |

In comparison to CEM IIB, PG is capable of attaining much higher compressive and tensile strength at early and latter ages. Based on the information acquired from the technical data sheet of the grout and Portland cement manufacturer, the minimum compressive strength of PG (at standard consistency) after 24 hours is greater than that of Portland cement after 7 days. The rapid strength development of the grout may be as a result of the very high fineness, the use of compatible admixtures (including cementitious materials), or the reduced water demand of the cementing grout. The inclusion of PFA/silica fumes, water reducers (plasticisers) and fine crystalline aggregate during milling all contribute to the low water demand of the grout. The crystalline aggregates also gave the material a gritty feel.

Some strength data and chemical properties of the grout and CEM IIB Portland cement obtained from the manufacturers technical data sheets and some physical properties obtained in the laboratory during the current research are shown in Table 3.4

Table 3.4: Some physico- mechanical and chemical properties of the Portland cement and Pozament ultra high strength grout

| *Properties* | *Portland cement* | *Pozament grout* |
|---|---|---|
| Colour | Grey | Off white |
| Bulk density ($kg/m^3$) | 1107 | 1225 |
| Sulfate $SO_3$ (%) | 2.3 -2.8 | 4 |
| Chloride Cl (%) | < 0.03 | 0.0 |
| $Na_2O$ (%) | < 1 | < 2 |
| Water content (%) | 0.59 | 1.3 |
| Compressive strength ($N/mm^2$)<br>1 day<br>7 days<br>28 days<br>90 days | <br>18 -28<br>30 – 40<br>47 – 52.5 | <br>35<br>65<br>80<br>92 |
| Flexural Strength ($N/mm^2$)<br>7 days<br>28 days | <br>3.7<br>4.4 | <br>9<br>11 |

## 3.2 AGGREGATES

### 3.2.1 Coarse aggregate

#### *3.2.1.1 Limestone aggregate*

In the current research, the physical, mechanical and durability properties of the encapsulated plastic systems were compared to those of conventional concrete developed with natural aggregates. In designing the concrete mix, crushed 10 mm limestone aggregate was selected due to its comparable maximum particle size with the plastic pellets. The aggregate was sourced in bulk from Jewson UK Limited in Caerphilly, South Wales, UK. The same batch was used throughout the current research. The aggregate was quarried from sedimentary rocks composed mainly of fossils and carbonate minerals including calcite and aragonite, which are both crystallised forms of calcium carbonate (Alexander and Mindess, 2005).

The (10 mm) limestone aggregates like the (0-10 mm) plastic aggregates are uniformly graded. However, the particle size distribution presented in Figure 3.3 indicates that, they contain higher fractions of coarse aggregates with particle sizes $\geq 5$ mm (up to 85%), and a lower fraction of fine aggregates with particle sizes $\leq 5$ mm. They have a maximum particle size of 10 mm, a distribution mode of 6.3 mm and fineness modulus of 5.8 mm. The proportions of non – uniform (flaky, elongated or other irregular shaped) aggregates were a lot lower in comparison to the (0-10 mm) plastic aggregates. Additionally, the (10mm) limestone aggregates also had a lower void percentage (0.42%) and higher bulk density (1280 kg/m$^3$), particle density (2530 kg/m$^3$), specific gravity (2.74) and water absorption percentage (0.42%) when compared to the (0-10mm) plastic aggregates. Some physical and mechanical properties of the material are shown in Table 3.5

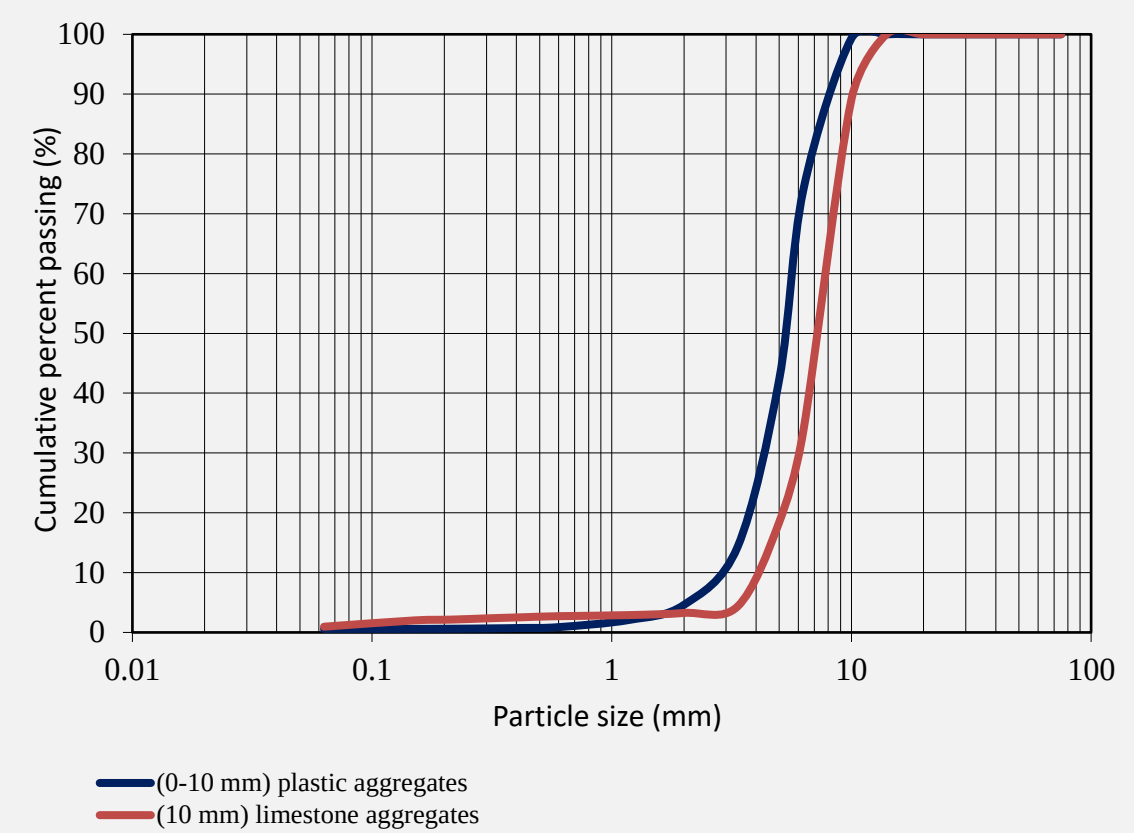


Figure 3.3: Particle size distribution curves of the coarse aggregates

Table 3.5: Some of the physical and mechanical properties of the coarse aggregate used in the current research

| *Properties* | *Coarse aggregates* | |
|---|---|---|
| | *0 -10 mm Plastic aggregate* | *10 mm aggregate* |
| Maximum particle size (mm) | 10 | 10 |
| Fineness modulus (mm) | 5.5 | 5.8 |
| Mode of the distribution (mm) | 5.0 | 6.3 |
| % fine aggregate (≤ 5 mm) | < 30 | 10 |
| % Particle size range (63μm – 2mm) | 4 | 4 |
| % Particle size range (2 – 5 mm) | 20 - 25 | 6 |
| % of coarse aggregate (≥ 5 mm) | ≥ 70 | 90 |
| % Particle size range (5 – 8 mm) | 60 - 65 | 50 |
| % Particle size range (8 -10 mm) | 10 | 40 |
| Flakiness index (%) | 30 – 35 | 18 |
| Elongation index (%) | 17 – 22 | - |
| Non - hollow cylindrical columns (%) | 10 | - |
| Bulk density (kg/m$^3$) | 768 | 1280 |
| Particle density (kg/m$^3$) | 1520 | 2740 |
| Specific gravity | 1.52 | 2.74 |
| Percentage void (%) | 0.50 | 0.42 |
| Water absorption (%) | 0.1 | 5.1 |
| Los Angeles coefficient | 2.4 | 10.1 |
| Melting point | 240$^0$C | - |

#### *3.2.1.2 Waste plastic*

The principal materials encapsulated in the current research work are waste plastics that are difficult and/or not economical to recycle. These waste plastics also referred to as end of life plastics (ELPs) are considered to have no economic value and as such disposed in landfills or incinerated. The waste plastics are mostly synthetic or semi synthetic polymers. In comparison to other commodity plastics, the waste plastics encapsulated in current work are lightweight, rigid and tough with relatively high mechanical and thermal resistant properties. They include bulk polyvinylchloride (PVC), acrylonitrile butadiene styrene (ABS), polyethylene (PE) acrylonitrile styrene acrylate (ASA), polyoxymethylene (POM), polycarbonates (PC) and other rigid plastics discarded as waste from the packaging, automobile, construction and aviation industries.

The waste plastics were collected from the various industries and disposed on behalf of the local authorities by waste management companies. Prior to the final disposal, the waste plastics are sent to polymer extrusion companies, where the bulk waste plastics are mechanical processed without sorting into aggregate sized pellets. The mechanical treatment was required to reduce the bulk waste plastics into manageable size particles suitable for land filling or incineration. The treatment procedure includes mechanical cycles of shredding, grinding and collection. This procedure is similar to that used for recyclable plastics (for example, HDPE and PET) but since the ELPs are not suitable for any further use and destined for land fill sites, grinding, washing, drying, re-granulating and compounding that may incur unnecessary additional costs are exempted.

In order to achieve an automatic division of aggregates into fractions with defined particle size, the unsorted bulk plastics are shredded into thin plastic strips of a 2 -7mm width before feeding into the grinding unit containing high precision cutting blades. The calibrated distance between the cutting blades in the grinding unit of the mechanical processor determines the maximum particle size of the pellets. According to the plastic recycling company, the distance between the blades (Polymer extrusion, Blackwood UK) can be vary between 2 – 20 mm. For the plastic aggregates encapsulated in the current work, the calibrated distance between the blades was maintained at 6 mm. After grinding, the pellets were collected, bagged and stored in a dry condition until burial in landfill sites or reuse (as in the current study).

The mechanically recovered (0-10mm) plastic aggregates were sourced from the extrusion company by the collaborating company, Speedbuild Limited (UK), who in turn supplied the material as it is, in batches to the material laboratory of the University of South Wales. The aggregates are also mostly black in colour although red, white, blue and opaque coloured particles were observed in some batches. The particle size distribution (Figure 3.3) indicated that each batch contains uniformly graded particles with up to 30% fine aggregates (particle size $\leq$ 5 mm) and 70 % coarse aggregates (particle size $\geq$ 5 mm) by mass. It also contains up to 60% non-uniform shaped aggregates, of which 30 – 35% are flaky shaped aggregates, 17 – 22% are elongated aggregates. About 10% of the elongated particles are shaped like non- hollow cylindrical columns. Furthermore, the maximum particle size and the fineness modulus (that is, the average particle size) were found to be 10 mm and 5.5 mm respectively while, the mode (most common particle size) of the distribution was 5 mm. The (0-10mm) plastic aggregates have a void percentage of 0.5% and surface water retention of 0.1%. It also has bulk and particle density of 768 kg/m$^3$ and 1520 kg/m$^3$ respectively, a specific gravity 1.52 and, a crushing resistance (*Los Angeles coefficient)* of 2.4. Some of the physical and mechanical properties of the (0-10mm) plastic aggregates determined by the researcher are shown in Table 3.5. In addition, some of the bulk waste plastics prior to the mechanical treatment are shown in Figure 3.4(a-f), while Figure 3.5(a-c) shows the equipment used for the mechanical recovery of the plastic aggregates. Some of the plastic pellets collected after the mechanical recycling are shown in Figure 3.6, while Figure 3.7(a-b) show some of the non-uniform shaped plastic aggregates.

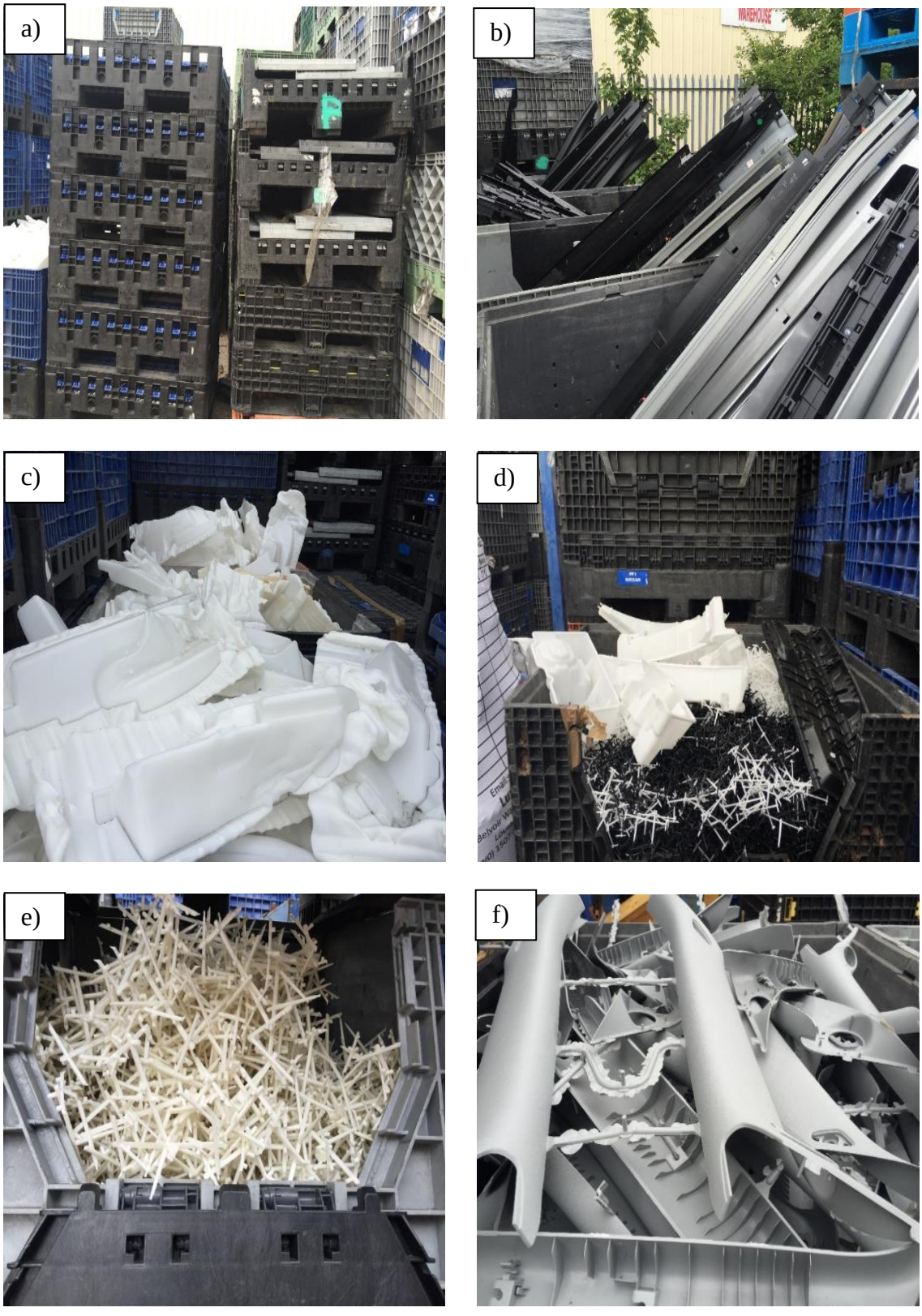


Figure 3.4 (a-f): Some of the bulk plastics prior to the mechanical recovery

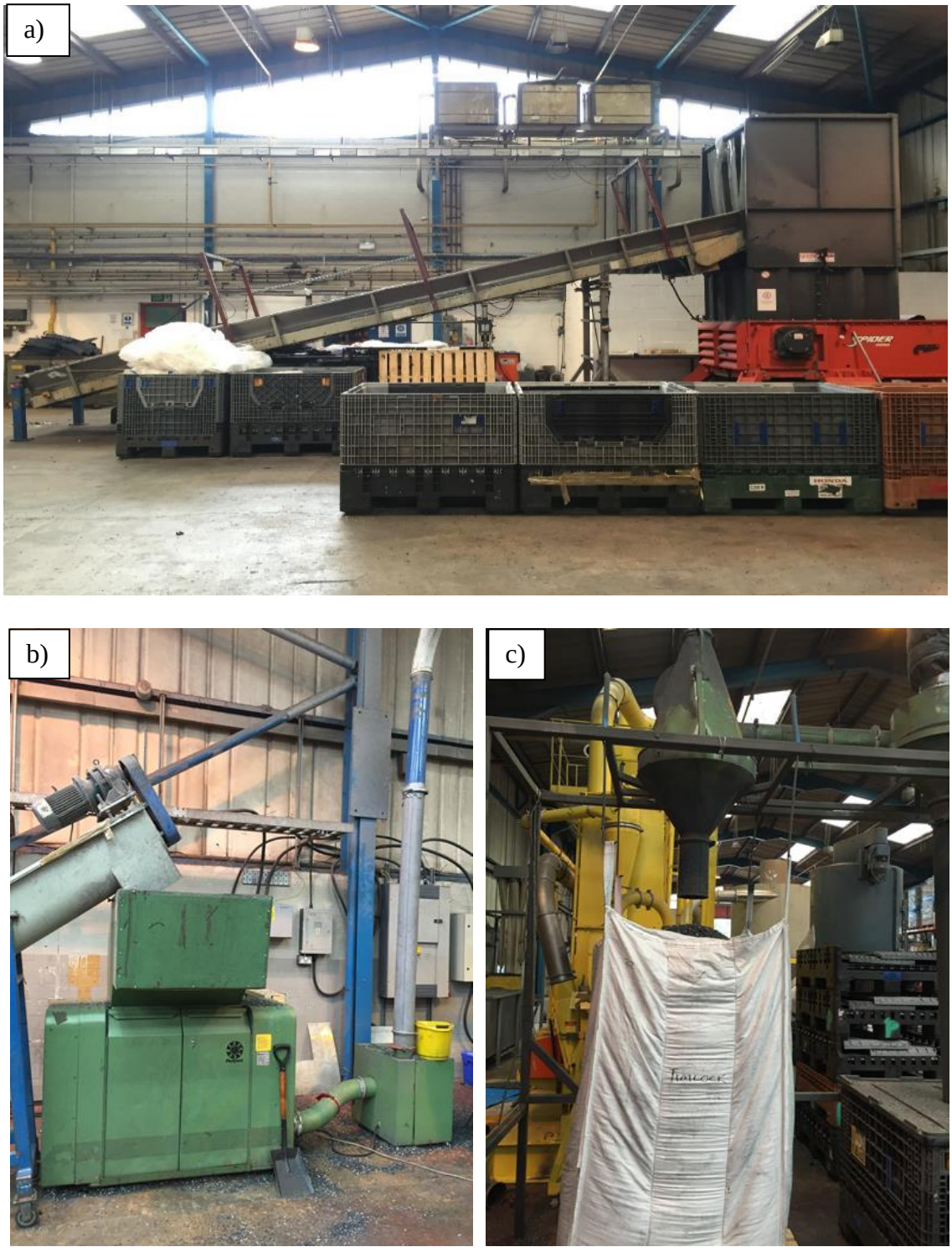


Figure 3.5 (a-c): Equipment used for the mechanical treatment of the bulk waste plastics, a) - shredder, b) - grinder, c) - extrusion funnel and collection point.

Figure 3.6: Sample of the granulated plastic pellets

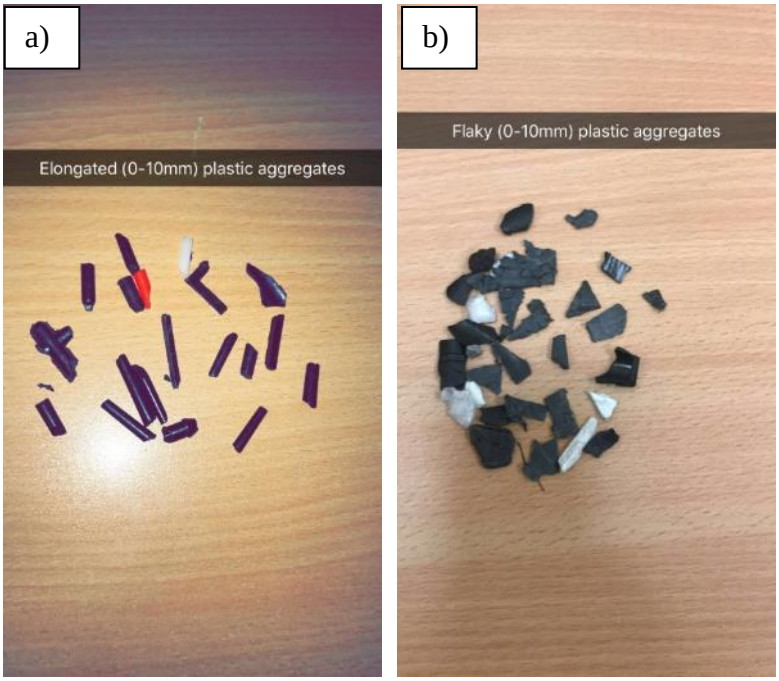


Figure 3.7: Some of the non-uniform shaped plastic aggregates, a) – Elongated particles and b) Flaky particles

### 3.2.2 Fine aggregates

#### *3.2.2.1 River sand*

River sand conforming to BS EN 13139: 2013 was used in the conventional concrete mixes as fine aggregates. River sand is a general-purpose material widely used in construction due to its inertness and considerable toughness. It is a finely divided naturally occurring granular aggregate comprising of rock and mineral particles. The most common constituent of the material is silica usually in the form of quartz. The aggregate was sourced from Jewson UK Limited in Caerphilly, South Wales, UK. The same batch was used throughout the current research.

The aggregates are mostly (up to 99%) fine grained particles with smooth texture. The particles are also uniformly distributed with a maximum particle size of 5 mm, fineness modulus (average particle size) of 1.6 mm and distribution mode (most common particle size) of 212 μm. The void percentage of river sand was 0.23%, the lowest of any of the aggregates used in the ongoing work.

The particle size distribution curves of the river sand used in the current work is shown in Figure 3.8, while the physical and mechanical properties of the river sand are presented in Table 3.6.

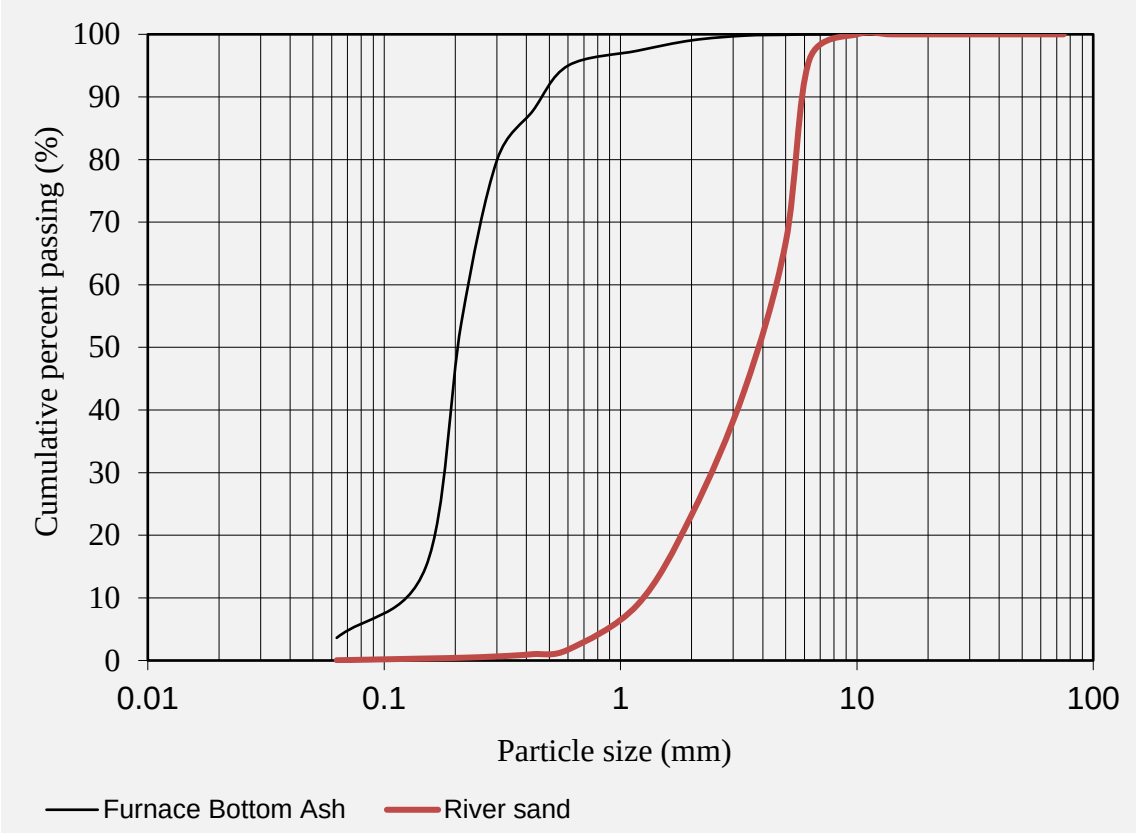


Figure 3.8: Particle size distribution curves of the fine aggregates

Table 3.6: Some of the physical and mechanical properties of the fine aggregate used in the current research

| *Properties* | *Fine aggregates* | |
|---|---|---|
| | *River sand* | *Furnace bottom ash* |
| Maximum particle size (mm) | 5 | 6.3 |
| Fineness modulus (mm) | 1.6 | 5.0 |
| Mode of the distribution | 212 µm | 5.0 |
| % fine aggregate (≤ 5 mm)<br>% Particle size range (63µm – 2mm)<br>% Particle size range (2 – 5 mm) | 99<br>99<br>1.0 | 50<br>25<br>25 |
| % of coarse aggregate (≥ 5 mm)<br>% Particle size range (5 – 8 mm)<br>% Particle size range (8 -10 mm) | 0<br>-<br>- | 50<br>50<br>- |
| Flakiness index (%) | 0 | 7.0 |
| Elongation index (%) | 0 | 10.0 |
| Non - hollow cylindrical columns (%) | - | - |
| Bulk density (kg/m$^3$) | 1530 | 918 |
| Particle density (kg/m$^3$) | 2590 | 1650 |
| Specific gravity | 2.6 | 1.7 |
| Percentage void (%) | 0.23 | 0.40 |
| Water absorption (%) | 29.7 | 24.3 |
| Los Angeles coefficient | 0 | 45 |
| Melting point | - | - |

#### *3.2.2.2 Furnace bottom ash*

The Furnace bottom ash (FBA) used in the current research work was obtained from the Aberthaw power station in South Wales by Speedbuild Limited UK. As with the (0-10mm) plastic aggregates, FBA was used as provided with no modifications. It conforms to specifications of lightweight aggregate as stipulated in BS EN 13055-2016, and was used primarily as low density fill in the encapsulated systems. Furnace bottom ash (FBA) is the coarse fraction of the ash produced in coal-fired power stations when pulverised fuel (coal) is fed into the boilers and burnt at high temperatures and pressures. Once combustion is completed, the finer pulverised fuel ash (PFA) is extracted from the flue gases discharged and captured in the precipitators. The coarser FBA drops into a hopper at the bottom of the boiler, from where it is later removed with high pressure water and pumped into storage lagoons. The material remains in the storage lagoons until it is discarded in landfill sites.

The material supplied in batches by Speedbuild Limited UK, contain (by mass) 50 % fine aggregates and 50 % coarse aggregates. The particle size distribution indicates that the aggregates are uniformly distributed. Their maximum particle size of aggregate ranges from 6.3 -20 mm (depending on the batch). The fineness modulus and the mode of the distribution were both 5.0 mm. The distribution also indicated that the material contains moderate amount of flaky and elongated particle shape (7 and 10 mm respectively). In comparison to FBA, the river sand has a higher particle density (2590 kg/m$^3$), bulk density (1530 kg/m$^3$), specific gravity (2.6) and water absorption percentage (29.7%). FBA was however more porous, with a void percentage of 0.40%. The particle size distribution curve of the FBA used in the current work is shown in Figure 3.8, while the physical and mechanical properties of the aggregates are presented in Table 3.6.

## 3.3 MICRO-FILLER

### 3.3.1 Pulverised fuel ash (PFA)

High carbon pulverised fuel ash (PFA) from the Aberthaw power station in Wales was considered for use in the encapsulated plastic concrete as micro filler, although the pozzolanic properties of the PFA also meant that it could also serve as a binder admixture. The material was classified as off-spec fly ash or waste at the Aberthaw works and stockpiled in settling basins or extracted mines. Large volumes of the stockpiled ash end up in landfills while, the rest are fed into burners and used as alternative raw materials in coal combustion. It was sourced from the power station and supplied by Speedbuild Limited to the materials laboratories of the University of South Wales.

The fly ash also resulted from the burning of pulverised coal in coal – fired electricity power stations. The PFA used in the current work was observed to be slightly darker than the commonly used PFA conforming to the specifications of BS EN 450. The dark coloration may be due to the presence of unburned carbon particles in the ash. Most PFAs contain up to 10% unburned carbon, generally present in the form of cellular particles larger than 45µm (Wu, 2002 and Naik et al., 2006). The presence of unburnt carbon in the fly ash according to, Skorupska (1993), DTI (1999) and Wu (2002) may be attributed mainly to two reasons. The first reason is that low nitrogen oxides (NOx) systems installed in coal – fired electricity power stations for the plant compliance with the stringent nitrogen oxide emission regulations, may limit the exhaustive burning of the coal particles. The second reason lies in the quality of the coal materials and the operating condition of the power plant. Changes in fuel type or operating conditions may also influence the coal combustion process (Skorupska, 1993). Larger amounts of carbon in PFA are considered harmful as the cellular particles of carbon tends to increase the water demand for a given consistency and also increases admixtures requirement for the entrainment of a given volume of air (Naik et al., 2006).

In order to evaluate the carbon content of the fly ash, a sieve analysis of the material was carried out using nested BS test sieves with aperture sizes 45 µm, 63 µm, 150 µm and 212 µm. The result of the sieve analysis indicates that the fly ash contains approximately 17.2% particles with particle sizes ≥ 45µm. The PFA used in the current work is shown in Figure 3.9, while the results of the sieve analysis are presented in Table 3.6. For

comparison purposes a PFA conforming to the specification of BS EN 450 has also been included.

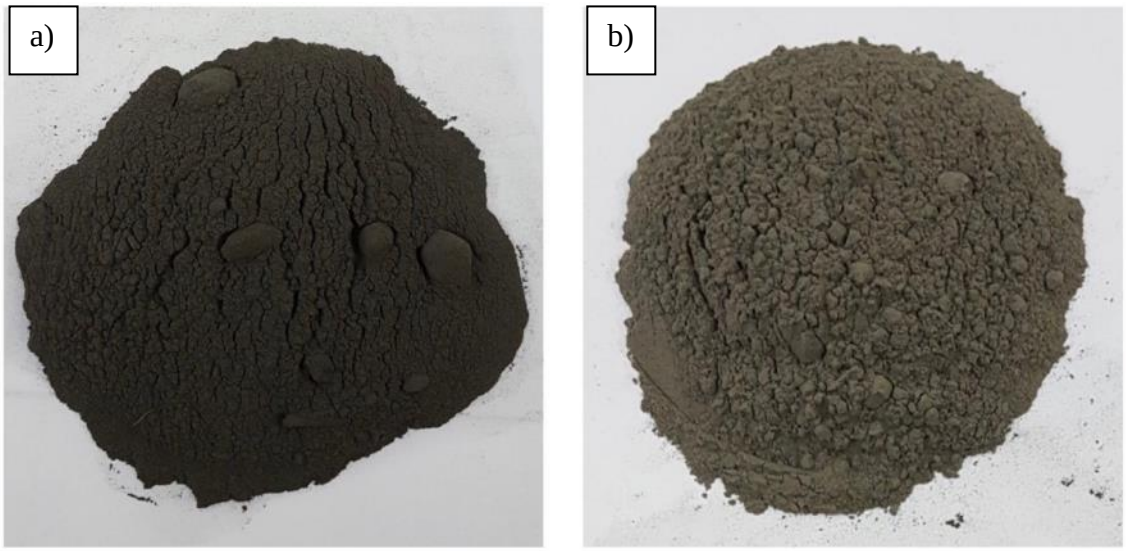


Figure 3.9: (a) high carbon PFA used in the research work and (b) the pulverised fly ash conforming to BS EN 450 (loss of ignition below 6%).

Table 3.7: Particle size distribution of the PFA used in the ongoing work

| *Particle size distribution* | *fly ash used in the research work* | *PFA conforming to BS EN 450* |
|---|---|---|
| < 45 µm | 83.5% | 90.3% |
| Retained on the 45µm | 11.5% | 5.2% |
| Retained of the 63 µm | 3.5% | 2.7% |
| Retained on the 150 µm | 2% | 1.4% |
| Retained on the 212 µm | 1.2% | 0.4% |

The inclusion of the PFA in the encapsulated plastic concrete involved the addition of the material to the binding materials (Portland cement or Pozament) before blending with the aggregate materials. The thermogravimetric analysis carried out on the blended CEM IIB-PFA binding system (Table 3.7) indicates that, the addition of PFA some delayed the temperature peaks and reduced the weight losses observed during the heat treatment of the CEM IIB binder on its own. The CEM IIB-PFA binding system recorded endothermic peaks within temperature range 110 – 120$^{o}$C, 410–420$^{o}$C and 770-780$^{o}$C during the first, second and third phases respectively. A fusion reaction accompanied by weight loss of 2.04% was observed at temperature between 900-910$^{o}$C during the thermal treatment of the PFA.

Table 3.8: Phase characterisation of the unhydrated CEM IIB-PFA binder

| *Phase* | *Temperature ranges ($^{o}$C)* | *Peak temperatures ($^{o}$C)* | *Weight loss (%)* | *Phase changes* |
|---|---|---|---|---|
| Phase 1 | 25- 350 | 115.91 | 0.01 | Loss of surface absorbed water and dehydration of ettringite ($C_6AS_3H_{32}$) |
| | | | | Dehydration of calcium aluminate hydrates |
| Phase 2 | 350 -450 | 418.97 | 0.12 | Dehydroxylation of $Ca(OH)_2$ |
| Phase 3 | 600 - 850 | 777.08 | 3.62 | Decarboxylation of $CaCO_3$, possibly dolomite, vaterite, aragonite or calcite |
| Phase4 | ≥ 850 | 908.87 | 2.04 | Fusion reaction |

According to BS EN 196-2:2005, the fusion reaction may be as a result of the loss of ignition of the cementitious material. The percentage weight lost on ignition gives an indication of the organic content of the cement. The loss of ignition is typically associated with the decomposition of carbon content, although it also includes the loss of water and $CO_2$ (BS EN 450). The specification and conformity criteria for use of fly ash in concrete (BS EN 450) suggest that PFA with loss of ignition above 6% are not suitable for use in

concrete due to the increased water demand. The loss of ignition of the PFA used in the ongoing work was approximately 17.5%, which is more or less representative of the 17.2% cellular particles of carbon with particle size ≥ 45μm. The loss of ignition was determined according to the specifications BS EN 15169:2007 and BS EN 196-2:2005. It was taken as the weight loss observed when 25 mg of the PFA powder was heated at constant temperature (950$^{o}$C) until a constant mass was obtained (EN 196-2:2005).

## 3.4 OTHER MATERIALS

### 3.4.1 Seawater

Sea-water is a complex solution containing dissolved salts and gasses, living matter, suspended silt and organic material. It has an average salt concentration of 3.5% (or 35 PPM) and a pH of 8.2. The compounds of chloride form the highest proportion of the total dissolved salt (88 -89%), while the sulfate compounds the second highest salt proportion constitute about 10%. The seawater was collected from Jackson bay in Barry Island, South Wales UK. The ion concentration of the sea water could not be determined due to lack of testing equipment, as such it was assumed to contain the typical ions ($Cl^-$, $SO_4^{2-}$, $CO_3^{2-}$, $HCO_3^-$, $Ca^{2+}$, $Mg^{2+}$, $Na^+$ and $K^+$) present in most seawater (Wegian, 2010). The seawater was used to evaluate the resistant of the optimised concrete mixtures to sulphate attack.

### 3.4.2 Precast curbing blocks

The precast curbing blocks from a previous landscaping work carried out by the Speedbuild UK Limited were also supplied for analysis as part of the ongoing work. They were developed by Speedbuild limited from a trial and error ad-hoc mixing of Pozament ultra high strength, (0-10mm) plastic aggregates, pulverised fuel ash (PFA) and furnace bottom ash (FBA). The actual mix proportion could not be established from Speedbuild Limited, but from anecdotal information the methodology included, mixing the materials with water in an automated mixer and placing the fresh mix in U-shaped silicon moulds where curing took place for the first 24 hours. For surface finishing, the moulds were pre-sprayed with a mortar mix of Bath stone dust and Pozament grout. An unorthodox curing regime which involve placing the moulds in a ‘heat box’ containing a 2kW portable heater for 24 hours. The heat box was mainly a small room (twelve feet by six feet) with the walls mostly cover with aluminium foil. After 24 hours, the curbing blocks were demoulded and placed on wooden platforms located in the workshop, where curing continued at room temperature until the blocks were used in landscaping applications. The curbing blocks supplied by Speedbuild Limited were air cured for at least 90 days old. They served as a model for the encapsulated plastic concrete mixtures developed in this work. A photographic image of a curbing block is presented in Figure 3.5.

Figure 3.10: Photographic image of the curbing block supplied by Speedbuild Limited

# CHAPTER 4 - METHODOLOGY

*This chapter gives the details of the mix design, sample preparation, curing regime and experimental program/methods used in the current work. The experimental program includes the preliminary tests used to evaluate some characteristics of the aggregate materials and the freshly mixed normal density concrete and encapsulated plastic systems (Encapsulated plastic systems). It also includes the analytical techniques used to investigate the engineering and durability performances of both systems.*

## 4.1 CONCRETE MIX DESIGN

The concrete mix design was based on the British method of mix design (Department of Environment, 1988) discussed by Neville (2012). This method recognises the durability of the concrete mix and it is applicable to conventional concrete mixtures made with Portland cement or Portland cement composites incorporating ground granulated blast furnace slags and fly ash. It is governed by five main factors namely; i) the maximum size of aggregates, ii) type and grading of aggregates, iii) specific gravity of aggregates, iv) required workability and v) the density of fully compacted fresh mixed concrete. The maximum aggregate sizes of aggregates recognised by the standard are 10 mm, 20 mm and 40 mm.

The mix design process broken down into five steps by Neville involves establishing a target mean compressive strength from which the water/cement ratio can be determined as the first step. Establishing the water content required to achieve an assumed workability expressed as slump as the second step. The water content and water/cement ratio then enable the determination of the cement content (third step), while estimating the total aggregate content from the fresh density of fully compacted concrete and proportioning of the fine and coarse aggregates are the fourth and fifth step respectively.

In this work, the five steps mentioned above were used to determine the proportions of materials required to develop an economically viable concrete with satisfactory workability that can be mirrored for the encapsulated plastic concrete blends. In order to achieve this, two reference CEM IIB concrete mix compositions were initially designed using the five steps stipulated by Neville (2012). The first mix (with a target compressive strength of 49N/mm$^2$) consisted of 360 kg/m$^3$ of Portland cement, 720 kg/m$^3$ of fine

aggregate, 1080 kg/m$^3$ of coarse 10- mm limestone aggregate and 180 kg/m$^3$ water (w/c – 0.5%). This equates to 15.4% CEM IIB, 30.8% fine and 46.2% coarse aggregate contents. The second mix in line with the objective of this study to maximise the use of waste materials at the expense of conventional concrete materials, contain increased quantity of coarse aggregates and reduced amount of binding material. It included 520 kg/m$^3$ (21.1%) fine aggregate, 260 kg/m$^3$ Portland cement (10.5%), and 1560 kg/m$^3$ coarse aggregate (63.1%). The water/cement ratio was maintained at 0.5 (130 kg/m$^3$).

The two mixtures were investigated for workability using slump test as described in Section 4.3.2 of the current work. The investigations revealed that the first mix was rich and complies with European slump class S2 (that is, concrete with slump values with the range 40 – 90 mm), while the second mix was lean and recorded no (0 mm) slump. In an attempt to reduce, the richness of the first mix and improve the workability of the second mix. Ten other mix compositions with varied proportion of cement, aggregate and water contents were investigated. The water/cement ratio was varied between 0.5 and 0.6 to obtain a wide range of slump values. All the mix compositions investigated and their respective workability (slump) values are shown in Table 4.1.

Table 4.1: The mix composition of normal density CEM IIB concrete

| *Mix No.* | *Mix ref.* | *Mix ratio* | *CEM IIB ($kg/m^3$)* | *Water content ($kg/m^3$)* | *w/b ratio* | *Sand ($kg/m^3$)* | *10 mm aggregates ($kg/m^3$)* | *Slump values (mm)* | *Slump class* |
|---|---|---|---|---|---|---|---|---|---|
| *1* | **C1** | 1:2:3 | 360 | 180 | 0.5 | 720 | 1080 | 45 | S2 |
| *2* | - | 1:2:6 | 260 | 130 | 0.5 | 520 | 1560 | 0 | S1 |
| *3* | **C2** | 1:2:3 | 360 | 216 | 0.6 | 720 | 1080 | 55 | S2 |
| *4* | - | 1:2:4 | 320 | 160 | 0.5 | 640 | 1280 | 20 | S1 |
| *5* | **C3** | 1:2:4 | 320 | 192 | 0.6 | 640 | 1280 | 50 | S2 |
| *6* | - | 1:2:5 | 290 | 145 | 0.5 | 580 | 1450 | 0 | S1 |
| *7* | **C4** | 1:2:5 | 290 | 174 | 0.6 | 580 | 1450 | 15 | S1 |
| *8* | - | 1:3:5 | 270 | 135 | 0.5 | 810 | 1350 | 0 | S1 |
| *9* | - | 1:3:5 | 270 | 162 | 0.6 | 810 | 1350 | 5 | S1 |
| *10* | **C5** | 1:2:6 | 260 | 156 | 0.6 | 520 | 1560 | 0 | S1 |
| *11* | - | 1:3:6 | 250 | 125 | 0.5 | 750 | 1500 | 0 | S1 |
| *12* | - | 1:3:6 | 250 | 150 | 0.6 | 750 | 1500 | 0 | S1 |

*w/b – water/binder ratio

### 4.1.1 Preliminary mix compositions

From the mix compositions shown in Table 4.1, five CEM IIB concrete mixtures were selected for further works, while the rest were discarded. The five mixtures referenced C1 – C5 are based on increasing volume of aggregate. The first three mix compositions (C1 – C3) were selected primarily due to their good (medium) slump values, while the last two compositions (C4 and C5) were selected due to the high volumes of coarse aggregates present. The latter mix compositions were at this stage considered necessary to develop an understanding of the impact of high volume of coarse aggregates on some engineering properties of the concrete mixtures (particularly the encapsulated plastic concrete). The selected CEM IIB concrete mixtures were replicated in equivalent mix designs for the encapsulated plastic systems in five stages. These stages are discussed below:

#### *4.1.1.1 Stage one- Introduction of FBA and waste plastics*

The first stage of the mix design for the encapsulated plastic systems retained CEM IIB as the binding material but replaced the conventional aggregates (river sand and 10 mm limestone aggregates) with recycled lightweight aggregates (FBA and plastic aggregates respectively). The conventional and recycled aggregates were used as supplied in their dry state. The mix ratio and unit weight ($kg/m^3$) of the materials in the conventional CEM IIB-concrete mixtures were initially maintained for the materials in the encapsulated plastic mixtures. The workability of the equivalent CEM IIB-encapsulated plastic concrete mixtures was investigated using the slump test described later in this chapter. The investigation was particularly difficult due to the high volumes of lightweight aggregates required to attain the same unit weight as the corresponding conventional aggregate. Mixing, placing and compacting were very strenuous. Furthermore, the mixtures were dry, not cohesive and highly segregated. The segregation and lack of cohesiveness observed during mixing increased with the increase in volume of lightweight aggregates included in the mix. The mix compositions designed at this stage were referenced CP1i – CP5i and shown in Table 4.2.

Table 4.2: The CEM IIB- based systems considered during the mix design stage of the current work

| *Mix type* | *Mix ref.* | *Mix ratio* | *Binding materials ($kg/m^3$)* | | *Water content ($kg/m^3$)* | *W/B* | *Micro-Filler ($kg/m^3$)* | *Conventional concrete materials ($kg/m^3$)* | | *Recycled waste materials ($kg/m^3$)* | |
|---|---|---|---|---|---|---|---|---|---|---|---|
| | | | *CEM IIB* | *PFA* | | | *PFA* | *Sand* | *10 mm limestone aggregates* | *FBA* | *(0-10mm) plastics aggregates* |
| CEM IIB-concrete | C1 | 1:2:3 | 360 | - | 180 | 0.5 | - | 720 | 1080 | - | - |
| | C2 | 1:2:3 | 360 | - | 216 | 0.6 | - | 720 | 1080 | - | - |
| | C3 | 1:2:4 | 320 | - | 192 | 0.6 | - | 640 | 1280 | - | - |
| | C4 | 1:2:5 | 290 | - | 174 | 0.6 | - | 580 | 1450 | - | - |
| | C5 | 1:2:6 | 260 | - | 156 | 0.6 | - | 520 | 1560 | - | - |
| (Stage one) CEM IIB-encapsulated plastic concrete | CP1i | 1:2:3 | 360 | - | 180 | 0.5 | - | - | - | 720 | 1080 |
| | CP2i | 1:2:3 | 360 | - | 216 | 0.6 | - | - | - | 720 | 1080 |
| | CP3i | 1:2:4 | 320 | - | 192 | 0.6 | - | - | - | 640 | 1280 |
| | CP4i | 1:2:5 | 290 | - | 174 | 0.6 | - | - | - | 580 | 1450 |
| | CP5i | 1:2:6 | 260 | - | 156 | 0.6 | - | - | - | 520 | 1560 |
| (Stage two) CEM IIB-encapsulated plastic concrete with correction factors | CP1 | 1:2:3 | 360 | - | 180 | 0.5 | - | - | - | 432 | 648 |
| | CP2 | 1:2:3 | 360 | - | 216 | 0.6 | - | - | - | 432 | 648 |
| | CP3 | 1:2:4 | 320 | - | 192 | 0.6 | - | - | - | 384 | 768 |
| | CP4 | 1:2:5 | 290 | - | 174 | 0.6 | - | - | - | 348 | 870 |
| | CP5 | 1:2:6 | 260 | - | 156 | 0.6 | - | - | - | 312 | 936 |
| (Stage three) CEM IIB/PFA-encapsulated plastic concrete | CPP1 | 1:1:4:6 | 360 | 360 | 360 | 0.5 | - | - | - | 864 | 1296 |
| | CPP2 | 1:1:4:6 | 360 | 360 | 432 | 0.6 | - | - | - | 864 | 1296 |
| | CPP3 | 1:1:4:8 | 320 | 320 | 384 | 0.6 | - | - | - | 768 | 1536 |
| | CPP4 | 1:1:4:10 | 290 | 290 | 348 | 0.6 | - | - | - | 696 | 1740 |
| | CPP5 | 1:1:4:12 | 260 | 260 | 312 | 0.6 | - | - | - | 624 | 1872 |
| (Stage four) CEM IIB/PFA-encapsulated plastic concrete with PFA as micro-filler | $CPP1_f$ | 1:1:2:3 | 360 | - | 180 | 0.5 | 360 | - | - | 432 | 648 |
| | $CPP2_f$ | 1:1:2:3 | 360 | - | 216 | 0.6 | 360 | - | - | 432 | 648 |
| | $CPP3_f$ | 1:1:2:4 | 320 | - | 192 | 0.6 | 320 | - | - | 384 | 768 |
| | $CPP4_f$ | 1:1:2:5 | 290 | - | 174 | 0.6 | 290 | - | - | 348 | 870 |
| | $CPP5_f$ | 1:1:2:6 | 260 | - | 156 | 0.6 | 260 | - | - | 312 | 936 |

#### *4.1.1.2 Stage two- Reduction of FBA and plastics aggregate*

In order to reduce the amount of FBA and plastic aggregates to a more manageable volume, a correction factor was applied to the unit weight of both materials. The correction factor ensures that the same volumes of materials are used in the encapsulated plastic concrete mixtures as the conventional materials in the replicated CEM IIB-concrete mixtures. It was obtained by expressing the unit weight of the recycled lightweight materials (FBA or plastic aggregate) as a ratio of the unit weight of an equal volume of the corresponding natural aggregate (river sand or limestone aggregate). Illustrations of how the correction factors were determined are shown in Figure 4.1 and 4.2.

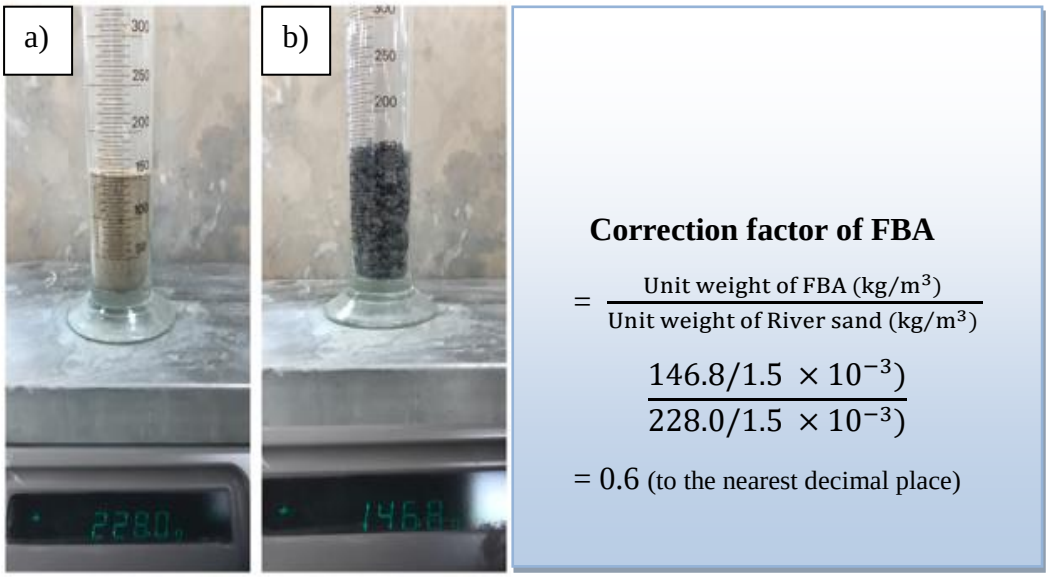


Figure 4.1: The correction factor of furnace bottom ash (FBA), (a) 150ml of river sand and (b) 150ml of FBA

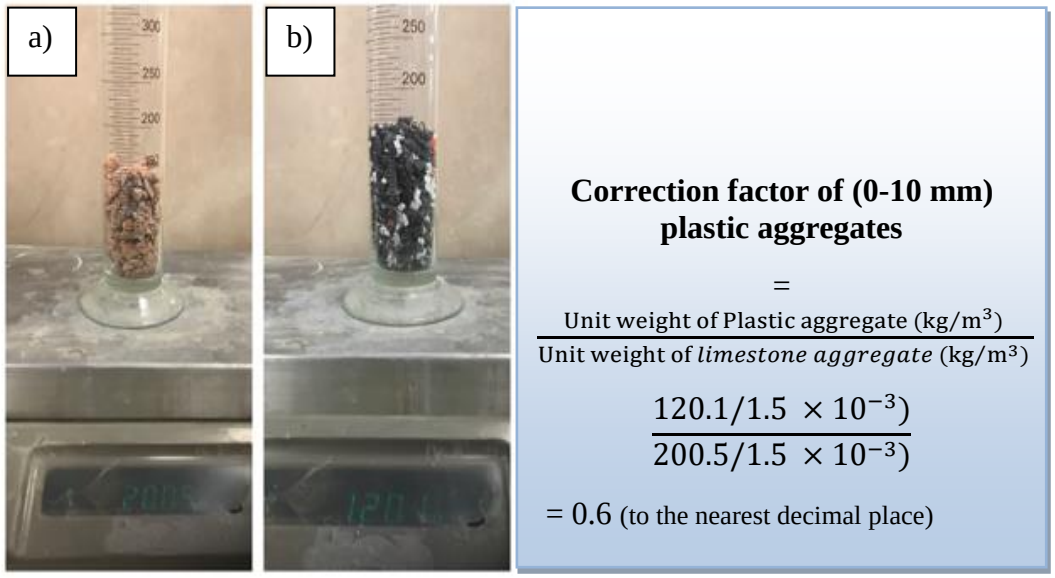


Figure 4.2: The correction factor of (0-10 mm) plastic aggregates. 150 ml (10 mm) limestone aggregates (a) and 150ml of (0-10 mm) plastic aggregates (b).

The determined correction factors were then applied to the unit weight of lightweight materials in stage one to obtain the revised mix compositions referenced CP1 – CP5 also shown in Table 4.2. The correction factors applied to each of the lightweight materials were the average of two evaluations carried out on each material. The CEM IIB-encapsulated plastic mix compositions without the correction factor (CP1i-5i) were discarded at this stage.

#### *4.1.1.3 Stage three – Introduction of pulverised fuel ash (PFA)*

This stage involves the addition of pulverised fuel ash (PFA) to the stage two mixtures. The inclusion of PFA in the encapsulated plastic concrete mixtures was considered necessary for the following reasons;

- The fresh and hydrated stage two mixtures were observed to be open textured with high percentages of visible void spaces. High void spaces (porosity) as reported in the literature negatively affect the mechanical and durability performance of conventional concrete. PFA due to its filler and pozzolanic properties was expected to reduce the void spaces and possibly improve the

mechanical and durability performance of the encapsulated plastic concrete mixtures.

- The stage two mixtures were also observed during mixing and placing to be non-cohesive and difficult to compact. The inclusion of PFA is anticipated to help improve the rheology and homogeneity of the encapsulated plastic concrete, and induce improved cohesion and easier compaction.

In order to determine the amount of PFA added to the mixtures, three trial mixtures including varied amount of PFA (CEM IIB: PFA ratios 1:0.50, 1: 0.75 and 1:1) were mixed with FBA and plastic aggregates and placed in 100 × 100 × 100 mm steel moulds. The stage two mix composition with water/binder ratio of 0.5 (mix CP1) was used in the trial mixtures. The fresh encapsulated plastic concrete with the highest proportion of PFA was observed to be more cohesive, better compacted and less segregated compared to the other two mixtures. Furthermore, as shown in Figure 4.3, the hydrated sample containing the highest proportion of PFA also provided the best finishing with least amount of exposed aggregates. As a result, CEM IIB/PFA ratio 1:1 was used throughout the current work.

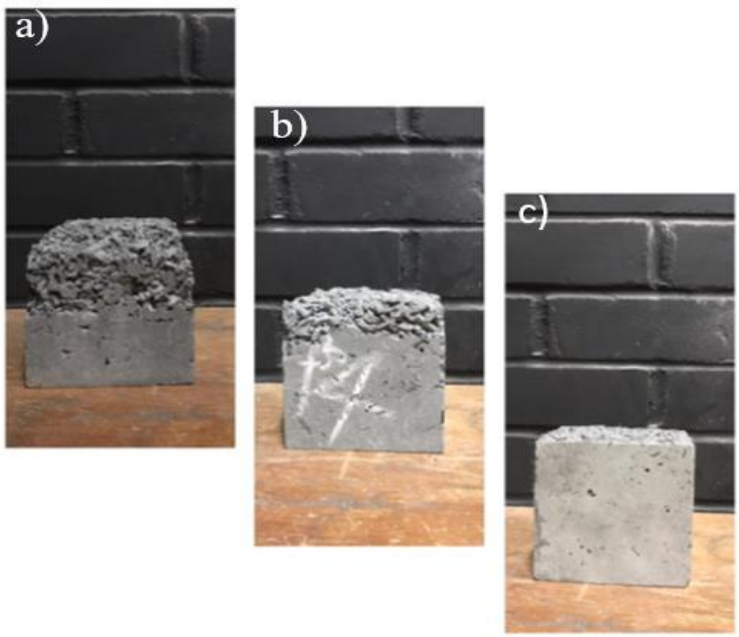


Figure 4.3: The trial mixtures with varied proportion of PFA. CEM IIB-PFA, (a) ratio - 1:0.50, (b) ratio -1: 0.75, and (c) ratio - 1:1.

PFA due to its associated cementitious properties was initially considered a binding material. That is, it was used as a CEM IIB admixture. The resulting CEM IIB-PFA encapsulated plastic concrete mixtures from this stage were referenced, CPP1–5. When PFA was included as an admixture, the aggregate content increased to reflect the increased binder content.

#### *4.1.1.4 Stage four – Consideration of PFA as a micro-filler*

The stage three-mix compositions were investigated for workability using both slump and degree of compactability tests, and for both physical and mechanical properties in hydrated state. The various test procedures are described later in this chapter. The physical and mechanical properties of (all) the stage three mixtures determined at 28 and 90 days fell short of the minimum specified requirement for structural lightweight concrete applications (BS EN 1992-1-1:2004). Thus, effort at optimising the performance of the systems was made by tweaking the mix compositions to consider PFA as a micro-filler rather than a mineral admixture. This allows for a reduction in the volume of aggregate materials used, as the aggregate content no longer need to increase with the increase in binder content. That is, the same mix compositions were maintained as in the stage two mixtures even though the binder content increased. These revised mix compositions are referenced CPP1$_f$ – CPP5$_f$ and are also shown in Table 4.2.

### 4.1.2 Optimised mix compositions

The result of the different analyses performed on the preliminary mix compositions helped in identifying an array of performance profiles from which the optimised mix compositions were decided. Four of the five CEM IIB-concrete mix types in Table 4.2 were considered for further works. The fifth concrete type, CEM IIB-encapsulated plastic concrete without the correction factor as previously mentioned were discarded. The top three mix compositions from each of the four concrete types considered were selected as the optimum mixtures. In addition to having superior performance in terms of workability, these mixtures also allowed for the influence of variations in water/binder and aggregate/binder ratios on the different concrete types to be evaluated.

Once the optimised mix compositions from the CEM IIB–concrete system has been decided. The selected mixtures from each concrete type were mirrored for the PG-concrete system. The same mix ratios and aggregate proportions as in the replicated

mixtures from the CEM IIB-concrete system were retained in the equivalent mixtures in the PG-concrete system. The only difference was that CEM IIB-binder was replaced with PG-binder. PFA was similarly used either as a mineral admixture or as a micro-filler. The use of the PG- binder helped in identifying the benefits likely to accrue from the use of high fluidity cementitious grout on the measured properties of the encapsulated plastic concrete. The optimised mix compositions selected for further work are shown in Table 4.3. The selected mixtures allowed for the effect of increased water to binder ratio and aggregate to binder ratio on the investigated properties of the conventional and encapsulated plastic concrete to be evaluated.

Table 4.3: The optimised CEM IIB and PG – concrete mix compositions carried forward for further works

| *Mix group* | *Mix type* | *Mix ref.* | *Mix ratio* | *Binding materials (kg/m³)* | | | *Water content (kg/m³)* | *W/B ratio* | *Micro-Filler (kg/m³)* | *Conventional concrete aggregates (kg/m³)* | | *Recycled waste materials (kg/m³)* | |
|---|---|---|---|---|---|---|---|---|---|---|---|---|---|
| | | | | *CEM IIB* | *PG* | *PFA* | | | *PFA* | *Sand* | *10 mm limestone aggregate* | *FBA* | *(0-10mm) plastics aggregate* |
| CEM IIB-concrete system | CEM IIB- concrete | C1 | 1:2:3 | 360 | - | - | 180 | 0.5 | - | 720 | 1080 | - | - |
| | | C2 | 1:2:3 | 360 | - | - | 216 | 0.6 | - | 720 | 1080 | - | - |
| | | C3 | 1:2:4 | 320 | - | - | 192 | 0.6 | - | 640 | 1280 | - | - |
| | CEM IIB-encapsulated plastic concrete | CP1 | 1:2:3 | 360 | - | - | 180 | 0.5 | - | - | - | 432 | 648 |
| | | CP2 | 1:2:3 | 360 | - | - | 216 | 0.6 | - | - | - | 432 | 648 |
| | | CP3 | 1:2:4 | 320 | - | - | 192 | 0.6 | - | - | - | 384 | 768 |
| | CEM IIB-PFA encapsulated plastic concrete | CPP1 | 1:1:4:6 | 360 | - | 360 | 360 | 0.5 | - | - | - | 864 | 1296 |
| | | CPP2 | 1:1:4:6 | 360 | - | 360 | 432 | 0.6 | - | - | - | 864 | 1296 |
| | | CPP3 | 1:1:4:8 | 320 | - | 320 | 384 | 0.6 | - | - | - | 768 | 1536 |
| | CEM IIB-encapsulated plastic concrete with PFA as micro-filler | $CPP1_f$ | 1:1:2:3 | 360 | - | - | 180 | 0.5 | 360 | - | - | 432 | 648 |
| | | $CPP2_f$ | 1:1:2:3 | 360 | - | - | 216 | 0.6 | 360 | - | - | 432 | 648 |
| | | $CPP3_f$ | 1:1:2:4 | 320 | - | - | 192 | 0.6 | 320 | - | - | 384 | 768 |
| PG-concrete system | PG-concrete | P1 | 1:2:3 | - | 360 | - | 180 | 0.5 | - | 720 | 1080 | - | - |
| | | P2 | 1:2:3 | - | 360 | - | 216 | 0.6 | - | 720 | 1080 | - | - |
| | | P3 | 1:2:4 | - | 320 | - | 192 | 0.6 | - | 640 | 1280 | - | - |
| | PG-encapsulated plastic concrete | PP1 | 1:2:3 | - | 360 | - | 180 | 0.5 | - | - | - | 432 | 648 |
| | | PP2 | 1:2:3 | - | 360 | - | 216 | 0.6 | - | - | - | 432 | 648 |
| | | PP3 | 1:2:4 | - | 320 | - | 192 | 0.6 | - | - | - | 384 | 768 |
| | PG--PFA encapsulated plastic concrete | PPP1 | 1:1:4:6 | - | 360 | 360 | 360 | 0.5 | - | - | - | 864 | 1296 |
| | | PPP2 | 1:1:4:6 | - | 360 | 360 | 432 | 0.6 | - | - | - | 864 | 1296 |
| | | PPP3 | 1:1:4:8 | - | 320 | 320 | 384 | 0.6 | - | - | - | 768 | 1536 |
| | PG-encapsulated plastic concrete with PFA as micro-filler | $PPP1_f$ | 1:1:2:3 | - | 360 | - | 180 | 0.5 | 360 | - | - | 432 | 648 |
| | | $PPP2_f$ | 1:1:2:3 | - | 360 | - | 216 | 0.6 | 360 | - | - | 432 | 648 |
| | | $PPP3_f$ | 1:1:2:4 | - | 320 | - | 192 | 0.6 | 320 | - | - | 384 | 768 |

## 4.2 PREPARATION AND CURING OF TEST SPECIMENS

1216, 100×100×100 mm test cubes and 18, 200 × 100 mm test cylinders were moulded using the mix compositions described in Section 4.1.2. The test specimens were prepared, mixed and placed under laboratory conditions. The materials were kept dry in lidded containers at room temperature and used as supplied with no other pre-treatment. To produce the test specimens, enough dry materials necessary for the fabrication of the required number of test specimens were taken and weighed, before thoroughly mixing in a Croker RP range pan mixer with a mixing speed of 74rpm for 3 minutes. The pre-weighed water was slowly poured into the mixer during this initial mixing period. To ensure a homogenous mix is achieved, the mixer was opened once, and the materials scooped from the edges back to the middle of the mixer with a hand-held shovel. After mixing, the workability tests were carried out before the fresh concrete were placed in cubic or cylindrical moulds and compacted on a vibrating table. The test specimens were removed from the vibrating table after a minute and placed on worktops at room temperature (20 ± 3 $^{o}$C), where they were air cured for 24 hours. The specimens after demoulding were placed in water tanks with temperatures 20 ± 3 $^{o}$C according to BS EN 12390-2:2009 until testing. The PG-concrete mixtures (conventional or encapsulated plastic concrete) were allowed an extra 24 hours air-curing period before immersing in the water tank due to their wetness and perceived weakness. Figure 4.4, 4.5 and 4.6 show the mixing chamber and some of the test specimens.

Figure 4.4: The Croker RP pan mixer used for mixing the materials in the current research

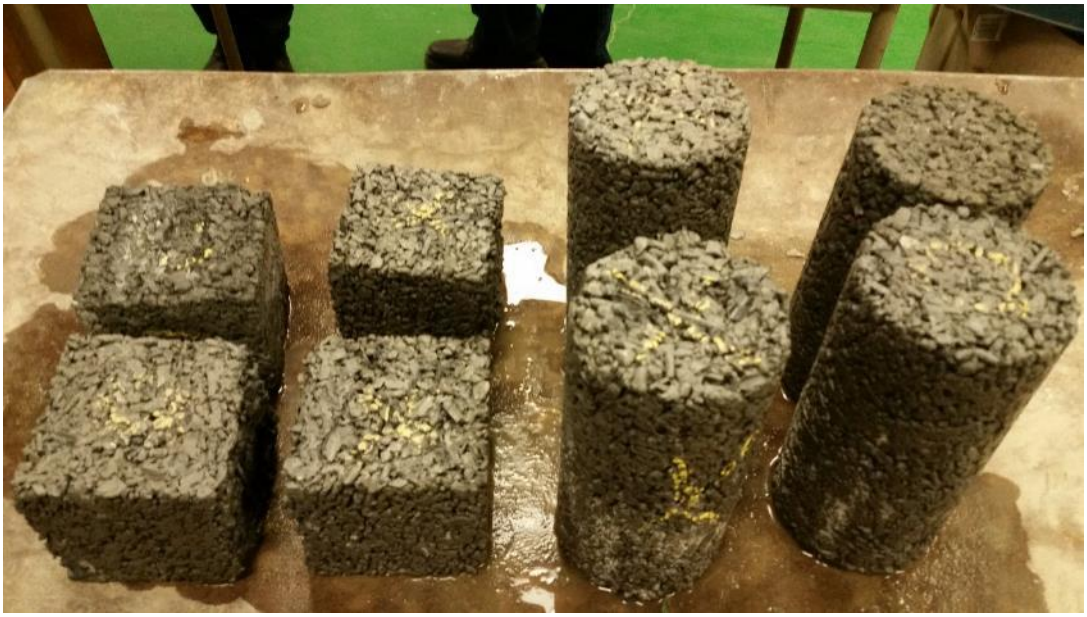

Figure 4.5: Some of the CEM IIB-encapsulated concrete plastic test specimens developed in the current research

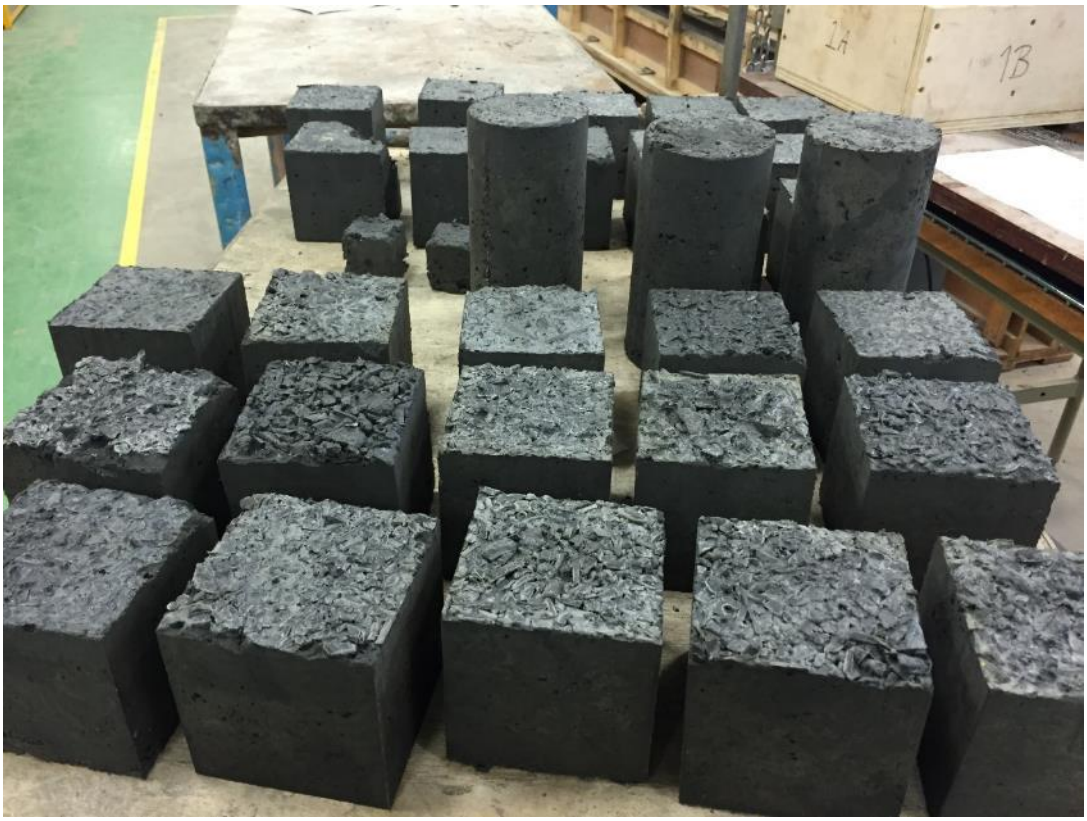

Figure 4.6: Some of the CEM IIB- PFA encapsulated plastic test specimens developed in the current research

## 4.3 TESTING

### 4.3.1 Preliminary tests

#### *4.3.1.1 Geometrical properties of (fine and coarse) aggregates used in the current work*

##### *4.3.1.1.1 Particle size analysis*

The particle size analysis was carried out using the dry sieve method described in BS EN 933-1: 2012. The investigation involves, shaking a sample of aggregate through the opening of a series of BS test sieves nested one above the other in order of size, with the sieve having the largest openings on top and the one with the smallest opening at the bottom. The result of the investigation was used to establish the grading, fineness modulus and the mode of distribution of the coarse and fine aggregates used in the current study. The grading relates to the proportioning of the fine and coarse aggregates in each material, while the fineness modulus gave an indication of the mean particle size in each aggregate distribution. The mode of distribution referred to the most common particle size in each distribution and was obtained from the sieve with the highest percentage mass of aggregate retained. The size distribution curves and the estimated parameters are presented in Chapter 3.

##### *4.3.1.1.2 Particle shape analysis*

The particle shape analysis was used to evaluate the percentage of flaky, elongate, round, and angular aggregates present in the bulk aggregate materials used in the current work. This investigation was significant because the particle shape (in addition to the particle sizes) influences the workability and engineering properties of concrete. The percentages of flaky and elongated particles were determined in accordance with BS 812 105 part 1 & 2 using the thickness and length gauges. For rounded, angular, and non-hollow cylindrical particle shapes, the aggregate particles after sieving were individually examined to determine their shapes. The different shape variations were expressed as a percentage of the total test portion. The estimated shape indices are shown in Chapter 3 of this work.

### *4.3.1.2 Physical and mechanical properties of the fine and coarse aggregates used in the current work.*

*4.3.1.2.1 Determination of loose bulk density and percentage void*

The loose bulk density ($\rho b$) indicate the mass of a unit volume of un-compacted aggregate including the void spaces, while the percentage of voids (v) is the volumetric proportion of voids in a container filled with aggregates. The loose bulk density was needed for calculating the percentage void (when the particle density is known), and for estimating the correction factor necessary to ensure equal volumes of lightweight materials are used in the encapsulated plastic concrete as the normal density materials in the conventional concrete. The investigations were carried out in accordance with the specifications of BS EN 1097-3:1998 on three test portions taken from bulk material using the quartering method described in BS EN 932-1:1997. In compliance with the BS EN 1097-3:1998, the loose bulk density (ρb) and percentage void (v) were determined using the following equations.

$$\rho b = \frac{M2-M1}{V} \quad \text{..... Equation 4.1}$$

Where;

$M_1$ = mass of the empty container, in kilograms

$M_2$ = mass of the container and test specimens, in kilograms

V = volume of the container, in litres

$$v = \frac{\rho\rho-\rho b}{\rho\rho} \times 100 \quad \text{.....Equation 4.2}$$

Where:

v = percentage of void

ρb = bulk density, in mega-grams per cubic metre

ρρ = particle density, in mega-grams per cubic metre

*4.3.1.2.2 Determination of particle density and water absorption*

The particle density ($\rho\rho$) indicate the mass of a unit volume of aggregate excluding the void spaces. It was used to evaluate the specific gravity of the aggregate materials used in this work. The investigation was carried out in accordance with the test procedure described in BS EN 1097-6:2013 annex E. Similarly, the water absorption was evaluated using the method described in BS EN 1097-6:2013. The method provides a measure for the total water absorbed and/or retained as film on aggregates after placing in a water filled container for 24 hours, and subsequently drying in an oven at a temperature of 105 ± 5 ºC until a constant mass is reached. As specified in the standards, the particle density (pρ) and the water absorption (%) were calculated using equations 4.3 and 4.4.

$$p\rho = \frac{M3}{V(F) - Vw} \quad \text{..... Equation 4.3}$$

Where;

ρρ = particle density, in mega-grams per cubic metre

$M_3$ = mass of dry aggregate, in grams

$V_{(F)}$ = volume of water and aggregates in container A, in millilitres

$V_w$ = volume of water in container B, in millimetres

$$WA_{24} = 100 \times \frac{M4 - M5}{M5} \quad \text{..... Equation 4.4}$$

Where;

$M_4$ = mass of the saturated surface-dry aggregate in the air, in grams,

$M_5$ = mass of the oven dried sample

*4.3.1.2.3 Determination of resistance to fragmentation*

The resistance to fragmentation of an aggregate is its ability to resist wearing, scraping or shattering by friction or impact. It is generally a measure of aggregate quality and resistance to degradation due to handling, stockpiling or mixing. The investigation was determined using the Los Angeles test procedure described in BS EN 1097-2:2010 annex B. It was performed only on the coarse aggregates (0-10mm plastic aggregates and 10 mm limestone aggregates), passing through the 10 mm but retained on the 6.3 mm BS test sieves. In compliance with BS EN 1097-2:2010, the Los Angeles coefficient (LA) was determined using the expression;

$$LA = \frac{5000-M}{50} \quad \text{..... Equation 4.5}$$

Where;

M is the mass retained on the 1.6 mm sieve after crushing the aggregate in the Los Angeles test machine for 15 minutes at 33 revs/minute.

***4.3.1.3 Engineering properties of the precast curbing blocks***

Some engineering properties of the precast blocks supplied by Speedbuild limited were also investigated as part of the preliminary investigation. The density, water absorption, porosity, and unconfined compressive strength (UCS) of the precast blocks were investigated using the test methods discussed below (Section 4.3.3). The test specimens were obtained by mechanically cutting out 100mm$^3$ samples from the blocks using a mounted concrete cutting saw. Three test specimens were obtained for each investigation. The investigations revealed that the 100 mm$^3$ precast cuts have an average density of 1405 kg/m$^3$, porosity 40%, water absorption of 33% and an average compressive strength of 7.5 N/mm$^2$. The recorded analytical values were taken as the baseline performance criteria for the encapsulated plastic concrete and the mix compositions in the current work were designed to improve on them.

#### *4.3.1.4 Phase transitions and hydration reactions of the binding materials.*

##### *4.3.1.4.1 Thermogravimetric analysis*

Thermogravimetric analysis was used to identify and characterise the different cement phase transitions and establish the relationships between the chemical composition and the hydration reaction of the binding materials. The investigation provides a quantitative measurement of weight changes associated with phase transitions and thermal degradations of the binding materials. It involves heating the unhydrated binder at controlled temperature programme over specified rates and, then measuring the change in mass as a function of temperature. The investigation was carried out according to the specifications of ASTM E1131, using a Hi - Res TGA 2950 thermogravimetric analyser (Figure 4.7). The analyser consists of a high – precision balance with a pan for loading the cement sample. The pan is located on a small electrically heated oven with a thermocouple to accurately measure the temperature increments.

At the start of the investigation, the pan was filled with 25 mg of the binding material to be tested and then placed on the oven. The cement samples were taken according to the specifications of BS EN 196-7:2007. Once filled, the pan was placed on the pan holder, which was then mechanically raised until the pan was completely enclosed in a plunger located right above the oven. The atmosphere around the pan was purge with inert gas ($N_2$) at 50ml/min to prevent oxidation or other undesired reactions. The analysis involved measuring the weight loss as the temperature was increased from 25 – 1000 $^oC$ at 10 $^oC$/min. The results presented as part of the material characterisation include both the thermogravimetric analysis (TGA) and derivative thermogravimetric (DTG) curves for the binding materials investigated. The TGA curves indicates the percentage decomposition of the unhydrated cement samples in descending increment, while the DTG curve shows the endothermic peaks (temperature peaks involving the evolution of water and carbon dioxide) as a function of temperature.

The weight losses observed between temperature ranges 25 – 350$^oC$ were assigned to the loss of surface absorbed water and the dehydration of the cement components including ettringite, gypsum and aluminate hydrates. The second and third phases include temperature peaks observed between temperatures ranging from 350 - 450 $^oC$ and 600 – 850 $^oC$ respectively. These phases coincide with the dehydroxylation of calcium

hydroxide and the decarboxylation of the calcium carbonates respectively. Each investigation lasted for 2 hours.

Figure 4.7: Hi - Res TGA 2950 thermogravimetric analyser

*4.3.1.4.2 Isothermal calorimetry*

The investigation was used to quantify the kinetics and extent of early age hydration reaction (up to 7 days) of the binding matrices used in the current work. The results of the analyses were used to characterise the setting and hardening behaviour of the binding materials used for encapsulating the plastic waste. The investigation was carried out according to the specifications of ASTM C1702, using a ToniCAL computer controlled Isothermal heat flow calorimeter. The instrument (Figure 4.8) permits a direct determination of the heat development rate (J/g) with elapsed time. To fabricate the paste required for the isothermal calorimetry measurement, a test tube was filled with 10 grams

of the unhydrated cement sample, while a syringe was filled with 5 grams of tap water (w/b ratio 0.5). The syringe was inserted into the test tube, such that, the end of the hollow needle was in the middle of the cement (in the test tube). The sample vial (test tube and syringe) was then stored in the calorimeter, while the equipment was allowed to equilibrate. The calorimeter was calibrated with a temperature regime of 25ºC. The hydration process was started after 4-6 hours of equilibration. The heat generated during the hydration reaction, was captured and recorded every 10 seconds continuously for 7 days, by the computing device connected to the ToniCAL calorimeter. The procedure was repeated for all the binding materials utilised in the current work.


Figure 4.8: Isothermal calorimeter equipment used in the current work

*4.3.1.4.3 Consistency and setting times*

The consistencies, initial and final setting time tests of the encapsulating (CEM IIB, CEM IIB-PFA, PG- and PG--PFA) matrices were carried out in accordance with BS EN 196-

3:2005 + A1:2008. The consistency was used to determine the minimum quantity of water required to complete the hydration reactions of the binding materials, while the initial and final setting times were the elapsed time between the moment water is added to the binding matrix and the moment at which it starts to lose and completely lose its plasticity respectively. The consistency and setting times were carried out using the Vicat and the Vicatronic apparatus shown in Figure 4.9 and 4.10.

Figure 4.9: Vicat apparatus used in determining the consistency of the cement pastes

Figure 4.10: The H3052 Vicatronics automatic machine used to determine the initial and final setting time of the cement pastes

*4.3.1.4.4 Flow-test*

In this study, the flow test was used to determine the fluidity and mobility of freshly mixed cement pastes. It was carried out in accordance to the specifications of BS EN 12350-5:2009 using the Matest flow table shown in Figure 4.11. The flow value of each cement paste was determined using the expression:

$F = \frac{d1+d2}{2}$ ..... Equation 4.6

Where:

F is the flowability of the cement paste

d1 is the maximum dimension of the concrete spread, parallel to one table edge

d2 is the maximum dimension of the concrete spread, parallel to the other table edge.


Figure 4.11: Matest time-tronic flow table used to determine the flowability of the binding materials

### 4.3.2 Physical property of fresh concrete

#### *4.3.2.1 Workability*

Workability refers to the consistency, mobility and compactability of the fresh concrete mixtures. In the current study, it was used to measure the wetness/fluidity, ease of flow (mobility) and compactability of the fresh conventional and encapsulated plastic concrete mixtures. The investigation was conducted using both the slump and degree of compactability tests. The slump test was carried out in accordance with BS EN 12350-2:2009, while the degree of compactability test was determined in accordance with the specifications of BS EN 12350 – 4: 2009. The degree of compactability test was particularly useful due to its ability to measure small variations in workability over a wide range of values. Figure 4.12 and 4.13 shows some of the optimised concrete mixtures under workability investigation.

Figure 4.12: Slump test carried out according to BS EN 12350-2:2009, using a 300-mm high, 200-mm wide slump test cone with a top opening of 100-mm

Figure 4.13: Degree of compactability test carried out according to BS EN 12350 – 4: 2009, using a 400-mm high and 200 mm square metal container

### 4.3.3 Physical and mechanical properties of the hydrated concrete and encapsulated plastic mixtures

#### *4.3.3.1 Density*

The densities of the conventional and encapsulated plastic concrete were determined in accordance with the water saturated method described in BS EN 12390-7:2009. The test was carried out using an electronic (Denison – Mayes) hydrostatic weight balance connected to a PC monitor (Figure 4.14). The weight balance consists of a water tank, steel support frame, mechanical lifting device and a stirrup suspended below the balance system. The test involves placing 100 $mm^3$ water cured test specimens on the stirrup and raising the water tank up with the lifting device until the specimen is submerged. The weight (in air and in water) and density values of the specimen were automatically determined by the weight balance and displayed on the connected monitor.

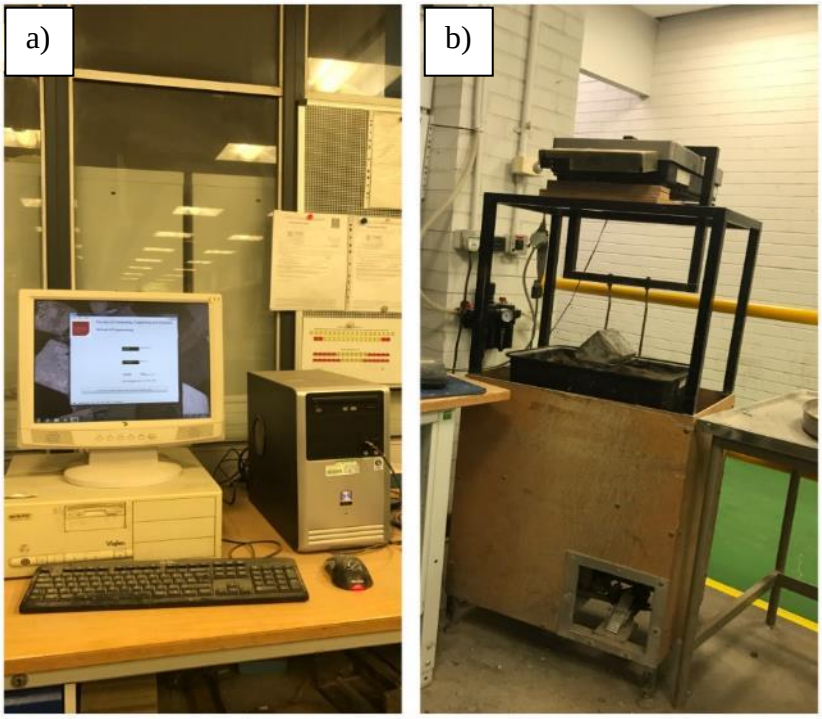


Figure 4.14: Hydrostatic weight balance. (a) The weight balance is on the right and, (b) PC monitor

#### *4.3.3.2 Porosity and water absorption*

The porosity and water absorption test of the concrete and encapsulated plastic concrete mixtures were carried out according to the specifications of BS 1881-122:2011, on test specimens water cured for 28 days. Porosity was used taken as a measure the percentage of void in each test specimen. It was estimated as the volume of void expressed as a percentage of the total volume of the test specimens (Equation 4.7). The water absorption of each specimen was taken as the change in mass of the test specimen immersed in water for 30 minutes and the oven dry mass to a constant mass expressed as a percentage of the dry mass (Equation 4.8).

$$porosity\ (n) = \frac{volume\ of\ void}{total\ volume\ of\ specimen} \times 100 \quad \text{..... Equation 4.7}$$

$$porosity\ (n) \quad = \frac{M_s - M_d}{M_s - M_w} \times 100$$

Where,

$M_s$ = mass of saturated specimen (specimen submerged in water for 28 days)

$M_d$ = mass of test specimens oven dried at 105$^o$C

$M_w$ = mass of specimen in water (specimen immersed in water for 30 minutes after drying in the oven).

$$\text{That is, Wa} = \frac{M_s - M_d}{M_d} \times 100 \quad \text{..... Equation 4.8}$$

Where

Wa = water absorption

$M_d$= mass of test specimens oven dried at 105$^o$C

$M_s$ = mass of saturated specimen (specimen submerged in water for 28 days)

#### *4.3.3.3 Unconfined compressive strength*

In order to understand the ability of the encapsulated plastic mixtures to gain strength, their unconfined compressive strength values were investigated at various curing ages (7, 28 and 90 days) and the results compared to those of the conventional concrete mixtures. The investigation was carried out in accordance with BS EN 12390-3:2009 using a 2000kN Hounsfield testing machine. Three water-cured (100-$mm^3$) test specimens per mix composition were used in the analyses. The test itself involves applying a vertical axial load at a constant rate of 0.06 ± 2 $N/mm^{2}$-sec on the test specimens until failure. The representative strength result of a mix composition was taken as the arithmetic average of the three-test specimens.

#### *4.3.3.4 Tensile splitting strength*

The tensile strength of the encapsulated plastic mixtures was used to determine the resistance of the conventional and encapsulated plastic concrete to splitting under tension. The test was carried out in accordance with the specifications of BS EN 12390-6:2009 on 200 x 100 mm diameter cylindrical test specimen water cured for 28 days. The results presented in this study are the mean of three measured values per mix composition.

### 4.3.4 Inferential Statistical analysis

In this analysis, the sample mean (average of three test specimens) relating to each of the physico-mechanical properties of the encapsulated plastic concrete (CEM IIB, CEM IIB-PFA, PG, PG-PFA-concrete), were aggregated and statistically compared to sample mean of the equivalent reference concrete (CEM IIB and PG-conventional concrete). The analysis was conducted with SPSS using the paired sample t-test. The paired sample t-test is a statistical analysis used to determine whether the mean difference of two sets of observation is zero. The data gathered from the analysis include the paired differences in mean, standard deviation, standard error and, t and p-values. The t-value measures the statistical difference between the sample mean of a given observation, while the p-value (or probability value) measures the level of marginal significance within a statistical hypothesis test. P-value provides the smallest level of significance at which a null hypothesis may be rejected. Null hypothesis is rejected for an alternative hypothesis, when the p-value is less than or equal to the alpha value and retained when the value of p is greater than or equal to the alpha value. The alpha value relates to the confidence level, which in this study correspond to 95% (thus, $\alpha = 0.05$). Likewise, the higher the value of t, the greater the evidence against the null hypothesis.

In this study, the null hypothesis ($p \geq 0.05$) assumes that, there is no relationship between the sample mean (average of 3 per investigation) reported for the physico-mechanical properties of the encapsulated plastic concrete and the control (the equivalent conventional concrete). Hence, the observed variation in measured properties is not statistically significant and may have occurred by chance. However, if $p \leq 0.05$, then the null hypothesis is rejected in favour of an alternative hypothesis, which in this work suggest that there, is a relationship between the test mean presented for each investigated property of the encapsulated plastic concrete and the equivalent conventional concrete. Hence, the observed variations are statistically significant and, unlikely to be due to chance.

### 4.3.5 Durability performance of the CEM IIB/PG–concrete systems.

#### *4.3.5.1 Freeze - thaw resistance*

The freeze and thaw resistance and other durability properties were investigated after the physical and mechanical properties of the encapsulated plastic mixtures have been determined. The freeze and thaw investigation was carried out to evaluate the potential of the encapsulated plastic mixtures to resist damage when subjected to successive freeze and thaw cycles. The test was carried out using the procedure described for aerated autoclave concrete (AAC) in BS EN 15304:2010. The standard was selected due to the lightweight property of the encapsulated plastic concrete.

Six 100-mm3 test specimens per mix compositions were used in this investigation. The test specimens were divided equally between the main and reference test specimens. The main test specimens were the specimens subjected to freeze thaw conditions, while the reference test specimens were the control test specimens. The investigation started with the specimen preparation period. All the test specimens were initially air cured at room temperature 23± 3$^{o}$C for 27 days. After the curing period, the test specimens were partially immersed in water baths containing 50 ± 2 mm deep water for 24 hours, followed by complete submersion in 100 ± 5 mm deep water for another 24 hours. After the submersion period, the specimens were removed from the bath and placed in lidded containers, where they were allowed to equilibrate for another 24.

After the specimen preparation period, the main test specimens were subjected to freezing at -15 ± 2$^{o}$C in a thermostatically regulated freezer for 8 hours. After the freezing period, the freezer was switched off while the test specimens were allowed to thaw for 8 hours at room temperature of 20 ± 3$^{o}$C and relative humidity ≥ 95%. The British standard a 0-4 and 0-6 hours' allowance was made for the temperature drop and rise respectively. The specimens were subjected to 20 uninterrupted freeze and thaw cycles, with each cycle completed after the thawing period. After the last freeze – thaw cycle, the all the test specimens (main and reference) were collected and oven dried at a 65$^{o}$C until a constant mass was achieved.

Deterioration due to freeze - thaw was evaluated in terms of changes in mass and compressive strength of the specimens subjected to the freeze and thaw cycles relative to the reference test specimens kept in the lidded containers at room temperature. These

changes were empirically evaluated as described in Section 4.3.5.1.1 - 4.3.5.1.2. In addition, the physical deterioration of the main test specimens was also evaluated through visual observation. For comparison purposes, the chemical deterioration of equivalent concrete mixtures was also determined.

*4.3.5.1.1 Change in mass of the hydrated test specimens due to freezing and thawing*

The change in mass ($M_{il}$) was taken as the measured mass of the test specimens after the completion of the freeze and thaw investigation, expressed as a percentage of the equivalent mass of the test specimen before the investigation. The equivalent mass of the test specimens before the freeze and thaw analysis was determined from the reference test specimens retained in the lidded containers using equation 4.9.

The equivalent mass as stipulated in the British standard was determined as follows:

$$M_{id,0}^{m} = M_{i,0}^{m} \times \left[\frac{M_{id,n}^{r}}{M_{i,0}^{r}}\right] \quad \text{Equation 4.9}$$

Where

$M_{id,0}^{m}$ = the equivalent oven-dry mass of the main test specimens immediately after removal from the lidded plastic container.

$M_{i,0}^{m}$ = the initial moist mass of the main test specimens after removal from the lidded container prior to commencing the freeze and thaw analysis

$M_{id,n}^{r}$ = is the measured oven dry mass of the reference test specimens after the completion of *20* freeze thaw cycles

$M_{i,0}^{r}$ = the measured initial moist mass of the reference test specimens after removal from the lidded container

Once the equivalent dry mass of the main specimens as being determined, the change in mass due to freezing and thawing was calculated using equation 4.10:

$$M_{il} = 100 \times \left(1 - \frac{M_{id,n}^{m}}{M_{id,0}^{m}}\right) \quad \text{Equation 4.10}$$

Where

$M_{il}$ = the mass loss of the main test specimens after n freeze and thaw cycles (n= 20)

$M_{id,n}^{m}$ = the measured oven-dry mass of the main test specimens immediately after 20 freeze and thaw cycles.

$M_{id,0}^{m}$ = the equivalent oven-dry mass of the main test specimens immediately after removal from the lidded plastic container prior to freeze and thaw (equation 4.9).

*4.3.5.1.2 Change in compressive strength of the hydrated test specimens due to freezing and thawing*

Compressive strength test was carried out on oven dried test specimens (after freeze-thaw cycles) using the standard described in Section 4.3.3.3. The strength loss of the main test specimens was taken as the relative decrease in the compressive strength values of the reference and main test specimens expressed as a percentage of the compressive strength values of the main test specimens. The residual compressive strength was empirically expressed as shown in equation 4.11:

$$f_{ci.rel} = 100 \times \left(1 - \frac{f_{ci,n}^{m}}{f_{cr,n}^{m}}\right) \quad \text{Equation 4.11}$$

Where,

$f_{ci.rel}$ = relative loss in compressive strength of the main test specimens (that is, test specimens subjected to freezing and thawing)

$f_{ci,n}^{m}$ = the average value of the compressive strength of the main test specimens after 20 repeated freeze and thaw cycles

$f_{cr,n}^{m}$ = the average value of the compressive strength of the reference test specimens

#### *4.3.5.2 Sulphate resistance of the concrete systems*

In addition to the freeze – thaw resistance, the performance of the encapsulated hydrated test specimens under sulphate attack was also investigated as part of the durability assessment of the encapsulated plastic test specimens. The test involved the immersion of test specimens in seawater and comparing their rate of degradation relative to test specimens immersed in fresh tap water. Seawater was chosen as the saline solution for two reasons, 1) it provides a medium rich in $SO^{2-}$ and $Cl^{-}$ ions, which may influence the long-term durability of the encapsulated plastic concrete mixtures. 2) It provides a measure for the performance of the hydrated encapsulated plastic mixtures when used in practical applications such as flood defence systems. This is dependent on the plastic systems achieving the required physical and mechanical characteristics. The analysis is expected to provide information on the progressive deterioration of the encapsulated plastic system due to $SO^{2-}$ attack, since the mechanism of chloride ($Cl^{-}$) induced attack mainly affects concrete reinforcements (which are not considered in the current work).

Eighteen 100×100×100 mm test specimens per mix composition were used in this analysis. Casting, de-moulding, curing and testing were all carried out at room temperature (20 ± 3$^{o}$C). After de-moulding, the test specimens were immersed completely in lidded plastic containers filled either with sea or with fresh water. The main test specimens were immersed in seawater, while the reference test specimens were immersed in fresh water. The lidded containers allow for protected exposure only. That is, they offer an environment devoid of frost action, wetting or drying, abrasion and different moisture content between the surface and core of the test specimens, thereby ensuring that only the interactions between immersed specimens and the ions in the solution were measured. Figures, 4.15 the lidded containers and some of the test specimens during the analysis.

Figure 4.15: Some of the test specimens immersed in seawater during the investigation

Deterioration due to sulphate attack (as with freeze and thaw) was also evaluated in terms of change in mass and compressive strength of the main specimens immersed in the saline solution relative to the reference test specimens immersed in tap water. These changes were empirically evaluated using equations 4.12 and 4.13. Visual inspections of the test specimens after immersion in seawater were also performed to evaluate any visible physical damage. For comparative purposes, the deteriorations of the respective equivalent concrete mixtures were also determined.

$$\% \text{ Mass loss} = \left(1 - \frac{W_2}{W_1}\right) \times 100 \quad \text{..... Equation 4.12}$$

$$\% \text{ change in compressive strength} = \left(1 - \frac{C_2}{C_1}\right) \times 100 \quad \text{..... Equation 4.13}$$

Where,

$W_1$ = mean weight of specimen immersed in tap water

$W_2$ = mean weight of specimen immersed in seawater

$C_2$ = mean compressive strength of specimen immersed in seawater water

$C_1$ = mean compressive strength of specimen immersed in tap water

#### *4.3.5.3 Behaviour of the encapsulated plastic systems at elevated temperatures*

As part of the robust durability performances investigated in the current work, the behaviour of the encapsulated plastic systems, particularly their structural stability and continued integrity at elevated temperatures were also investigated. This investigation is particularly pivotal due to the susceptibility of the plastic materials to deform/melt when exposed to high temperatures. Deformation of plastic at high temperatures often result in plasticizer, stabilisers, biocides (chemical compounds which can be harmful to living organisms) and other materials with low vapour pressure capable of forming aerosols (smoke) being released into the environment. Understanding the temperature limitations of the plastic blend therefore may help in defining the safety measures required to mitigate against the hazard.

The procedure employed in this study was based on the understanding that the physical and mechanical properties concrete is change substantially at elevated temperatures. The changes in mechanical property were considered in terms of the extent of strength loss, while the physical deformation was examined in terms of mass loss, spalling, scaling, peeling or crack formation in the concrete member. The test was conducted on 100 ×100 × 100 mm conventional and encapsulated plastic concrete test specimens water cured at room temperature (20 ± 3$^{o}$C) for 28 days and, subsequently oven dried at a temperature of 40$^{o}$C until a constant mass was attained.

Two main and two reference test specimens per optimum mix were used in the investigation. The main test specimens were the specimens subjected to temperature increments, while the reference test specimens were kept at room temperature. Prior to testing, the initial weights and dimensions of the main test specimens were determined. The specimens were then heated in an oven with a maximum heating capacity of 200$^{o}$C at six different target temperatures (30, 40, 50, 100, 150 and 200$^{o}$C) for 2 hours. A relative humidity of ≥ 70% was maintained for each temperature range. Silica xerogel was used as a desiccant to control the relative humidity of the oven. Some of the test specimens in a pre-heated oven during the heat treatment are shown in Figure 4.16.

Figure 4.16: Some of the test specimens in a pre-heated oven during the freeze and thaw investigation

After the heating period, the specimens were removed and allowed to cool at room temperature for 2 hours before visual inspections were carried out. The dry mass and the compressive strength of each of the test specimens were also determined. The mass loss and strength loss due to temperature increase were determined using equation 4.14 and 4.15.

$$\% \text{ weight change} = \frac{W_1 - W_2}{W_1} \times 100 \quad \text{.....Equation 4.14}$$

$$\% \text{ change in compressive strength} = \frac{C_1 - C_2}{C_1} \times 100 \quad \text{.....Equation 4.15}$$

Where,

$W_1$ = mean weight of specimen prior to immersion in seawater

$W_2$ = mean weight of specimen immersed in seawater

$C_2$ = mean compressive strength of specimen immersed in seawater water

$C_1$ = mean compressive strength of specimen immersed in tap water

# CHAPTER 5 - RESULTS

*This chapter describes the detailed results of the various tests performed on the cementing matrices and the concrete systems.*

## 5.1. HYDRATION REACTION OF THE BINDING MATERIALS

### 5.1.1 Rate of heat evolution.

The heat evolution of the cement samples over time (up to 7 days) are shown in Figure 5.1, while the time of peaks and the rate of heat evolution are presented in Table 5.1. The results like most calorimetry curves were characterised by three main hydration stages. According to Neville (2012), the first stage (stage I, on the heat evolution curve) represents the rapid initial hydration process typically associated with the reaction of tricalcium aluminate ($C_3A$) phase. In ordinary Portland cement, this stage is usually observed within the initial 5 minutes post hydration (Mukesh et al., 2012). The stage is understood to be brief (usually only a few minutes) but highly exothermic. The rate of heat evolution drops very low after about 5 minutes and remains almost constant for about 2 hours during the second stage. This stage denoted by 'stage II' on the heat evolution curve, represents the induction (dormant) period, where little or no reaction takes place, instead the different ions in solution combine to form critical size nucleis (Mukesh et al., 2012).

During the third stage (stage III, the rapid reaction period), the hydration reaction accelerate increases rapidly reaching a maximum peak (known as the main hydration peak) after about 6 hours, before decelerating again rapidly to almost half its original height. This period is also exothermic and entirely related to the hydration of the alite ($C_3S$) phases of the cement samples. It includes both the initial and final setting periods where the cement starts to gain its strength. A second main peak may also be observed during the hydration of Portland cement. This secondary peak (also referred to as shoulder peak) according to Mukesh et al., (2012), occur at about 12 – 20 hours of hydration (in OPC) any maybe due to the depletion of sulphate or renewed $C_3A$ dissolution and an accelerated ettringite precipitation. There are also the fourth and fifth hydration stages, which represent the deceleration stage characterised by retarded hydration and the steady hydration stage, which relate to the long-term hydration of the

cement paste. The belite ($C_2S$) dominates the long-term hydration stage particularly after 28 days of hydration.

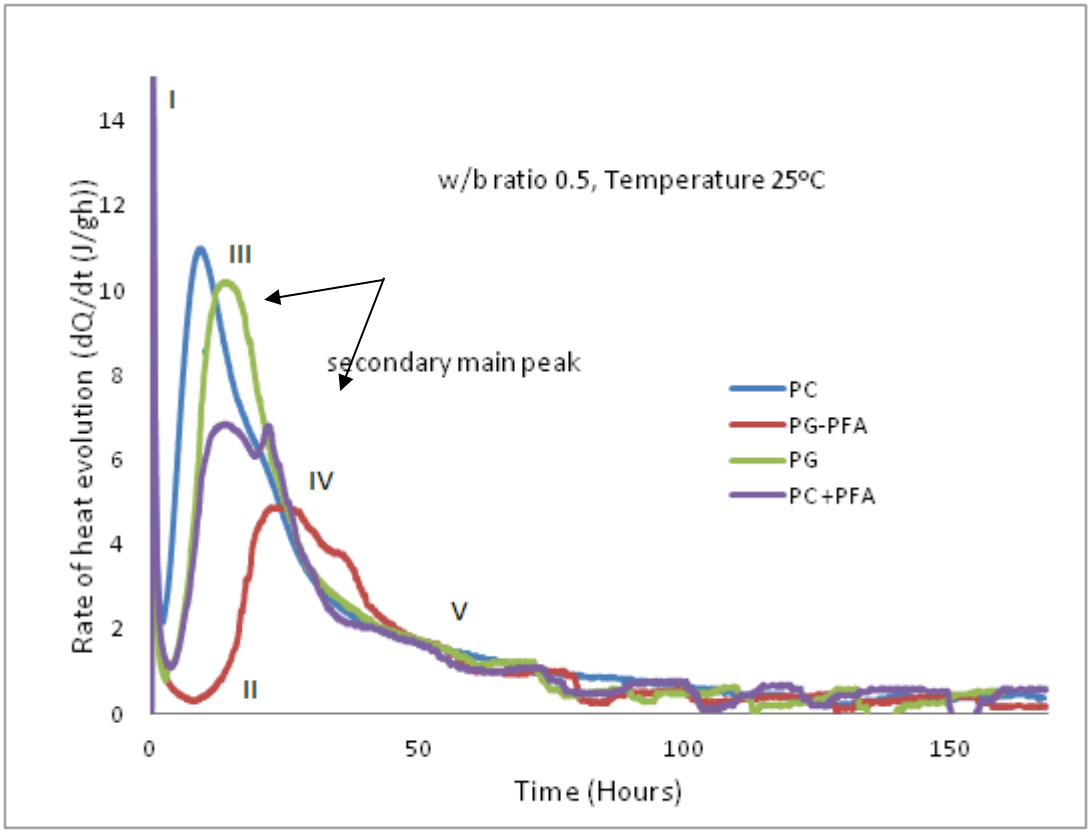


Figure 5.1: The rate of heat evolution vs time graph for the cement samples used in the current work.

Table 5.1: Peak times and rate of heat evolution of the binding materials used in the present work

| *Binding material* | *Initial Peak (Stage I)* | | *Dormant period (Stage II)* | | *Main peak (Stage II)* | | *Secondary main peak (Shoulder peak)* | |
|---|---|---|---|---|---|---|---|---|
| | *Time (hours)* | *dQ/dt (J/gh)* | *Time (hours)* | *dQ/dt (J/gh)* | *Time (hours)* | *dQ/dt (J/gh)* | *Time (hours)* | *dQ/dt (J/gh)* |
| Portland cement (CEM IIB) | 0.146 | 32.15 | 1.95 | 2.16 | 9.43 | 10.99 | - | - |
| Pozament grout (PG) | 0.108 | 36.98 | 2.61 | 0.78 | 13.50 | 10.21 | - | - |
| CEM IIB – PFA | 0.07 | 26.31 | 3.38 | 1.1 | 21.86 | 6.81 | 22.05 | 6.81 |
| PG – PFA | 0.86 | 7.59 | 8.4 | 0.28 | 22.33 | 4.87 | 31.65 | 4.0 |

From Figure 5.1, the Pozament grout (PG) paste recorded the highest rate of heat evolution during the rapid initial hydration stage. The Portland cement (CEM IIB), Portland cement and pulverised fuel ash (CEM IIB-PFA) and, the Pozament and PFA (PG –PFA) paste followed in that order. As shown in the results, the PG-paste evolved 36.98J/gh heat energy after 0.108 hours (6.32 minutes), while, the CEM IIB-paste evolved 32.15J/gh heat after 0.146 hours (8.48 minutes). The inclusion of PFA was observed to retard the initial hydration of both the CEM IIB and PG pastes. The heat evolved by the CEM IIB-PFA paste was about 18% lower than that of the CEM IIB-paste while, the heat evolved by PG–PFA sample was about 79.5% lower than the PG-paste sample. In addition, the CEM IIB-PFA sample recorded its initial hydration peak after 0.072 hours (4.22 minutes), while the PG-PFA paste recorded its initial peak after 0.86 hours (51.32 minutes) the longest time taken by any of the cement samples investigated. This suggests that PFA had a higher retarding effect on the PG than on the CEM IIB.

During the second stage (stage II), all the cement samples experienced a rapid decrease in heat evolution, confirming a reduction in the hydration process. The heat evolved by CEM IIB–paste reduced by about 93%, while that evolved by the CEM IIB-PFA, the PG, and the PG-PFA pastes reduced by about 96, 98 and 96% respectively. The dormant

period was also observed to last over an hour for the PG– PFA paste, and about 0.5 hours for the other 3 cement samples, further confirming the effects of PFA on the PG paste.

The dormant period as mentioned earlier was followed by the rapid reaction period (Stage III) characterised by another rapid increase in heat evolution resulting in the main hydration peaks. During stage III, the CEM IIB-paste evolved 10.99J/gh of heat energy while, the PG-paste evolved 10.21J/gh energy. The use of PFA as Portland cement and/or Pozament grout admixture resulted in CEM IIB-PFA paste evolving lower (6.81J/gh) heat energy while, the PG-PFA paste also evolved lower (4.87 J/gh) energy. In addition, the main hydration peaks of CEM IIB and PG-pastes were attained after 9.43 and 13.50 hours respectively, while those of their respective equivalents with PFA were attained after 21.86 and 22.33 hours respectively.

Overall, the timing and heat evolved by the PG-paste was the highest recorded (only) during the first stage. During the other four stages, Portland cement demonstrated quicker and higher heat evolution compared to all other cement samples. The addition of PFA in equal proportions to CEM IIB and PG influenced the timing and heat evolved for all the five stages. The CEM IIB-PFA paste, although less affected by the addition of PFA compared with the PG–PFA, demonstrated quicker timing during the initial hydration stage relative to the CEM IIB-paste. The hydration time and rate of heat evolution of the CEM IIB-PFA were however lower than that of the CEM IIB-paste. The timings and rates of heat evolution of the PG–PFA paste were also lower compared to those of the PG-paste throughout the investigation.

The CEM IIB-PFA and PG-PFA pastes have shoulder peaks on the descending branch of the main hydration peaks. This may suggest the presence of secondary aluminate – phase, which may be because of the PFA reacting with calcium hydroxide, which would have otherwise coated the face of the aluminate phase, and/or the gradual release of mix water absorbed by the carbon in the PFA back into the solution. The factors, both promote the renewed dissolution of aluminate ions. The main hydration peaks were followed by the deceleration and steady stages where the hydration of the cement samples continued with a low rate of heat evolution for the entirety of the investigation. The hydration of the CEM IIB, PG and CEM IIB-PFA pastes appears to continue at almost a similar rate, while the hydration of the PG-PFA paste appears to be slightly lower than the other binding system during the steady state.

### 5.1.2 Total heat evolved during the hydration reactions

The rate and amount of energy evolved during cement hydration are closely contributory to the total heat evolved. The total heat evolved by the cement samples during the hydration process are shown in Figure 5.2. As with the rate of heat evolution, some test data relevant to the interpretation of the cumulative curves are presented in Table 5.2.

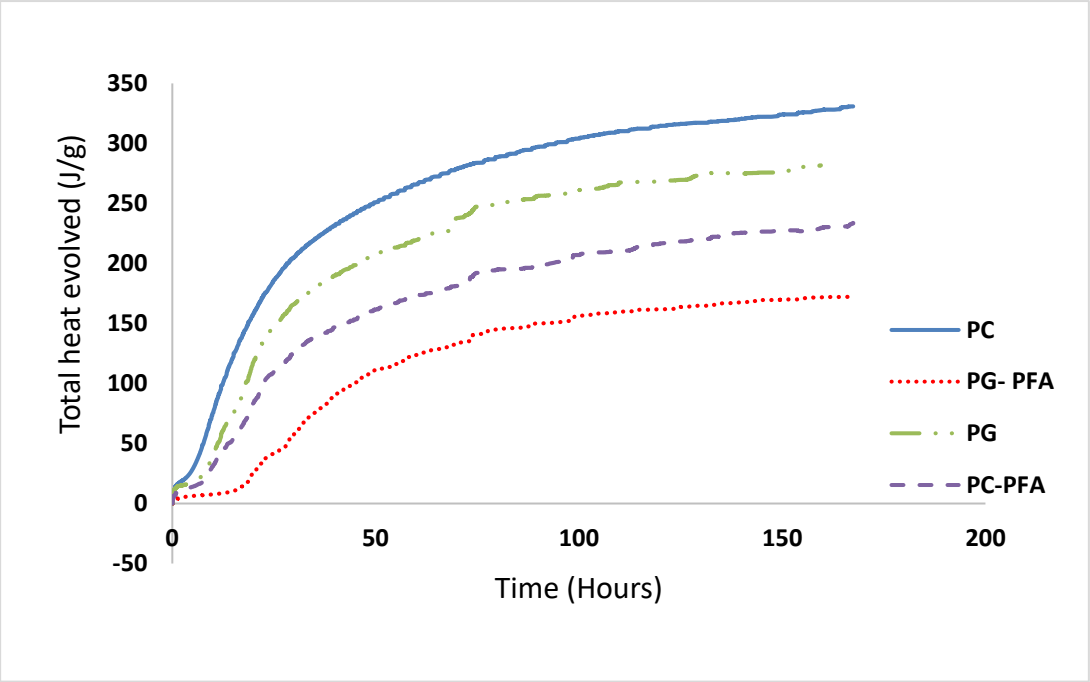


Figure 5.2: Cumulative heat vs. time behaviour of the binding materials.

Table 5.2: Cumulative heat evolved by the binding materials with time

| *Time (hours)* | *Total heat evolution (J/g)* | | | |
|---|---|---|---|---|
| | *Portland cement (CEM IIB)* | *Pozament grout (PG)* | *CEM IIB–PFA* | *PG-PFA* |
| 0.146 | 3.59 | 3.9 | 3.28 | 0.59 |
| 0.5 | 14.3 | 12.82 | 8.08 | 2.85 |
| 1 | 16.69 | 14.34 | 10.06 | 4.35 |
| 24 | 206 | 166 | 126.36 | 58.83 |
| 168 | 341.13 | 281.78 | 235.52 | 175.64 |

From Figure 5.2, the total heat evolved at any time during the hydration process was significantly higher for the cement and grout without PFA than their equivalents with PFA. The total heat evolved was highest for PG-paste during the very early stage of hydration (up to 0.45 hours). This may be related to the rapid increase in heat development observed during the initial hydration stage of the grout as shown by heat evolution curve Figure 5.1. After about 0.5 hours, the total heat evolved by CEM IIB-paste was observed to be higher in relation to all the other cement samples. The total heat emitted by the CEM IIB-paste after 30 minutes was 10% higher than that of the PG-paste. This sustained increase in the heat evolution of the CEM IIB paste was observed to be about 17% higher that of the grout after 168 hours (7 days). Likewise, the heat evolved by Portland cement (alone) sample was over 40% that of the CEM IIB- PFA paste after 0.5 hours and about 30% after 168 hours.

The variation in the total heat evolution was even more pronounced between the PG and PG-PFA paste. The total heat evolved by the PG-paste after 0.5 hours was at least four times that evolved by the PG-PFA paste. It reduced to about three times the total heat produced by the PG–PFA matrix after 24 hours and less than double after 168 hours. A sudden spike in the total heat evolved was observed for the hydrated, PG and PG–PFA binder around the 25-hour mark. This period coincides with the secondary main peak stage observed in the heat evolution curve for the PG-PFA paste. There was also a spike in the total heat evolved by the CEM IIB-PFA paste during the period corresponding to the secondary peak, although this was observed to be subtle relative to that of the PG–PFA sample. The total heat evolved by the CEM IIB, PG, CEM IIB-PFA and PG–PFA (in that order) continued to increase throughout the duration of the investigation.

In summary, the timing of the reactions and the energy evolved during the initial hydration stage suggest that the aluminate ($C_3A$) content of Pozament grout may be higher than that of the CEM IIB Portland cement. Relative to the other binding systems investigated, the PG-paste demonstrated quicker timing and evolved the most heat during the initial hydration stage associated with the dissolution of $C_3A$. $C_3A$ plays a major role on the property of fresh concrete (Mukesh et al., 2012). It helps in maintaining consistency and workability of concrete. As such, the PG-concrete is likely to be more workable in comparison to the CEM IIB-concrete. The addition of PFA retarded the hydration reaction of the aluminate phases in both the CEM IIB and PG pastes. PFA had

a higher retarding effect on the PG than on the CEM IIB, probably due to the presence of other retarding agents in the PG-binder.

At the water/binder ratio (0.5) investigated, the CEM IIB-pastes lost its plasticity quicker and evolved more energy than the PG-paste during the third hydration stage. This stage as previously mentioned is associated with the main peak and involve the hydration of the alite ($C_3S$) phase of the binding materials. From the results, it can be deduced that, the CEM IIB contains higher amount of $C_3S$ or the presence of retarders in the PG may have reduced the hydration reaction of the $C_3S$ during this stage. Either way, the CEM IIB-paste is likely to produce concrete with higher early age strength relative to the PG-paste. As observed during the initial hydration stage, the addition of PFA also retarded the hydration reaction observed during the third stage for the CEM IIB-PFA and PG-PFA pastes. Again, the addition of PFA appears to have higher retarding effect on the PG-PFA paste.

The shoulder peaks observed after the main peaks during the hydration of CEM IIB-PFA and PG-PFA pastes suggest that the addition of PFA prolonged the dissolution of the $C_3A$ phase. This may be due to the introduction of more $C_3A$ by the fly ash or the slow release of water absorbed by the carbon content of the ash. The secondary aluminate phase may cause spontaneous over heating in large masses of concrete or may induce sulphate attacks in mature concrete. In sulphate rich environment, the excess aluminate may react with sulphates (in solution) to form expansive ettringite.

## 5.2 STANDARD CONSISTENCY AND SETTING TIME

The result of the standard consistency and setting times of the different binding materials used as solidifying reagents during the encapsulation process are shown in Table 5.3.

Table 5.3: Consistency and setting times of the cementing materials

| *Encapsulating matrix (binding materials)* | *Consistency (w/c ratio)* | *Initial setting time (Minutes)* | *Final setting time (Minutes)* | *Flow value (mm)* |
|---|---|---|---|---|
| Portland cement (CEM IIB) | 0.31 | 160 | 380 | 190 |
| Pozament grout (PG) | 0.17 | 40 | 220 | 220 |
| CEM IIB-PFA | 0.37 | 240 | 620 | 175 |
| PG-PFA | 0.33 | 340 | 500 | 185 |

The Portland cement and Pozament paste, have standard consistencies (water/binder ratios) of 0.31 and 0.17 respectively. The addition of PFA to Portland cement increased the standard consistency of the cement sample to 0.37, while adding PFA to the Pozament grout increased the standard consistency of the grout to 0.33. The PG paste was observed during mixing to have higher fluidity and mobility in comparison to the CEM IIB (CEM IIB) paste. Similarly, the inclusion of PFA was observed to reduce the fluidity/mobility of both CEM IIB-PFA and PG–PFA paste. This may be attributed to the high carbon content of the PFA increasing the water demand of the CEM IIB-PFA or PG-PFA binding materials. The PG–PFA paste showed better flow in comparison to the CEM IIB-PFA paste. A flow analysis carried out to assess the fluidity of the pastes confirmed the visual observation. The result of the investigation is shown in Figure 5.3 (a-d).

The initial setting time was taken as the time between the moment water was added to the binding materials to the time when the paste starts to lose its plasticity. The results shown in Table 5.3 indicate that, the initial setting time of the cements without PFA were lower than those with PFA. The PG paste lost its plasticity after 40 minutes, while PG–PFA paste lost its plasticity after 340 minutes. The Portland cement and CEM IIB-PFA pastes recorded initial setting times of 160 and 240 minutes respectively.

The final setting times were the time taken for the wet paste to completely lose its plasticity and attain a level of firmness to resist applied pressure to a certain degree. The results presented in Table 5.3 shows that the Portland cement and Pozament pastes recorded final setting times of 380 and 220 minutes respectively, while the CEM IIB-PFA and PG–PFA pastes recorded final setting times of 620 and 500 minutes respectively

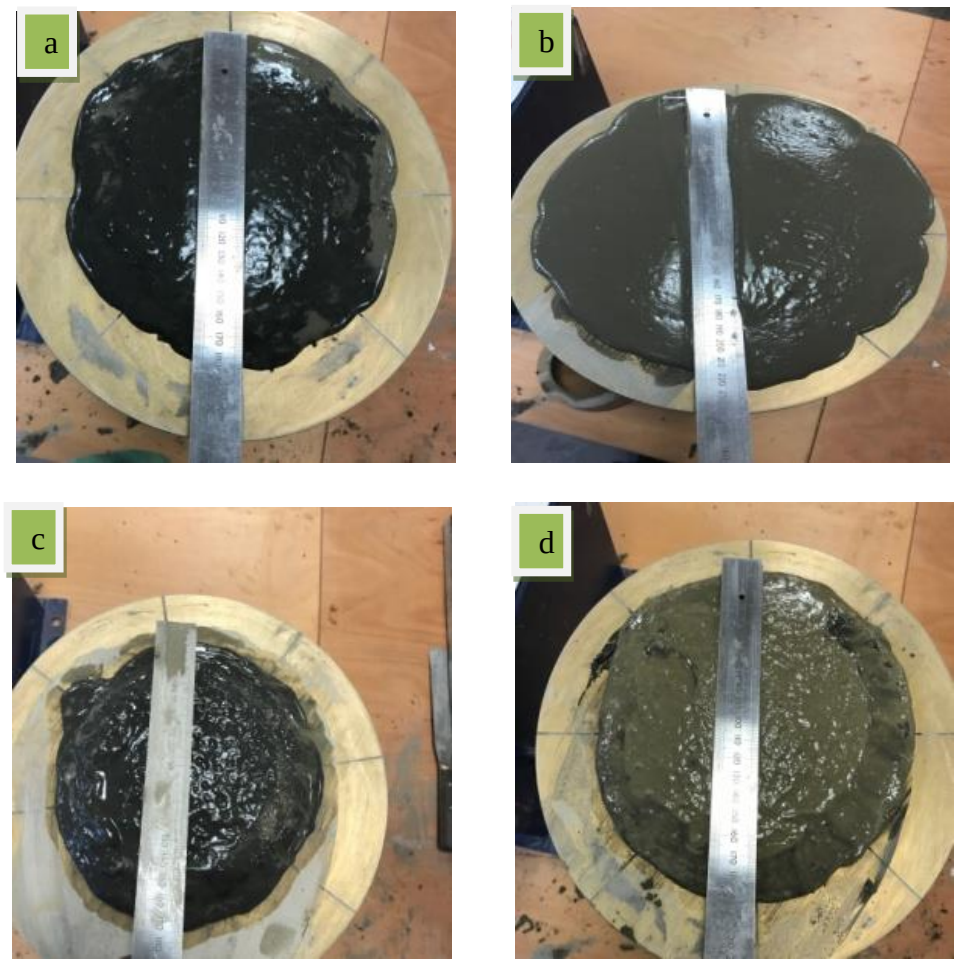


Figure 5.3: Flow analysis result of (a) Portland cement paste - 190 mm, (a) Pozament paste - 220 mm, (c) Portland cement - PFA sample - 175 mm and (d) PG-PFA paste - 185 mm

## 5.3 PROPERTIES OF THE FRESH CONCRETE MIXTURES

### 5.3.1 Workability

#### *5.3.1.1 Slump and compaction index of the CEM IIB-concrete system*

The results of the workability assessment carried out on the CEM IIB-concrete, CEM IIB-encapsulated plastic concrete and the CEM IIB-PFA encapsulated plastic concrete mixtures are presented in Table 5.4. PFA as mentioned in the mix design (Chapter 4, Section 4.3.1) was considered for use as both a mineral admixture and a micro-filler. The specified slump class were based on BS EN 206:2013+A1:2016 and BS EN 8500–1:2015, and only applicable to slump values greater than 10 mm.

Table 5.4: Workability assessment of the CEM IIB-concrete system

| *Mix ref* | *Mix ratio* | *w/b ratio* | *a/b ratio* | *Slump* | | | *Compaction index* | |
|---|---|---|---|---|---|---|---|---|
| | | | | *(mm)* | *Class* | *Type* | *Index (mm)* | *Compaction Class* |
| C1 | 1:2:3 | 0.5 | 5/1 | 45 | S2 | True | 1.25 | $C_{.I}2$ |
| C2 | 1:2:3 | 0.6 | 5/1 | 55 | S2 | True | 1.21 | $C_{.I}2$ |
| C3 | 1:2:4 | 0.6 | 6/1 | 50 | S2 | True | 1.24 | $C_{.I}2$ |
| CP1 | 1:2:3 | 0.5 | 5/1 | 0 | - | No slump | 1.42 | $C_{.I}1$ |
| CP2 | 1:2:3 | 0.6 | 5/1 | 0 | - | No slump | 1.36 | $C_{.I}1$ |
| CP3 | 1:2:4 | 0.6 | 6/1 | 0 | - | No slump | 1.44 | $C_{.I}1$ |
| CPP1 | 1:1:4:6 | 0.5 | 5/1 | - | - | Collapse | 1.33 | $C_{.I}1$ |
| CPP2 | 1:1:4:6 | 0.6 | 5/1 | - | - | Collapse | 1.29 | $C_{.I}1$ |
| CPP3 | 1:1:4:8 | 0.6 | 6/1 | - | - | Collapse | 1.35 | $C_{.I}1$ |
| $CPP1_f$ | 1:1:2:3 | 0.5 | 5/1 | 20 | S1 | True | 1.27 | $C_{.I}1$ |
| $CPP2_f$ | 1:1:2:3 | 0.6 | 5/1 | - | - | Shear | 1.07 | $C_{.I}3$ |
| $CPP3_f$ | 1:1:2:3 | 0.6 | 6/1 | - | - | Shear | 1.18 | $C_{.I}2$ |

*C1-3 - CEM IIB- concrete; CP1-3 – CEM IIB - encapsulated plastic concrete; CPP1-3 – CEM IIB-PFA encapsulated plastic concrete (PFA mineral admixture), $CPP_f1$-3 – CEM IIB-PFA encapsulated plastic concrete (PFA micro-filler). *w/b – water/binder ratio. a/b – aggregate/binder ratio, *S1 and $C_I1$- low workability, S2 and $C_I2$ - medium workability, $C_I3$ – high workability (BS 8500 and 206).

The result in Table 5.4 shows that only the CEM IIB-concrete mixtures (C1, C2 and C3) and mix CPP1$_f$, an encapsulated plastic mix utilising PFA as mineral filler recorded true slump values. The Slump types observed in the ongoing work are shown in Figure 5.4.


Figure 5.4: Slump types, a) - true slump, b) - shear slump, c) - collapsed slump and d) – no slump

The CEM IIB–concrete trio C1, C2 and C3 recorded slump values ranging between 45-55 mm, while mix CPP1$_f$ recorded a slump of 20 mm. The slump result indicates that the

workability of the CEM IIB-concrete mixtures increased with increase in water/binder ratio but decreased with increase in aggregate/binder ratio at the higher water/cement ratio. In addition to the slump result, the workability of the CEM IIB-concrete mixtures based on the compaction index also confirmed an increase in workability with increased water content and decreased workability with increased aggregate contents.

The CEM IIB - encapsulated plastic mixtures (CP1, CP2 and CP3) all recorded zero-millimetre slump values. That is, they all experienced no change (reduction) in height when the test cone was removed during the slump investigation (Figure 5.7). The workability assessment made from the compaction index however suggests that increasing the water/binder ratio from 0.5 to 0.6 increased the workability of the CEM IIB-encapsulated plastic concrete mixtures, while increasing the aggregate/binder ratio from 5/1 to 6/1 at the higher water/binder ratio led to a decrease in workability. The first mix 'CP1' recorded a compaction index of 1.42 mm while, the second and third mixtures recorded compaction indexes of 1.36 and 1.44 mm respectively. These results (slump and compaction index) suggested that the three CEM IIB-encapsulated concrete mixtures were not as workable as their CEM IIB-concrete equivalents.

Similar to the three mixtures from the preceding encapsulated concrete, the encapsulated plastic mixtures with PFA included as a mineral admixture (CPP1, CPP2 and CPP3) recorded no slump values. They all recorded collapsed -slumps as shown in Figure 5.4. Like the CEM IIB-encapsulated plastic concrete mixtures, an increase in the water/cement ratio increased the workability of the CEM IIB- PFA mix CPP1, CPP2 and CPP3, while subsequent increase in aggregate/binder ratio (at w/b, 0.6) decreased the workability of the concrete mixtures. The mixtures (CPP1-3) recorded compaction indices within the range of 1.29 – 1.35 mm. Efforts at optimising the performance of the plastic concrete by incorporating PFA as micro-filler rather than a mineral admixture increased the workability of the fresh plastic concrete. The first mixture ($CPP1_f$,), with the lower water/binder ratio (0.5), as mentioned earlier recorded a true slump of 20 mm, while the other two mixtures ($CPP2_f$ and $CPP3_f$) with w/b 0.6 but different aggregate/binder ratios both demonstrated shear slumps. Based on the compaction indices, mix $CPP2_f$ demonstrated an increased workability relative to $CPP3_f$. The former mix recorded a compaction index of 1.07 mm, while the latter mix recorded a compaction index of 1.18 mm. The compaction index of 1.07mm recorded by mix $CPP2_f$ was the

lowest recorded for any of the encapsulated concrete mixtures investigated in the ongoing work. As with the case of the workability of the other two encapsulated plastic concrete types investigated in this system, the workability of the CEM IIB-encapsulated plastic concrete mixtures with PFA micro-filler increased with increase in water/binder ratio and decreased slightly with increase in aggregate/binder ratio.

Finally, when specified according to BS EN 206:2013+A1:2016 and BS 8500, the CEM IIB-concrete mixtures can be classified into slump consistency class S2 (that is, concrete mixtures with medium range workability), while the encapsulated plastic concrete mixtures based on the compaction index can be classified as low – medium apparent workability concrete. The usage concrete with low-medium class workability includes kerb bedding and backing, wall/strip footings (house and garage floors), cast in-situ paving (drives and domestic parking) and sliding concrete formwork (ICF blocks). Powerful vibration and compaction in thin layers may however be necessary for the encapsulated plastic concrete mixtures

#### *5.3.1.2 Slump and compaction index test of the PG-concrete system*

The results of the workability assessment for the PG-concrete system are shown in Table 5.5. As with the CEM IIB-concrete system, the result presented include the slump and compaction index, the slump type and the workability classifications based on BS 8500 – 1:2015 + A1:2016 and BS EN 206:2013+A1:2016. PFA was also used as both a mineral admixture and a micro-filler, while the slump classes were as specified in BS 8500 – 1:2015 + A1:2016 and only applicable to slump values greater than 10 mm.

Table 5.5: Workability assessment of the PG-concrete systems

| *Mix ref* | *Mix ratio* | *w/b ratio* | *a/b ratio* | *Slump* | | | *Compaction* | |
|---|---|---|---|---|---|---|---|---|
| | | | | *(mm)* | *Type* | *Consistency class* | *Index (mm)* | *Consistency Class* |
| P1 | 1:2:3 | 0.5 | 5/1 | 15 | True | S1 | 1.33 | C.$_I$1 |
| P2 | 1:2:3 | 0.6 | 5/1 | 60 | True | S2 | 1.18 | C.$_I$2 |
| P3 | 1:2:4 | 0.6 | 6/1 | 25 | True | S2 | 1.25 | C.$_I$2 |
| PP1 | 1:2:3 | 0.5 | 5/1 | 0 | Collapse | - | 1.45 | C.$_I$1 |
| PP2 | 1:2:3 | 0.6 | 5/1 | 0 | Collapse | - | 1.38 | C.$_I$1 |
| PP3 | 1:2:4 | 0.6 | 6/1 | 0 | Collapse | - | 1.47 | C.$_I$1 |
| PPP1 | 1:1:4:6 | 0.5 | 5/1 | - | Collapse | - | 1.38 | C.$_I$1 |
| PPP2 | 1:1:4:6 | 0.6 | 5/1 | - | Collapse | - | 1.19 | C.$_I$2 |
| PPP3 | 1:1:4:8 | 0.6 | 6/1 | - | Collapse | - | 1.24 | C.$_I$2 |
| PPP1$_f$ | 1:1:2:3 | 0.5 | 5/1 | 20 | True | S1 | 1.36 | C.$_I$1 |
| PPP2$_f$ | 1:1:2:3 | 0.6 | 5/1 | - | Collapse | - | 1.08 | C.$_I$3 |
| PPP3$_f$ | 1:1:2:3 | 0.6 | 6/1 | - | Shear | - | 1.18 | C.$_I$2 |

*(P1-3)-PG-concrete; (PP1-3) – PG-encapsulated plastic concrete; (PPP1-3) – PG-PFA encapsulated plastic concrete, (PPP1-3) – PG-encapsulated plastic concrete with PFA considered as micro-filler. *w/b – water/binder ratio. a/b – aggregate/binder ratio. *S1 and C.$_I$1- low workability, S2 and C.$_I$2 - medium workability, C.$_I$3 – high workability (BS 8500 and 206).

As in the case of the CEM IIB-concrete mixtures (C1-3), the results in Table 5.5 indicate that only four of the twelve mix compositions with PG-binder recorded true slumps. The three PG-concrete mixtures (P1, P2 and P3) recorded slumps of 15, 60 and 25 mm, and compaction index values 1.33, 1.18 and 1.25 mm respectively, while mix PPP1$_f$, (an encapsulated plastic mix with PFA used as micro filler) recorded a 20-mm slump and a compaction index of 1.36 mm. The encapsulated plastic mixture (PPP1$_f$) maintained the same mix composition as the CEM IIB-encapsulated system with the True slump value (CPP1$_f$). All the remaining PG-encapsulated plastic concrete mixtures recorded either collapse or shear slumps. Overall, the workability of the all the concrete mixtures from PG–concrete system (like the CEM IIB equivalents), increased with increase in water/binder ratio, but decreased with increase in aggregate/binder ratio.

The PG-encapsulated plastic mixtures (PP1, PP2 and PP3) all recorded collapsed slumps. Hence, the workability assessment was made from the compaction index. In comparison to the corresponding CEM IIB-encapsulated plastic concrete mixtures (CP1-3), the PG-encapsulated plastic concrete equivalents (PP1-3) recorded lower compaction indices, which indicate a decrease in workability. The PG–encapsulated plastic concrete mixtures (with or without PFA) were also observed to have higher flow in comparison to their CEM IIB counterparts. The high flow of the PG–encapsulated plastic concrete mixtures resulted in leaching of acidic water from the fresh concrete as shown in Figure 5.5.

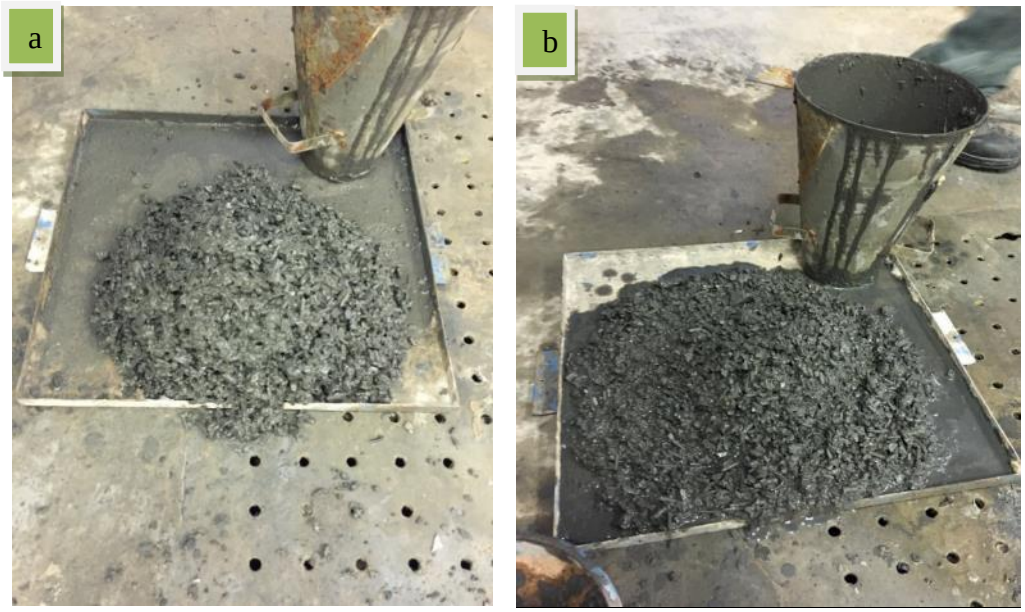


Figure 5.5: Photographic illustration of the encapsulated plastic concrete showing (a) the less fluid CEM IIB- encapsulated plastic concrete mixture and (b) its PG equivalent with high fluidity.

In addition, as with the CEM IIB equivalents, all the PG encapsulated plastic concrete mixtures with PFA included as a mineral admixture (PPP1, PPP2 and PPP3) recorded collapsed slumps. Nonetheless, the workability of the mixtures observed from the compaction index increased with increase in consistency (w/b ratio) but decreased with increase in aggregate/binder ratio. The mixtures (PPP1, PPP2 and PPP3) recorded compaction indices of 1.38, 1.19 and 1.24 mm respectively. These represent a decrease

in workability when compared to the equivalent CEM IIB-PFA encapsulated plastic concrete mixtures (CPP1, CPP2 and CPP3)

Switching the use of PFA from mineral admixture to micro-filler in $PPP1_f$, $PPP2_f$ and $PPP3_f$, resulted in the mixture with lower water/binder ratio ($PPP1_f$), having a true slump of 20 mm. When the water/binder ratio was increased to 0.6 in mix $PPP2_f$, the encapsulated plastic demonstrated a collapse slump, while maintaining the water/binder ratio at 0.6 but increasing the aggregate/binder ratio in mix $PPP3_f$ led to a shear slump. The compaction index indicates that, the mix with the collapsed slump ($PPP2_f$) demonstrated a higher workability compared to the mix with shear slump ($PPP3_f$). Mix $PPP2_f$ recorded the lowest compaction index (1.08mm) of all the PG-encapsulated plastic concrete mixtures investigated. The three mixtures ($PPP1_f$, $PPP2_f$ and $PPP3_f$) demonstrated increased workability when compared to the PG-encapsulated plastic concrete mixtures (PP1, PP2 and PP3) or PG–PFA encapsulated plastic mixtures (PPP1, PPP2 and PPP3) but slightly decrease in workability when compared to the CEM IIB equivalents ($CPP1_f$, $CPP2_f$ and $CPP3_f$).

When specified according to BS EN 206 and BS 8500, using both the slump values and compaction indices, mix P1, PP1-3, PPP1 and $PPP1_f$ demonstrated low range workability, while mix P2, P3, PPP2 – 3 and $PPP3_f$ demonstrated medium range workability and mix $PPP2_f$ demonstrated high range workability.

## 5.4 PHYSICAL PROPERTIES OF THE HYDRATED CONCRETE SYSTEM

### 5.4.1 CEM IIB-concrete system

The details of the physical properties of the test specimens prepared from the optimised mix compositions with Portland cement (CEM IIB) as the primary binding material are shown in Table 5.6. The results presented for each evaluated property are the average obtained from three test specimens per mix composition, water cured for 28 days.

Table 5.6: Physical properties of the CEM IIB-concrete system

| *CEM IIB-concrete system* | *Mix ref* | *Mix ratio* | *w/b ratio* | *a/b ratio* | *Density ($kg/m^3$)* | *Porosity (%)* | *Water absorption (%)* |
|---|---|---|---|---|---|---|---|
| CEM IIB-concrete | C1 | 1:2:3 | 0.5 | 5/1 | 2440 | 8.9 | 3.7 |
| | C2 | 1:2:3 | 0.6 | 5/1 | 2400 | 9.0 | 3.7 |
| | C3 | 1:2:4 | 0.6 | 6/1 | 2390 | 9.3 | 3.8 |
| CEM IIB - encapsulated plastic concrete | CP1 | 1:2:3 | 0.5 | 5/1 | 1600 | 26.0 | 21 |
| | CP2 | 1:2:3 | 0.6 | 5/1 | 1590 | 26.7 | 21.7 |
| | CP3 | 1:2:4 | 0.6 | 6/1 | 1520 | 27.0 | 22 |
| CEM IIB-PFA encapsulated plastic concrete (PFA used as mineral admixture) | CPP1 | 1:1:4:6 | 0.5 | 5/1 | 1630 | 18.1 | 12.5 |
| | CPP2 | 1:1:4:6 | 0.6 | 5/1 | 1600 | 18.4 | 12.8 |
| | CPP3 | 1:1:4:8 | 0.6 | 6/1 | 1600 | 19.4 | 13.9 |
| CEM IIB-PFA encapsulated plastic concrete (PFA used as micro-filler). | $CPP1_f$ | 1:1:2:3 | 0.5 | 5/1 | 1640 | 12.2 | 8.04 |
| | $CPP2_f$ | 1:1:2:3 | 0.6 | 5/1 | 1590 | 13.8 | 9.67 |
| | $CPP3_f$ | 1:1:2:3 | 0.6 | 6/1 | 1570 | 15.1 | 11.3 |

#### *5.4.1.1 Density*

From Table 5.6, the densities of the cubic test specimens made with Portland cement (CEM IIB) and natural aggregates (river sand and 10 mm limestone aggregates) were within the ranges of 2390 – 2440 $kg/m^3$, while those made from CEM IIB (with or without PFA) and lightweight aggregates (FBA and 0-10 mm plastic aggregates) were between 1520 – 1640 $kg/m^3$. The measured densities of the hydrated encapsulated plastic test

specimens all fall within the specified density range for lightweight concrete (BS EN 206:2013+A1:2016). The results in Table 5.6 also indicate that the density of the encapsulated plastic mixtures decreased when the water/binder and aggregate/binder ratios were increased. This may be due to the increase in void volumes. When PFA was added to the encapsulated plastic mixtures (as either mineral admixture or micro – filler) the densities of the mixtures (CPP1-3 or CPP$1_f$-$3_f$) marginally increased relative to those recorded by the CEM IIB-encapsulated mixtures without PFA. At high water/binder ratio (0.6), the mixtures utilising PFA as mineral admixtures (CEM IIB-PFA encapsulated plastic concrete mixtures) demonstrated higher densities relative to the CEM IIB-encapsulated plastic mixtures with PFA micro-filler.

#### *5.4.1.2 Porosity (void percentage)*

The details of the porosity (void percentages) of the cubic test specimens presented in Table 5.6, shows that the porosity of the mixtures from the CEM IIB-concrete (C1-3), CEM IIB-encapsulated plastic concrete (CP1 -3), CEM IIB-PFA encapsulated plastic concrete with PFA utilised as mineral admixture (CPP1-3) and CEM IIB-PFA encapsulated plastic concrete with PFA used as micro-filler (CPP$1_f$- $3_f$). The result also indicated that the CEM IIB-concrete mixtures (C1 -3), were the least porous with void percentages of 8.9, 9 and 9.3% respectively, while the CEM IIB-encapsulated plastic mixtures (CP1-3) recorded void percentages of 26, 26.7 and 27% respectively. The inclusion of PFA in the plastic mixtures as observed in Table 5.6 led to a reduction in porosity. The blends from the encapsulated plastic mixtures utilising PFA as a mineral admixture (CPP1-3) all recorded over 28% reduction in porosity relative to the CEM IIB - encapsulated plastic mixtures, while the blends from the encapsulated plastic mixtures with PFA micro-filler (CPP$1_f$-$3_f$) demonstrated over 43% reduction in porosity, also relative to the equivalent CEM IIB-encapsulated plastic blends. The hydrated CEM IIB-encapsulated plastic mixtures were the most pervious of the entire CEM IIB-concrete system investigated, while the CEM IIB-PFA encapsulated plastic mixtures with PFA used as micro-filler recorded the lowest porosity for all the encapsulated plastic concrete investigated.

#### *5.4.1.3 Water absorption*

The water absorption results from Table 5.6 indicate that, when the test specimens were dried in an oven at 105$^{o}$C to a constant mass before being completely immersed in water

for 30 minutes at room temperature, the denser CEM IIB-concrete system with relatively lower porosity absorbed the least amount of water. The concrete mixtures C1, C2 and C3 as shown in the table recorded water absorption percentages of 3.7, 3.7 and 3.8 respectively. Meanwhile, the more pervious lightweight encapsulated plastic test specimens absorbed considerably higher volumes of water in relation to the reference concrete test specimens. The test specimens from the CEM IIB-encapsulated plastic concrete absorbed the most amount of water amongst all the specimens tested. When PFA was included in the encapsulated plastic mix either as mineral admixtures or as micro-filler, the water absorption appears to reduce. The CEM IIB-encapsulated plastic mixtures were shown to demonstrate the lower water absorption percentages.

The results also indicate that the water absorption of the encapsulated plastic concrete increased with increase in both water/binder and aggregate/binder ratios, while the water absorption of the CEM IIB-concrete mixtures remained the same following the increase in water to binder ratio but increased when the aggregate/binder ratio was increased.

### 5.4.2 PG-concrete system

The details of the physical performance of the test specimens prepared from the optimised mix compositions with Pozament grout as the primary solidifying reagent are shown in Table 5.7. Like the CEM IIB-concrete, the results presented for the evaluated properties are the average obtained from three water cured test specimens per mix composition.

Table 5.7: Physical properties of the PG-concrete systems

| *PG-concrete system* | *Mix ref* | *Mix ratio* | *w/b ratio* | *a/b ratio* | Density ($kg/m^3$) | Porosity (%) | Water absorption (%) |
|---|---|---|---|---|---|---|---|
| PG-concrete | P1 | 1:2:3 | 0.5 | 5/1 | 2390 | 11.7 | 5.1 |
| | P2 | 1:2:3 | 0.6 | 5/1 | 2370 | 13.6 | 6.2 |
| | P3 | 1:2:4 | 0.6 | 6/1 | 2360 | 13.9 | 7.1 |
| PG-encapsulated plastic concrete | PP1 | 1:2:3 | 0.5 | 5/1 | 1490 | 29.2 | 21.2 |
| | PP2 | 1:2:3 | 0.6 | 5/1 | 1460 | 30.7 | 22 |
| | PP3 | 1:2:4 | 0.6 | 6/1 | 1420 | 31.6 | 24 |
| PG-PFA encapsulated plastic concrete (PFA used as mineral admixture) | PPP1 | 1:1:4:6 | 0.5 | 5/1 | 1590 | 19.3 | 13.2 |
| | PPP2 | 1:1:4:6 | 0.6 | 5/1 | 1580 | 19.5 | 13.4 |
| | PPP3 | 1:1:4:8 | 0.6 | 6/1 | 1560 | 20.1 | 14.3 |
| PG-PFA encapsulated plastic concrete (PFA used as micro-filler). | $PPP1_f$ | 1:1:2:3 | 0.5 | 5/1 | 1600 | 13.0 | 9.1 |
| | $PPP2_f$ | 1:1:2:3 | 0.6 | 5/1 | 1590 | 15.7 | 11.1 |
| | $PPP3_f$ | 1:1:2:3 | 0.6 | 6/1 | 1550 | 21.2 | 15.4 |

#### *5.4.2.1 Density*

As with the CEM IIB-concrete, the test specimens from the PG-concrete mixtures recorded higher densities relative to their respective PG-encapsulated plastic equivalents. The conventional PG-concrete (P1 – 3) recorded densities ranging from 2360-2390 $kg/m^3$, while the encapsulated plastic concrete (including those with PFA) recorded densities ranging between 1420-1600 $kg/m^3$. The average densities of the encapsulated plastic test specimens utilising PFA as mineral admixture or micro-filler were 6–11% higher than their respective equivalents without PFA. Test specimens from the mixtures

utilising PFA as mineral admixture (PPP1, PPP2 and PPP3) recorded density values of 1590, 1580 and 1560 kg/m$^3$ respectively, while the specimens from the mixtures utilising PFA as micro-filler (PPP1$_f$, PPP2$_f$ and PPP3$_f$) recorded density values of 1600, 1590 and 1550 kg/m$^3$ respectively.

In comparison with the CEM IIB equivalents, the PG-(conventional and encapsulated plastic) concrete all recorded lower densities except PPP2$_f$. As with its CEM IIB equivalent 'CPP2$_f$', mix PPP2$_f$ recorded a density of 1590kg/m$^3$. Furthermore, as with the CEM IIB-equivalents, the densities of the PG- (conventional or encapsulated plastic) concrete decreased when both the water/binder and aggregate/binder ratios were increased. A comparative graph showing the densities of the mixtures from both the CEM IIB and PG-concrete systems measured in the current work is provided in Figure 5.6.

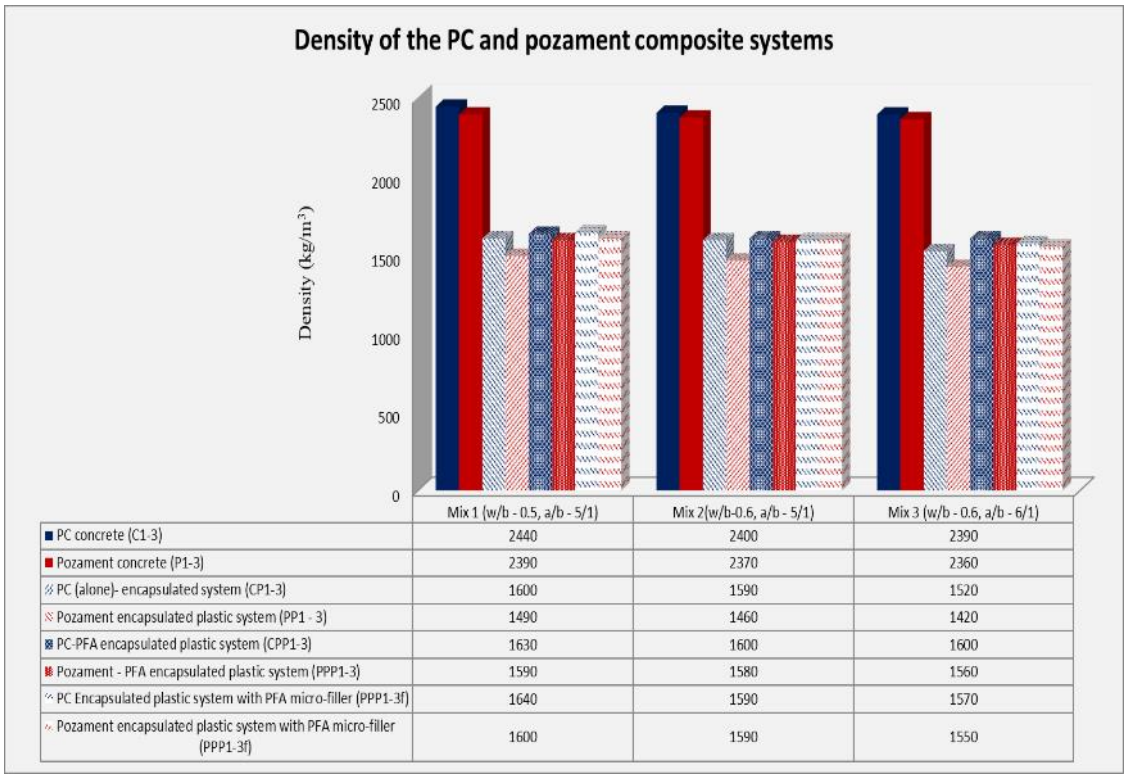


| | Mix 1 (w/b - 0.5, a/b - 5/1) | Mix 2(w/b-0.6, a/b - 5/1) | Mix 3 (w/b - 0.6, a/b - 6/1) |
|---|---|---|---|
| PC concrete (C1-3) | 2440 | 2400 | 2390 |
| Pozament concrete (P1-3) | 2390 | 2370 | 2360 |
| PC (alone)- encapsulated system (CP1-3) | 1600 | 1590 | 1520 |
| Pozament encapsulated plastic system (PP1 - 3) | 1490 | 1460 | 1420 |
| PC-PFA encapsulated plastic system (CPP1-3) | 1630 | 1600 | 1600 |
| Pozament - PFA encapsulated plastic system (PPP1-3) | 1590 | 1580 | 1560 |
| PC Encapsulated plastic system with PFA micro-filler (PPP1-3f) | 1640 | 1590 | 1570 |
| Pozament encapsulated plastic system with PFA micro-filler (PPP1-3f) | 1600 | 1590 | 1550 |

Figure 5.6: Density of the CEM IIB and PG-concrete systems investigated in the current work

### *5.4.2.2. Porosity*

From the results in Table 5.8, the conventional PG-concrete (P1-3) recorded the lowest percentage porosities, while PG-encapsulated plastic concrete (PP1-3) recorded the highest. The inclusion of PFA in the encapsulated plastic mixtures reduced the porosity of the hydrated test specimens. The encapsulated plastic concrete with PFA recorded lower porosities relative to the encapsulated plastic concrete with PG-binder used on its own. The porosities of the concrete utilising PFA as mineral additive (PPP1-PPP3) were higher than those of the mixtures with PFA used as micro-filler ($PPP_1f$-$PPP3_f$). Furthermore, the porosity of the test specimens from the PG-conventional and encapsulated plastic concrete increased when the water/binder and aggregate/binder ratios were increased. In comparison to the CEM IIB – equivalents, the PG- (conventional and encapsulated plastic) concrete demonstrated higher porosity. A comparative graph showing the behaviour of the mixtures from both the CEM IIB and PG-concrete systems during the investigation is provided in Figure 5.7.

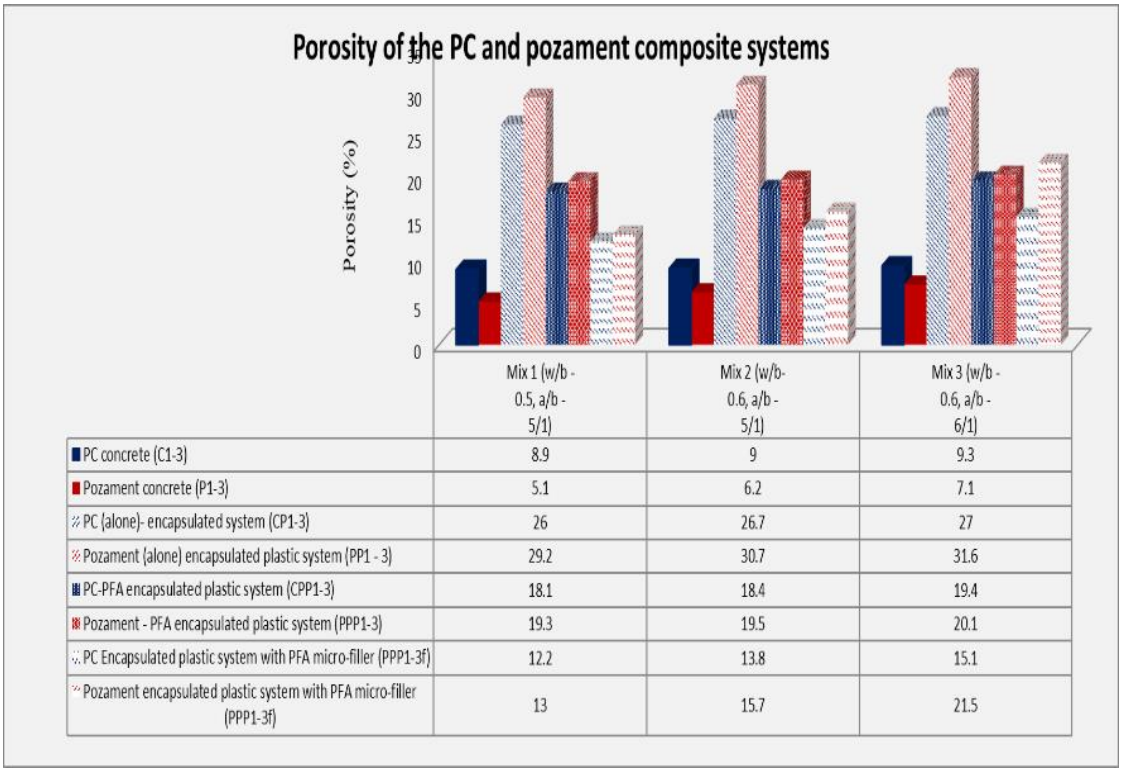


| | Mix 1 (w/b - 0.5, a/b - 5/1) | Mix 2 (w/b- 0.6, a/b - 5/1) | Mix 3 (w/b - 0.6, a/b - 6/1) |
|---|---|---|---|
| PC concrete (C1-3) | 8.9 | 9 | 9.3 |
| Pozament concrete (P1-3) | 5.1 | 6.2 | 7.1 |
| PC (alone)- encapsulated system (CP1-3) | 26 | 26.7 | 27 |
| Pozament (alone) encapsulated plastic system (PP1 - 3) | 29.2 | 30.7 | 31.6 |
| PC-PFA encapsulated plastic system (CPP1-3) | 18.1 | 18.4 | 19.4 |
| Pozament - PFA encapsulated plastic system (PPP1-3) | 19.3 | 19.5 | 20.1 |
| PC Encapsulated plastic system with PFA micro-filler (PPP1-3f) | 12.2 | 13.8 | 15.1 |
| Pozament encapsulated plastic system with PFA micro-filler (PPP1-3f) | 13 | 15.7 | 21.5 |

Figure 5.7: Porosity of the CEM IIB and PG-concrete of the systems investigated in the current work

### *5.4.2.3 Water absorption*

The results shown in Table 5.7 indicate that the replacement of conventional aggregates (river sand and 10 mm limestone aggregates) with recycled aggregates (FBA and 0-10mm plastic aggregates) decreased the water absorption of the conventional PG-concrete by over 70%. As with the other measured physical properties, the water absorption (%) of the encapsulated plastic concrete decreased with the inclusion of PFA. The inclusion of PFA as mineral admixtures led to approximately 40% reduction in the water absorption capacity of the PG–encapsulated plastic concrete (PPP1, PPP2 and PPP3). Likewise, the water absorption percentages of the PG-encapsulated plastic concrete decreased by 36 – 57% when PFA was included as a micro-filler. Overall, the water absorption (%) of the PG-concrete (conventional and encapsulated plastic) increased with increase in both water/binder and aggregate/binder ratios. In comparison to the CEM IIB-concrete (conventional or encapsulated plastic), the PG-equivalents recorded higher absorption (%). A comparative graph showing the CEM IIB and PG-concrete is shown in Figure 5.8.

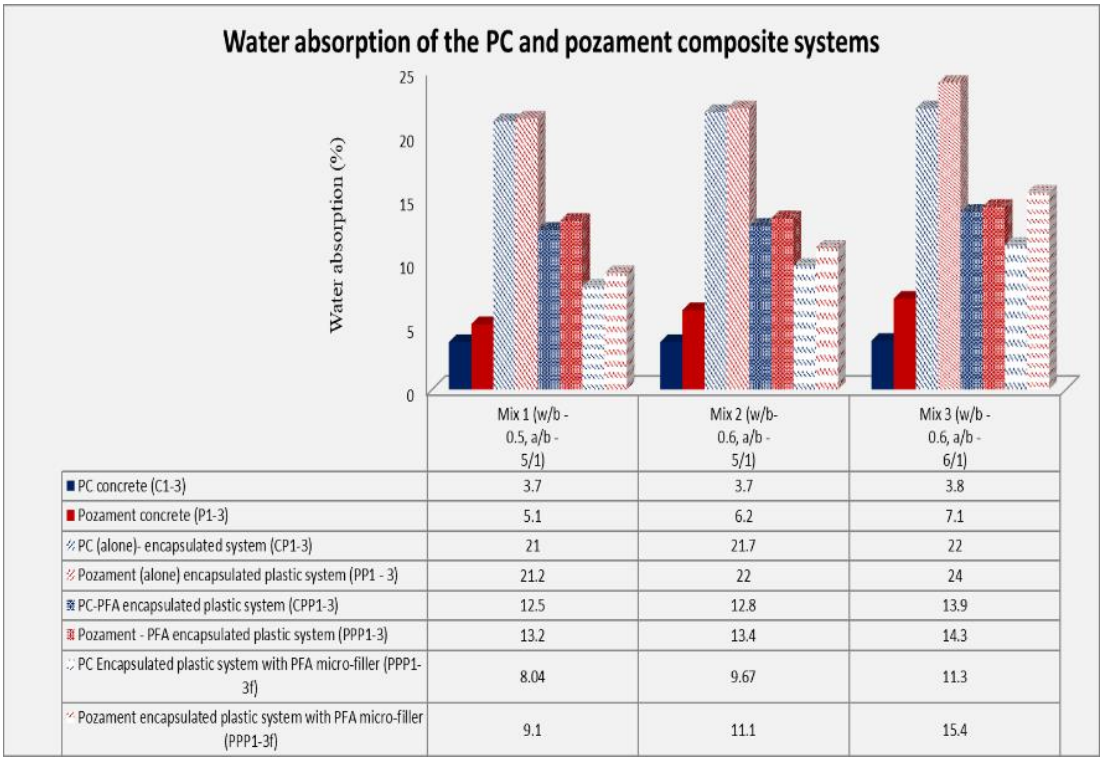


| | Mix 1 (w/b - 0.5, a/b - 5/1) | Mix 2 (w/b- 0.6, a/b - 5/1) | Mix 3 (w/b - 0.6, a/b - 6/1) |
|---|---|---|---|
| PC concrete (C1-3) | 3.7 | 3.7 | 3.8 |
| Pozament concrete (P1-3) | 5.1 | 6.2 | 7.1 |
| PC (alone)- encapsulated system (CP1-3) | 21 | 21.7 | 22 |
| Pozament (alone) encapsulated plastic system (PP1 - 3) | 21.2 | 22 | 24 |
| PC-PFA encapsulated plastic system (CPP1-3) | 12.5 | 12.8 | 13.9 |
| Pozament - PFA encapsulated plastic system (PPP1-3) | 13.2 | 13.4 | 14.3 |
| PC Encapsulated plastic system with PFA micro-filler (PPP1-3f) | 8.04 | 9.67 | 11.3 |
| Pozament encapsulated plastic system with PFA micro-filler (PPP1-3f) | 9.1 | 11.1 | 15.4 |

Figure 5.8: Water absorption of the CEM IIB and PG-concrete of the systems investigated in the current work

## 5.5 MECHANICAL PROPERTIES OF THE CEM IIB AND PG CONCRETE SYSTEM

### 5.5.1 Unconfined compressive strength

The compressive strength results for the different concrete systems investigated in the ongoing work for easier presentation have also been divided into two parts. The first part provides the details of the strength development of the Portland cement (CEM IIB) concrete system while the second part presents the detailed result of the PG-concrete system. The unconfined compressive strength data presented were for strength development observed in test specimens water cured for 7, 28 and 90 days.

#### *5.5.1.1 Strength development of the Portland cement (CEM IIB) concrete systems*

Figure 5.9 illustrates the unconfined compressive strength development for the CEM IIB-concrete, CEM IIB - encapsulated plastic concrete; CEM IIB- PFA encapsulated plastic concrete (with PFA used as mineral additive). CEM IIB-encapsulated plastic concrete with PFA used as micro-filler. The results in Figure 5.9 indicates that for all curing ages tested the mixtures (C1-3) from the reference concrete system outperformed their equivalents from all the encapsulated plastic concrete. The CEM IIB-concrete mix (C1) developed using the British concrete mix design method (as described by Neville, 2012) achieved its minimum target compressive strength of 49 N/mm$^2$ after 28 days of water curing. Its early age (at 7 days) compressive strength was about 47% lower than the minimum target value, while its strength development at 90 days was about 22% higher than the minimum value. Increasing the water/cement ratio of the concrete mix to 0.6 in mix C2 (whilst maintaining the aggregate/binder ratio as in mix C1) reduced the compressive strength of the CEM IIB-concrete by about 9.18% and 13.5% at 28 days and 90 days. Similarly, when the water/binder ratio was maintained but the aggregate/binder ratio was increased to 6/1 in mix C3, the compressive strength of the concrete mixture reduced by about 11.2% at 28 days and 13.3% at 90 days. At 7 days, mix C2 and C3 demonstrated higher compressive strength values relative to mix C1.

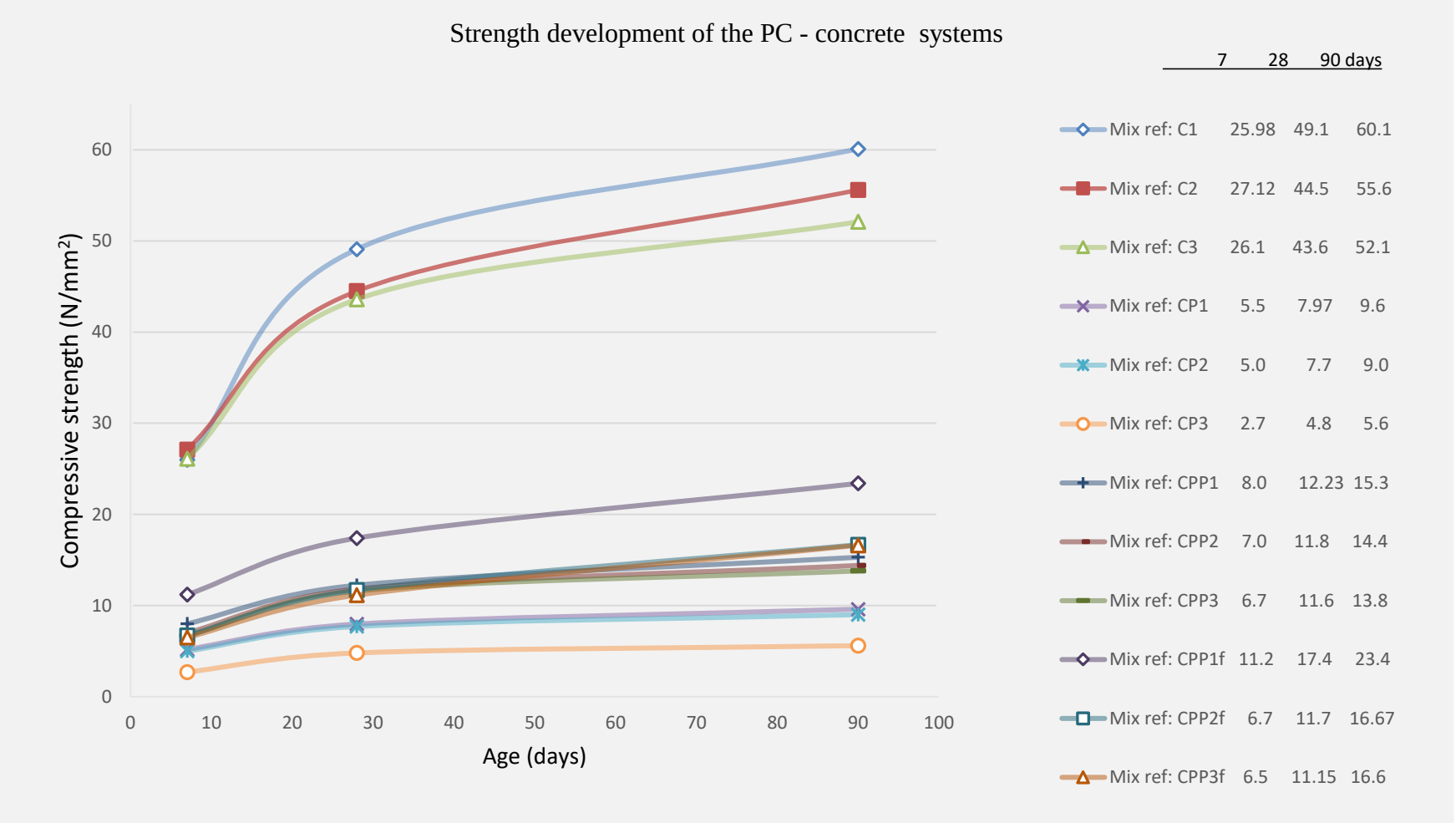


Figure 5.9: The strength development of the CEM IIB-concrete system

The substitution of natural aggregate (river sand and 10mm limestone aggregates) with the lightweight aggregates (furnace bottom ash and 0-10mm plastic aggregates) led to a significant reduction in the compressive strength of the resulting encapsulated plastic concrete specimens. The encapsulated plastic concrete test specimens from the first mix utilising CEM IIB-binder (CP1), recorded strength developments of 5.5, 7.97 and 9.6 $N/mm^2$ at 7, 28 and 90 days respectively, while the test specimens from the second mixture (CP2) recorded strength values of 5.0, 7.7 and 9.0 $N/mm^2$ respectively after 7, 28 and 90 days of water curing. The third encapsulated plastic concrete mixture (CP3), similarly recorded strength values of 2.7, 4.8 and 5.6 $N/mm^2$ after 7, 28 and 90 days of water curing. In comparison to the CEM IIB-concrete mixtures, these strength values represent up to 85% reduction in compressive strength when the natural aggregate aggregates were replaced with the lightweight aggregates.

When PFA was included in the encapsulated plastic mixtures either as mineral admixture or micro-filler, the strength gain of the resulting concrete for the curing ages observed improved slightly relative to the CEM IIB-concrete mixtures. For example, the recorded strength values of the first mix from the encapsulated plastic concrete with PFA included as a mineral admixture (CPP1) was approximately 31, 35 and 33% higher than that of the CEM IIB - encapsulated plastic concrete (CP1), after 7, 28 and 90 days of water curing respectively. Similarly, the same mix adjusted to include PFA as a micro-filler ($CPP1_f$) demonstrated strength gains of 51, 54 and 59% higher than CP1 for the same curing ages. $CPP1_f$ recorded the highest compressive strength values of all the encapsulated plastic mixtures at every age tested.

When the second encapsulated plastic mixture was designed to include PFA as a mineral admixture, the resulting concrete mixture (CPP2) relative to CP2, demonstrated strength gains higher by about 29, 35 and 37.5% at 7, 28 and 90 days respectively. The modification of the same mixture to include PFA as micro-filler ($CPP2_f$) also resulted in unconfined compressive strength increase of 25, 34 and 46% for the 7, 28 and 90 days water cured test specimens relative to the equivalent CEM IIB-encapsulated concrete mix (CP2). Nonetheless, relative to CP3, CPP3 with PFA as mineral admixture recorded approximately 60, 59 and 59% higher unconfined compressive strength values at 7, 28 and 90 days respectively, while the unconfined compressive strength values of mix $CPP3_f$

with PFA utilised as micro-filler were about 58.5, 57 and 66% higher than those of CP3 for the same curing ages.

Also, as shown by the result in Figure 5.9, the strength gain of mix CPP1f was higher than that of CPP1 for all the curing ages investigated. In contrast, mix CPP2f recorded marginally lower compressive strength values at 7 and 28 days, but a higher strength value at 90 days relative to mix CPP2. The same inter play was observed for the third set of mixtures with PFA (CPP3 and CPP3f). CPP3 performed better up to 28 days, while CPP3f recorded the higher strength at 90 days. The improved packing density of mix CPP2 and CPP3 due to high aggregate volumes may be responsible for the higher compressive strength reported up to 28 days. The lower aggregate proportions together with the reactivity of PFA at later ages may have improved the bonding between the aggregates and cement paste in CPP2f and CPP3f resulting in the higher compressive strength observed at 90 days.

#### *5.5.1.2 Strength development of the PG-concrete systems*

The strength development of the concrete system utilising PG-binder as the primary binding material instead of CEM IIB are shown in Figure 5.10. Like with the CEM IIB–concrete system, this investigation was also conducted on test specimens water cured at room temperature (20 ± 2 $^{o}$C) for 7, 28 and 90 days. The results reported are also the arithmetic averages of three test specimens per mix per curing age. For comparison purposes, illustrations of the results for both the CEM IIB and PG-concrete systems are included in Figure 5.11.

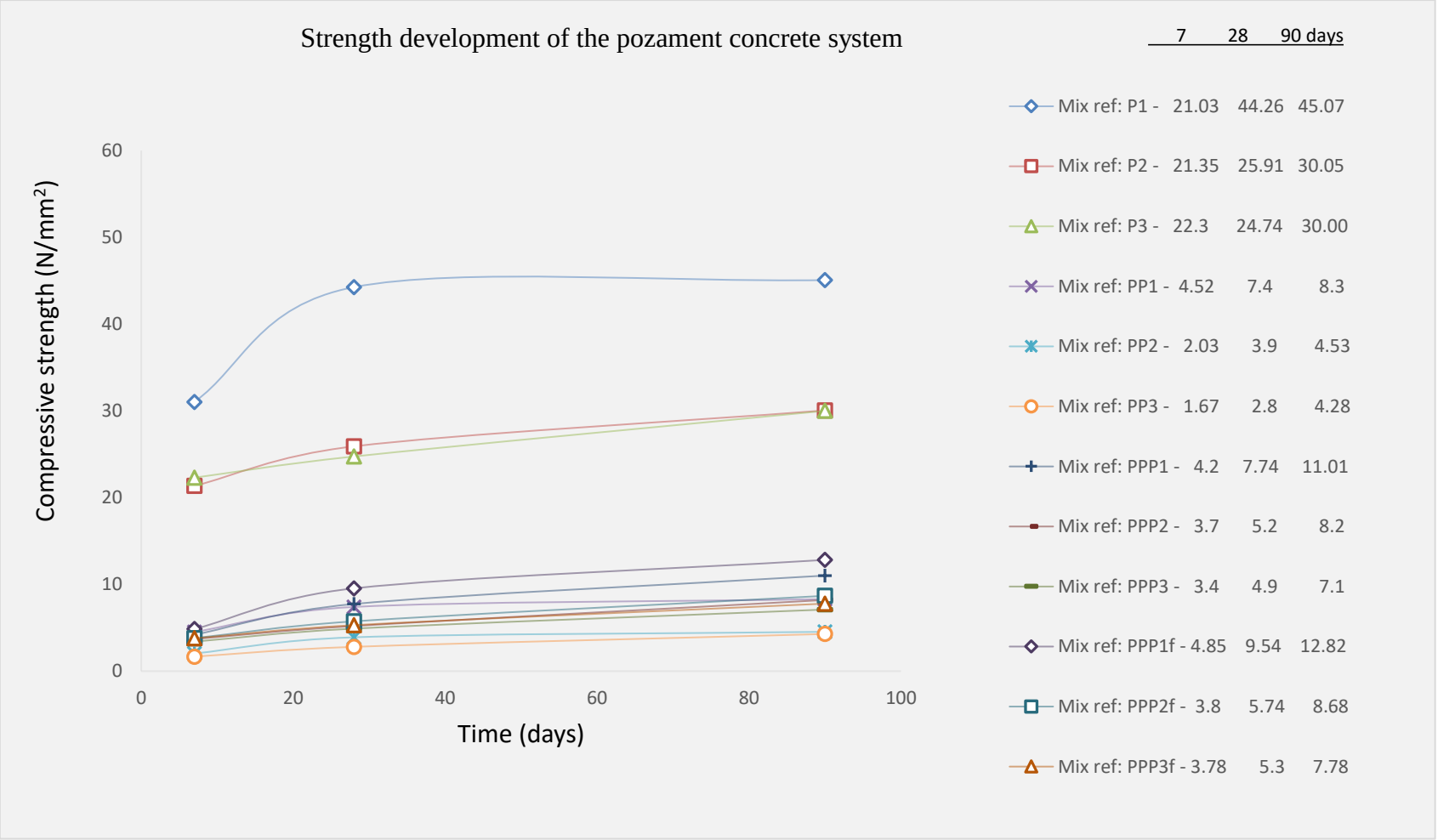


Figure 5.10: Strength development of the PG-concrete system

From Figure 5.10, the compressive strength of the all the mixtures increased with increase in curing age. The PG-concrete recorded the highest compressive strength values, while the PG-encapsulated plastic concrete recorded the lowest, for all curing ages. The inclusion of PFA as observed in the graph improved the compressive strength of the encapsulated plastic concrete. The encapsulated mixtures utilising PFA as micro-filler, when compared to the system utilising PFA as mineral admixture throughout the evaluation recorded higher compressive strengths.

The test specimens from PG-concrete 'mix P1' designed using the British method of concrete mix design but with PG replacing CEM IIB as the primary binder, recorded compressive strength values of 21.03, 44.26 and 45.07N/mm$^2$ for tests conducted after 7, 28 and 90 days of water curing respectively. Increasing the water/binder ratio to increase workability in mix P2 resulted in a reduction in compressive strength of the PG–concrete mix at 28 and 90 days. For tests conducted after 7, 28 and 90 days of water curing, the test specimens from mix P2 recorded average compressive strength of 21.32, 25.91 and 30.05 N/mm$^2$. At 7 days, mix P2 demonstrated higher compressive strength values in comparison to mix P1. Similarly, reducing the binder quantity and increasing the coarse aggregate content of the PG-concrete resulted in further strength reductions at 28 and 90 days. For investigations conducted after 7, 28 and 90 days of water curing, mix P3 recorded compressive strength values of 22.3, 24.94 and 30.00 N/mm$^2$ respectively. Mix P3, recorded the highest compressive strength at 7 days, but for subsequent curing days, it recorded the lowest. In comparison to the CEM IIB equivalent (mix C1), the hydrated PG-concrete, mix P1, demonstrated strength development approximately 19, 11 and 25% lower at 7 days, 28 and 90 days respectively. Likewise, relative to mix C2 and C3, the test specimens from mix P2 and P3 demonstrated a reduction in strength by approximately 21, 19 and 45% and, 15, 43 and 42%, respectively after 7, 28 and 90 days of water curing.

For the encapsulated plastic concrete utilising the lightweight aggregates (FBA and 0-10 mm plastic aggregates) and PG binder on its own, the first mix (PP1) recorded compressive strength values of 4.52, 7.4 and 8.3 N/mm$^2$ after 7, 28 and 90 days of water curing. These results indicate a compressive strength reduction of over 80% (for all curing ages) when compared to the compressive strength of the reference PG-concrete mixture (P1). In addition, when compared to the CEM IIB-encapsulated plastic

counterpart (CP1), the result represents a reduction in strength of between 4 – 18% for the curing ages investigated.

A similar trend was also observed with the second and third mixtures from this system (mix PP2 and PP3). The strength values of PP2 measured after 7, 28 and 90 days of water immersion (2.03, 3.9 and 4.53 N/mm$^2$) were also over 80% lower than the compressive strength of the reference concrete equivalent (P2), and 49 – 59% lower than the encapsulated plastic counterpart (CP2). Furthermore, the compressive strength values obtained after the curing ages for mix PP3 (1.67, 2.8 and 4.28 N/mm$^2$), were about 85% lower than the values recorded for the reference concrete equivalent (mix P3). The strength values were also between 14 – 41% lower than the strength values demonstrated by CP3 (the CEM IIB equivalent). PP3 recorded the lowest compressive strength values of any of the hydrated test specimens investigated.

The unconfined strength values of the PG-PFA encapsulated plastic mixtures after 7, 28 and 90 days of water curing ranges between 3.4 - 11.01 N/mm2. The best performing mixture, PPP1, recorded compressive strength values of 4.2, 7.7 and 11.01 N/mm$^2$, while second mix PPP2 recorded lower strength values of 3,7, 5.2 and 8.2 N/mm$^2$ for investigations carried out at 7, 28 and 90 days respectively. As observed in the preceding PG-encapsulated plastic concrete, the test specimens from third mixture (PPP3) in this system also recorded the lowest compressive strength values of all the mixtures in this system. The test specimens (from PPP3) under compression recorded an unconfined compressive strength of 3.4 N/mm$^2$ at 7 days, 4.8 N/mm$^2$ at 28 days and 7.1 N/mm$^2$ at 90 days. When compared to their respective reference PG-concrete equivalents (P1-3), the compressive strength results of mix PPP1-3 (for the ages investigated) reduced significantly by more than 70, and by more than 40% when compared to their CEM IIB-PFA encapsulated plastic counterparts (CPP1-3).

The unconfined compressive strength result of the hydrated mixtures utilising PFA as micro-filler (PPP1$_f$, PPP2$_f$ and PPP3$_f$) were also significantly lower than those of the reference concrete mixtures (P1-3) and their CEM IIB - encapsulated plastic equivalents (CPP1$_f$, CPP2$_f$ and CPP3$_f$). The first mix from this system (PPP1$_f$) recorded strength values of 4.85, 9.54 and 12.82 N/mm$^2$ after 7, 28 and 90 days of water curing. Likewise, the test specimens from PPP2$_f$ (the second mix from the system) recorded an average compressive strength of 3.8, 5.74 and 8.68 N/mm$^2$ at 7, 28 and 90 days respectively, while

the test specimens from PPP3$_f$ recorded an average strength value of 3.78, 5.3 and 7.78 N/mm$^2$ also at 7, 28 and 90 days respectively.

In comparison to the average results obtained for the hydrated PG-concrete (P1- P3) test specimens, the strength development of the PG-encapsulated plastic test specimens with PFA micro-fillers (PPP1$_f$ - PPP3$_f$) reduced by over 70% per curing age. The compressive strength results of the hydrated PG-encapsulated plastic test specimens with PFA micro-filler to the compressive strength results obtained for the CEM IIB equivalents test specimens suggest a strength reduction of more than 45%.

As mentioned earlier a bar chart illustration of the results for both the CEM IIB and PG-concrete systems is shown in Figure 5.11.

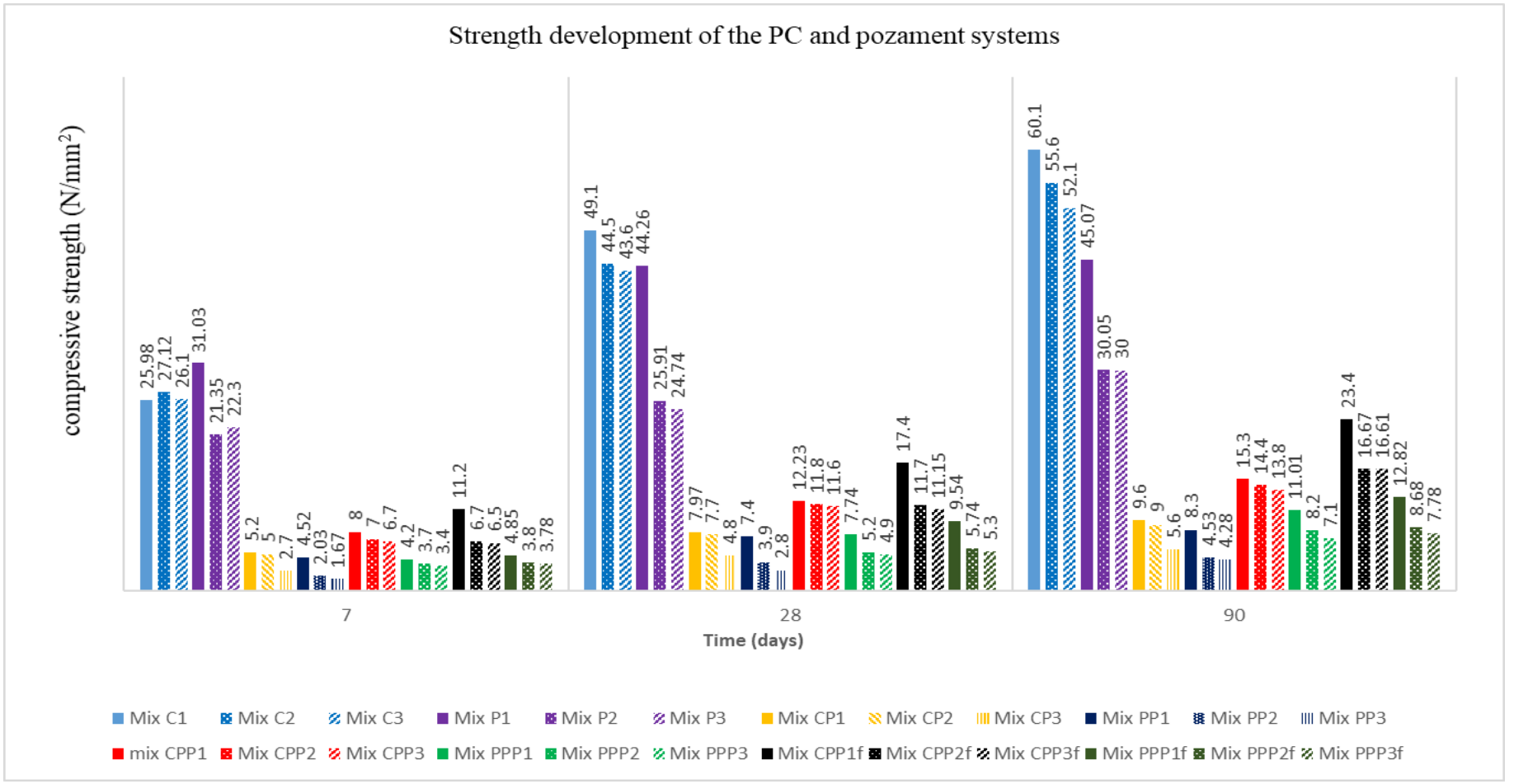


Figure 5.11: The combined unconfined compressive strength graph for the CEM IIB and PG-concrete systems.

### 5.5.2 Split tensile strength.

The split tensile strength of the test cylinders from the CEM IIB and PG concrete systems are shown in Figures 5.12 and 5.13. The results presented are the arithmetic averages of three test specimens per mix optimum per curing age.

#### *5.5.2.1 Tensile strength of the CEM IIB-concrete system*

Figure 5.12 shows the variation in tensile strength for the CEM IIB-concrete, CEM IIB - encapsulated plastic concrete, CEM IIB-PFA encapsulated plastic concrete and the CEM IIB-encapsulated plastic concrete with PFA used as micro-filler water cured for 28 days.

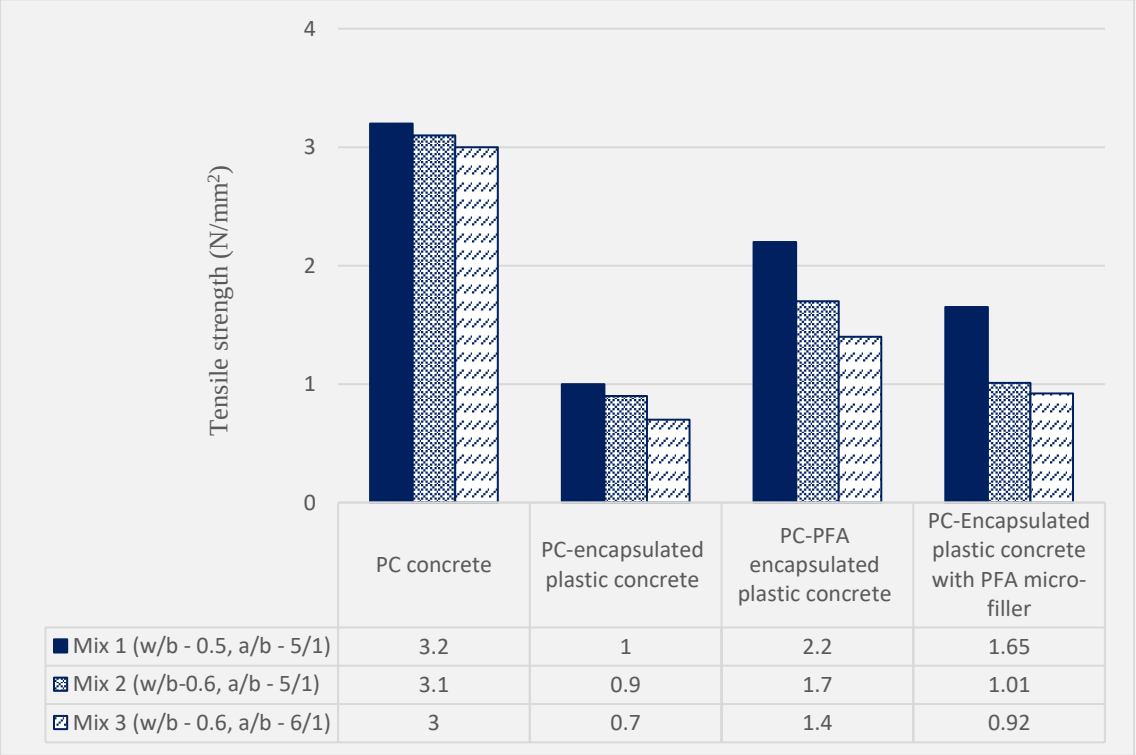


Figure 5.12 Variation in tensile strength of the mixtures from the CEM IIB-concrete system

From Figure 5.12, it can be observed that the test specimens from the CEM IIB-concrete system recorded higher tensile strength in comparison to the test specimens from the encapsulated plastic concrete. The test cylinders from the concrete mixtures (C1, C2 and C3) as observed in Figure 5.12, recorded a tensile strength values between 3.0 and 3.2

$N/mm^2$. The first concrete mix as noted utilises a water/binder ratio of 0.5 and aggregate/binder ratio of 5/1, while second mix retained the aggregate/binder ratio but increased the water/binder ratio to 0.6, and the third mix, similarly maintained the water/binder ratio at 0.5 but increased the aggregate/binder ratio to 6/1. Hence judging by these results, a slight decrease in tensile strength took place when the water/binder and aggregate/binder ratios were increased. This may be as a result of increased porosity between the two systems.

The combination of Portland cement with the lightweight materials (0-10 mm plastic aggregates and FBA) also demonstrated similar tensile strength development. That is, the tensile strength decreased with increase in water/binder and aggregate/binder ratio. The CEM IIB - encapsulated plastic concrete recorded an average tensile strength of 1 $N/mm^2$ for the first mix (CP1), 0.9 $N/mm^2$ for mix 2 (CP2) and 0.7 $N/mm^2$ for mix 3 (CP3). In comparison to the mirrored conventional CEM IIB-concrete (C1-3), these results signify a 69 – 77% reduction in tensile strength. When PFA was added to the encapsulated plastic concrete, the tensile strength improved significantly. The inclusion of PFA as a mineral admixture increased the tensile strength of the CEM IIB-encapsulated plastic concrete by approximately 50%, while the inclusion of PFA as micro-filler increased the tensile strength of the CEM IIB- encapsulated plastic concrete by 49-69 %.

#### *5.5.2.2 Tensile strength of the PG-concrete system*

The variation in tensile strength of the conventional and encapsulated plastic PG-concrete test specimens water cured for 28 days are shown in Figure 5.13. The result presented in Figure 5.13 indicate that, the tensile strength of the conventional and encapsulated plastic concrete (as with the CEM IIB-concrete) decreased when the water/binder and aggregate/binder ratios were increased. The conventional PG-concrete mixtures (mix P1-3) recorded the highest tensile strength. When the conventional aggregates (river sand and 10 mm aggregates) were replaced with (recycled aggregates) FBA and 0-10 mm plastic aggregates, the tensile strength of the resulting encapsulated plastic concrete were 68- 89% lower than the equivalent conventional concrete (P1-3). The inclusion of PFA in the encapsulated plastic concrete generally increased the tensile strength of the PG-encapsulated plastic concrete. The tensile strength of the PG-encapsulated plastic concrete increase by 56-76%, when PFA was incorporated in the mix. The mix utilising PFA (PPP1-PPP3) recorded the higher tensile strength gain relative to ($PPP1_f$-$PPP3_f$).

When compared to their CEM IIB equivalents (Figure 5.12), some of the test specimens from the PG concrete blends (P1-3 and PP1) recorded slightly higher tensile strength, while the rest of the mixtures recorded lower tensile strength values.

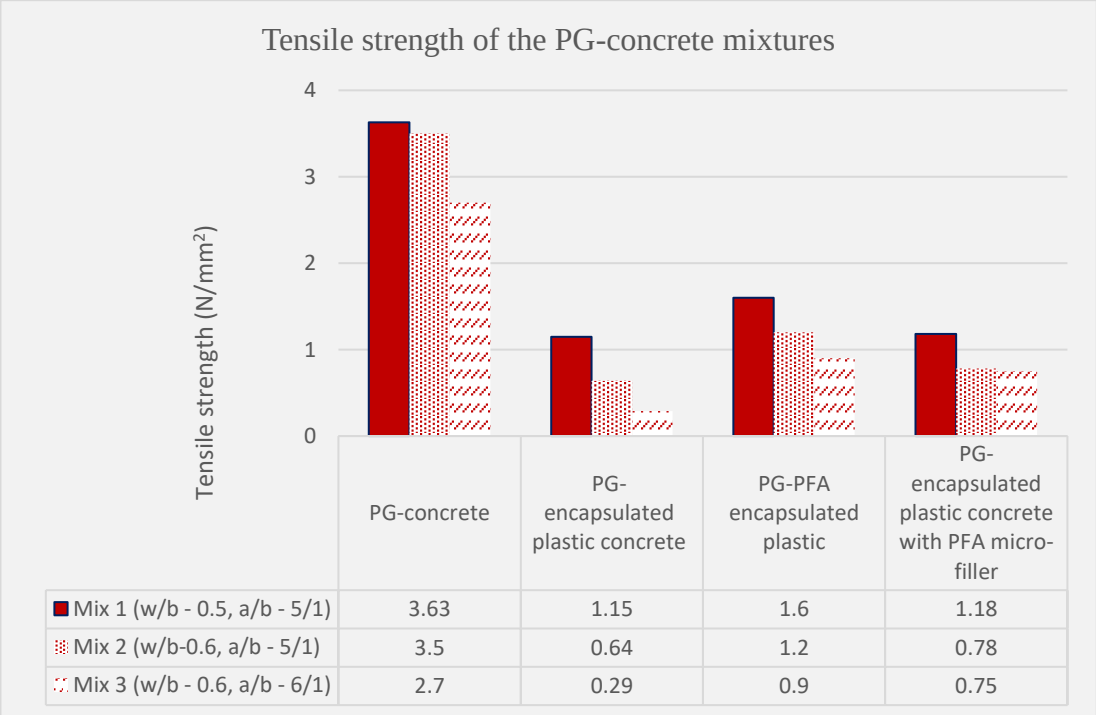


| | PG-concrete | PG-encapsulated plastic concrete | PG-PFA encapsulated plastic | PG-encapsulated plastic concrete with PFA micro-filler |
|---|---|---|---|---|
| Mix 1 (w/b - 0.5, a/b - 5/1) | 3.63 | 1.15 | 1.6 | 1.18 |
| Mix 2 (w/b-0.6, a/b - 5/1) | 3.5 | 0.64 | 1.2 | 0.78 |
| Mix 3 (w/b - 0.6, a/b - 6/1) | 2.7 | 0.29 | 0.9 | 0.75 |

Figure 5.13: Variation of tensile strength of the PG-concrete system

## 5.6 STATISTICAL ANALYSIS OF THE PHYSICAL AND MECHANICAL PROPERTIES OF THE CEM IIB AND PG-CONCRETE

The results of the statistical analyses for the CEM IIB and PG-concrete blends are presented in Table 5.8 and Table 5.9 respectively. The results presented include number of samples (n), the differences in mean, standard deviations (STD), standard errors (Std error) and, t-values and p-values obtained from. The p values were compared to an alpha value of 0.05, which represent a 95% confidence level. As shown in Table 5.8, the CEM IIB-encapsulated plastic concrete all recorded p values lower than 0.05. In most cases, the encapsulated plastic concrete incorporating PFA (CPP1-CPP3 and $CPP1_f$-$CPP3_f$) also recorded p-values lower than 0.05. The few exceptions include, the recorded tensile strength results by CPP1, CPP2 and $CPP1_f$ and the recorded porosity of CP1, CP2 and $CPP1_f$ , where $p \geq 0.05$. Negative t-values (or negative mean difference) were also observed for 28-days porosity and 28-days water absorption of the CEM IIB-encapsulated plastic concrete (including those with PFA). The negative t-values indicate that, the mean data obtained for the properties of the encapsulated plastic concrete (porosity and water absorption), were higher than those obtained for the equivalent conventional concrete. As with the CEM II-B encapsulated plastic concrete, the p-values recorded by most of the PG-encapsulated plastic concrete (including those with PFA) were lower than 0.05 (Table 5.9). The exceptions observed include, the 28-days porosity of the concrete blends PP3, PPP2, PPP3, $PPP1_f$ and $PPP2_f$, 28- days water absorption of PP3, PPP1, PPP2, $PPP1_f$ and $PPP3_f$ and the 90-days compressive strength of PP3, PPP3, $PPP3_f$, with $P \geq 0.05$. Negative t-values were also observed for porosity and water absorption properties of the PG-encapsulated plastic concrete (including those with PFA) as the recorded mean was higher than those of the equivalent conventional PG-concrete.

Table 5.8: Inferential statistical analysis for the CEMIIB-encapsulated plastic concrete (Including those with PFA)

| Analysis | n | Mix | Mean | STD deviated | STD error mean | T value | p-value | Mix | Mean | STD | Std error | T value | p-value | Mix | Mean | STD | Std error | T value | p-value |
|---|---|---|---|---|---|---|---|---|---|---|---|---|---|---|---|---|---|---|---|
| 28-days Density ($kg/m^3$) | 3 | CP1 | 836.67 | 49.33 | 28.48 | 29.377 | 0.001 | CPP1 | 806.67 | 55.08 | 31.78 | 25.368 | 0.002 | CPP1f | 800 | 52.92 | 30.55 | 26.186 | 0.001 |
| | 3 | CP2 | 830.1 | 10.01 | 5.7735 | 143.76 | 0.001 | CPP2 | 813.33 | 61.1 | 35.27 | 23.06 | 0.002 | CPP2f | 820 | 5 | 2.89 | 284.056 | 0.001 |
| | 3 | CP3 | 865.01 | 25.01 | 14.43 | 59.929 | 0.003 | CPP3 | 786.67 | 15.28 | 8.82 | 89.2 | 0.001 | CPP3f | 813.33 | 5.77 | 3.33 | 244.01 | 0.001 |
| 28-days Porosity (%) | 3 | CP1 | -17.1 | 3.9 | 2.25167 | -7.594 | 0.17 | CPP1 | -9.2 | 0.4 | 0.23 | -39.84 | 0.001 | $CPP1_f$ | -3.3 | 3.4 | 1.96 | -1.681 | 0.235 |
| | 3 | CP2 | -17.7 | 1.8 | 1.039 | -17.03 | 0.003 | CPP2 | -9.4 | 2.9 | 1.67 | -5.61 | 0.03 | $CPP2_f$ | -4.8 | 3.01 | 1.732 | -2.777 | 0.109 |
| | 3 | CP3 | -17.7 | 3.6 | 2.08 | -8.516 | 0.014 | CPP3 | -10.1 | 2 | 1.15 | -5.287 | 0.013 | $CPP3_f$ | -5.8 | 1.9 | 1.1 | -5.287 | 0.034 |
| 28-days Water absorption (%) | 3 | CP1 | -17.3 | 2 | 1.15 | -14.98 | 0.004 | CPP1 | -8.8 | 2.1 | 1.21 | -7.258 | 0.018 | $CPP1_f$ | -4.34 | 0.26 | 0.15 | -28.91 | 0.001 |
| | 3 | CP2 | -18 | 0.5 | 0.289 | -62.35 | 0.001 | CPP2 | -9.1 | 0.3 | 0.173 | -52.54 | 0.001 | $CPP2_f$ | -5.97 | 0.67 | 0.39 | -15.43 | 0,004 |
| | 3 | CP3 | -18.2 | 3.2 | 1.84 | -9.851 | 0.01 | CPP3 | -10.1 | 1.4 | 0.81 | -12.5 | 0.006 | $CPP3_f$ | -7.5 | 1.2 | 0.69 | -10.83 | 0.008 |
| 7-days Compressive strength ($N/mm^2$) | 3 | CP1 | 20.9 | 3.15 | 1.82 | 11.5 | 0.007 | CPP1 | 17.91 | 2.45 | 1.41 | 12.66 | 0.006 | $CPP1_f$ | 14.75 | 2.24 | 1.29 | 11.39 | 0.008 |
| | 3 | CP2 | 22.15 | 3.04 | 1.756 | 12.62 | 0.006 | CPP2 | 20.05 | 3.25 | 1.88 | 10.68 | 0.009 | $CPP2_f$ | 20.45 | 3.09 | 1.78 | 11.47 | 0.008 |
| | 3 | CP3 | 20.38 | 1.34 | 0.78 | 26.28 | 0.001 | CPP3 | 16.35 | 1.02 | 0.59 | 27.88 | 0.001 | $CPP3_f$ | 16.27 | 0.67 | 0.4 | 42.9 | 0.001 |
| 28-days Compressive strength ($N/mm^2$) | 3 | CP1 | 38.51 | 5.12 | 2.3 | 13.015 | 0.006 | CPP1 | 34.47 | 4.21 | 2.43 | 14.16 | 0.005 | $CPP1_f$ | 29.5 | 5.19 | 2.3 | 9.83 | 0.01 |
| | 3 | CP2 | 36.86 | 0.98 | 0.57 | 65.068 | 0.001 | CPP2 | 32.79 | 0.93 | 0.54 | 61.058 | 0.001 | $CPP2_f$ | 32.83 | 0.48 | 0.28 | 118.12 | 0.001 |
| | 3 | CP3 | 38.29 | 0.84 | 0.46 | 79.45 | 0.001 | CPP3 | 31.69 | 0.8 | 0.46 | 68.52 | 0.001 | $CPP3_f$ | 32.17 | 0.62 | 0.36 | 89.77 | 0.001 |
| 90-days Compressive strength ($N/mm^2$) | 3 | CP1 | 52.69 | 1.72 | 0.1 | 52.94 | 0.001 | CPP1 | 46.8 | 1.12 | 0.65 | 72.15 | 0.001 | $CPP1_f$ | 35.53 | 1.7 | 0.98 | 39.29 | 0.001 |
| | 3 | CP2 | 46.53 | 0.29 | 0.17 | 279.2 | 0.001 | CPP2 | 41.16 | 0.64 | 0.37 | 110.7 | 0.001 | $CPP2_f$ | 37.77 | 0.64 | 0.24 | 159.35 | 0.001 |
| | 3 | CP3 | 47.1 | 1.04 | 0.6 | 78.5 | 0.001 | CPP3 | 38.87 | 1.08 | 0.62 | 62.42 | 0.001 | $CPP3_f$ | 36.04 | 2.07 | 1.2 | 30.139 | 0.001 |
| 28-days Tensile strength | 3 | CP1 | 2.2 | 0.1 | 0.06 | 38.105 | 0.001 | CPP1 | 1.1 | 0.46 | 0.26 | 4.158 | 0.53 | $CPP1_f$ | 1.55 | 0.55 | 0.32 | 4.881 | 0.4 |
| | 3 | CP2 | 2.2 | 0.26 | 0.15 | 14.402 | 0.005 | CPP2 | 1.4 | 0.41 | 0.24 | 5.925 | 0.027 | $CPP2_f$ | 2.1 | 0.35 | 0.2 | 10.318 | 0.009 |
| | 3 | CP3 | 2.3 | 0.2 | 0.16 | 19.92 | 0.003 | CPP3 | 1.6 | 0.5 | 0.29 | 5.543 | 0.31 | $CPP3_f$ | 2.08 | 0.26 | 0.15 | 13.856 | 0.005 |

Table 5.9: Inferential statistical analysis for the PG-encapsulated plastic concrete (Including those with PFA)

| Analysis | n | Mix | Mean | STD | Std error | T value | p-value | Mix | Mean | STD | Std error | T value | p-value | Mix | Mean | STD | Std error | T value | p-value |
|---|---|---|---|---|---|---|---|---|---|---|---|---|---|---|---|---|---|---|---|
| 28-days Density | 3 | PP1 | 896.67 | 5.77 | 3.33 | 269.01 | 0.001 | PPP1 | 796.67 | 15.28 | 8.82 | 90.33 | 0.002 | $PPP1_f$ | 790 | 45.83 | 26.46 | 29.9 | 0.001 |
| | 3 | PP2 | 903.3 | 11.55 | 6.67 | 135.5 | 0.002 | PPP2 | 786.67 | 5.77 | 3.33 | 236.01 | 0.002 | $PPP2_f$ | 776.67 | 20.82 | 12.01 | 64.62 | 0.001 |
| | 3 | PP3 | 943.33 | 5.77 | 3.33 | 283.01 | 0.001 | PPP3 | 800 | 17.32 | 10 | 80.01 | 0.002 | $PPP3_f$ | 810 | 20 | 11.55 | 70.14 | 0.001 |
| 28-days Porosity | 3 | PP1 | -17.5 | 2.3 | 1.33 | -13.18 | 0.006 | PPP1 | -7.6 | 3.8 | 2.19 | -3.464 | 0.74 | $PPP1_f$ | -1.3 | 0.7 | 0.4 | -3.22 | 0.085 |
| | 3 | PP2 | -17.1 | 0.3 | 0.17 | -98.73 | 0.001 | PPP2 | -5.9 | 0.9 | 0.52 | -11.36 | 0.008 | $PPP2_f$ | -6.2 | 3.3 | 1.91 | -6.06 | 0.026 |
| | 3 | PP3 | -5.4 | 3.8 | 2.19 | -2.461 | 1.133 | PPP3 | -2.1 | 0.6 | 0.35 | -3.254 | 0.83 | $PPP3_f$ | -7.3 | 2.9 | 1.67 | -4.36 | 0.49 |
| 28-days Water absorption | 3 | PP1 | -16.07 | 1.85 | 1.063 | -15.04 | 0.004 | PPP1 | -16.9 | 2.5 | 1.44 | -11.71 | 0.007 | $PPP1_f$ | -18.9 | 3.8 | 2.19 | -8.62 | 0.013 |
| | 3 | PP2 | -7 | 0.4 | 0.23 | -30.31 | 0.001 | PPP2 | -7.2 | 3 | 1.75 | -4.157 | 0.53 | $PPP2_f$ | -8.1 | 0.1 | 0.06 | -140.3 | 0.001 |
| | 3 | PP3 | -2 | 1.9 | 1.1 | -1.823 | 0.21 | PPP3 | -4 | 2.2 | 1.27 | -3.149 | 0.88 | $PPP3_f$ | -8.3 | 2.3 | 1.33 | -6.25 | 0.25 |
| 7-days Compressive strength ($N/mm^2$) | 3 | PP1 | 26.42 | 0.2 | 0.12 | 223.5 | 0.002 | PPP1 | 26.81 | 0.55 | 0.38 | 84.122 | 0.001 | $PPP1_f$ | 26.19 | 1.81 | 1.05 | 25.064 | 0.002 |
| | 3 | PP2 | 19.43 | 1.19 | 0.69 | 28.22 | 0.001 | PPP2 | 17.65 | 1.11 | 0.64 | 27.645 | 0.001 | $PPP2_f$ | 17.55 | 0.89 | 0.514 | 34.16 | 0.001 |
| | 3 | PP3 | 20.61 | 1.89 | 1.09 | 18.884 | 0.003 | PPP3 | 18.9 | 1.95 | 1.13 | 16.772 | 0.004 | $PPP3_f$ | 19.27 | 1.14 | 0.66 | 29.166 | 0.001 |
| 28-days Compressive strength ($N/mm^2$) | 3 | PP1 | 36.83 | 1.68 | 0.97 | 37.886 | 0.001 | PPP1 | 36.52 | 1.57 | 0.91 | 40.177 | 0.001 | $PPP1_f$ | 34.73 | 1.22 | 0.7 | 49.476 | 0.001 |
| | 3 | PP2 | 20.77 | 2.36 | 1.36 | 15.262 | 0.004 | PPP2 | 19.48 | 2.42 | 1.4 | 13.963 | 0.005 | $PPP2_f$ | 18.94 | 2.22 | 1.29 | 14.725 | 0.005 |
| | 3 | PP3 | 21.91 | 0.73 | 0.42 | 51.724 | 0.001 | PPP3 | 20.44 | 1.6 | 0.93 | 22.068 | 0.002 | $PPP3_f$ | 19.64 | 1.18 | 0.68 | 28.924 | 0.001 |
| 90-days Compressive strength ($N/mm^2$) | 3 | PP1 | 34.49 | 8.26 | 4.77 | 7.228 | 0.19 | PPP1 | 30.11 | 6.62 | 3.82 | 7.876 | 0.16 | $PPP1_f$ | 28.2 | 7.3 | 4.21 | 6.688 | 0.22 |
| | 3 | PP2 | 25.84 | 0.85 | 0.49 | 52.518 | 0.001 | PPP2 | 23.27 | 1.1 | 0.64 | 36.523 | 0.001 | $PPP2_f$ | 22.59 | 0.56 | 0.32 | 69.811 | 0.001 |
| | 3 | PP3 | 25.78 | 1.07 | 0.62 | 41.59 | 0.001 | PPP3 | 22.33 | 1.48 | 0.85 | 26.165 | 0.001 | $PPP3_f$ | 21.56 | 1.66 | 0.96 | 22.5 | 0.002 |
| 28-days Tensile strength | 3 | PP1 | 2.48 | 0.03 | 0.02 | 143.18 | 0.001 | PPP1 | 2.03 | 0.28 | 0.16 | 12.56 | 0.006 | $PPP1_f$ | 2.45 | 0.26 | 0.15 | 16.3 | 0.004 |
| | 3 | PP2 | 2.86 | 0.36 | 0.21 | 13.76 | 0.005 | PPP2 | 2.3 | 0.36 | 0.21 | 11.07 | 0.008 | $PPP2_f$ | 2.72 | 0.16 | 0.09 | 29.45 | 0.001 |
| | 3 | PP3 | 1.953 | 0.33 | 0.19 | 10.21 | 0.009 | PPP3 | 1.833 | 0.03 | 0.02 | 110 | 0.001 | $PPP3_f$ | 1.983 | 0.28 | 0.16 | 12.2 | 0.007 |

## 5.7 DURABILITY ASSESSMENT OF THE CEM IIB AND PG-CONCRETE SYSTEMS

### 5.7.1 Freeze – thaw analysis

The ability of the hydrated encapsulated plastic concrete mixtures to resist frost damage when subjected to successive freeze – thaw conditions were assessed in terms of mass loss, compressive strength loss and visually observed physical damages to the test specimens. The investigation was carried out on six test specimens per mix composition divided equally between the test specimens subjected to the freeze and thaw regime and reference test specimens kept in covered containers. After the last freeze and thaw cycle, the test specimens were inspected for any physical damages before the mass and strength losses were determined. The mass loss or residual mass (in percentage) as discussed in Chapter 4, was taken as the percentage ratio of the measured mass (mass of the test specimens measured after the last freeze/thaw cycle) and the equivalent mass of the test specimens determined from the reference test specimens. The loss in compressive strength was treated in a similar way. The residual mass and compressive strength percentages recorded are the average of three test specimens per mix composition.

#### *5.7.1.1 Freeze – thaw analysis of the CEM IIB-concrete systems*

The result of the physical assessments carried out on the test specimens from the CEM IIB – concrete systems after the last freeze and thaw cycle, along with the residual mass (%) and residual compressive strength (%) of the test specimens subjected to the freeze and thaw cycles relative to the reference test specimens are presented below:

##### *5.7.1.1.1 Physical assessment of the deterioration of the CEM IIB-concrete test specimens after the 20$^{th}$ freeze and thaw cycle*

The visual representations of some of the test specimens from the CEM IIB-concrete mixtures (C1-3), CEM IIB-encapsulated plastic mixtures (CP1-3), CEM IIB-PFA encapsulated test specimens (CPP1-3) and the CEM IIB-encapsulated test specimens with PFA used as micro fillers (CPP1-3$_f$) after the freeze – thaw analysis is presented in Figure 5.14 (a-f). The description of the physical deteriorations of the test specimens observed is provided in Table 5.10.


Figure 5.14: Some test specimens from (a) mix C1-3, (b) mix CP1, (c) mix CP2, (d) mix CP3, (e) mix CPP1 – 3 and (f) mix CPP1$_f$ – 3$_f$ after the freeze and thaw cycles

Table 5.10: Assessment of the damages to the test specimens from the CEM IIB – concrete systems as observed after the last freeze and thaw cycle

| *Description of damage* | *Remarks* |
|---|---|
| Crack ≥ 0.2mm | None observed |
| Crack ≤ 0.2 mm | None observed |
| Crater | None observed |
| Chipping, peeling and scaling | No chipping, peeling or scaling was observed in the concrete or encapsulated plastic mixtures with PFA. However, after about 7 cycles, the test specimens from the encapsulated plastic concrete with CEM IIB binder used on its own started to lose some of the aggregates closer to the corners. Chipping around the edges continued throughout the remaining cycles. |
| Fracture | None observed |
| Spalling and delamination | None observed |

*5.7.1.1.2 Residual mass of the CEM IIB-concrete systems*

Figure 5.15 shows the residual mass (%) of the test specimens from the CEM IIB-concrete mixtures (C1-3), CEM IIB-encapsulated plastic concrete mixtures (CP1-3), CEM IIB-PFA encapsulated plastic concrete mixtures (CPP1-3) and the CEM IIB-encapsulated plastic concrete mixtures with PFA micro filler (CPP1-$3_f$) after 20 successive freeze and thaw cycles. From the result in Figure 5.15, the test specimens from the hydrated CEM IIB- concrete mixtures showed better resistance to freeze and thaw conditions than their equivalent encapsulated - plastic concrete (with or without PFA). The test specimens from the CEM IIB-concrete specimens recorded the lowest mass losses (between 0.3 -0.6 %), whereas the test specimens from the encapsulated plastic concrete with CEM IIB binder own its own recorded the highest (1-1.5%). The inclusion of PFA (both as mineral admixture and as micro-filler) seems to mitigate the effect of frost action on the mass loss of the encapsulated plastic test specimens. The test

specimens from the CEM IIB-PFA encapsulated plastic concrete mixtures recorded mass losses ranging between 0.5 – 0.7% while the test specimens from the CEM IIB-encapsulated plastic concrete mixtures with PFA utilised as micro filler recorded mass losses ranging between (0.4 – 0.7).

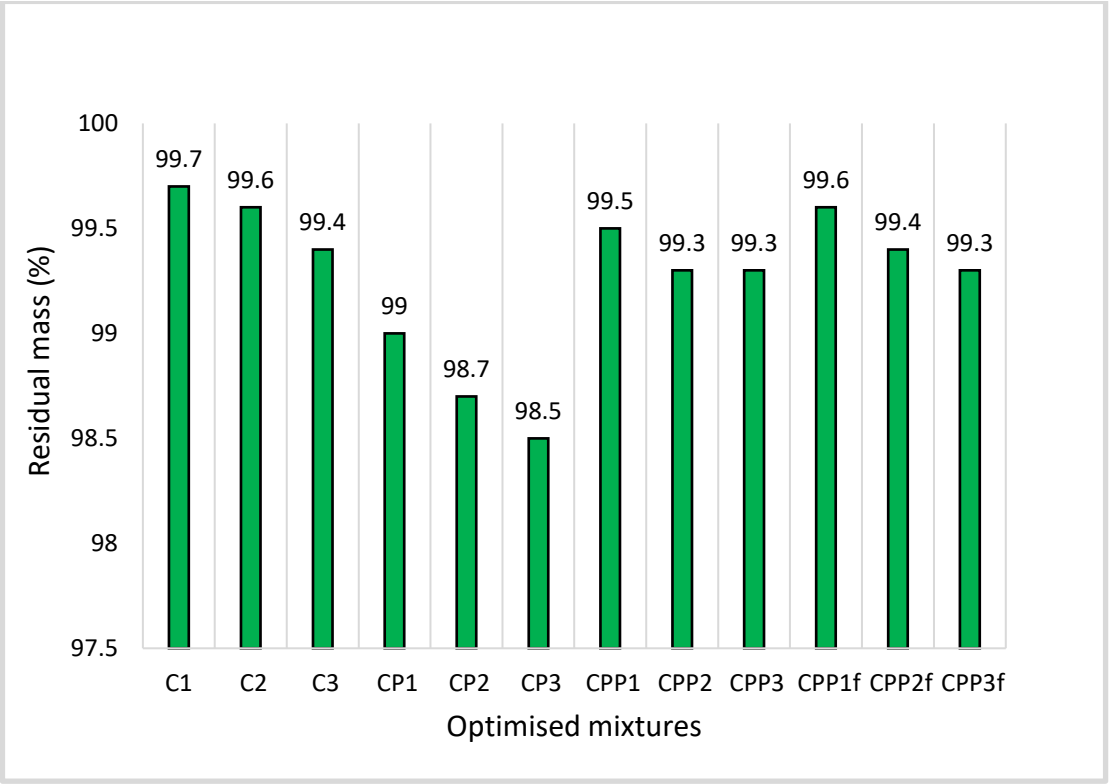


Figure 5.15: Residual mass (%) of the test specimens from the CEM IIB-concrete systems after 20 successive freeze and thaw cycles

*5.7.1.1.3 Residual compressive strength of the CEM IIB-concrete systems*

The residual compressive strength of the test specimens from the CEM IIB–concrete mixtures (C1-3), CEM IIB-encapsulated plastic mixtures (CP1- 3), CEM IIB-PFA encapsulated plastic concrete mixtures (CPP1-3) and CEM IIB-encapsulated plastic mixtures with PFA micro fillers (CPP1-$3_f$) due to successive freeze and thaw cycles is shown in Figure 5.16.

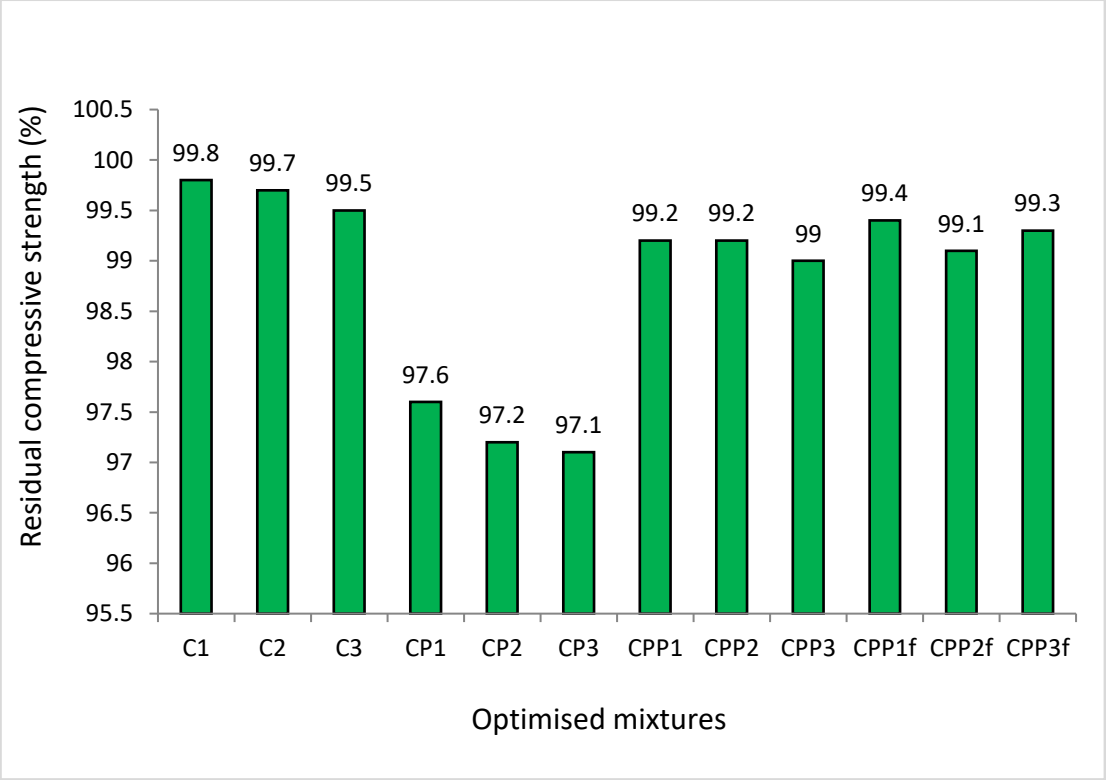


Figure 5.16: Residual compressive strength (%) of the test specimens from the CEM IIB systems after 20 successive freeze and thaw cycles

From Figure 5.16, the CEM IIB-concrete test specimens demonstrated better resistance to freeze and thaw conditions relative to the encapsulated plastic concrete specimens. The mixtures (C1-3) recorded residual compressive strength ranging between 0.2 -0.5%. Optimised mix C1 with a water/binder ratio of 0.5 and aggregate/binder ratio of 5/1 recorded the highest residual compressive strength among the CEM IIB – concrete mixtures, while mix C3 with a water/binder ratio of 0.6 and aggregate/binder ratio of 6/1 recorded the lowest. In comparison to the CEM IIB1–concrete specimens, the test specimens from the CEM IIB-encapsulated plastic mixtures (CP1 – 3) recorded a higher

mass loss ranging between 2.4 – 2.7%. The first mix from the CEM IIB-encapsulated plastic concrete (CP1) also with a water/binder ratio of 0.5 and aggregate/binder ratio of 6/1 outperformed the other two mixtures in the group. The third mix CP3 demonstrated the least resistance to freeze and thaw (in terms of strength loss). Like the residual mass, the inclusion of PFA also appears to reduce the harsh effect of successive freezing and thawing on the encapsulated plastic concrete test specimens. The specimens with PFA micro fillers (CPP1-3$_f$) as observed performed slightly better under freeze and thaw conditions than the encapsulated plastic mixtures with PFA used as binder admixture (CPP1-3). The specimens with PFA micro filler recorded strength losses ranging between 0.6 – 0.9%, while the specimens with PFA mineral admixtures recorded strength losses between 1–1.8%. Again, the first optimised mix form each concrete type demonstrated better freeze and thaw resistance, while the third mixtures demonstrated the least resistance.

### *5.7.1.2 Freeze – thaw analysis of the PG-concrete systems*

The result of the physical assessments carried out on the test specimens from the PG–concrete systems after the last freeze and thaw cycle, along with the residual mass (%) and residual compressive strength (%) of the test specimens subjected to the freeze and thaw cycles relative to the reference test specimens are presented below:

*5.7.1.2.1 Physical assessment of the deterioration of the PG-concrete test specimens after the 20$^{th}$ freeze and thaw cycle*

The visual representations of the test specimens from PG-concrete systems are shown in Figure 5.17 (a-f), while a tabulated description of the damages caused by frost action is presented in Table 5.11.

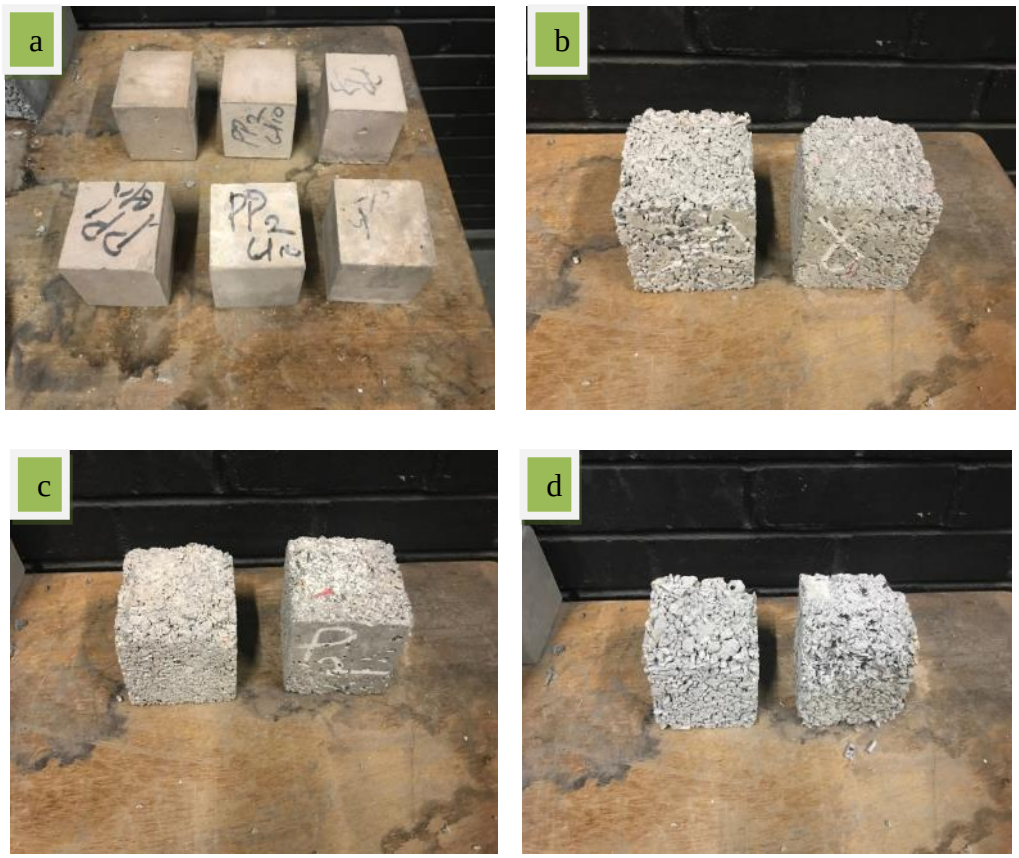


Figure 5.17: Some test specimens from (a) mix P1-3, (b) mix PP1, (c) mix PP2, (d) mix PP3, (e) mix PPP1 – 3 and (f) mix PPP1$_f$ – 3$_f$ after the freeze and thaw cycles

Table 5.11: Assessment of the damages to the test specimens from the PG – concrete as observed after the last freeze and thaw cycle

| *Description of damage* | *Remarks* |
|---|---|
| Crack ≥ 0.2mm | None observed |
| Crack ≤ 0.2 mm | None observed |
| Crater | None observed |
| Chipping, peeling and scaling | No chipping, peeling and scaling was observed in the concrete or encapsulated plastic mixtures with PFA. However, after about 5 cycles the test specimens from the PG-encapsulated plastic system started to lose some of the aggregates closer to the corners. |
| Fracture | None observed |
| Spalling and delamination | None observed |

*5.7.1.2.2 Residual mass of the PG-concrete systems*

The changes in mass of the PG-concrete system and the PG-encapsulated plastic systems expressed in terms of the residual mass (%) are shown in Figure 5.18.

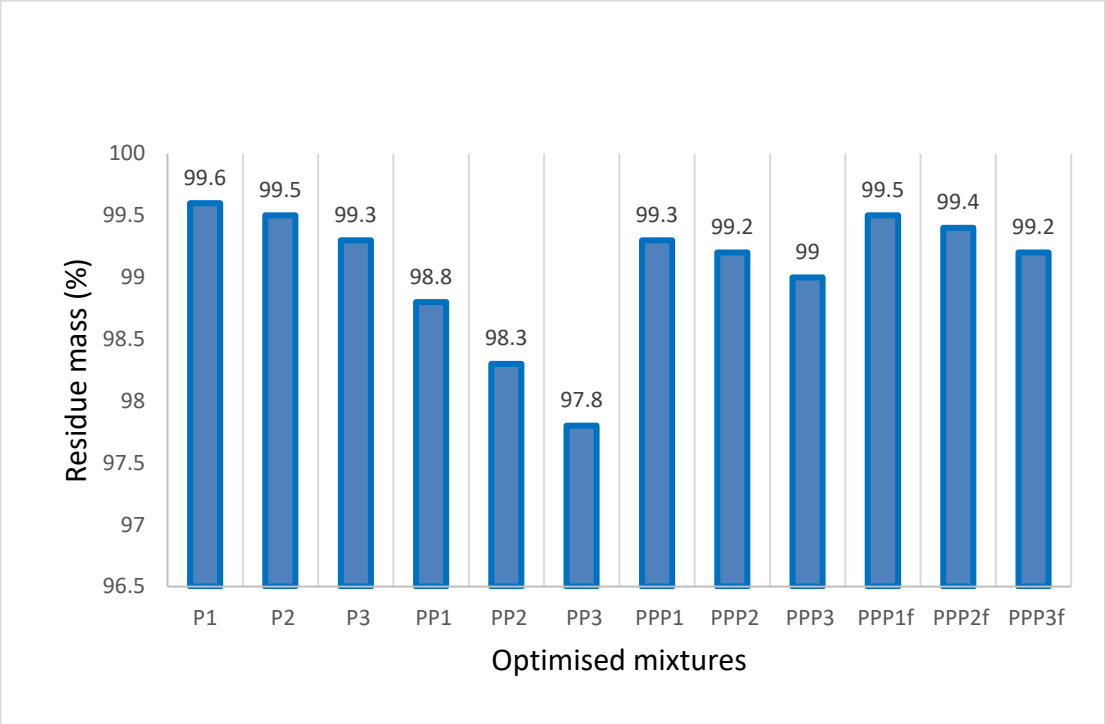


Figure 5.18: Residual mass (%) of the test specimens from the PG-concrete systems after 20 freeze and thaw cycles

The results indicate that the test specimens from the PG-concrete system recorded weight losses ranging between 0.4 – 0.7%, while the test specimens from the PG-encapsulated plastic concrete recorded weight losses ranging between 1.2 – 2.2%. The inclusion of PFA slightly reverses the weight loss of the encapsulated plastic concrete, with the test specimens from the mixtures utilising PFA as micro-filler recording the highest strength improvements. The hydrated specimens from the encapsulated mixtures including PFA as micro-fillers (CPP1$_f$ – 3$_f$) recorded weight losses ranging between 0.5 -0.7%, while the test specimens from the mixtures utilising PFA mineral admixture recorded weight losses within the range of 0.7 – 1.0%.

Overall, the PG-concrete mixtures performed better than their respective encapsulated plastic equivalents with or without PFA. The hydrated specimens from the PG-encapsulated plastic concrete recorded the highest average weight losses of all the concrete specimens subject to freeze and thaw conditions. In addition, the percentage weight loss of the PG-concrete increased with increase water/binder and aggregate/binder ratios. Also, in comparison to the CEM IIB equivalents, the PG-concrete recorded higher percentage weight losses.

*5.7.1.2.3 Residual compressive strength of the PG-concrete systems*

The changes in compressive strength of the PG-concrete system and the PG-encapsulated systems expressed in terms of the residual compressive strength percentages are shown in Figure 5.19

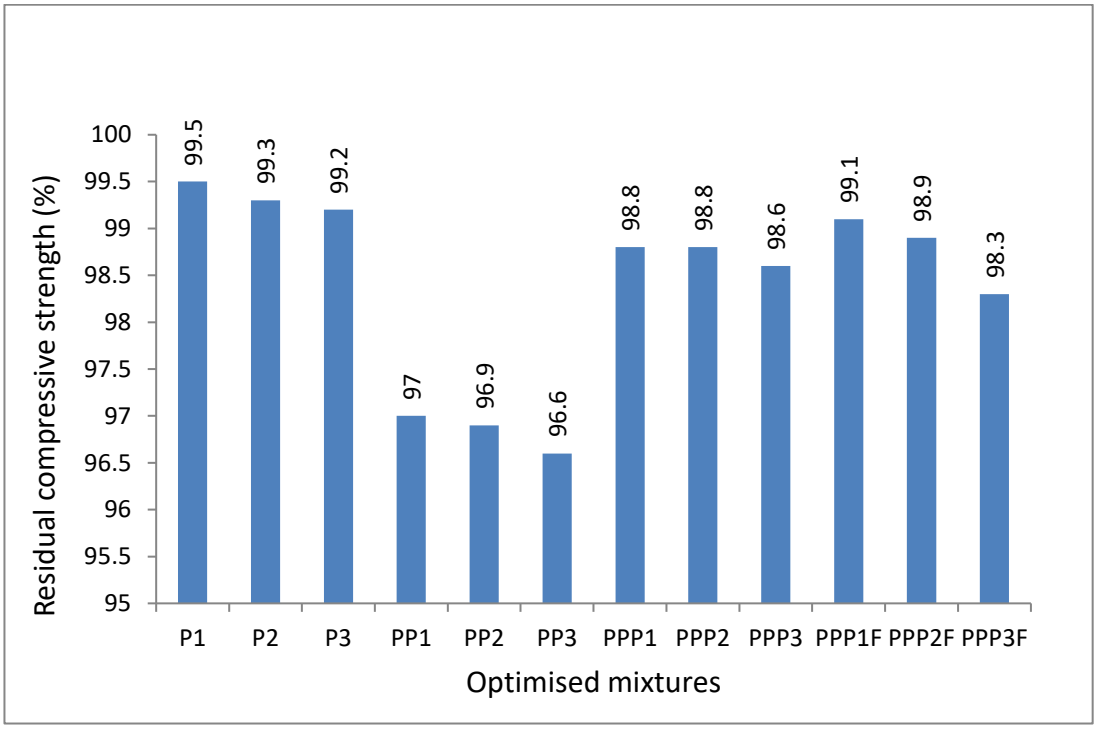


Figure 5.19: Residual compressive strength of the test specimens from the PG-concrete systems due to successive freeze and thaw cycles.

From the results in Figure 5.19, the hydrated PG-concrete mixtures (P1-3) retained most of their compressive strength after being subjected to the freeze and thaw cycles. The test specimens from this system lost between 0.5 – 0.7% of their unconfined compressive strength. When compared to the PG-encapsulated plastic concrete test specimens from PP1-3, the deterioration of the PG-concrete test specimens from P1-3 under freeze and thaw conditions were slower. After 20 successive freeze and thaw cycles, the compressive strength of the test specimens from the PG–encapsulated plastic concrete mixture, the PG–PFA encapsulated plastic concrete mixtures and the PG–encapsulated concrete mixtures with PFA utilised as micro filler reduced by 3 – 3.4%, 1.2 – 1.4% and 0.9 – 1.7% respectively. In comparison to the deterioration of the test specimens from the CEM IIB-concrete systems, the reduction in compressive strength of the equivalent test specimens from the PG-concrete systems after the last freeze and thaw cycle was slightly higher.

### 5.7.2 Sulphate resistance of the concrete systems

As part of the durability assessment, the physical and mechanical deteriorations of the hydrated tests specimens were also established in terms of the changes in weight and compressive strength. The measurements were made after 7, 28 and 90 days of continued immersion of the reference test specimens in tap and seawater for specimens subjected to sulphate attack. Also presented as part of the result are the visually observed physical damages to the test specimens from immersion in seawater.

#### *5.7.2.1 Resistance of the CEM IIB-concrete systems to sulphate attack*

##### *5.7.2.1.1 Visual observation of the test specimens from the CEM IIB-concrete systems after the immersion in seawater for 90 days*

There were no changes in dimensions (expansion) observed in any of the test specimens immersed in seawater. The surfaces (particularly the upper surface) of the test specimens as shown in Figure 5.20 (a-b) were covered with crystallised salt when they were extracted from the seawater-filled container. The level of salt crystallization was observed to increase with immersion age. For the CEM IIB-PFA encapsulated plastic concrete test specimens with PFA utilised either as mineral admixture or micro-filler immersed in seawater for 90 days, surface indentations/cavities (bug – holes) were observed, once the crystallised salt was mopped. The indentations are small irregular cavities less than 0.5 mm deep and ≤ 1mm wide.


Figure 5.20 (a – b): A test specimens with crystallised salt and indentations on the upper and anterior surface after 90 days of continuous immersion in seawater.

*5.7.2.1.2 Mass loss (%)*

The mass loss (%) of the test specimens from the CEM IIB-concrete and CEM IIB-encapsulated plastic concrete mixtures (including those with PFA) are shown in Figure 5.21 (I - IV). The mass (%) for each mix composition as expressed in equation 17 (Chapter 4, Section 4.3.4.2), is percentage ratio of the average mass of three main test specimens immersed in sea water to the average mass of three reference test specimens immersed in fresh water. The relative changes were determined after 7, 28 and 90 immersion days.

From the results, the mass loss (%) of all the specimens increased as the immersion period increase. The mass loss (%) of the test specimens from the CEM IIB – concrete mixtures were much lower than the equivalent encapsulated plastic test specimens. From Figure 5.21 (I), the hydrated specimens from the CEM IIB–concrete mixtures (C1-3) recorded mass losses within the range of 0.03 – 0.26%, while the specimens from CEM IIB-encapsulated plastic concrete mixtures (CP1-3) recorded mass losses within the range of 0.08 – 0.75% (Figure 5.21 II). The inclusion of PFA (as either mineral admixture or micro-filler) appears to reduce the mass losses of the encapsulated plastic concrete. The test specimens from the CEM IIB-PFA encapsulated plastic concrete mixtures (CPP1 – 3) and the CEM IIB-encapsulated systems with PFA micro fillers ($CPP1_f$ – $3_f$) recorded mass losses ranging from 0.06 – 0.44% and 0.04 – 0.38% respectively (Figure 5.21 III and IV).

The results also confirmed that, the mass loss of the test specimens from the CEM IIB-concrete systems increased with increase in both water/binder and aggregate/binder ratios. Hence, for the immersion periods investigated, the first mix in each system (C1, CP1, CPP1 and $CPP1_f$) with the water/binder ratio of 0.5 and aggregate/binder ratio of 5/1 recorded the lowest percentage mass losses, while third mixtures utilising a w/b ratio of 0.6 and aggregate/binder ratio of 6/1 (mix C3 CP3, CPP3 and $CPP3_f$) recorded the highest mass losses.

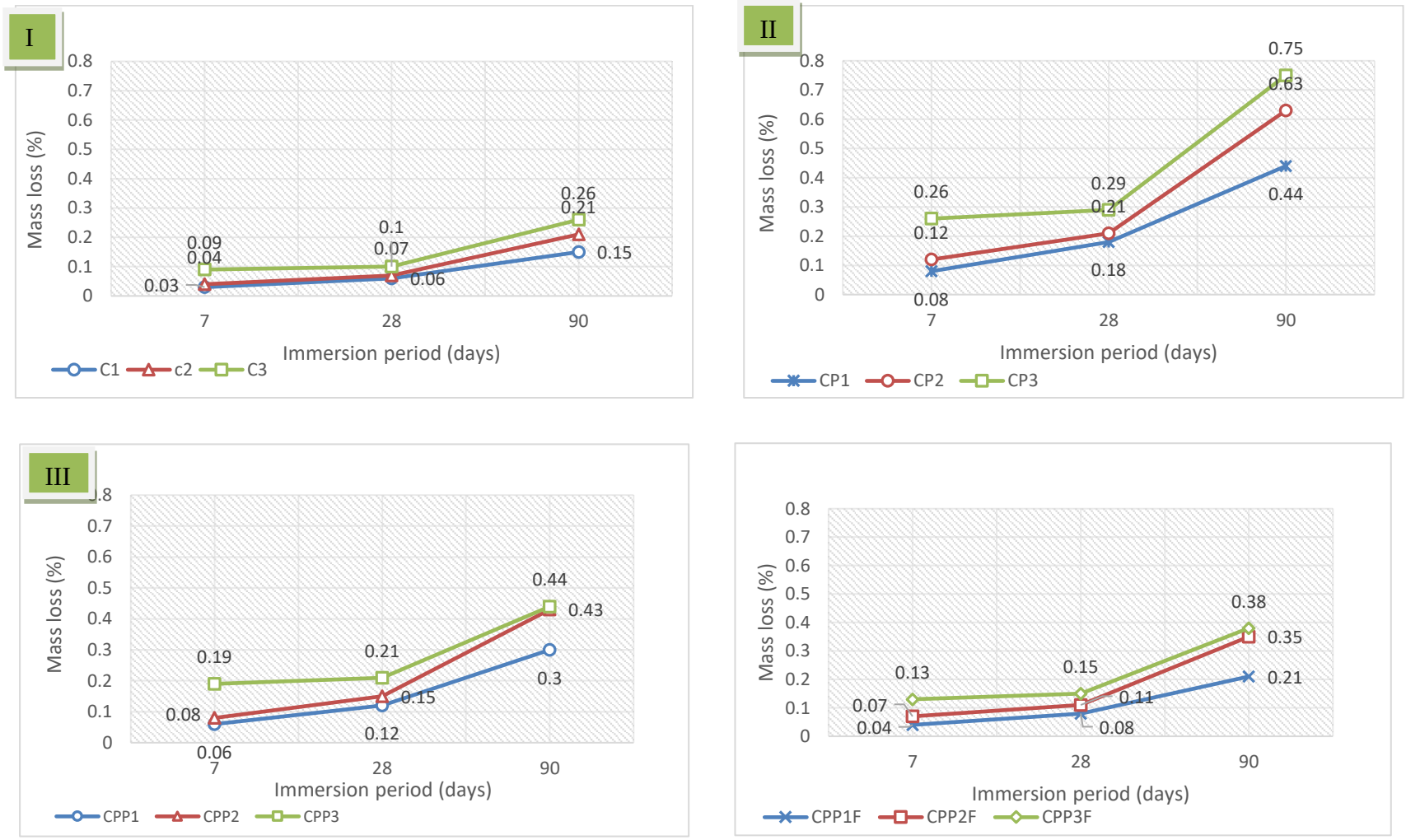


Figure 5.21: Mass loss (%) of the test specimens from - I) CEM IIB-concrete, II) PC–encapsulated plastic concrete, III) PC–PFA encapsulated plastic concrete and IV) PC–encapsulated plastic concrete with PFA micro filler

*5.7.2.1.3 Compressive strength loss (%)*

The relative compressive strength change (%) of the test specimens from the conventional CEM IIB-concrete and the encapsulated plastic concrete mixtures are shown in Figure 5.22 (I-IV). As with the mass loss (%), the compressive strength loss (%) were also expressed as percentage ratio of the average compressive strength of three main test specimens (specimens immersed in seawater) and the average compressive strength of the reference test specimens immersed in fresh water. The compressive strength values were determined after 7, 28 and 90 days of separate continuous immersion in sea and fresh water.

From the result, the compressive strength of all the specimens decreased gradually as the exposure period increased. The deterioration in strength of the CEM IIB-concrete system was observed to range between 0.18 – 0.26% for the immersion period up to 90 days, while that of the encapsulated plastic concrete ranges between 0.53 – 1.92% for the same period. When PFA was added to the encapsulated plastic mixtures, the percentage changes in compressive strength observed for all the encapsulated plastic test specimens decreased slightly. For all immersion periods, the specimens with PFA included as mineral admixture recorded strength changes within the range of 0.37 and 1.34%, while those including PFA as micro filler recorded strength changes between 0.25 – 1.97%. Overall, the residual compressive strength of the specimen from the CEM IIB-concrete systems were all above 98% after 90 days of seawater immersion suggesting a minimal rate of deterioration of the test specimens. The increase in strength with immersion periods, may also suggest deterioration continued beyond the immersion periods (90 days) investigated in this work.

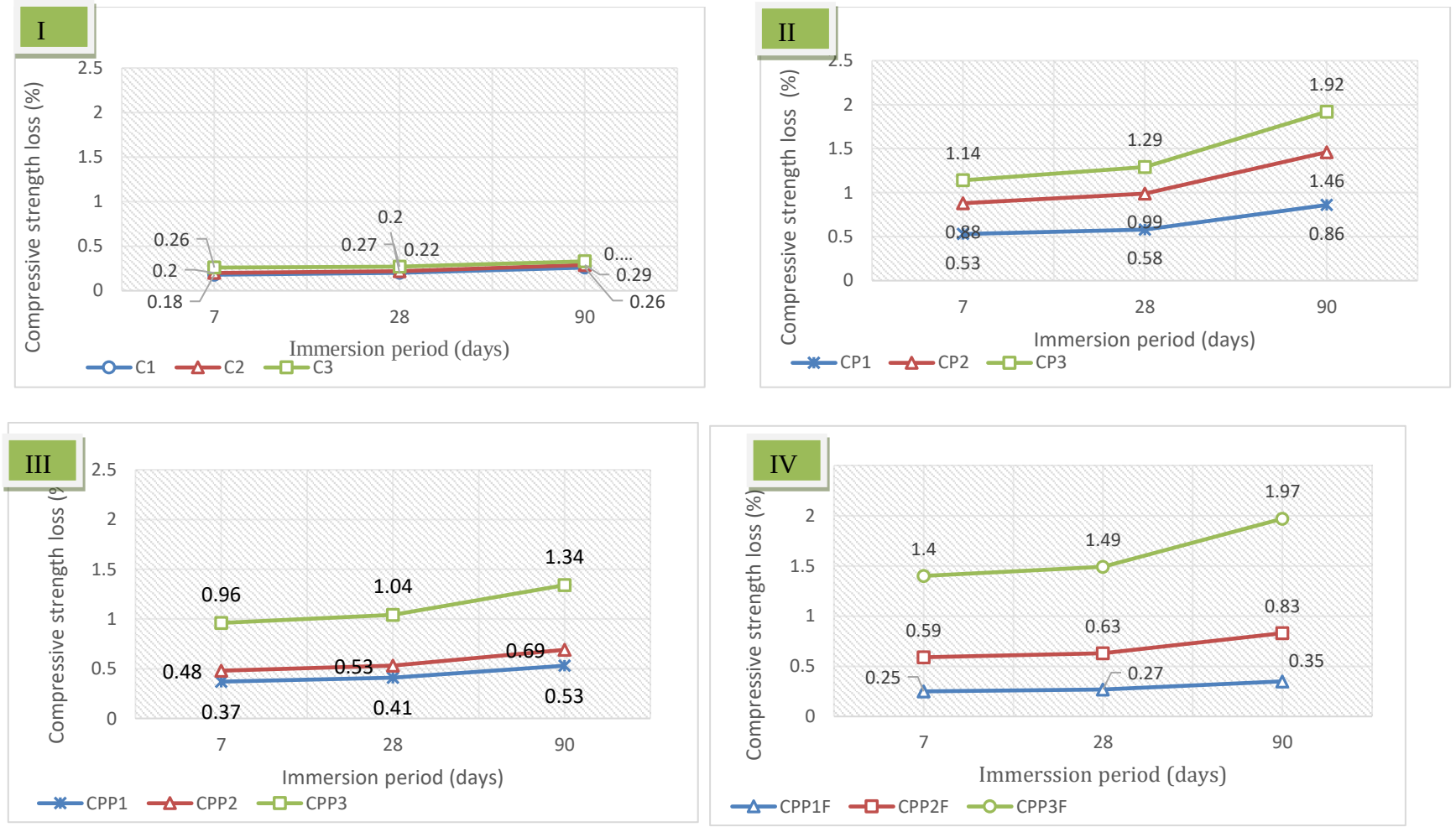


Figure 5.22: Compressive strength loss (%) of the test specimens from - I) PC concrete II) PC – encapsulated plastic concrete, III) PC – PFA encapsulated plastic concrete and IV) PC – encapsulated plastic concrete with PFA micro filler

### *5.7.2.2 Sulphate resistance of the PG-concrete systems*

*5.7.2.2.1 Visual observation of the test specimens from the PG-concrete systems after the immersion in seawater for 90 days*

Similar to the test specimens from the CEM IIB-concrete system, there were no visible changes in dimensions but surface indentaions were observed when the test specimens from the PG-encapsulated plastic concrete specimens with PFA were extracted from the saline water. The surface of the test specimens were also covered with crystallised salts like the CEM IIB – concrete equivalent.

*5.7.2.2.2 Mass loss (%)*

The change in mass of the main test specimens from the PG-concrete systems when immersed in seawater expressed as a percentage ratio of the reference test specimens immersed in fresh water are shown in Figure 5.23 (I – IV). The result presented in Figure 5.23 (I), indicates that the mass loss (%) of the all the hydrated test specimens from conventional PG-concrete mixtures (P1-3) increased as the immersion period increased. The specimens from the three groups of mixtures making up this concrete recorded mass loss ranging from 0.4% - 0.36% for the immersion periods investigated. In comparison to the PG-concrete mixtures, the CEM IIB - encapsulated plastic mixtures recorded higher percentage mass losses. The specimens from the first mix (PP1) recorded mass losses ranging between 0.10 – 0.88% for the immersion periods investigated. The mass losses observed with the specimens from this system (PG-encapsulated plastic concrete) also increased with immersion periods (Figure 5.23 II). The addition of PFA as observed in Figure 5.23 III and IV led to slight reductions in mass losses observed with the encapsulated plastic test specimens. The mass loss (%) of the encapsulated concrete with PFA utilised either as a micro-filler of mineral admixture (PPP1-3 and $PPP1_f$ -$3_f$), like the PG-encapsulated plastic concrete (PP1-3), also increased with immersion periods. The mixtures utilising PFA as micro filler ($PPP1_f$ -$3_f$) appears to perform better than the mixtures with PFA deployed as mineral admixture (PPP1-3). The former recorded mass losses within the range of 0.04 – 0.40%, while the latter recorded mass losses within the ranges of 0.07 – 0.56% for the immersion periods. In comparison to their CEM IIB counterparts, the test specimens from the PG-concrete recorded higher mass losses (%).

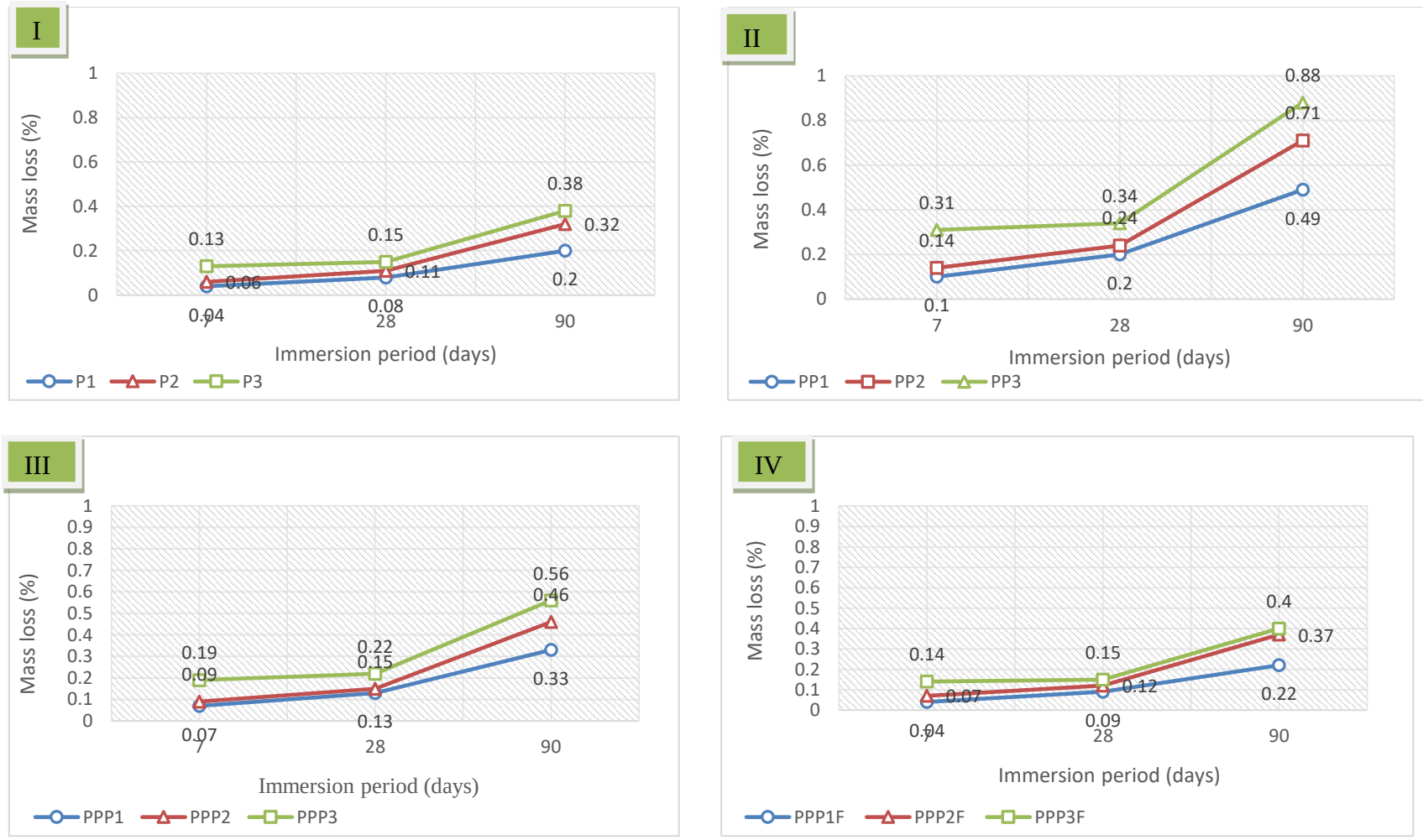


Figure 5.23: Mass loss (%) of the test specimens from - I) PG-concrete (P1-3), II) PG–encapsulated plastic concrete (PP1-3), III) PG–PFA encapsulated plastic concrete (PPP1-3) and IV) PG–PFA encapsulated plastic concrete ($PPP1_f$-$3_f$)

*5.7.2.2.3 Compressive strength loss (%)*

The relative difference in compressive strength (%) between the test specimens immersed in sea and test specimens immersed in freshwater are shown in Figures 5.24 (I-IV). Like the results of the CEM IIB-concrete, the compressive strength loss (%) of all the test specimens decreased as the exposure period increased. The compressive strength loss of the PG-concrete system was observed to range between 0.24 – 1.43 % for the immersion periods 7, 28 and 90 days, while that of the encapsulated plastic concrete ranges between 0.28 - 1.92% for the same period. When PFA was added to the encapsulated plastic mixtures, the changes in compressive strength slightly decreased. The encapsulated plastic specimens with PFA included as mineral admixture recorded relative compressive strength values ranging between 0.34 and 0.85%, while those including PFA as micro filler recorded strength values within the range of 0.27 – 3.36%. The latter system recorded the highest strength loss of any of the concrete systems investigated. When compare to CEM IIB equivalents the individual PG-concrete mixture demonstrated a higher level of deterioration after continuous immersion in seawater for 90 days.

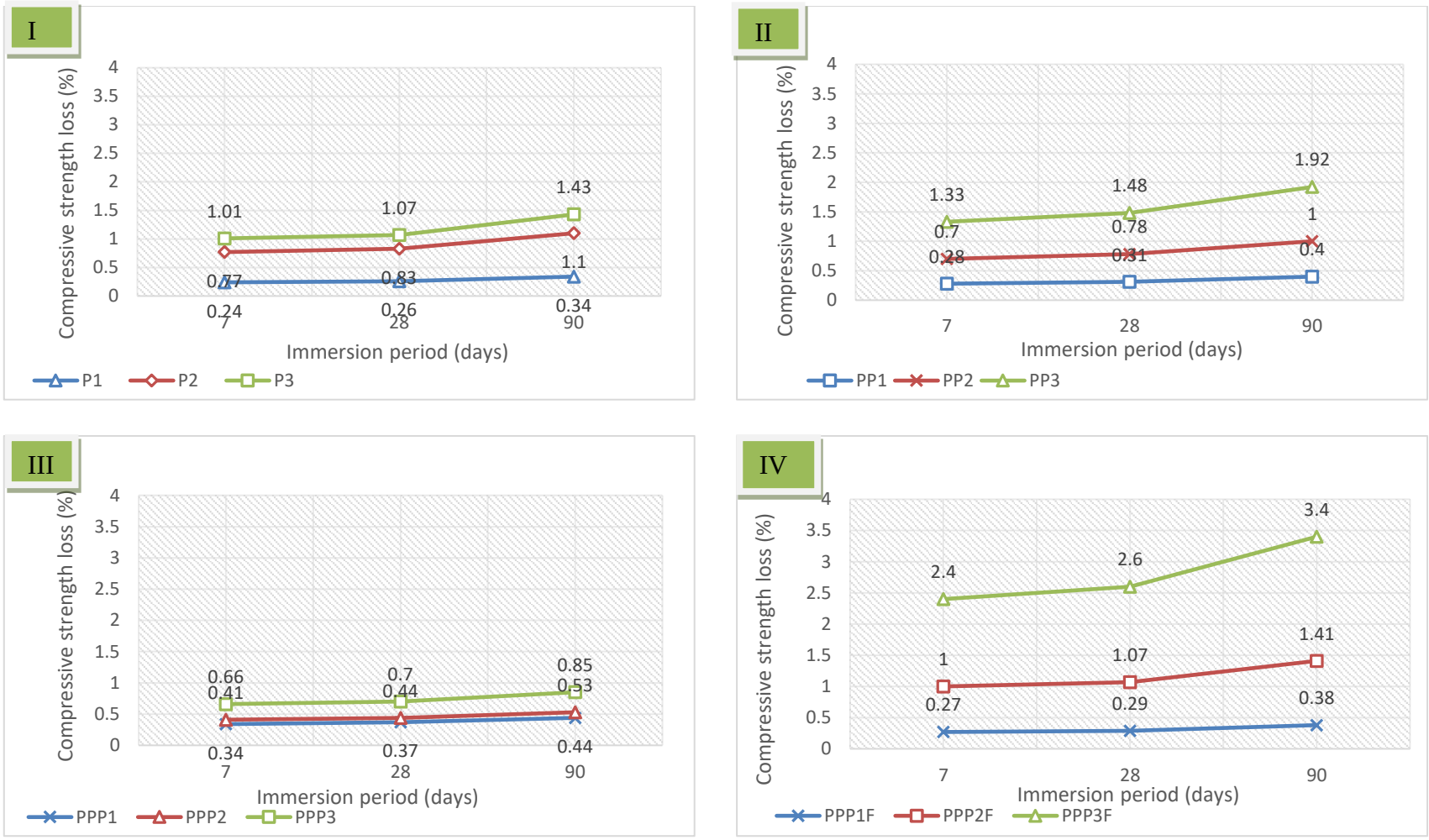


Figure 5.24: Compressive strength loss (%) of the test specimens from - I) PG-concrete (P1-3), II) PG–encapsulated plastic concrete (PP1-3), III) PG–PFA encapsulated plastic concrete (PPP1-3) and IV) PG–PFA encapsulated plastic concrete ($PPP1_f$-$3_f$)

### 5.7.3 Thermal properties of the test specimens from the CEM IIB-concrete systems

The performances of the concrete and encapsulated plastic concrete at elevated temperatures were part of the current work. Unlike the results of other two durability properties previously presented (freeze and thaw and sulphate resistance), the results of the deterioration of conventional concrete and encapsulated plastic concrete due to temperature increments were determined only for the best performing CEM IIB-concrete and the CEM IIB-PFA encapsulated plastic concrete test specimens. A fire scare scenario stopped the investigation. Excessive smoke from the melting plastic in the encapsulated plastic test specimens was released into the work environment when the target temperature of 200 $^{o}$C was adopted. This was not envisaged, as it had been assumed that at about 200$^{o}$C, even though near the melting point, the plastic encapsulated in cementitious materials, as in the current work, would still maintain its solid form. The melting point of the plastic aggregate was reported to be between 240 – 270$^{o}$C in Chapter 3. Nonetheless, the result obtained from the CEM IIB-PFA encapsulated plastic concrete test specimens investigated, to a certain degree gave an understanding of the mode and extent of physical (mass loss) and mechanical deformation (compressive strength change) of the encapsulated plastic system subjected to heat treatment at target temperatures of 30, 40, 50, 100, 150 and 200$^{o}$C for 2 hours. The results presented focus on the mass and compressive strength loss.

#### *5.7.3.1 Visual observation of the test specimens subjected to heat treatment*

There were no crack marks observed on the CEM IIB-concrete test specimens throughout the investigation. However, as shown in Figure 5.25 (I), chipping around the edges and small hollow shaped depressions were observed on the surface of the concrete test specimens after the last target temperature (200 $^{o}$C). The same indentations and some crack lines were observed on the encapsulated plastic concrete test specimens at temperatures above 50 $^{o}$C onwards (Figure 5.25 II – IV). These indentations and crack lines appear to be more pronounced as the temperature increased. At 200 $^{o}$C, the plastic aggregates appear to have melted and were extruding through the matrix possibly unto the oven floor. The number of visible crack lines has more than doubled, while the surface indentations previously noticed have disappeared completely. It appears the melted plastic had proceeded to the surface through these hollow openings. The specimens at the stage were however, all still sound and in a solid form. Furthermore, after crushing the

encapsulated test specimens, it was observed that the melting was limited to the plastic aggregates closest to the surface. About 5mm from the cover/surface of the specimens through to the core of the specimens, the plastic aggregates were observed to still be in a solid form.

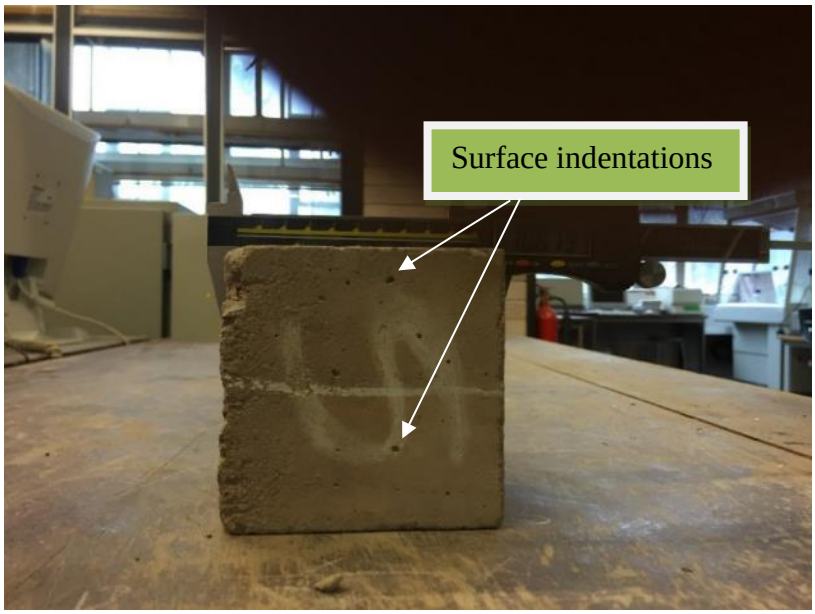


Figure 5.25 (I): CEM IIB-concrete test specimens with hollow indentations on the surface and spalling at the edges after being subjected to heat treatment at 200ºC for two hours

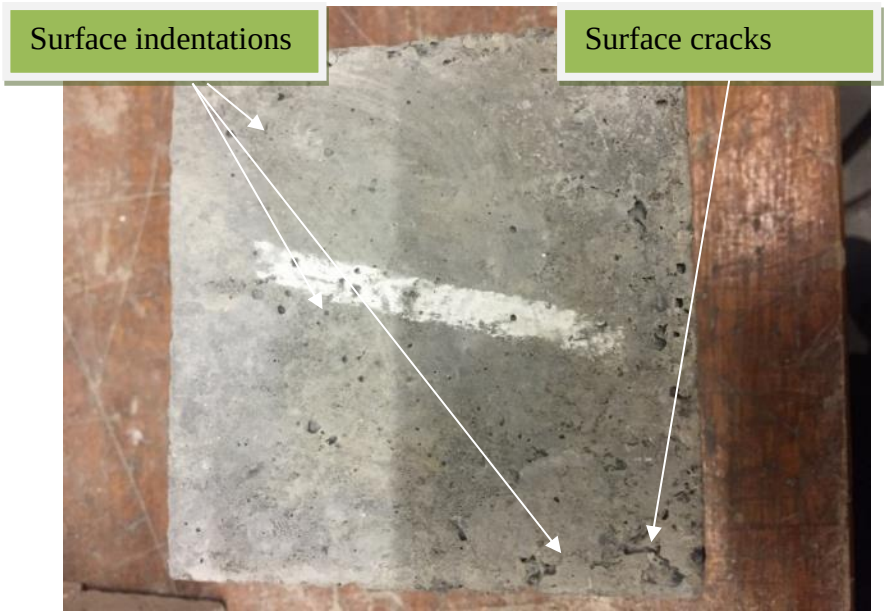


Figure 5.25 (II): CEM IIB - PFA encapsulated plastic test specimens with hollow indentations and crack lines on the surface after being heated at 50$^{o}$C for two hours

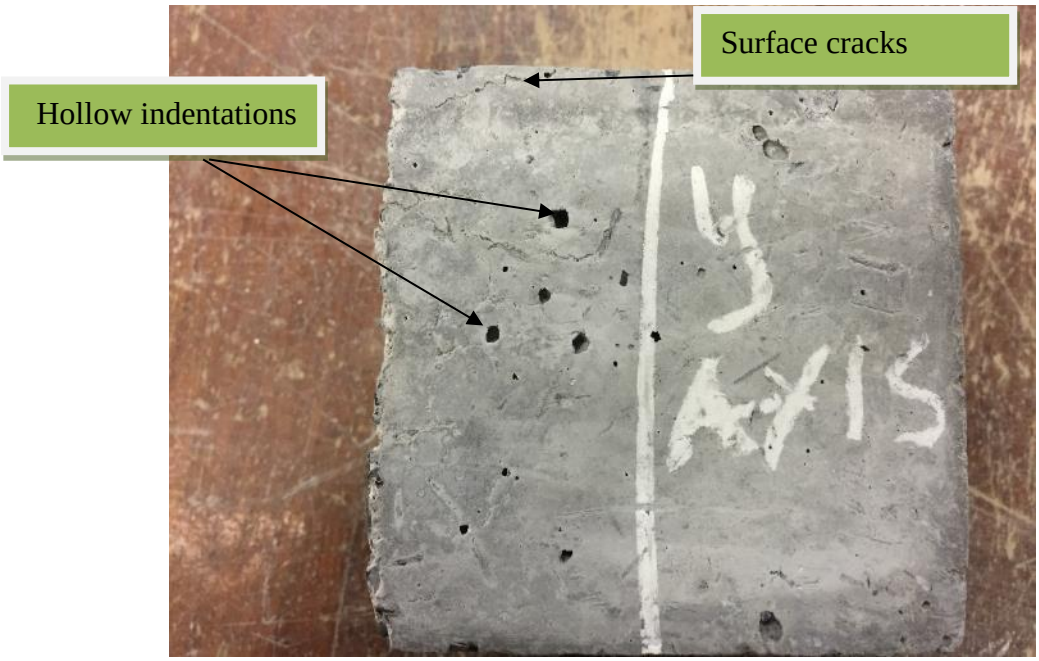


Figure 5.25 (III): CEM IIB - PFA encapsulated plastic test specimens with more pronounced hollow indentations and crack lines on the surface after being heated at 100$^{o}$C for two hours


Figure: 5.25 (IV): CEM IIB- PFA encapsulated plastic test specimens with more pronounced hollow indentations and crack lines on the surface after being heated at 150$^{o}$C for two hours

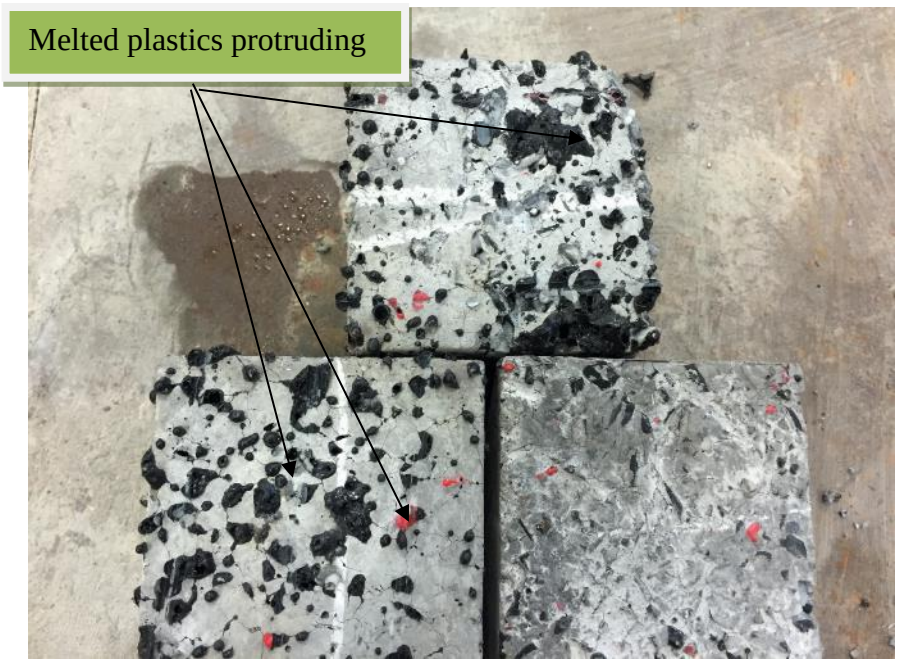


Figure 5.25 (V): CEM IIB-PFA encapsulated plastic concrete test specimens after being heated at 200$^{o}$C for two hours

### *5.7.3.2 Mass loss (%) of the test specimens subjected to elevated temperature*

The result in Figure 5.26 represents the residual mass (in %) of the conventional CEM IIB-concrete (C1) and the encapsulated plastic concrete (CPP1). The residual mass was obtained from the difference in average masses of three (main) test specimens and three-reference test specimens (per mix composition), expressed as a percentage of the average mass of the reference test specimens. The main test specimens as mentioned in Chapter 4, Section 4.3.4.3, were the specimens subjected to heat treatment, while the reference test specimens were retained at room temperature (20 ±3$^{o}$C) in the laboratory.

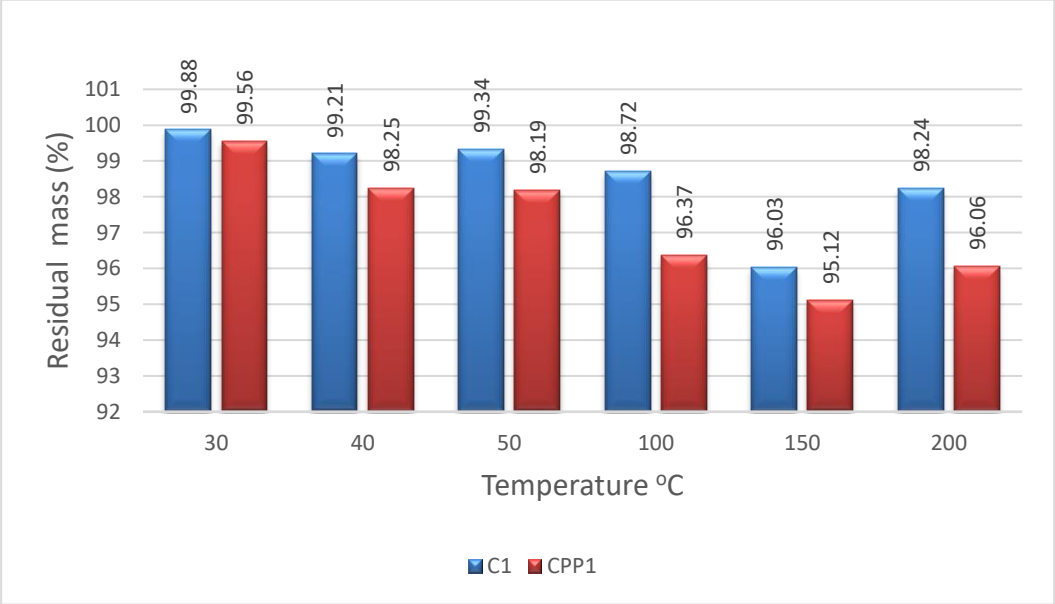


Figure 5.26: Variation in mass of the CEM IIB-concrete (CP1) and CEM IIB-PFA encapsulated plastic concrete (CPP1) subjected to thermal treatment up to 200$^{o}$C for two hours

From Figure 5.26, the residual mass (%) of the test specimens investigated decreased as the temperature was increased. The residual masses (%) of the CEM IIB concrete test specimens ranges between 0.12 and 1.31% while, the residual mass (%) of the CEM IIB-PFA encapsulated plastic system ranges between 0.44 – 3.94%. In relation to the concrete specimens, the mass loss (%) of the encapsulated plastic test specimens was a slightly higher at all temperatures. The difference in mass is more pronounced in test specimens subjected to higher temperatures above 50 $^{o}$C. Overall, both the CEM IIB concrete and

the CEM IIB-encapsulated plastic concrete test specimens demonstrated a slight reduction in mass follow the thermal treatment. The difference in mass between the reference and the main test specimens from both concrete types appear to increase as the temperature increased.

### *5.7.3.3 Relative compressive strength (%) of the test specimens subjected to elevated temperature*

Similar to the mass loss, the result presented in Figure 5.27 represents the relative compressive strength change (%) of the concrete mix (C1) and the encapsulated plastic mix (CPP1). The results indicate that temperature increments from room temperature, up to 100 $^{o}$C have no significant effect on the compressive strength of the CEM IIB-concrete test specimens. However, between 150 and 200 $^{o}$C, the concrete test specimens lost approximates 0.03 - 0.06% of its compressive strength. Meanwhile, the encapsulated plastic test specimens subjected to thermal treatment recorded relative compressive strength (%) of 99.92, 98.89, 97.6, 96 and 100.05 at temperatures 30, 40, 50, 100, 150 and 200 $^{o}$C respectively. This equates to 0.08 – 4% compressive strength loss between room temperature (20 ± 3$^{o}$C) and 150 $^{o}$C, but a strength gain of 0.5% was recorded at 200 $^{o}$C.

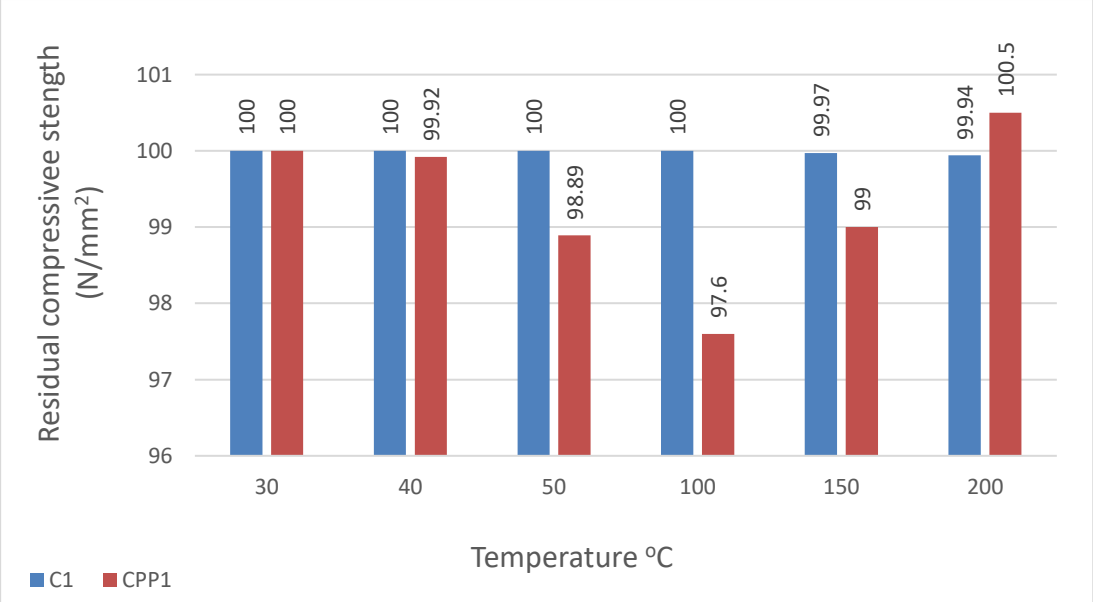


Figure 5.27: Variation in compressive strength CP1 and CPP1 subjected to thermal treatment up to 200$^{o}$C

# CHAPTER 6-DISCUSSION

*This chapter discusses the overall results of the research, their interpretations and practical implications. For easier presentation, the chapter has been divided into three sections. The first section, Section 6.1, discusses the workability, physio-mechanical and durability performance of the CEM IIB- concrete and encapsulated plastic concrete mixtures (with CEM IIB binder or CEM IIB-PFA). The second section, Section 6.2, discusses the same parameters but for the equivalent mixtures from the PG-concrete. The chapter concludes with the analysis of the economic benefits and practical application of the encapsulated plastic concrete mixtures and both the CEM IIB- and the PG-concrete systems (Section 6.3).*

## 6.1 CEM IIB- CONCRETE SYSTEM

### 6.1.1 Variations in workability of the fresh mixtures from the CEM IIB – concrete system

Workability was used in the current work to determine the ease in placing or consolidating concrete with the least amount of segregation. The variations in workability of the mixtures from each of the four concrete mix types (CEM IIB-concrete, CEM IIB-encapsulated plastic concrete, CEM IIB-PFA encapsulated plastic concrete and the CEM IIB-encapsulated plastic concrete with PFA micro filler may be attributed mainly to the water content and the aggregate (fine or coarse) type and quantity. Water content was recognised in the literature as the main factor influencing the workability of concrete. The addition of water beyond standard consistency (that is, the water needed for the complete hydration of the cement) decreases the viscosity of the concrete thereby increasing its workability (Neville, 2012 and Lamond and Pielert, 2006). It is also important to note that, the increase in water content beyond the standard consistency and the water absorption capacity of the aggregate in a concrete mix may also increase the porosity and decrease the compressive strength (Neville, 2012).

#### *6.1.1.1 CEM IIB–concrete*

As observed with the CEM IIB-concrete mixtures (C1-3), workability (slump and compaction index) increased when the water/binder ratio was increased. The workability of the mixtures (C1-3) was also observed to decrease with increase in aggregate/binder ratio. This may also be attributed to the influence of water content. A reduction in the

water content may also decrease workability (Neville, 2012). The increase in aggregate/binder ratio, during the mix design was achieved by increasing the aggregate content and reducing the cement content. A reduction in cement content at a given water/binder ratio implies a reduction in water content. Hence, also consistent with the literature the decrease in workability with a reduction in water content at a constant water/binder ratio was also observed.

#### *6.1.1.2 Effect of aggregate replacement on workability of the CEM IIB – concrete mixtures*

The replacement of natural aggregates (river sand and 10 mm limestone aggregates) with the recycled lightweight aggregates (FBA and 0 – 10 mm - plastic aggregates) significantly decreased the workability (slump) of the CEM IIB-encapsulated plastic concrete mixtures (CP1-3). The mixtures (CP1-3) recorded zero (mm) slump values, which represents 100% reduction in workability (slump) compared to the equivalent conventional CEM IIB-concrete mixtures (C1-3). The CEM IIB-PFA encapsulated plastic mixtures (CPP1-3) and the CEM IIB-encapsulated plastic concrete with PFA micro fillers ($CPP1_f$-$3_f$) demonstrated collapse or shear slump. As a result, the variation in workability was evaluated from the compaction index investigation (compaction index). The result of the compaction index (Table 5.2) indicated that, the workability of the encapsulated plastic concrete mixtures (including those with PFA), increased with increase in water/binder ratio but decreased with increase in aggregate/binder ratio.

The variations observed in workability of the CEM IIB-concrete and the encapsulated concrete mixtures were mostly dependent on the amount and physical characteristics of the fine (FBA) and coarse (0-10 mm) plastic aggregates, and the use of supplementary cementitious material (PFA). In the literature, the use of high substitution percentages of waste plastic in polymer concrete as either fine or coarse aggregate replacement is shown to decrease workability (Ismail and Al-Hashmi, 2008, Gu and Ozbakkaloglu, 2016, Manjunath, 2016 and Albano et al., 2009). Ismail and Al- Hashmi (2008), and Manjunath (2016), in their separate works on the use of waste plastic (PET and E-plastic waste) as fine or coarse aggregate replacement, observed that the workability (slump values) of fresh polymer concrete mixtures investigated, reduced by over 50%, when the substitution levels increased up to 20%. Both researchers attributed the decrease in workability to changes in flow behaviour and high segregation of polymer concrete due

to the low bulk density and particle shape of waste plastic. In this work, 100% volumetric replacement of conventional limestone aggregate was replaced with recycled plastic aggregates, as such the decrease in workability observed was anticipated

It is widely acknowledged in conventional concrete mixtures, that uniform (shape) aggregates (smooth, round or equidimensional particles) increase the workability of concrete, while non–uniform aggregates (angular, flaky, elongated particles) increase segregation, and thus decrease workability (Neville, 2012, Lamond and Pielert, 2006, and Mindess et al., 2003). The FBA and (0-10 mm) plastic aggregates used in the current study contain a high percentage of non – uniform shaped particles (Table 3.2). They (the materials) were also lightweight with specific gravities lower than specific gravity of the conventional aggregates (river sand and coarse aggregates (Table 3.2). The specific gravity of the FBA and (0-10mm) plastic aggregates used in the current work have specific gravities of 1.7 and 1.5 respectively, while the river sand and 10 mm limestone aggregates have specific gravities of 2.7 and 2.6 respectively. These physical properties (particle shape, textures and specific gravities) combined may all increase the void volume (porosity) of the CEM IIB-encapsulated plastic concrete mixtures (CP1-3).

The water absorption capacity and particle size distribution of the lightweight aggregates is another factor, which may increase the porosity of the encapsulated plastic concrete mixtures. The water absorption percentages of the FBA and (0-10mm) plastic aggregates used in the current work at 24% and 0.1% respectively were also lower than the water absorption percentages of river sand and (10 mm) limestone aggregates (29% and 5.2 % respectively). Since there is no capacity to reduce the water content of the encapsulated mixtures, the unabsorbed free water retained in the concrete, which does not react with Portland cement, may increase the porosity and reduce the workability of the concrete. The water/binder ratio indicated in the mix design does not take into account the amount of excess water provided by the low-water absorption of the encapsulated plastic. This was mainly to ensure a direct comparison between the conventional and encapsulated plastic concrete could be made. However, as observed by Senhadji et al., (2015) in their work on the effect of incorporating PVC waste as aggregate on the physical, mechanical, and chloride ion penetration behaviour of concrete, workability improvement can be achieved if the unit weight of water is reduced to reflect the low water absorption percentage of recycled waste plastics. Additionally, the particle size distribution (Table

3.2) shows that, FBA contains about 50% fine or coarse aggregates, while (0-10mm) plastic aggregates contain approximately 75% coarse and 25% fine aggregates. The deficiency in fine aggregates and high proportion of similar sized coarse aggregates (particle size 4 – 10 mm) may increase segregation of the plastic concrete mixtures (Nursyamsi et al., 2017).

#### *6.1.1.3 Effect of PFA*

The addition of PFA however, improved the placing and compactability of the encapsulated plastic mixture. This may be due to the improved microstructure and/or increased water demand of the cementing matrix due to the high carbon content of the PFA used in the current work. The spherical particles of alumina-silicate glass and the high-water absorption capacity of the PFA may densify the cement paste. The high carbon content of the PFA may mitigate the problem of excess water observed in the CEM IIB-encapsulated concrete mixtures (Metha and Monteiro, 2006). The PFA used in the current work contains cellular carbon particles with particle size larger than 45μm. Its loss of ignition determined using BS EN 15169:2007 was 17.5%. BS EN 450 typifies the loss of ignition with carbon content, although loss of ignition also includes evaporated of water and $CO_2$. In concrete, the use of PFA with over 10% carbon content has been reported to increase the water demand of concrete. This was demonstrated in the flow analyses carried out as part of the current work (Figure 5.6). A 10% reduction in flow value (fluidity) of Portland cement was observed, when the PFA was added to the Portland cement in the CEM IIB-PFA matrix. The same PFA was used throughout this study and the water demand of the CEM IIB-PFA paste to achieve the same consistency (flow) as the CEM IIB paste was not meet. That is, the water content of the CEM IIB-PFA paste was not increased to attain the same workability as the CEM IIB paste. The only problem envisaged with the use of the high carbon PFA is the water absorption properties of high carbon PFA, which may affect the long- term durability of the encapsulated plastic mixtures. Some of such durability issues were evaluated in the current work using the freeze and thaw and the sulphate resistance analyses.

When PFA was utilised as a mineral admixture in the encapsulated plastic concrete mixtures (CEM IIB-PFA encapsulated plastic concrete mixtures, CPP1-3), the workability of the concrete decreased in comparison to the CEM IIB-encapsulated plastic concrete mixtures utilising PFA as a micro-filler ($CPP1_f$ -$3_f$). The only difference between

the two groups of encapsulated concrete mixtures is that the CPP1-3 contained a higher amount of water and aggregate (fine or coarse) than the equivalent CPP$1_f$ -$3_f$. Hence, the difference in the workability of the two groups of mixtures may be attributed to both the water and aggregate content, which as discussed previously may both negatively influence the workability of the plastic mixtures.

### 6.1.2 Variations in density of the hydrated mixtures from the CEM IIB–concrete system

The variations observed between the average densities of test specimens from the CEM IIB–concrete mixtures (C1-3), the CEM IIB-encapsulated plastic concrete mixtures (CP1-3) and the CEM IIB-PFA encapsulated plastic concrete mixtures CPP1-3 and CPP$1_f$-$3_f$), may be attributed to the water content, quantity and physical properties of the aggregates including, particle size, shape and texture, water absorption percentage, bulk density and specific gravity. As observed with workability, these factors all influenced the porosity of the hydrated concrete mixtures.

#### *6.1.2.1 Relationship between density and porosity of the hydrated mixtures*

The use of high quantity of waste plastic in polymer concrete and FBA as fine aggregate replacements in mortar have been reported in the literature to decrease concrete density. In a critical review on the use of plastic aggregates in concrete as fine or coarse aggregate replacement carried out by Gu and Ozbakkaloglu (2016), observed an upwards of 30% reduction in density was observed in the works reviewed, when up to 70% normal weight coarse conventional aggregates were replaced with plastic. The previous works attributed the loss in density of polymer concrete to the specific gravity of the lightweight aggregates. In a similar work on the use of Furnace Bottom Ash (FBA) as fine aggregate replacement, Aggarwal et al., (2007), concluded that the density of concrete decreased with increase in bottom ash content due to the low specific gravity of bottom ash compared to fine aggregates. The specific gravity of the FBA and 0-10 mm plastic aggregates (1.7 and 1.5 respectively) are considerably lower than those of river sand and 10 mm limestone aggregates (2.6 and 2.7 respectively). Hence, coupled with the 100% replacement of both fine and coarse aggregates adopted in the current work, the density of test specimens from the encapsulated plastic concrete (CP1-3, CPP1-3 and CPP$1_f$-$3_f$) were relatively lower than those of the test specimens from the conventional CEM IIB – concrete equivalents (C1-3).

In addition to quantity and specific gravity of aggregates, the measured density of the encapsulated plastic concrete test specimens, may also have been influenced by the water content, and some other physical properties of the aggregate components such as particle size, shape, texture and water absorption (%). These factors as observed with workability of the fresh concrete mixtures may increase the size and volume of voids in concrete and decrease the density of hydrated test specimens. In concrete technology the relationship between densities and porosity are commonly regarded as inversely linear. That is density increases with decrease in porosity and decreases with increase in porosity. As shown in Figure 6.1, the relationships (with experimental errors) between the average densities and porosities of the CEM IIB-concrete (C1-3) and encapsulated plastic concrete test specimens (CP1-3, CPP1-3 and CPP1$_f$-3$_f$) are inversely linear.

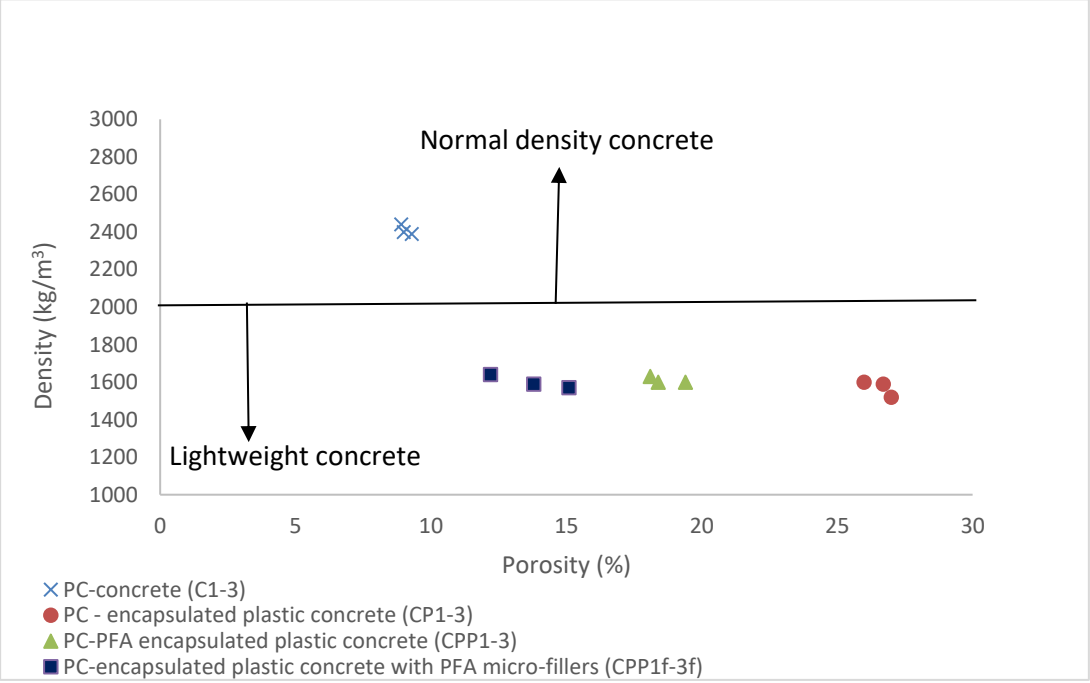


Figure 6.1: Relationship between the density and porosity of the hydrated test specimens from the CEM IIB-concrete system

From Figure 6.1, the average density of all the hydrated test specimens from the CEM IIB-system decreased, when porosity increased. The test specimens from the CEM IIB-concrete mixtures (C1-3) recorded the lowest porosities and as such the highest densities

of all the concrete members/types in the CEM IIB-concrete system. The conventional concrete specimens with the highest average density (C1) demonstrated the lowest porosity while, the concrete specimens with the lowest average density demonstrated the highest porosity. The equivalents in the encapsulated plastic concrete mixtures followed a similar pattern. That is, the test specimens from each encapsulated concrete mix type with the highest density demonstrated the lowest porosity while the test specimens with the lowest density demonstrated the highest porosity. In comparison with the equivalent test specimens from the CEM IIB-concrete mixtures (C1-3) and the encapsulated plastic concrete, the test specimens from the CEM IIB-encapsulated plastic concrete mixtures were the most porous and as such demonstrated the lowest densities.

When PFA was included in the encapsulated concrete mixtures (CPP1-3 and CPP$1_f$-$3_f$), the porosity of the plastic concrete mixtures decreased and density marginally increased. This may be due to the improvement in microstructure of the concrete resulting from better particle size distribution, increased packing density and the formation of more C-S-H gel by PFA. The encapsulated plastic concrete mixtures with PFA used as micro-filler (CPP$1_f$-$3_f$) demonstrated lower porosities relative to the concrete with PFA used as mineral admixtures (CPP1-3). This may also be attributed to the influence of higher aggregate proportion on the microstructure of the CEM IIB-PFA encapsulated plastic mixtures with PFA used as mineral admixtures (CPP1-3). This group of mixtures (CPP1-3) contain twice the amount of (fine and coarse) aggregates in the equivalents from CPP$1_f$-$3_f$. The high aggregate fraction in ‘CPP1-3’ may increase the volume and the distribution of the interface zone in the matrix (Portland cement and FBA), hence increase the porosity of the concrete mixtures. However, even with the higher porosities, the average densities of the test specimens from the CEM IIB-PFA encapsulated plastic concrete mix CPP2 and 3 were slightly higher than those of the equivalents from the CEM IIB-PFA encapsulated plastic concrete (CPP$2_f$ and $3_f$) with the lower porosities. This may be attributed to the increased packing density (arrangement and orientation) of the vibrated concrete. Mix CPP2 and CPP3 contain higher water content and higher fractions of fine and coarse aggregates. The higher water content may have improved the mobility of the aggregate during vibration thereby improving the packing of the aggregates in the hydrated mixtures.

### *6.1.2.2 Relationship between porosity and water absorption of the hydrated mixtures*

The porous nature of concrete according to Neville (2012) also allows it to absorb and retain water easily. The water absorption concrete increases with increase in porosity (Figure 6.2). Due to higher porosities, the water absorption (%) of the test specimens from the encapsulated plastic concrete (CP1-CP3, CPP1-CPP3 and CPP1$_f$-CPP3$_f$) were higher than the equivalents from the CEM IIB-concrete (C1-C3). The test specimens from the CEM IIB-encapsulated plastic concrete (CP1-CP3), the most porous concrete type, also recorded the highest water absorption (%). In comparison to the equivalent test specimens from the conventional CEM IIB–concrete (C1-C3), the mean water absorption (%) of CP1-CP3 test specimens were approximately 82% higher. The inclusion of PFA in CPP1-3 and CPP1$_f$-3$_f$, decreased the water absorption (%) of the encapsulated plastic concrete mixtures. Relative to the C1-3, the water absorption (%) of test specimens from the CPP1-3 and CPP1-3$_f$ were approximately about 70 and 50% higher. Furthermore, as observed with the porosity (%), the test specimens from the CEM IIB-PFA encapsulated plastic concrete (CPP1-3) demonstrated higher water absorption (%) relative to the CEM IIB-encapsulated plastic concrete with PFA used either as micro-filler (CPP1$_f$-3$_f$).

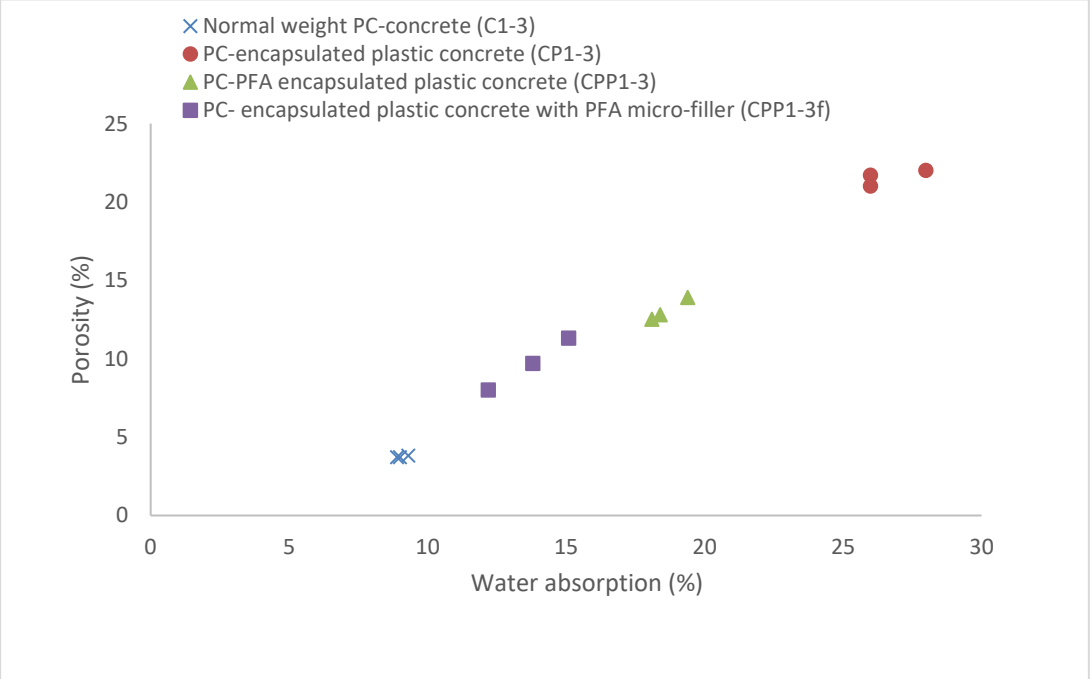


Figure 6.2: Relationship between porosity and water absorption of the hydrated test specimens from the CEM IIB-concrete system

### *6.1.2.3 Relationship between density and water absorption of the hydrated mixtures*

The density of concrete is inversely proportional to its porosity (Figure 6.1), and porosity is directly proportional to water absorption (Figure 6.2). A linear relationship may also be established between water absorption and density (Figure 6.3). Figure 6.3 indicates that water absorption (%) of the test specimens from the different concrete mix types decreased when the average densities of all the concrete mixtures increased. The test specimens from the conventional CEM IIB-concrete mixtures (C1-3) with densities between 2350 - 2440 kg/m$^3$ recorded the lowest water absorption (%) of all the concrete test specimens in this system. The water absorption (%) of the lightweight concrete test specimens from the encapsulated plastic mixtures (CP1-3, CPP1-3 and CPP1$_f$-3$_f$) were 100% higher that the equivalent specimens from C1-3. The densities of the encapsulated mixtures range between 1520 – 1640 kg/m$^3$.

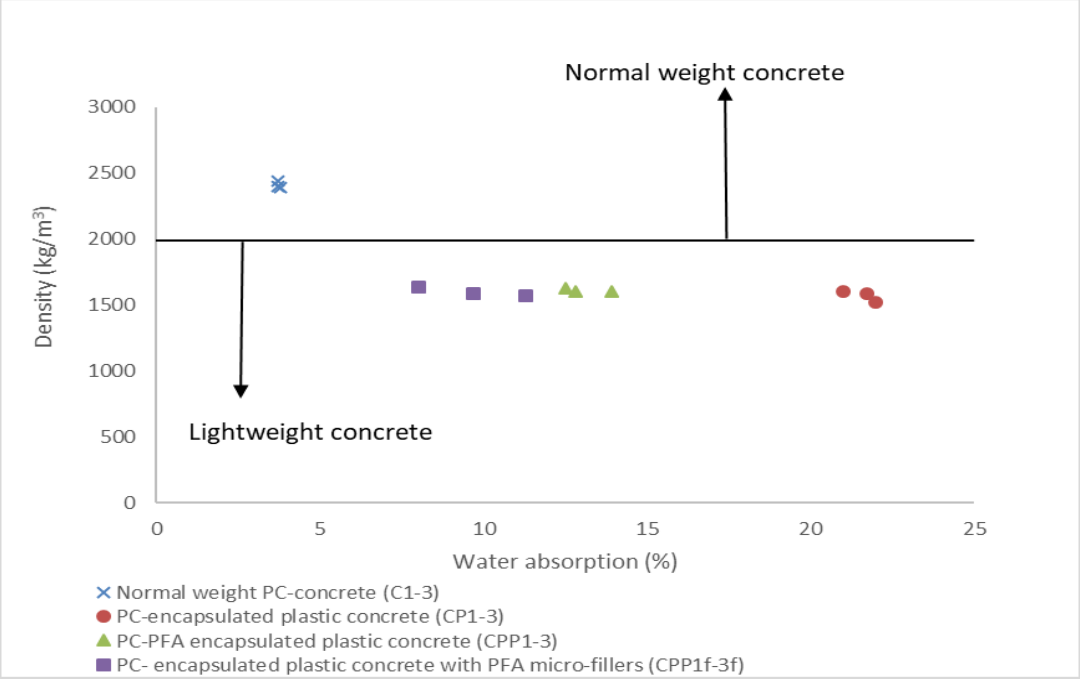


Figure 6.3: Relationship between density and water absorption of the hydrated mixtures from the CEM IIB-concrete system

### 6.1.3 Variations in mechanical performance of the hydrated mixtures from the CEM IIB–concrete system

#### *6.1.3.1 Unconfined compressive strength*

The compressive strength of the test specimens from the CEM IIB-concrete mixtures (C1-3) and the test specimens from the encapsulated plastic concrete mixtures (C1-3, CP1-3, CPP1-3 and CPP$1_f$-$3_f$) as observed in the results increased with increase in curing age. The CEM IIB-concrete mix (C1) developed using the British concrete mix design method (as described by Neville, 2012) achieved its minimum target compressive strength of 49 N/mm$^2$ after 28 days of water curing. Attempts at increasing the workability of the mix by increasing the water/binder in mix C2, slightly decreased the compressive strength of the concrete by almost 10%. Likewise, attempts at reducing the cement content (higher aggregate/binder ratio) to make the concrete leaner (mix C3) at the higher water/binder ratio, led to further reduction (about 11%) in the compressive strength of the concrete.

The compressive strength demonstrated by most of the test specimens from the encapsulated plastic mixtures conform to the strength requirement for lightweight concrete ($\geq$ 7 N/mm$^2$) as specified in BS EN 1992-1-1:2004+A1:2014. The only exceptions are the test specimens from mix CP3, the CEM IIB-encapsulated plastic concrete with the higher water/binder and aggregate/binder ratios (0.6 and 6/1 respectively). This concrete recorded strength of 2.7, 4.8 and 5.6 N/mm$^2$ after 7, 28 and 90 days of water curing. The relatively high water/binder and aggregate/binder ratios of CP3 may be credited with the strength reduction. The two factors increased the porosity, and as such decreased the recorded strength values of CP3 relative to C1 and C2. Increase in water content (water/binder ratio) according to Neville (2012) is the primary factor responsible for the increase in porosity, while the utilisation of high volumes of waste plastics according to Gu and Ozbakkaloglu, (2016), Nibudey et al., (2013) and, Prahallada and Prakash (2013) decrease the compactability and increase the porosity of concrete. Furthermore, the reduction in cement content to achieve the increased aggregate/binder ratio may be another factor responsible for the higher porosity and lower compressive strength of CP3. The reduction in cement content may imply a reduction in the volume of hydrates formed by the CEM IIB cement (particularly C-S-H gel) and an increase in void ratio. This may also reduce the aggregate/paste bonding.

Nonetheless, one of the encapsulated plastic concrete mixtures conform to the ≥ 17 N/mm$^2$ strength specified for structural lightweight concrete in the BS EN 1992-1-1:2004+A1:2014. Mix CPP1$_f$, the CEM IIB–encapsulated plastic concrete with PFA micro – filler and a water/binder ratio and aggregate/binder ratio '0.5 and 5/1' recorded compressive strength values of 17.4 N/mm$^2$ at 28 days and, 23.4 N/mm$^2$ at 90 days. The strength developed by the concrete may be because of the increased compactability, reduced porosity and, strength enhancing characteristics of PFA.

It is important to know that in the utilisation of waste, control mixes are generally included for the sole purpose of reference. The mixes containing waste are not necessarily expected to perform better or even close to those of the control. The key question and way forward, in the utilisation of waste is the establishment of the likely applications that the test results obtained would suggest. In this particular instance, whereas one mix design as argued above met the specifications for structural lightweight concrete, other mixes in the C10-C20 category have applications in low-strength concrete such as bulk fill situations in trenches, concrete surround in structures, for blinding concrete, and use in foot/cycle paths and playfields, among many other applications. The results obtained in the current work suggest that the PC-system was closer to achieving this threshold, while more work is needed with the PG-system in order to optimise the design and hence achieve usable strength magnitudes. In general, form the results obtained in the current work, the low-concrete applications cited suggest that these already available "sinks" for the large volumes of plastic available, as more research work is undertaken.

*6.1.3.1.1 Effect of porosity on the unconfined compressive strength of the CEM IIB-concrete system*

The variations observed in unconfined compressive strength between, the CEM IIB-concrete (C1-3) and the encapsulated plastic concrete test specimens (CP1-3, CPP1-3 and CPP1$_f$-3$_f$) may be attributed to the water/cement ratio and, the chemical composition, quantity, and physical properties (particle shape, texture and low water absorption capacity) of the constituent aggregates. These factors may influence the porosity of the concrete, particularly at the interfacial transition zones. That is, the spaces between the hydrated cement and the (fine or coarse) aggregate. The increase in water content according to Metha and Monteiro, (2006) beyond standard consistency increases the

porosity of concrete due to the formation of capillary voids between the mortar (hydrated cement pastes and fine aggregates) and the coarse aggregates.

Table 6.1: Variations in strength development of the concrete mixtures from the CEM IIB- system

| *Mix reference* | *w/b ratio* | *a/b ratio* | *Density ($kg/m^3$)* | *Porosity (%)* | *Compressive strength* ($N/mm^2$) | | | *Tensile strength* |
|---|---|---|---|---|---|---|---|---|
| | | | *28 days* | *28 days* | *7 days* | *28 days* | *90 days* | *28 days* |
| C1 | 0.5 | 5/1 | 2440 | 8.9 | 25.98 | 49.1 | 60.1 | 3.2 |
| C2 | 0.6 | 5/1 | 2400 | 9.0 | 27.12 | 44.5 | 55.6 | 3.1 |
| C3 | 0.6 | 6/1 | 2390 | 9.3 | 26.1 | 43.6 | 52.1 | 3 |
| CP1 | 0.5 | 5/1 | 1600 | 26.0 | 5.2 | 7.97 | 9.6 | 1 |
| CP2 | 0.6 | 5/1 | 1590 | 26.7 | 5 | 7.7 | 9 | 0.9 |
| CP3 | 0.6 | 6/1 | 1520 | 27.0 | 2.7 | 4.8 | 5.6 | 0.7 |
| CPP1 | 0.5 | 5/1 | 1630 | 18.1 | 8 | 12.23 | 15.3 | 2.2 |
| CPP2 | 0.6 | 5/1 | 1600 | 18.4 | 7 | 11.8 | 14.4 | 1.7 |
| CPP3 | 0.6 | 6/1 | 1600 | 19.4 | 6.7 | 11.6 | 13.8 | 1.4 |
| CPP1F | 0.5 | 5/1 | 1640 | 12.2 | 11.2 | 17.4 | 23.4 | 1.65 |
| CPP2F | 0.6 | 5/1 | 1590 | 13.8 | 6.7 | 11.7 | 16.67 | 1.01 |
| CPP3F | 0.6 | 6/1 | 1570 | 15.1 | 6.5 | 11.15 | 16.61 | 0.92 |

The increase in water/binder ratio due to increased porosity, decreased the compressive strength for all curing ages (Table 6.1 and Figure, 6.4a-c). The only exception was observed at early age (7 days), where there was no direct correlation between the strength of the reference concrete (mix C1-C3) and the recorded porosity values. Mix C2 and C3 with higher porosity values also demonstrated higher compressive strength values relative to mix C1 with the lowest porosity. The 28 and 90 days strength of the concrete (C1-C3) however, all decreased with increase in porosity. The observation recorded at 7 days may be an anomaly or may be as a result increased hydration at early age due to the higher water content of C2 and C3. The two concrete mixtures utilised the higher water/binder ratio of 0.6, while mix C1 utilised the lower water/binder ratio of 0.5. The

compressive strength of all the encapsulated plastic concrete from the CEM IIB-concrete system decreased when the porosity increased.

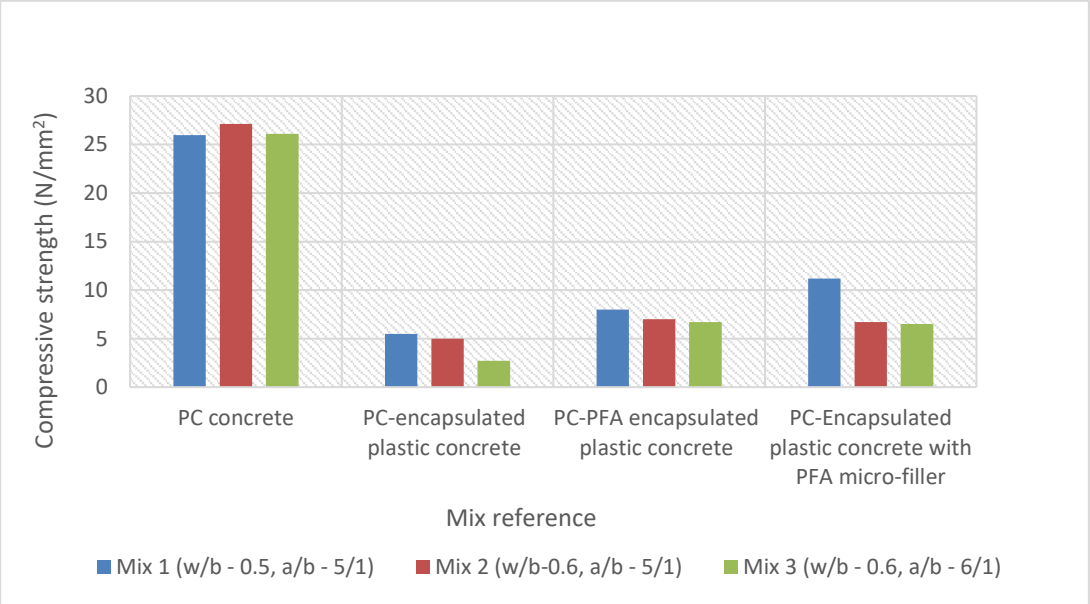


Figure 6.4a: Influence of water/binder and aggregate/binder ratios on the 7 days compressive strength of the CEM IIB-concrete mixtures

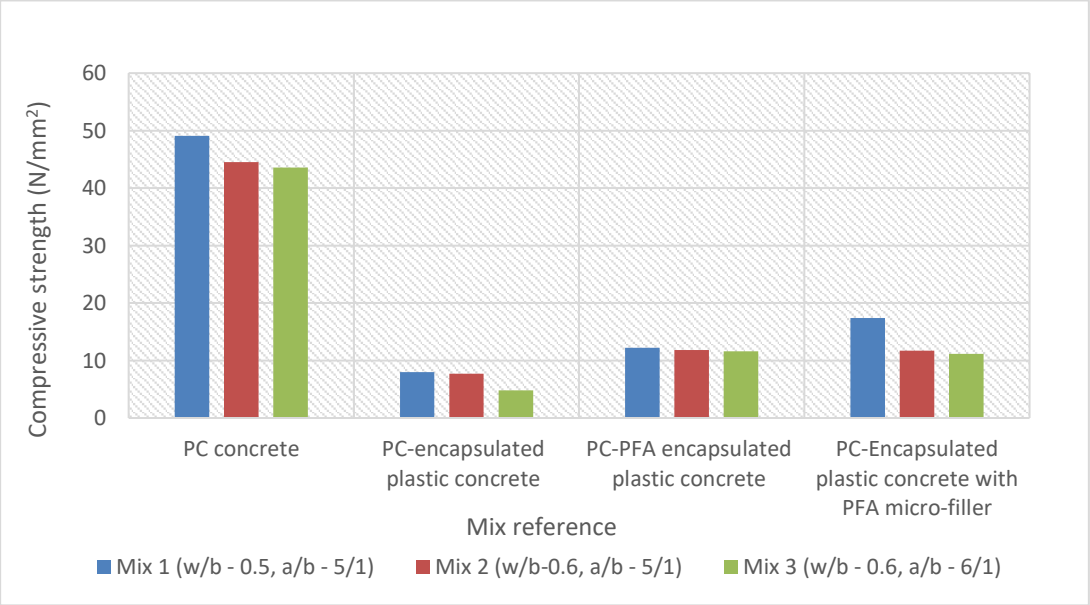


Figure 6.4b: Influence of water/binder and aggregate/binder ratios on the 28 days compressive strength of the CEM IIB-concrete mixtures

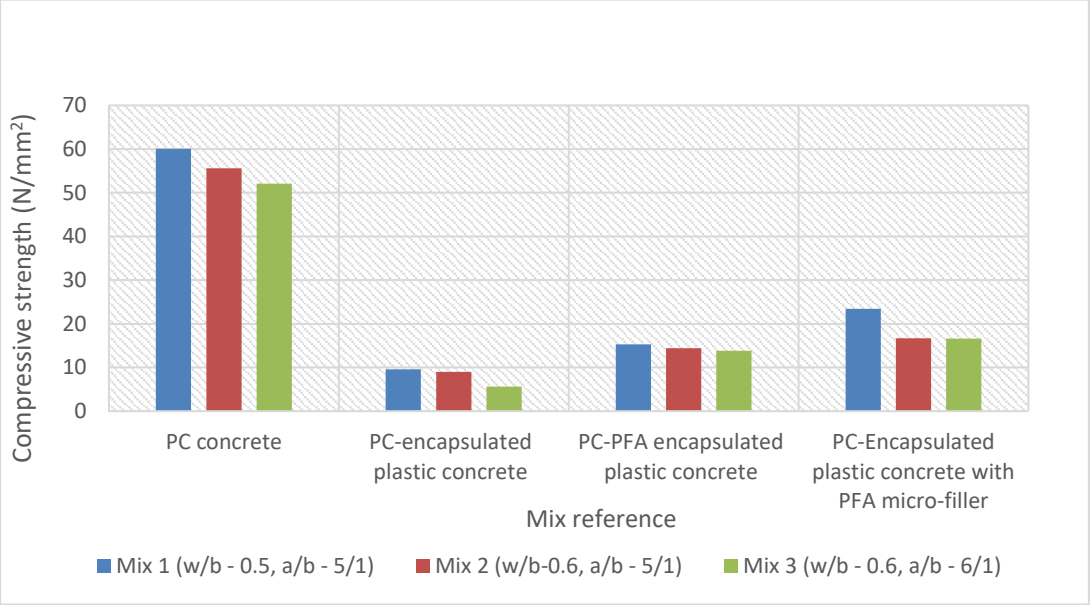


Figure 6.4c: Influence of water/binder and aggregate/binder ratios on the 90 days compressive strength of the CEM IIB-concrete mixtures

From Figure 6.4(a-c), the increase in aggregate/binder ratio generally resulted in a decrease in compressive strength of the concrete (conventional and encapsulated) for all the curing ages investigated. When the water/binder ratio was maintained at 0.6, but the aggregate/binder ratio was varied between 5/1 and 6/1 for second and third mixtures, the compressive strength of the concrete decreased. This may be attributed to the degree of hydration of the binding materials. The volume occupied by the hydration products C-S-H, $Ca(OH)_2$ and calcium sulfoaluminates ($C_6AS_3H_{32}$) formed during the hydration of Portland cement are twice the sum of the volume of the unhydrated cement and the volume of water (Metha and Monteiro, 2006). The volume of hydrates influences the microstructure (density) of the concrete due to the reduction in gel pore and capillary voids. The more hydration products formed, the lower the void spaces (Metha and Monteiro, 2006).

To increase the aggregate/binder ratio, the water and cement contents were reduced while the aggregate content was increased. An increase in aggregate content will imply more void spaces that require filling with cement paste. Hence, when volume of fine and coarse

aggregate in the concrete were increased and the paste (water and cement) was reduced, the concrete became more porous thus, the compressive strength decreased. The inclusion of PFA in the encapsulated plastic concrete reduced the porosity and increased the compressive strength of the encapsulated plastic concrete with PFA utilised as either a mineral admixture (CPP1-3) or micro filler (CPP1f-3f). The production of more cementitious products (C-S-H) improves the microstructure (densification) of concrete, decrease porosity and increase compressive strength according to Metha and Monteiro (2006). Hence, relative to the CEM IIB-encapsulated plastic concrete (CP1-3), the mixtures containing PFA demonstrated higher compressive strength.

The density of concrete according to Metha and Monteiro (2006) is directly proportional to its compressive strength. An increase in density typifies an increase in compressive strength, because the relationship between density and porosity is inverse. As observed in Table 6.1, after 28 days of water curing, the compressive strength of all the mixtures from each concrete mix type (C1-3, CP1-3, CPP1-3 or $CPP1_f$-$3_f$) decreased as (28-days) density decreased. In addition, the equivalent mixtures in the different concrete types, with the lower densities also demonstrated lower compressive strength except for mix CPP2 and CPP3 where the density stayed the same. The two mixtures from the CEM IIB-PFA encapsulated plastic concrete mixtures (CPP2 and CPP3) with the higher water/cement ratios, demonstrated higher densities but similar range of compressive strength as the equivalent from the CEM IIB-encapsulated plastic concrete with PFA used as micro filler ($CPP2_f$ and $CPP3_f$) up to 28 days. At 90 days however, the mixtures with the lower densities $CPP2_f$ and $CPP3_f$ demonstrated slightly higher compressive strength. Since both concrete mix types contain the same amount of PFA, the pozzolanic activities of PFA were expected to be the same. Hence, the marginal variations in the compressive strength observed between the two equivalent mix types at 90 days may be attributed to the increased porosity at the interfacial transition zone.

The microstructure at the interfacial zone according to Neville (2012) include a 10µm duplex film (0.5µm crystalline $Ca(OH)_2$ behind a 0.5µm C-S-H) and 50µm larger crystal of $Ca(OH)_2$. In concrete containing natural aggregates such as (10 mm) limestone aggregate, the large crystals of calcium hydroxide may react with the calcium carbonate from the limestone aggregates to form calcium carbonate – calcium hydroxide complexes which improves the microstructure at the interface zone (Neville, 2012 and, Metha and Monteiro,

2006). Metha and Monteiro (2006) also suggested a reaction might also occur between any unreacted calcium aluminate ($C_3A$) and calcium carbonates to form carboaluminate hydrates. These reactions reduce the porosity at the interfacial zone and increase the resistance of concrete to cracks and fractures along the zone. In concrete containing plastic aggregates as used in the current work, the possibility of such reactions taking place is highly unlikely. Plastics possess no cementitious properties and lack the chemical reactivity required for such reactions. That is, there are no ion exchange and/or oxy/hydroxyl precipitation following the interaction of plastic aggregates with the cementing materials. Therefore, the resistance of the encapsulated plastic concrete mixtures to cracking and fracture formation along the interface unlike CEM IIB-concrete mixtures (C1-3) were expected to be much lower. The compressive strength results confirmed the lower bond strength of encapsulated plastic concrete mixtures.

In the case of the marginal variations observed between CPP2 and 3 and $CPP2_f$ and $3_f$, the use of high volume of plastic aggregates in the CEM IIB-PFA encapsulated concrete mixtures (CPP1-3) may increase the volume and the distribution of the interfacial zone in the matrix (Portland cement and FBA). The increase in the volume and distribution of the interfacial zone coupled with the high water/binder ratio and low resistance of plastic to deformation are bound to decrease the compressive strength of the concrete. The increase in the volume and distribution of the interfacial zone and the high water/cement ratio may increase the porosity.

#### *6.1.3.2 Tensile strength*

As in the case of the compressive strength, porosity also played an important role in the variation in split tensile strength observed between the conventional and encapsulated CEM IIB-concrete. As shown in Table 6.1, the tensile strength of the conventional (C1-C3) and encapsulated plastic concrete (CP1-CP3, CPP1-CPP3 and $CPP1_f$-$CPP3_f$) decreased with increase in porosity. The same factors (water/binder and aggregate/binder ratios) accountable for the variation observed between the compressive strength of the conventional and encapsulated plastic CEM IIB-concrete may also be attributed with the variation observed in tensile strength of the concrete. The relationship between 28-days tensile strength and water/binder and aggregate/binder ratios are shown in Figure 6.5

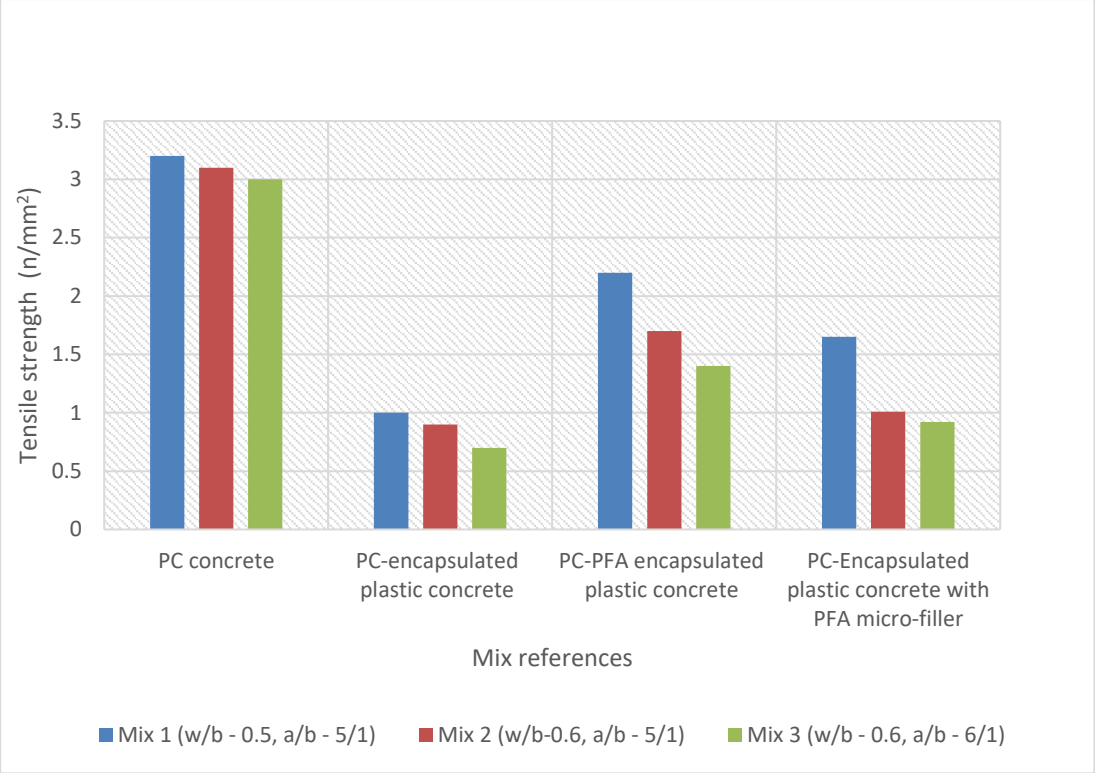


Figure 6.5: Influence of water/binder and aggregate/binder ratios on the 28 days tensile strength of the CEM IIB-concrete mixtures

The increase in water/binder and aggregate/binder ratios increased the porosity and as such decreased tensile strength (Table 6.1 and Figure 6.5). The CEM IIB-encapsulated plastic concrete (CP1-CP3) were the most pervious and as such demonstrated the lowest compressive strength. The addition of PFA improved the microstructure at the interface zone due to the formation of more C-S-H. Hence, relative to the encapsulated plastic concrete with CEM IIB binder used on its own (CP1-CP3), the equivalent encapsulated concrete with PFA (CPP1-3 and $CPP1_f$-$3_f$) demonstrated higher tensile strength values. The CEM IIB-PFA encapsulated plastic concrete mixtures (CPP1-CPP3) recorded higher tensile strength relative to the equivalent mixtures from the CEM IIB - encapsulated plastic concrete ($CPP1_f$-$CPP3_f$). This may be because of the higher packing density of mixes CPP1-CPP3 identified earlier in Section 6.1.2. According to Patil et al., (2017) the packing density and tensile strength of concrete increase as the coarse aggregate content increases. Mix CPP1-CPP3 utilised high coarse aggregates content relative to $CPP1_f$-$CPP3_f$.

The tensile strength of the mixtures from the CEM IIB- concrete system were also observed to increase as the compressive strength increased. The tensile strength (at 28 days) for the conventional and encapsulated plastic concrete evaluated in the current work increased with increase in compressive strength. The increase in tensile strength of the concrete with increase in compressive strength was consistent with the findings of Choi and Yuan, (2005), Kou et al., (2009) and Lavanya and Jegan, (2015). The three works observed that the tensile strength and compressive strength of conventional concrete (reinforced with glass and polypropylene fibre), lightweight concrete (containing recycled plastic aggregates) and geopolymer concrete respectively, had a linear relationship. The relationship between the compressive strength and the tensile strength of the conventional and encapsulated plastic CEM IIB-concrete is presented in Figure 6.6

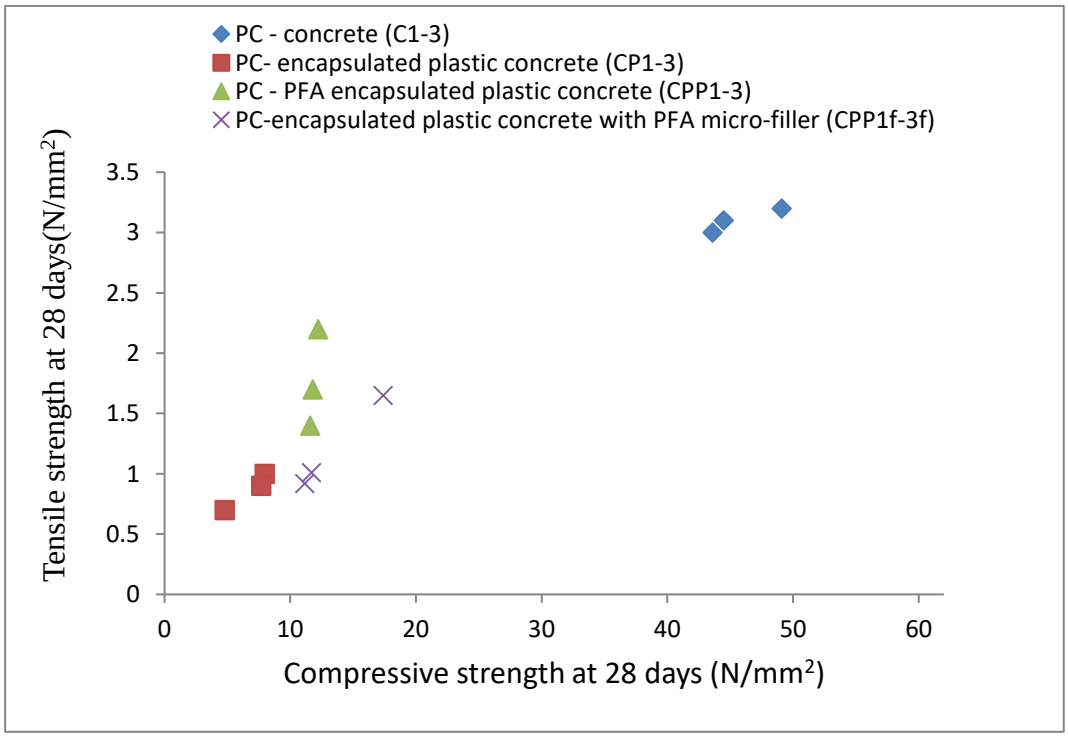


Figure 6.6: Power law relationships between the 28-days split tensile strength and compressive strength of the CEM IIB-concrete

### 6.1.4 Statistical analysis for the physico-mechanical properties of the CEM IIB-concrete

As mentioned in Section 4.3.4, the null hypothesis ($p \geq 0.05$) in this study assumes that, there is no relationship between the samples mean (average of 3 per investigation) reported for the physico-mechanical properties of the encapsulated plastic concrete and the control (the equivalent conventional concrete). Hence, the observed variation in measured properties is not statistically significant and may have occurred by chance. However, if $p \leq 0.05$, then the null hypothesis is rejected in favour of an alternative hypothesis, which in this work suggest that there, is a relationship between the sample mean presented for each investigated property of the encapsulated plastic concrete and the equivalent conventional concrete. Hence, the observed variations are statistically significant and, unlikely to be due to chance.

As observed from the results, the CEM IIB-encapsulated plastic concrete (CP1-CP3), recorded p-values lower than the alpha value ($p < 0.05$). The analysis affirmed that there are statistically significant variations between the mean values reported for the determined properties of the encapsulated plastic concrete and the conventional concrete equivalents. Hence, the compared results are not due to chance and the null hypothesis can be rejected in all instance in favour of the alternate hypothesis. Therefore, the result of the analysis supports the findings so far, that the volume and physical properties (particularly the particle shape, water absorption and cementitious characteristics) of the aggregates played an important role on the performance observed for the CEM IIB-encapsulated plastic concrete. Relative to the conventional concrete, the substitution of conventional aggregates with recycled aggregates significantly decreased the physical and mechanical properties of the CEM IIB-concrete. This was attributed to the quantity, particle shape, texture, and water absorption capacity of the recycled aggregates (FBA and 0-10mm plastic aggregates) and, the lack of cementitious properties of the 0-10 mm plastic aggregates.

The addition of PFA to the encapsulated plastic concrete (CPP1-CPP3 and $CPP1_f$-$CPP3_f$) in most cases also caused highly significant changes and very unlikely to have occurred by chance as the p-values were lower than the alpha value. This may be attribute again to the composition of the CEM IIB-encapsulated plastic concrete (CPP1-CPP3 and $CPP1_f$-$CPP3_f$), which knowingly differs from those of the conventional concrete (C1-C3). The

only exceptions were observed in the tensile strength results by CPP1, CPP2 and CPP1$_f$ and the recorded porosity of CP1, CP2 and CPP1$_f$, where $p \geq 0.05$. In these cases, the null hypothesis could not be rejected, as there is not enough statistical evidence to suggest a statistically significant difference exist between the highlighted properties of the related concrete groups. The effect of replacing conventional aggregates with recycled aggregates and, the differential effect of PFA on the highlighted properties may be the cause of these exceptions. The arrangement and orientation of the plastic aggregates may cause variations in the porosity of the tested specimens. The fly ash used in this work generally contain high carbon content, which may absorb and retain water. The disparity in the transmission of mix water through the concrete and rate of evaporation of mix water may have a sequential influence on the porosity of the encapsulated plastic concrete containing PFA. The smooth surface and free water on the surface of the recycled plastic aggregates can also cause weaker bonding between the aggregates and cement paste, hence the observed exceptions in tensile strength.

### 6.1.5 Durability of the CEM IIB–concrete system

#### *6.1.5.1 Freeze-thaw resistance*

The resistance of the hydrated encapsulated plastic concrete test specimens and CEM IIB-concrete specimens to frost action was determined using the procedures stipulated for aerated autoclave concrete in BS EN 15304:2010. The procedure entails an accelerated dry technique that measures the damage to porous concrete by repeated freezing and thawing of moisture held within the cavities of the concrete. It is better suited to encapsulated plastic concrete mixtures due to their high porosity (%). The porous nature of concrete allows it to absorb and retain water easily, which may weaken the encapsulating matrix.

Deterioration of concrete due to frost action is fundamentally a function of the porosity of the concrete. In freeze-thaw conditions, the moisture/water held in the cavities in the concrete freezes and exerts (ice) capillary pressure, which may cause the concrete to expand. Continuous cycles of freezing and thawing may eventually result in scaling, chipping or the eventual cracking of the concrete/mortar (Oti et al., 2010, and Wang et al., 2014). As observed in the results presented in Chapter 5 (Section 5.7.1.1), only the test specimens from the CEM IIB-encapsulated plastic concrete mixtures (CP1-3) recorded any noticeable physical damage. The concrete specimen subjected to freeze-

thaw cycles all recorded chipping of aggregates around the edges. The weak aggregate/paste bonding and/or the high porosity of the hydrated test specimens may have made them susceptible to damages by frost action. When the development of expansion forces exceeds the maximum tensile stress that concrete can take before failure, the tendency of the weak bonding between the aggregate to disintegrate becomes higher. The pozzolanic activity of PFA improved the microstructure of the encapsulated plastic concrete. As such, no physical disintegration was observed in the CEM IIB-PFA encapsulated plastic concrete mixtures (CPP1-3 and CPP1$_f$-3$_f$).

Besides the visual observation, the deteriorations of the test specimens subjected to freeze and thaw analyses was evaluated in terms of weight and compressive strength losses. As shown in Figure 6.7, the mass losses of the conventional and encapsulated plastic concrete increased with increase in porosity. The least porous concrete (the conventional concrete, C1, C2 and C3) recorded the highest residual mass (%), that is the lowest mass losses after the last freeze and thaw cycle. The CEM IIB-encapsulated plastic concrete (CP1, CP2 and CP3) were the most porous and as such, demonstrated the highest mass losses (lowest residual mass). Because of the improved microstructure, the CEM IIB-encapsulated plastic concrete mixtures with PFA (CPP1-3 and CPP1$_f$ -3$_f$) demonstrated lower mass losses relative to the hydrated CEM IIB-encapsulated plastic concrete mixture (CP1-3). The concrete utilising PFA as mineral admixtures (CPP1-3) recorded higher mass losses relative to the equivalents with PFA micro filler (CPP1-3$_f$). The porosity of the concrete blends (CPP1-3) were higher than the equivalent (CPP1-3$_f$). Nonetheless, all the hydrated concrete mixtures only demonstrated minor residual mass (98.5-99.7%), which was considered a good performance for the concrete mix types investigated.

As in the case of the mass loss, the compressive strength losses of the test specimens can also be analysed using percentage voids. The CEM IIB-concrete (conventional concrete or encapsulated plastic concrete), also recorded minor losses in compressive strength, which as shown in Figure 6.8, increased with increase in porosity. All the mixtures followed a similar pattern to those observed with mass loss. The minor losses in compressive strength (0.2 – 2.9%) were also considered good performance. The most porous concrete, the CEM IIB-encapsulated plastic concrete (CP1-3) also recorded the highest drop in compressive strength when subjected to freeze-thaw conditions. The

CEM IIB-concrete mixtures (C1-3) due to the relative low porosity recorded the least drop in strength after the freeze-thaw analysis.

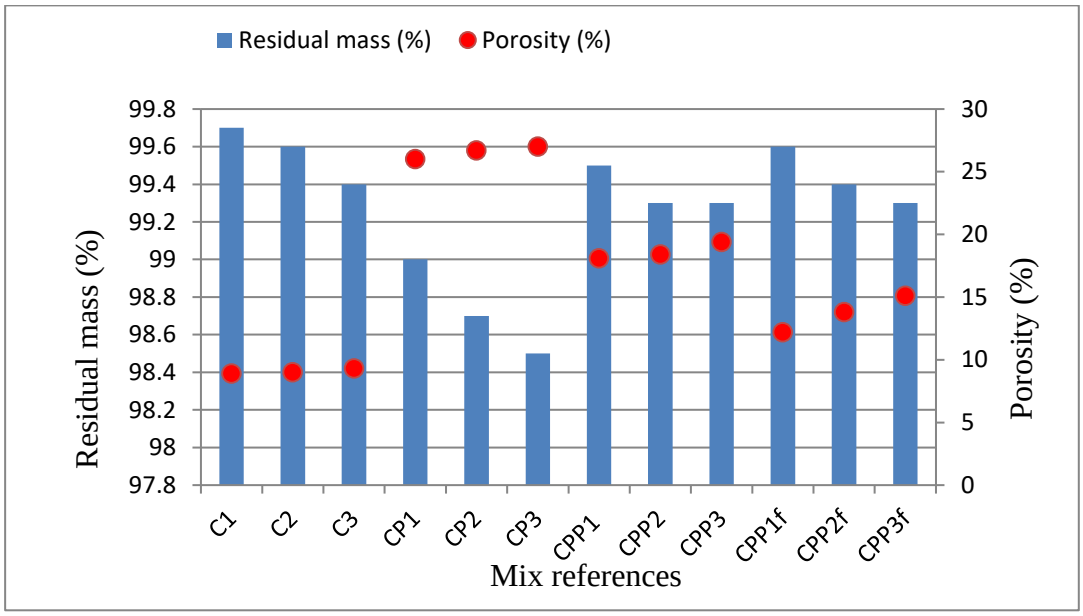


Figure 6.7: Relationship between 28-days porosity (%) and the residual mass (%) of the CEM IIB-concrete after the last freeze and thaw cycle

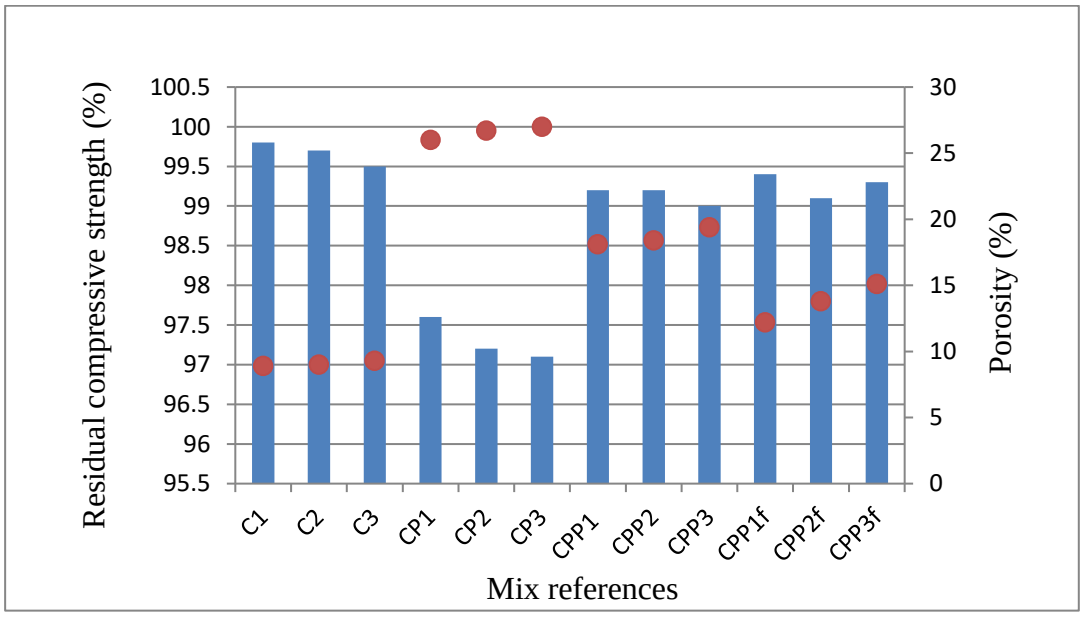


Figure 6.8: Relationship between 28-days porosity (%) and the residual compressive strength (%) of the CEM IIB-concrete after the last freeze and thaw cycle

### *6.1.5.2 Sulphate resistance of CEM IIB–concrete and encapsulated plastic concrete*

As with the case of freeze and thaw analysis, the conventional CEM IIB-concrete (C1-3) and encapsulated plastic concretes (CP1-3, CPP1-3 and CPP1f-3f) hydrated also experienced minor weight and compressive strength (%) losses when subjected to sulphate attacks. As shown in the results, the weight and compressive strength (%) losses increased as the immersion period (days) increased. The loss in weight and compressive strength may be attributed to formation ettringite in the cavities of the concrete by the infiltrating sulphate ions. When sulphate ions diffuse into concrete, they may react with calcium aluminate ($C_3A$) and the calcium sulphate hydrates (C-Ŝ-H) to form ettringite, which induces expansion and cracking, and eventually disintegrate the matrix. No physical damage was observed in the dimensions of any of the test specimens subjected to sulphate resistance.

The average mass and strength (%) lost by the test specimens from the encapsulated plastic concrete (CP1-3, CPP1-3 and CPP$1_f$-$3_f$) were relatively higher than those of the conventional CEM IIB – concrete (C1-3). This may be due to the higher water absorption percentages of the encapsulated plastic concrete relative to the CEM IIB-concrete. Zhang and Zong, (2014) associated the resistance of concrete to sulphate attack to the water absorption capacity of the concrete. The lower the hydraulic conductivity of concrete the higher the resistance to sulphate attack. As shown in Figure 6.9 and 6.10, the weight and compressive strength (%) losses of the CEM IIB- conventional and encapsulated plastic concrete are also fairly linear with the water absorption (%) of respective concrete.

From Figure 6.9, the mass loss (%) resulting from sulphate attack increased with increase in water absorption for all the concrete types investigated. The test specimens from the CEM IIB- concrete mixtures (C1-3) due to their relatively low water absorption (%) demonstrated the lowest mass loss (%), while the test specimens from the hydrated CEM IIB-encapsulated plastic concrete mixtures due to the higher water absorption demonstrated highest mass loss (%). The Portland cement, as mentioned in Chapter 3, contains about 8% PFA, which helps to militate against the sulphate attack. The addition of the high carbon PFA to the encapsulated plastic concrete mixtures (CPP1-3 and CPP$1_f$-$3_f$) also reduced the mass losses of the hydrated 'CP1-3' test specimens. This may be because the addition of PFA to Portland cement according to Ayub et al., (2013), increases the small diameter pores, which makes the concrete less permeable and resistant

to the infiltration of the sulphate ions. The CEM IIB-PFA encapsulated plastic concrete mixtures (CPP1-3) as shown in Figure 6.8, demonstrated higher mass losses relative to the CEM IIB-encapsulated plastic concrete with PFA micro-filler (CPP1-$3_f$). This variation as with the variation in water absorption (%) may be attributed to the higher aggregate fraction in the CPP1-3 mixtures.

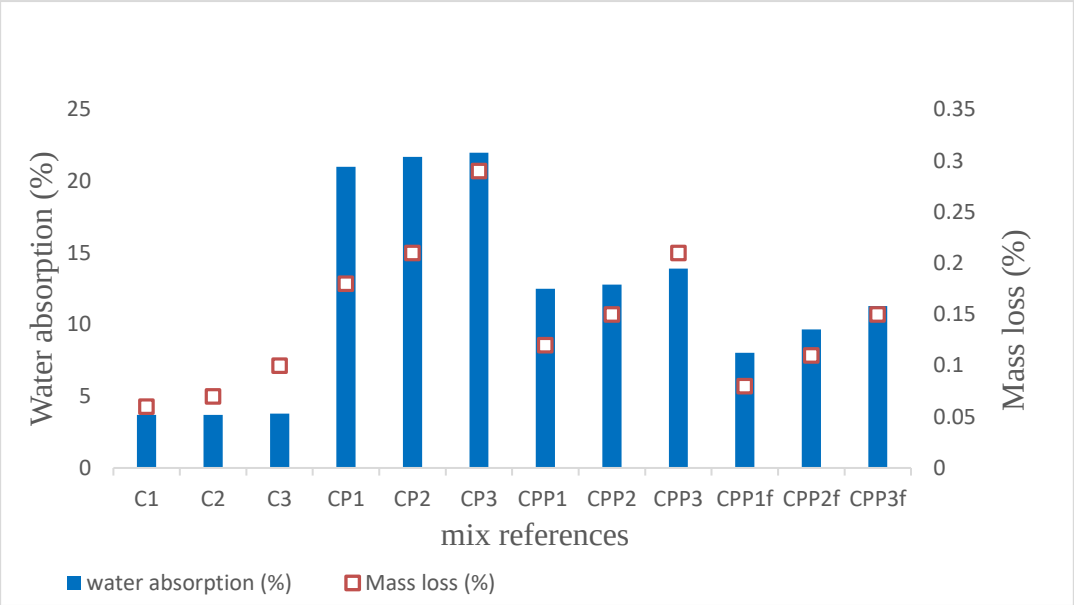


Figure 6.9: Relationship between water absorption (%) of the test specimens from the CEM IIB-concrete system after 28 days of water curing and the mass loss (%) after 28 days of curing in sulphate water

The losses in compressive strength may also be linearly related to the water absorption (%) of the concrete mixtures. As shown in Figure 6.10, the CEM IIB-concrete mixtures (C1-3) demonstrated the lowest compressive strength losses due to their relatively lower water absorption (%). In comparison to the replicated CEM IIB-concrete (C1-3), the CEM IIB-encapsulated plastic concrete (CP1-3), demonstrated higher compressive strength losses (%) due to their higher water absorption percentages. As shown in Figure 6.9, the deterioration in compressive strength of the CEM IIB-PFA encapsulated plastic concrete mixtures (CPP1-3 and $CPP1_f$-$3_f$) was also observed to increase with increase in water absorption (%). The CEM IIB-PFA encapsulated plastic concrete with PFA mineral

admixtures ‘CPP2 and CPP3’ demonstrated lower compressive strength (%) losses, relative to the equivalent CEM IIB-PFA encapsulated plastic concrete with PFA micro-filler ($CPP2_f$ and $CPP3_f$). This may be attributed to the differential volume and high sorptivity of the PFA in the encapsulated plastic concrete (PPP1-3 and $PPP1_f$-$3_f$). The higher binder to aggregate proportion of the CEM IIB-encapsulated plastic concrete with PFA micro-filler ($CPP1_f$-$3_f$) relative to the CEM IIB-PFA encapsulated plastic concrete mixtures with the lower binder to aggregate proportion may also suggest higher portion of cellular carbon particles. In sulphate ion-rich environment, owing to the high-water retention capacity of the carbon particles, the high binder content of mix ‘$CPP1_f$-$3_f$’ may increase the expansion due to the formation of ettringite and rate of degradation of the concrete mixtures. The immersion of the test specimens in the seawater immediately after demoulding may also have contributed to the above phenomenon. Curing the test specimens prior to immersing in seawater may reduce the water retention of the cellular carbon particles in the concrete. As observed with the freeze – thaw analysis, the hydration and pozzolanic reactions could have restrained carbon particles within the gel pores. Thereby limiting the absorption and retention of sulphate ions in the concrete, as such, reduce the expansion and possibly reduce the rate of degradation.

The impact of the high sorptivity of the carbon-rich PFA on the compressive strength loss (%) was less noticeable at low water/binder ratio. The resistance of the CEM IIB-encapsulated plastic concrete mixture with PFA micro-filler utilising water/binder ratio of 0.5 (mix $CPP1_f$) to sulphate attack, based on the compressive strength loss (%) was slightly higher than that the of CEM IIB-PFA encapsulated plastic concrete equivalent (CPP1). Overall, the recorded mass loss by the hydrated PG-concrete (conventional concrete or encapsulated plastic concrete) ranges between 0.03 -0.75%, while the recorded compressive loss (%) ranges between 0.18 and 1.97%. This as with the CEM IIB-concrete equivalent can be considered a good performance.

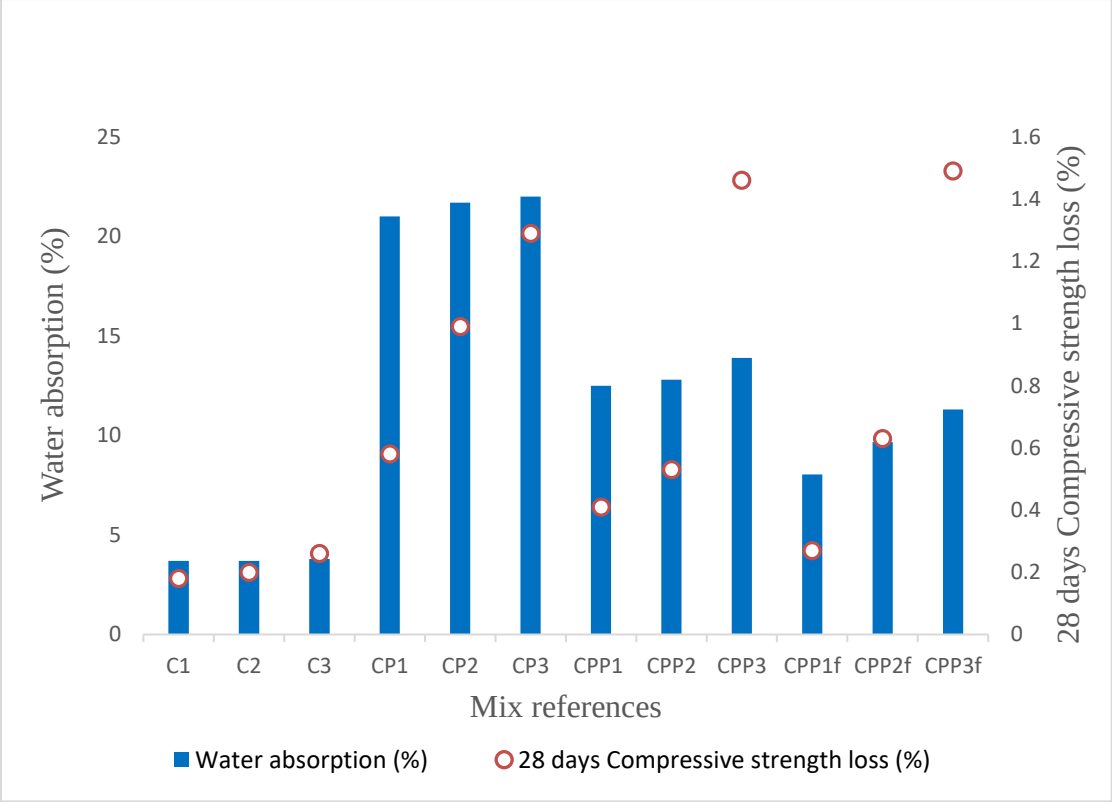


Figure 6.10: Relationship between water absorption (%) after 28 days of water curing and the compressive strength loss (%) of the mixtures from the CEM IIB-concrete system after 28 days of curing in sulphate water

***6.1.5.3 Thermal properties of the CEM IIB-concrete and encapsulated plastic concrete***

As with the freeze and thaw, and sulphate resistance, the behavioural characteristics of the tests specimens from the CEM IIB-concrete systems were also evaluated in terms of visual observation, weight and compressive strength losses. For the reasons given in Chapter 5 (Section 5.5.3) only the thermal properties of the best performing mixtures from the CEM IIB–concrete mix C1 and the CEM IIB-PFA encapsulated plastic concrete (CPP1) were investigated. As observed in the results, under visual observations, the CEM IIB–concrete mixtures suffered only minor spalling around the edges after being subjected to heat treatment at 200$^{o}$C for 2 hours. This may be because concrete exhibits good thermal performance at elevated temperatures of up to 300$^{o}$C. It is only beyond these temperatures that significant physio-chemical changes leading to the degradation of the hydrate structure occur (Bailey and Khoury, 2011). Also for the same reasons the concrete test specimens only suffered minute changes in weight and compressive strength

for all the temperature ranges investigated. The average mass (%) losses of the test specimens from the CEM IIB-concrete mixture (C1) ranged between 0.12 – 1.26% for all the temperature ranges. Additionally, the test specimens recorded compressive strength (%) losses ranging from 0 – 0.06%. No change in compressive strength was observed between 30- 150$^{o}$C. According to Bailey and Khoury, (2011), concrete only suffers significant strength changes at temperature above 500$^{o}$C.

As with the conventional CEM IIB-concrete, the encapsulated plastic concrete mixture (CPP1) under visual observation suffered only minor physical deformation between 30-50$^{o}$C. At temperatures above 50$^{o}$C, surface cracking lines and visible indentations that increased with temperature elevation, shrinkage and extrusion of melted plastic materials from the test specimens were visually observed. According to Albano et al., (2009) the hollow indentations, which formed the extrusion points for the melted plastic may be due to the formation of gas products (smoke). As mentioned in the results, the test was stopped due to a fire scare which resulted from the formation of these gaseous products. At 200$^{o}$C, the encapsulated plastic concrete generated enough smoke/gas in less than 30 minutes to trigger the fire sensors in the laboratory. In addition, volume changes caused by the loss of excess water, which would have otherwise been retained by the PFA, may be the source of the crack lines observed from 50$^{o}$C onwards.

In addition to the visual observations, the encapsulated plastic concrete also recorded mass losses (%) ranging between 0.44 – 4.88% between temperatures 30 – 200$^{o}$C. At 200$^{o}$C however the densification of the test specimens by the melted plastic increased the residual mass (%) reducing the mass loss (%) to approximately 4%. Similarly, the average compressive strength loss (%) as observed in the results also increased with temperature increments between 40 – 150$^{o}$C. No changes in compressive strength were observed at 30$^{o}$C, while at 200$^{o}$C, the densification of the concrete by the molten plastic increased the compressive strength beyond that of the reference test specimens. Also at 200$^{o}$C, the average residual compressive strength of the test specimens was 100.5%, which suggest an increase in strength by 0.5%.

## 6.2 PG-CONCRETE SYSTEM

### 6.2.1 Variations in workability of the fresh mixtures from the PG–concrete system

The PG-concrete system consists of the conventional PG–concrete (P1-3), the PG–encapsulated plastic concrete (PP1-3), the PG–PFA encapsulated plastic concrete (PPP1-3) and the PG–encapsulated plastic concrete with PFA used as micro-filler ($PPP1_f$-$3_f$). Similar to the fresh mixtures from the CEM IIB-concrete system, the workability of the PG-concrete mixtures (conventional and encapsulated plastic with or without PFA) were also observed to increase with increase in water/binder ratio but to decrease with increase in aggregate/binder ratio. The PG-concrete mixtures P1, P2 and P3 recorded slump values of 15 mm, 60 mm and 25 mm and, compaction indices of 1.33, 1.18 and 1.25 mm. The only PG-encapsulated plastic concrete mixture that demonstrated a true slump value was mix $PPP1_f$. Similar to its CEM IIB-concrete equivalent ($CPP1_f$) it recorded a true slump of 20 mm. All the remaining encapsulated plastic concrete mixtures from the PG–concrete system demonstrated collapse or shear slump. As a result, the variations in workability of the encapsulated plastic concrete (PP1-3, PPP1-3 and $PPP1_f$-$3_f$) were evaluated using the compaction indices.

As in the case of the mixtures from the CEM IIB–concrete system (P1-3, PP1-3, PPP1-3 and $PPP1_f$-$3_f$), the variations observed in the workability of the mixtures from the PG–concrete mixtures may be attributed to the water content and, the quantity and physical properties of the constituent aggregates. The quantity and physical properties of the aggregate materials (FBA and 0-10 mm plastic aggregates) may also be responsible for the low workability demonstrated by the PG-encapsulated plastic mixtures (with or without PFA). Additionally, the inclusion of PFA increased the cohesiveness and compactability of the plastic concrete mixtures (PPP1-3 and $PPP1_f$-$3_f$) relative to the mixtures from the encapsulated plastic mixtures utilising PG-binder on its own (PP1-3).

In comparison to the equivalent mixtures from the CEM IIB-concrete system however, the mixtures from the PG–concrete system except for mix P2, all demonstrated lower workability. The relatively low workability of the mixtures from the PG-concrete system may be attributed to the relatively high segregation of the PG-concrete mixtures due to the reduced water demand of the PG-binder. The PG-binder as described in Chapter 3 (Section 3.1.2) is a complex blend of very fine low alkali, high specific surface area Portland cement, inter-ground with fine pozzolans (PFA and silica fumes), high purity

crystalline aggregates and other compatible admixtures. The pozzolans and other admixtures reduced the water demand of the grout. The amount of water required for the complete hydration of the grout as observed in the standard consistency was approximately 0.17 per unit weight of the material compared to 0.31 per unit weight of material for CEM IIB-binder. Increasing the water demand of binder beyond the standard consistent (0.17) may increase the porosity (segregation) and decrease the workability of the fresh concrete mixtures (Neville, 2012). The PG-concrete mix 'P2' with water/binder and aggregate/binder ratios of 0.6 and5/1 respectively, demonstrated increased workability relative to the CEM IIB-concrete equivalent mix C2. This may be due to the higher aluminate content of the PG-binder influencing the workability at high water/binder ratio.

### 6.2.2 Variations in density of the hydrated mixtures from the PG–concrete system

As with the CEM IIB–concrete equivalents, the measured density of the conventional PG-concrete (P1-3), PG–encapsulated plastic concrete (PP1-3), PG–PFA encapsulated plastic concrete (PPP1-3) and PG–encapsulated plastic concrete with PFA used as micro-fillers ($PPP1_f$-$3_f$) were also observed to decrease with increase in water/binder and increase in aggregate/binder ratios. Also, as with the CEM IIB–concrete equivalents, the variations observed between the test specimens from the conventional concrete and the encapsulated plastic concrete (including those with PFA), may be attributed to the water content, volume and physical properties of the aggregate constituents, including specific gravity, particle shape, texture and water absorption (%). These factors as observed with the test specimens from the CEM IIB-concrete system may also increase the porosity and decrease the density of the test specimens from the PG-concrete system (conventional or encapsulated plastic concrete).

#### *6.2.2.1 Relationship between density and porosity of the hydrated mixtures from the PG-concrete system*

As shown in Figure 6.11, the densities of all the test specimens from the PG–concrete systems decreased with increase in porosity. The mixtures with the lowest porosities (%) from each PG-concrete type (P1-3, PP1-3, PPP1-3 and $PPP1_f$-$3_f$) recorded the higher densities, while the mixtures with the highest porosity demonstrated the lowest densities. In addition, the conventional PG–concrete test specimens from mix P1, P2 and P3 with porosities of 11.7, 13.6 and 13.9% recorded densities of 2390, 2370 and 2360kg/m$^3$

respectively. Similarly, the test specimens from the PG–encapsulated plastic concrete mixtures PP1, PP2 and PP3 recorded porosities between 29.2, 30.7 and 31.6% and densities of 1490, 1460 and 1420 kg/m$^3$ respectively. The inclusion of PFA as mineral admixtures in the hydrated PG-PFA encapsulated plastic concrete mixtures (PPP1, 2 and 3) decreased the porosity of the mixtures by at least 30% and increased the densities by at least 6%, relative to the equivalents in the PG–encapsulated plastic concrete mixtures (PP1,2 and 3). In addition, the utilisation of PFA as micro-filler in PPP1$_f$, PPP2$_f$ and PPP3$_f$ decreased the porosity of the mixtures by 33 – 55 % and increased the densities by at least 8%. The reduction in porosity and increase in density of the PG-encapsulated plastic concrete with PFA (PPP1-3 and PPP1$_f$-3$_f$) relative to those with PG-binder used on its own (PP1-3) may be attributed to the improvement in microstructure of the concrete due to the formation of more C-S-H gel upon the inclusion of PFA. Furthermore, the test specimens from mix PPP1 and PPP2 recorded higher porosities and marginally lower densities relative to the equivalent test specimens from PPP1$_f$ and PPP2$_f$. The third mix PPP3 as shown in Figure 6.11 demonstrated lower porosities but higher densities than PPP3$_f$. This may be as a result of increased packing density of the vibrated concrete due to the higher amount of coarse and fine aggregates in the former mix.

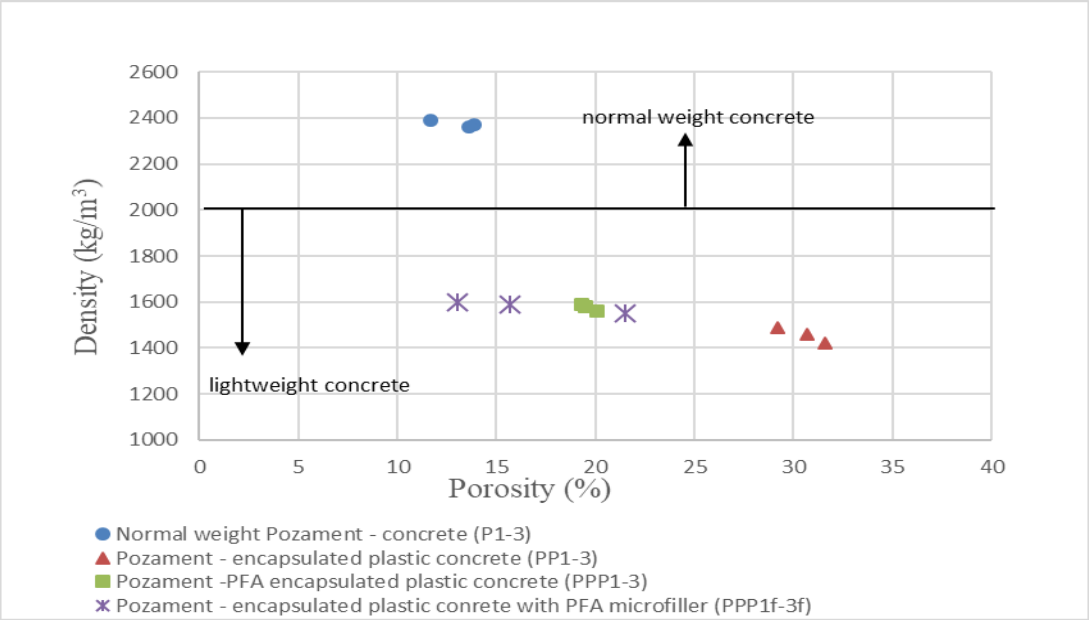


Figure 6.11: relationship between density and porosity of the hydrated mixtures from the PG-concrete system

#### *6.2.2.2 Relationship between porosity and water absorption (%) of the hydrated mixtures from the PG-concrete system*

As with the hydrated specimens from the mixtures in the CEM IIB-concrete system, a linear relationship also exists between the porosity (%) and water absorption (%) of the test specimens from the PG–concrete mixtures (P1-3, PP1-3, PPP1-3 and in $PPP1_f$ - $3_f$). As shown in Figure 6.12, the water absorption (%) of the test specimens from each of the encapsulated plastic concrete mixtures (PP1-3, PPP1-3 and $PPP1_f$-$3_f$) were higher than the equivalents from the conventional PG-concrete mixtures (P1-3). The PG-encapsulated plastic concrete test specimens (PP1-3), due to their relatively high porosity, recorded the highest water absorption (%) relative to the other concrete types (P1-3, PPP1-3 and in $PPP1_f$-$3_f$) in this system. The water absorption (%) of the test specimens from PG-encapsulated plastic concrete mixtures were 70 -75% higher, when compared to the equivalents test specimens from the PG–concrete mixtures (P1-3). The inclusion of PFA in mix PPP1-3 and mix $PPP1_f$-$3_f$ decreased the water absorption (%) of the encapsulated plastic concrete mixtures. Relative to the conventional PG-concrete (P1-3), the water absorption (%) of the PG-encapsulated plastic concrete (PP1-3) decreased by 50 -60% when PFA was included in the encapsulated concrete mix as a mineral binder admixture (PPP1-3) and 44 – 53% in the encapsulated concrete mix with PFA included as a micro-filler ($PPP1_f$-$3_f$). Similar to the relationship observed between the densities and porosities of the test specimens from mix PPP1-3 and PPP1f-$3_f$. The mixture with the higher water/binder and aggregate/binder ratios from the PG-PFA encapsulated plastic concrete mixture (PPP3) demonstrated lower porosity and water absorption (%) relative to the test specimens from the equivalent mix from the PG–encapsulated concrete mixture with PFA micro–filler ($PPP3_f$). This may be attributed to the increased packing density of mix PPP3 due to increased aggregate content.

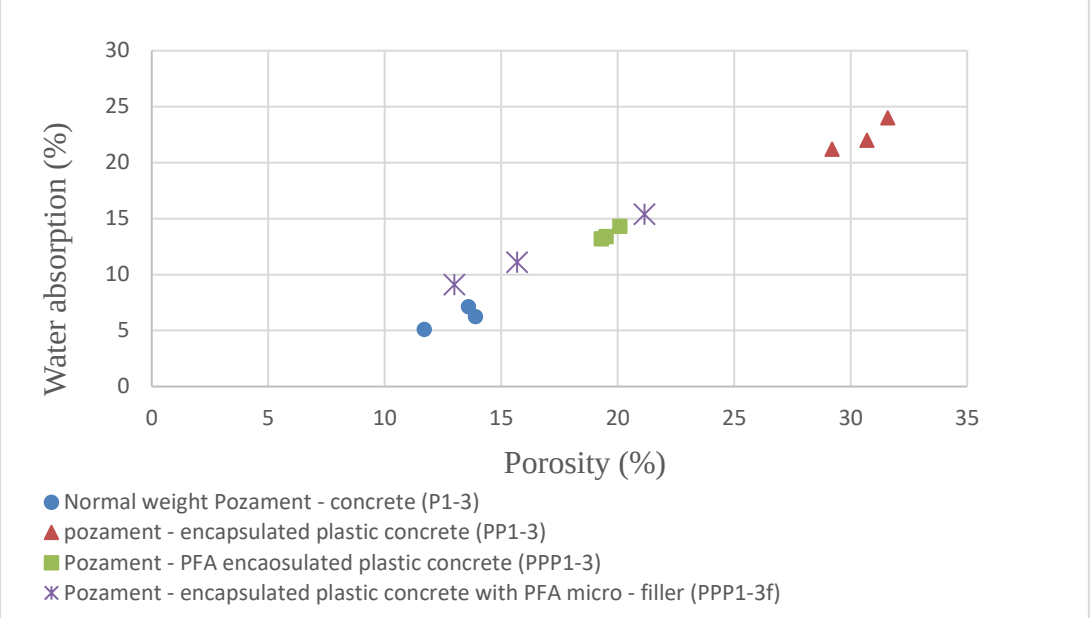


Figure 6.12: Relationship between porosity (%) and water absorption (%) of the hydrated mixtures from the PG-concrete system

### *6.2.2.3 Relationship between density and water absorption (%) of the hydrated mixtures from the PG-concrete system*

As was the case of the CEM IIB-concrete mixtures, linear relationships may also be established between the density and the water absorption (%) of the PG-concrete mixtures (conventional and encapsulated plastic concrete). These relationships (Figure 6.13) are similar to those observed between the porosity and density shown in Figure 6.12.

When compared to the test specimens from the equivalent CEM IIB-concrete mixtures (C1-3, CP1-3, CPP1-3 and CPP1$_f$-3$_f$), the test specimens the PG-mixtures (P1-3, PP1-3, PPP1-3 and in PPP1$_f$-3$_f$) recorded higher porosities and water absorption (%) but lower densities. These variations may be attributed to the low water demand of the PG-paste. As observed with the workability assessment, increasing the water/cement ratio to 0.5 and 0.6 (as opposed to the 0.17 required for the hydration of the Pozament paste) may increase the porosity and in essence decrease the density of the test specimens from the mixtures in the PG-concrete system. In general, the physical properties (density, porosity and water absorption) demonstrated by the test specimens from the PG-concrete mixtures (P1-3, PP1-3, PPP1-3 and in PPP1$_f$ - 3$_f$) were lower in comparison to the physical properties demonstrated by the test specimens from equivalent CEM IIB-concrete

mixture (C1-3, CP1-3, CPP1-3 and in CPP1$_f$-3$_f$). The variations observed in the physical properties (density, porosity and water absorption) of the test specimens from the hydrated mixtures in the PG–concrete system relative to the test specimens from the mixtures in the CEM IIB-concrete system may all be attributed to the low water demand of the Pozament grout.

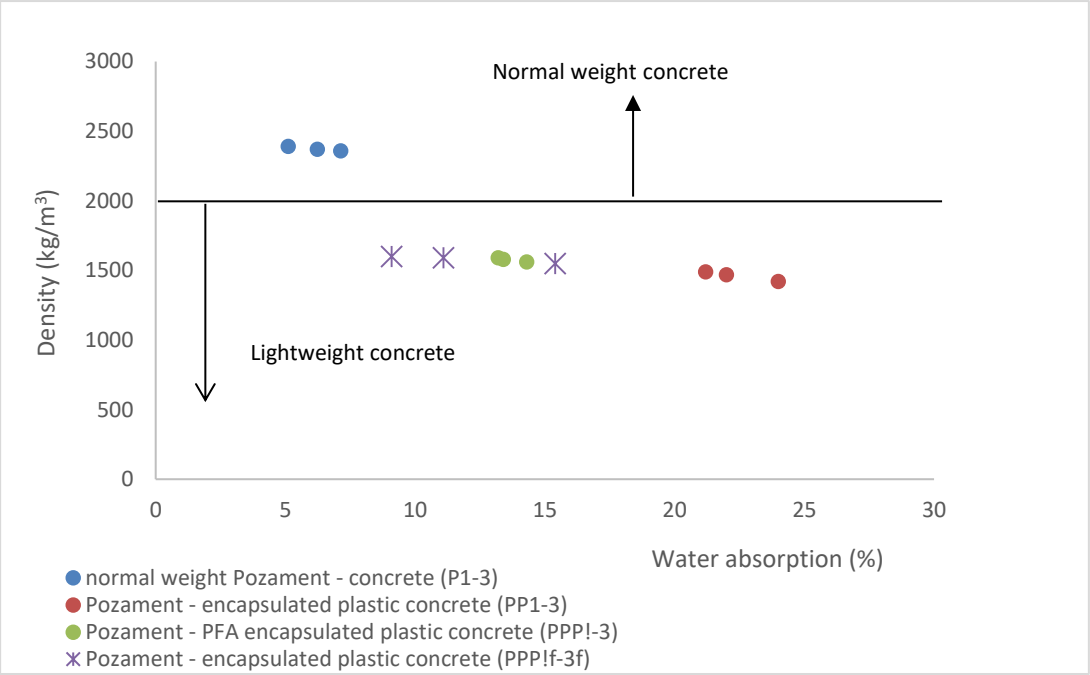


Figure 6.13: Relationship between density and water absorption of the hydrated mixtures from the CEM IIB-concrete system

### 6.2.3 Variations in mechanical performance of the hydrated mixtures from the PG–concrete system

#### *6.2.3.1 Unconfined compressive strength*

The compressive strength of the test specimens from the PG-concrete and the PG-encapsulated plastic concrete mixtures (including those with PFA) as observed with the CEM IIB-equivalents also increased with increase in curing age. For the ages tested, the test specimens from all the PG-concrete mixtures (conventional or encapsulated plastic) achieved at least 70% of their compressive strength within the first 28 days. The usage of PFA in the PG–PFA encapsulated plastic concrete as either a mineral admixture (PPP1-3) or micro-filler (PPP$1_f$-$3_f$) increased the compressive strength. PFA usually influences the long-term strength development of concrete, due to the hydration of belite at the latter ages. Hence, at 90 days due to the formation of more C-S-H gel, the compressive strength values of mix PPP1-3 were 25 -40% higher than those of the mixtures with PG-binder used on its own (PP1-3). Similarly, the compressive strength values of mix PPP$1_f$-$3_f$ were 35 -40% higher than PP1-3. In addition, the strength values of mix PPP1-3 were 11 -14% lower than those of mix PPP$1_f$-$3_f$. This may be due to the higher amount of fine and coarse aggregates in PPP1-3.

##### *6.2.3.1.1 Effect of porosity on the unconfined compressive strength of the PG-concrete system*

Porosity played a major role in the variations observed between the unconfined compressive strength values of the test specimens from the concrete mix types investigated in the PG–concrete system. As shown in Table 6.2, compressive strength of each concrete type for all the curing ages tested decreased as porosity increased. Due to their lower porosity, the conventional PG–concrete demonstrated higher compressive strength relative to the encapsulated plastic concrete (PP1-3, PPP1-3, and PPP1f-$3_f$). At 7 days, similar to the CEM IIB-concrete, the conventional PG-concrete with the higher water/cement ratio (mix P2 and P3) demonstrated higher compressive strength development compared to the mixture with lower water/cement ratio. Figure 6.14 -6.17 shows the variations in compressive strength of the PG-concrete with water/binder and aggregate/binder ratios. The availability of more water may have also increased the degree of hydration of the PG-concrete at the early age. Likewise, the higher water

content may have increased the porosity and as such decrease the compressive strength of the test specimens at latter ages (28 and 90 days).

The higher the porosity, the lower the compressive strength of the hydrated encapsulated plastic concrete. The PG–concrete tests specimens from PP1-PP3, due to the high porosity recorded the lowest strength values of all the concrete mix types investigated in this system. The inclusion of PFA both as micro-filler or mineral admixtures generally decreased the porosities and increased the compressive strength of the PG-encapsulated plastic concrete. For all curing ages, the concrete utilising PFA as micro-filler ($PPP1_f$-$3_f$) due to the lower amount of aggregate and decreased porosity maintained higher compressive strengths, relative to the mixtures utilising PFA as mineral admixtures. The influence of PFA as already discussed was observed to be more prevalent at 90 days.

Table 6.2: Variations in strength development of the concrete mixtures from the PG–concrete system

| *Mix reference* | *w/b ratio* | *a/b ratio* | *Density (kg/m$^3$)* | *Porosity (%)* | *Compressive strength (*N/mm$^2$) | | | *Tensile strength* |
|---|---|---|---|---|---|---|---|---|
| | | | *28 days* | *28 days* | *7 days* | *28 days* | *90 days* | *28 days* |
| P1 | 0.5 | 5/1 | 2390 | 11.7 | 21.03 | 44.26 | 45.07 | 3.6 |
| P2 | 0.6 | 5/1 | 2370 | 13.9 | 21.35 | 25.91 | 30.05 | 3.5 |
| P3 | 0.6 | 6/1 | 2360 | 13.6 | 22.30 | 24.74 | 30.00 | 2.7 |
| PP1 | 0.5 | 5/1 | 1490 | 29.2 | 4.52 | 7.40 | 8.30 | 1.2 |
| PP2 | 0.6 | 5/1 | 1460 | 30.7 | 2.03 | 3.90 | 4.53 | 0.6 |
| PP3 | 0.6 | 6/1 | 1420 | 31.6 | 1.67 | 2.80 | 4.28 | 0.3 |
| PPP1 | 0.5 | 5/1 | 1590 | 19.3 | 4.20 | 7.74 | 11.01 | 1.6 |
| PPP2 | 0.6 | 5/1 | 1580 | 19.5 | 3.70 | 5.20 | 8.20 | 1.2 |
| PPP3 | 0.6 | 6/1 | 1560 | 20.1 | 3.40 | 4.90 | 7.10 | 0.9 |
| $PPP1_f$ | 0.5 | 5/1 | 1600 | 13.0 | 4.85 | 9.54 | 12.82 | 1.18 |
| $PPP2_f$ | 0.6 | 5/1 | 1590 | 15.69 | 3.80 | 5.74 | 8.68 | 0.78 |
| $PPP3_f$ | 0.6 | 6/1 | 1550 | 21.5 | 3.78 | 5.30 | 7.78 | 0.75 |

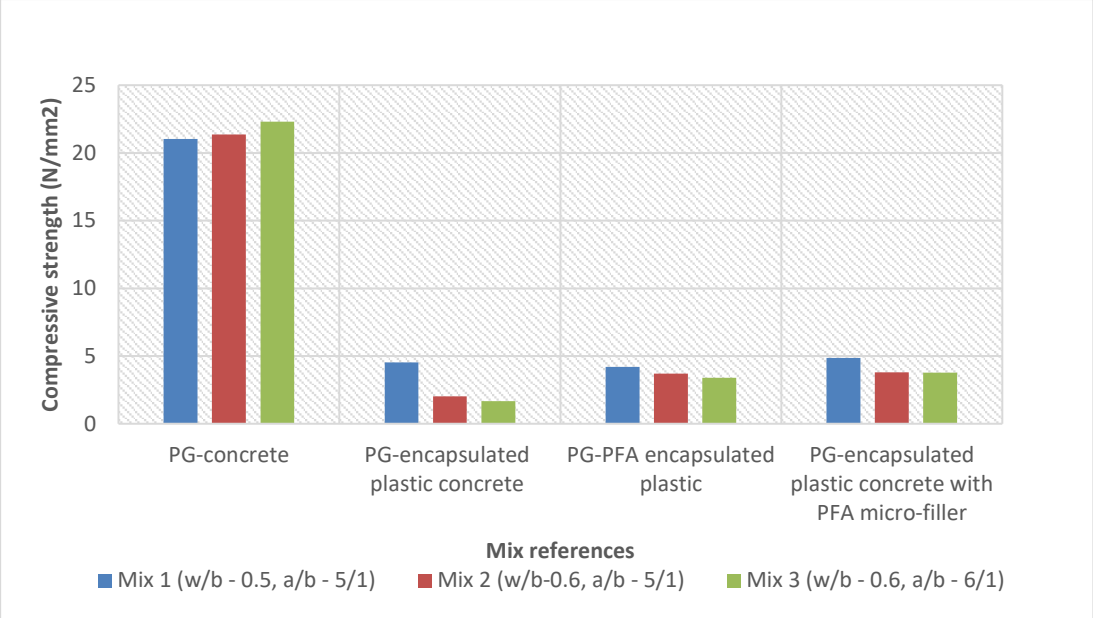


Figure 6.14: Influence of water/binder and aggregate/binder ratios on the 7 days compressive strength of the PG-concrete mixtures

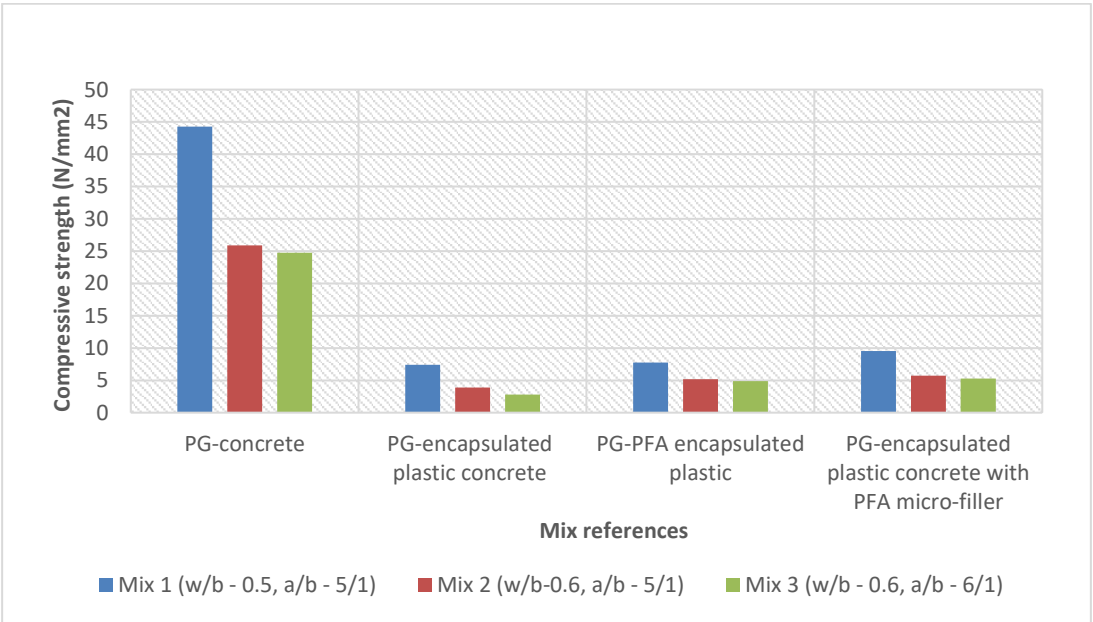


Figure 6.15: Influence of water/binder and aggregate/binder ratios on the 28 days compressive strength of the PG-concrete mixtures

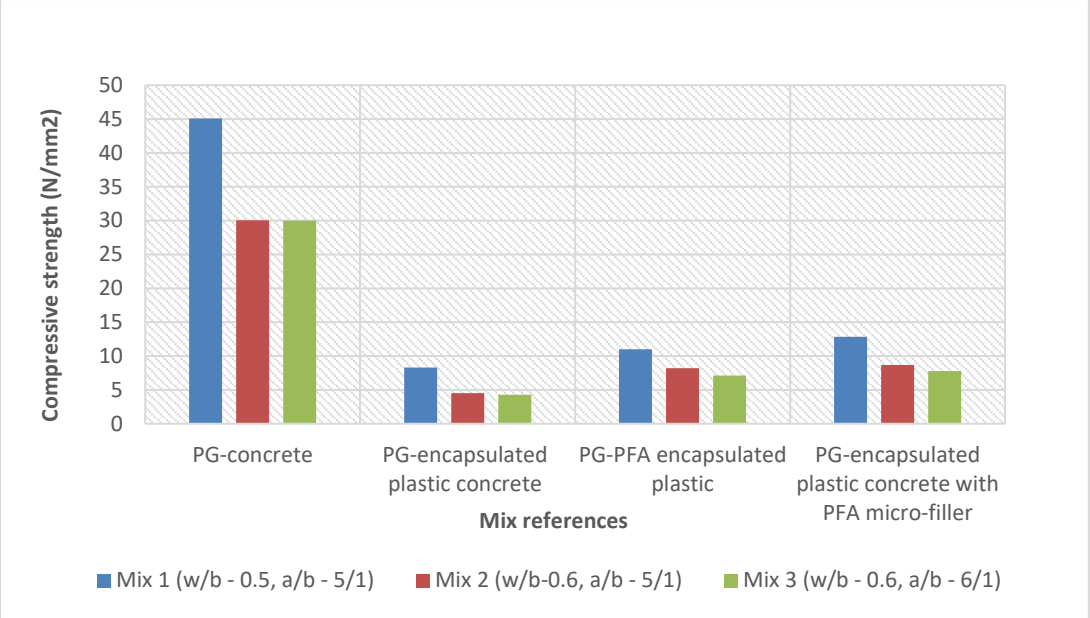


Figure 6.16: Influence of water/binder and aggregate/binder ratios on the 90 days compressive strength of the PG-concrete mixtures

In comparison to the CEM IIB–equivalents, all the PG concrete mixtures demonstrated higher porosities and lower compressive strength for all the curing ages tested. In addition, none of the test specimens from the conventional PG-concrete mixtures (P1-3) meets the minimum target compressive strength of 49N/mm$^2$, from the mix design. In addition, the 28 days strength values of most of the encapsulated plastic concrete mixtures (with or without PFA) were below the minimum compressive strength specified in BS EN 1992-1-1:2004+A1:2014 for lightweight concrete. The only exceptions were PP1, PPP1 and PPP1$_f$, the mixtures from each of the Pozament based encapsulated plastic concrete types utilising the lower water/binder and aggregate/binder ratios. The compressive strength values recorded by the mixtures (PP1, PPP1 and PPP1$_f$) after 28 days of water curing were slightly higher than the minimum strength value (7N/mm$^2$) specified in the standard for lightweight concrete. At 90 days, only the PG–encapsulated plastic concrete mixes ‘PP2 and PP3’ did not meet the minimum strength specified for lightweight concrete in the standard. In addition, for all the curing ages investigated none of the test specimens from the PG-encapsulated plastic concrete (with or without PFA) conform with the compressive strength specified in BS EN 1992-1-1:2004+A1:2014 for

structural lightweight concrete. The standard specified a conformity criterion of 17N/mm$^2$ for structural lightweight concrete.

#### *6.2.3.2 Tensile strength*

The tensile strength of the test specimens from the conventional concrete and the encapsulated plastic concrete mixtures (P1-3, PP1-3, PPP1-3 and PPP1$_f$-3$_f$) as with the CEM IIB equivalents was also influenced by the porosity and density. An increase in porosity and the associated decrease in density resulted in a decrease in split tensile strength. As shown in table 6.2, the split tensile strength of the hydrated mixtures from each concrete type decreased with increase in porosity. The hydrated PG-concrete mixtures (P1-2) demonstrated the highest split tensile values while, the PG-encapsulated plastic concrete mixtures (PP1-3) demonstrated the lowest. The addition of PFA as with compressive strength increased the tensile strength values of the test cylinders from PPP1-3 and PPP1$_f$-3$_f$. The PG-PFA encapsulated plastic concrete mixtures (PPP1-3) recorded higher tensile strength relative to the equivalent mixtures from the CEM IIB - encapsulated plastic concrete (PPP1$_f$-3$_f$). This as with the CEM IIB equivalent with PFA may be attributed to the higher packing density of mixes PPP1-3 due to the increased aggregate content.

As with the case of the hydrated mixtures from the CEM IIB–concrete systems, the tensile strength of the PG-concrete mixtures (conventional and encapsulated plastics) also increased with increase in compressive strength (Figure 6.18). This relationship was also consistent with the previous works on the use of polymer material in concrete, but none of the mixtures complies with the power coefficient law. Additionally, all the test cylinders from the PG- concrete (except P1, P2 and PP1) recorded lower tensile strength values in comparison to the CEM IIB–equivalents. The tensile strength of P1, P2 and PP1 at 28 days was relatively higher than the equivalents from the CEM IIB-concrete system. This may be because of either the mineral admixtures utilised in the PG-binder, low water demand of the PG-binder or the effect of PFA on the PG-binder.

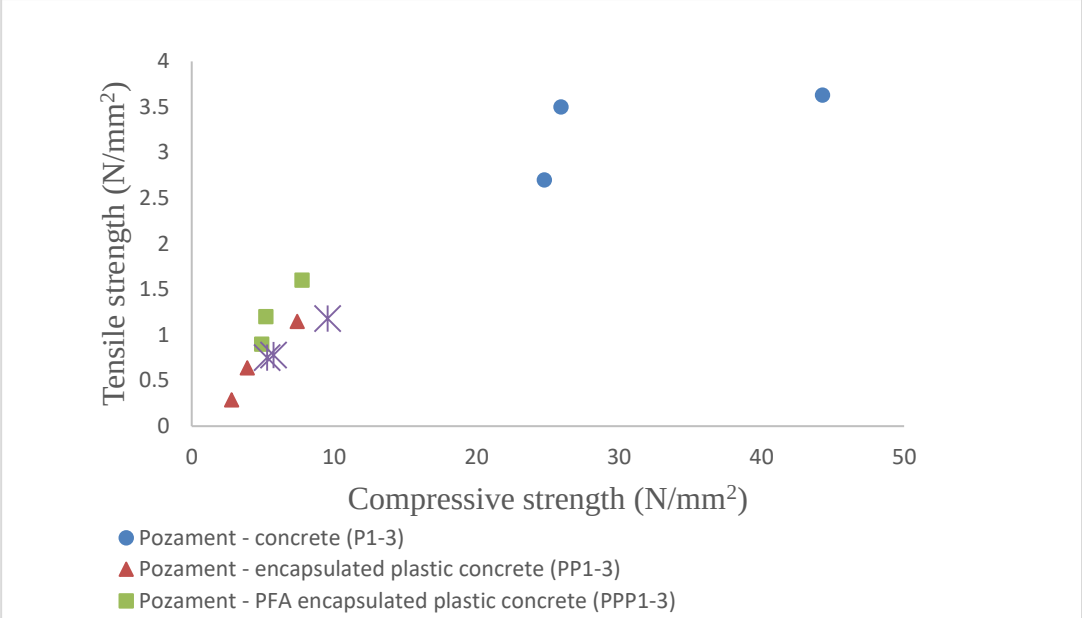


Figure 6.18: Relationships between the 28-days split tensile strength and compressive strength of the PG-concrete

### 6.2.4 Statistical analysis of the physico-mechanical properties of the CEM IIB-concrete

As with the CEM IIB concrete, the PG-encapsulated plastic concrete (including those with PFA) mostly observed p-values greater than 0.05 (alpha value), implying the null hypothesis can be rejected in most cases. As with the discussions on the physical and mechanical properties of the PG and PG-PFA encapsulated plastic concrete, the replacement of conventional aggregates with recycled aggregates and the subsequent addition of PFA led to significant variations in the determined properties relative to the control (P1-P3). Exceptions were however observed in the aggregated results for the 28-days porosity of the concrete blends PP3, PPP2, PPP3, $PPP1_f$ and $PPP2_f$, 28- days water absorption of PP3, PPP1, PPP2, $PPP1_f$ and $PPP3_f$ and the 90-days compressive strength of PP3, PPP3, $PPP3_f$, where the p-values are greater than 0.05. Hence, the null hypothesis could not be rejected for the observations in these instances, as there was not enough statistical evidence to suggest that there is a relationship between the highlighted properties for the concrete mixtures involved relative to the control. The low water demand of Pozament grout combined with the quantity and aggregate properties, high water and aggregate content and, varied degree of compaction (direction and orientation

of aggregates) may cause disparity in the porosity and water absorption properties of the encapsulated plastic concrete. They may have resulted in dissimilarity between the tests results obtained for each specimen pertaining to the porosity and water absorption. Similarly, the quantity and aggregate properties and the differential effect of PFA may cause disparity in the compressive strength of the encapsulated plastic concrete at high water/binder and aggregate/binder ratio (PP3, PPP3, PPP3$_f$).

### 6.2.4 Durability of the PG–concrete system

#### *6.2.4.1 Freeze-thaw resistance*

The deterioration of the PG (conventional concrete and encapsulated plastic) concrete mixtures due to frost action was not different to that observed with the CEM IIB-concrete mixtures. The weak aggregate/paste bonding and the high porosity of the PG–encapsulated plastic concrete mixtures (PP1-3) resulted in chipping around the edges. Also, as with the CEM IIB–concrete equivalents, the weight and compressive strength losses observed with the conventional PG–concrete mixtures (P1-3) and the PG-encapsulated plastic concrete including those with PFA (PP1-3, PPP1-3 and PPP1$_f$-3$_f$) increased as the porosity increased. The mixtures with the highest porosity (PP1-3) recorded the highest weight and strength losses, while the mixtures with the lowest porosity (P1-3) recorded the lowest mass losses. Due to the improved microstructure, the hydrated test specimens from the mixtures with PFA (PPP1-3 and PPP1$_f$-3$_f$) also demonstrated lower mass losses relative to the hydrated test specimens from the PG-encapsulated plastic concrete mixture (PP1-3). The mixtures utilising PFA as mineral admixtures (PPP1-3) recorded lower residual mass relative to the equivalents with PFA micro filler (PPP1-3$_f$). PPP1-3 mixes were also more porous. Nonetheless, all the concrete mixtures from the PG–concrete system demonstrated minor weight (0.4 – 2.2 %) and compressive strength (05 -3.4) losses, which is considered a good performance.

The relationships between the porosity (%) and the residual mass (%) of the mixtures from the PG-concrete system are presented in Figure 6.19 while, the relationships between the porosity (%) and the residual compressive strength (%) of the mixtures from the PG-concrete system are presented in Figure 6.20.

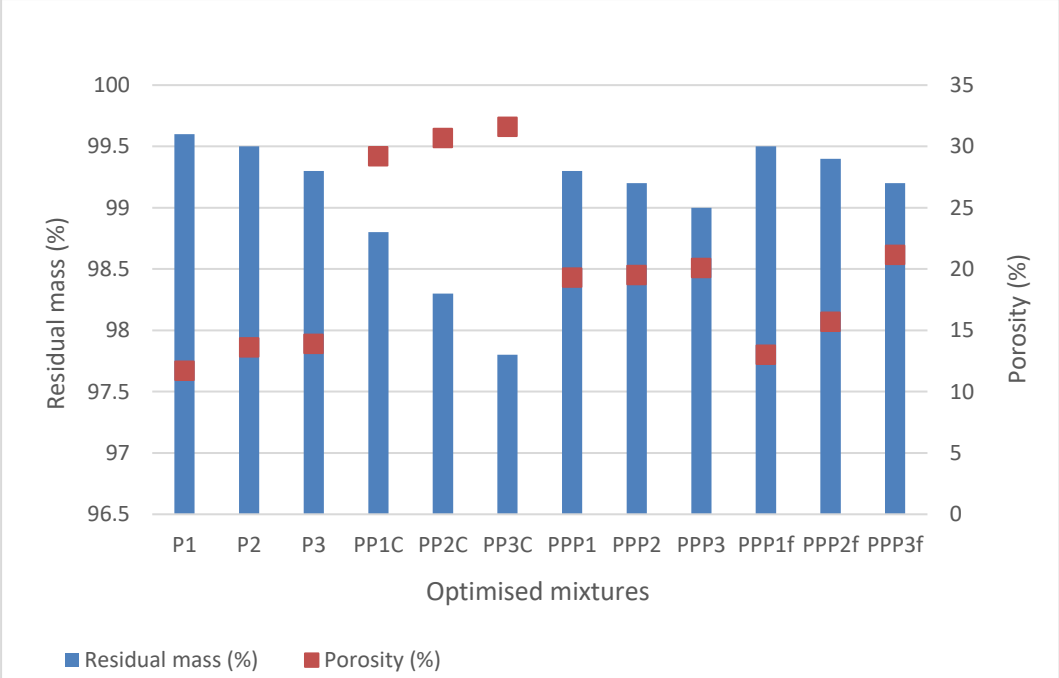


Figure 6.19: Relationship between porosity (%) and residual mass (%) of the PG-concrete system after 20 last freeze and thaw cycles

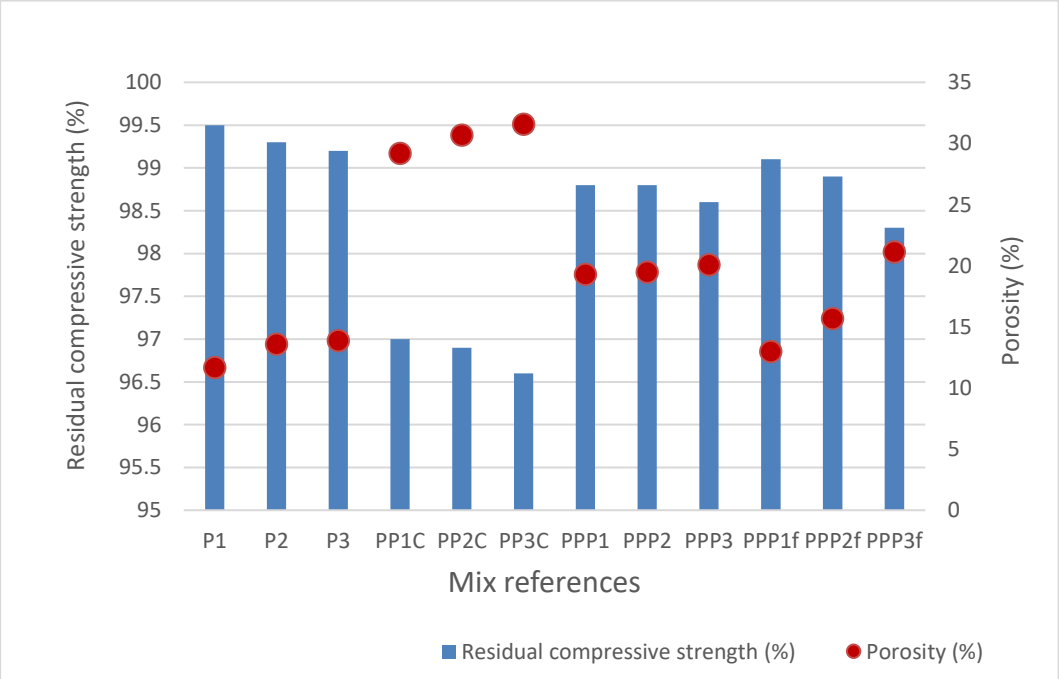


Figure 6.20: Relationship between porosity (%) and residual compressive strength (%) of the PG-concrete system after 20 last freeze and thaw cycles

### *6.2.4.2 Sulphate resistance of the PG–concrete and the encapsulated plastic concrete test specimens*

The resistance of the PG-concrete mixture (conventional concrete and encapsulated plastic concrete) to sulphate attack was similar to that observed in the equivalents from the CEM IIB-concrete system. The test specimens from the PG-concrete mixtures (conventional and encapsulated plastic concrete) recorded minor weight and compressive strength losses after continuous immersion in seawater for up to 90 days. As shown in Figure 6.21 and Figure 6.22, the mass and compressive (%) losses of the PG-concrete mixtures (P1-3, PP1-3, PPP1-3 and $PPP1_f$-$3_f$) resulting from sulphate attack increased with increase in water absorption (%).

The hydrated test specimens from the PG-concrete mixtures (P1-3) due to their relatively low water absorption (%) demonstrated the lowest mass and compressive strength (%) losses. In comparison to the PG-concrete mixtures (P1-3), the test specimens from the PG-encapsulated plastic concrete mixtures due to the higher water absorption (%) demonstrated higher mass and compressive loss (%). The infiltration of water into the PG-encapsulated plastic concrete mixtures (PP1-3) due to the higher water absorption (%), enhanced the deterioration of the mixtures relative to the conventional PG-concrete (P1-3).

The inclusion of PFA in the PG-PFA encapsulated plastic concrete improved the resistance of the encapsulated plastic concrete mixtures (PPP1-3 and $PPP1_f$-$3_f$) to sulphate attack. The PG-PFA encapsulated plastic concrete (PPP1-3 and $PPP1_f$-$3_f$) demonstrated lower mass (%) losses relative to the PG-encapsulated plastic concrete (PP1-3). This may be attributed to the lower water absorption (%) of the PG-PFA encapsulated plastic concrete (PPP1-3 and $PPP1_f$-$3_f$) relative to the PG-encapsulated plastic concrete.

From Figure 6.21, the PG-PFA encapsulated plastic concrete with PFA utilised as mineral admixture (PPP1-3) recorded lower (%) mass losses, compared to the equivalent PG-PFA encapsulated plastic concrete mixtures with PFA used as micro-fillers ($PPP1_f$-$3_f$). From Figure 6.22, the first PG-PFA encapsulated plastic concrete mix ‘PPP1’ demonstrated higher water absorption percentages and lower compressive strength (%) loss relative to its equivalent with PFA utilised as micro-filler $PPP1_f$. The second (PPP2) and third (PPP3) mixes however, demonstrated higher water absorption (%) and higher

compressive strength (%) losses relative to the equivalent with PFA utilised as micro-filler ($PPP2_f$ and $PPP3_f$). The variations in compressive strength (%) losses may be attributed to the differential effect of PFA on the sulphate resistance of the encapsulated plastic concrete mix. The PFA used in the current work, due to the high carbon content, had the tendency to absorb and retain moisture. The PG-PFA encapsulated plastic concrete with PFA used as micro-filler ($PPP1_f$-$3_f$) contain lower aggregate/binder ratios, while the PG-PFA encapsulated plastic concrete equivalents with PFA mineral admixture (PPP1-3) contain higher aggregate/paste ratios. That is, $PPP1_f$-$3_f$ contain more paste and lesser aggregates (FBA and 0-10mm plastic aggregates) relative to the respective PPP1-3 equivalents. At higher water/binder ratio, the increased cavities in $PPP2_f$ and $PPP3_f$ may enable the concrete to absorb and retain more sulphate ion rich moisture, which may react with the aluminate in the PFA resulting in expansion and as such losses in compressive strength.

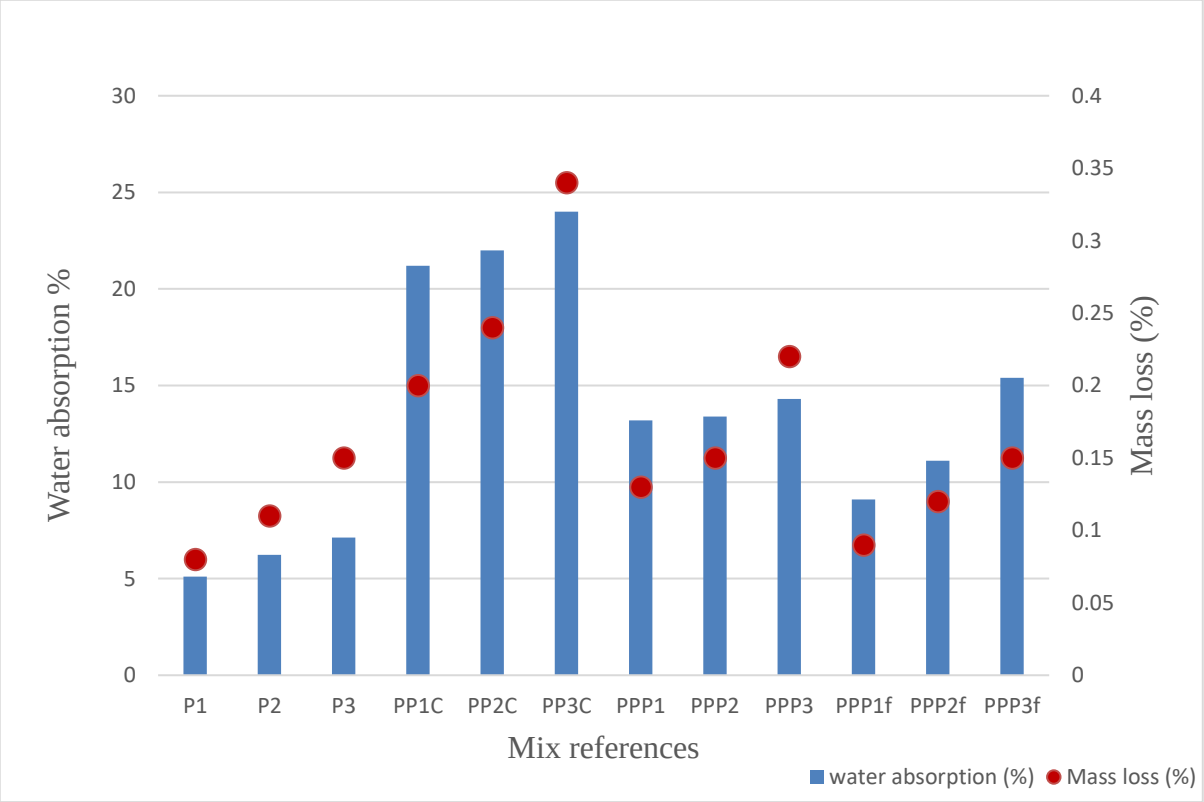


Figure 6.21: Relationship between water absorption (%) after 28 days of water curing and the mass loss (%) of the mixtures from the PG-concrete system after 28 days of curing in sulphate water

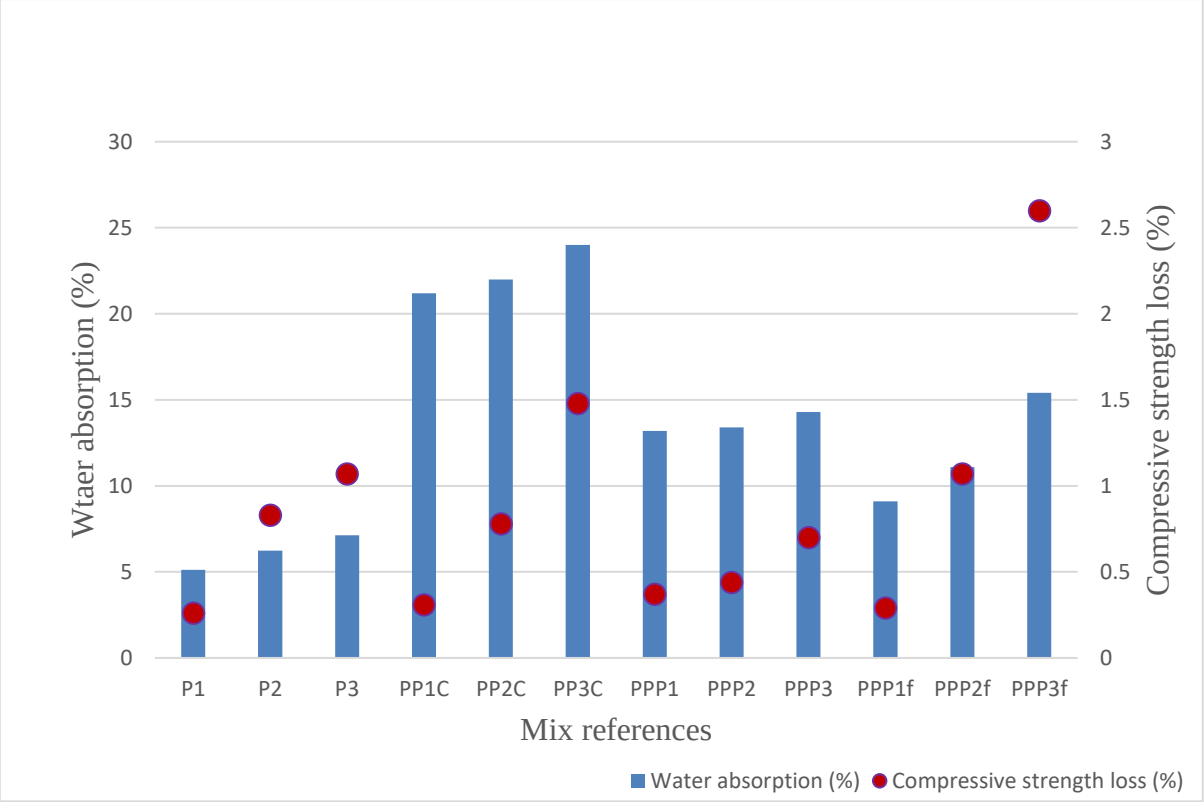


Figure 6.22: Relationship between water absorption (%) after 28 days of water curing and the mass loss (%) of the mixtures from the CEM IIB-concrete system after 28 days of curing in sulphate water

## 6.3 PRACTICAL IMPLICATIONS AND ECONOMIC BENEFITS

Waste plastics, as identified earlier in this work, are a problematic waste. Some of the properties such as its low cost, lightweight and durability that make it so beneficial also ensure that it is hard to dispose of to landfill as waste. The environmental and health concerns of waste plastics disposal are diverse and include amassing the waste in huge quantities in landfills and natural habitats, physical harm caused to wildlife by the ingestion and entanglements, leaching of chemical additives and endocrine disruptors from plastic products, which based on growing number of research works (Svenson et al., 2009, Thompson et al., 2009a&b, Tsuchida et al., 2011, Koch and Calafat, 2009, and Hirai et al., 2011), may adversely affect living organisms (including humans). Hence, attempts at recycling or reusing waste plastics, in addition to contributing to the various government (zero) waste legislations, will also contribute towards the current global alliance towards sustainable economic and environmental goals. In 2015, 186 United Nations member countries adopted a 15 years sustainable development plan, which includes equitable economic growth and targets to prevent and significantly reduce land and marine pollution, including plastic litters (EU infographic on plastic waste, 2015). Recycling or reusing waste plastic will reduce also help reduce the negative health effect and the burden (including chemical burden) of the material on the environment. Furthermore, utilising waste plastics in construction may contribute towards the reduction of concrete's hefty carbon footprint and resource efficiency through smarter, more efficient and sustainable use of natural resources.

The optimised encapsulated plastic concrete mixtures designed in the current work predominantly utilise waste materials (waste plastics, FBA and PFA), which would have otherwise been land filled or incinerated. Disposal through landfill or incineration would have resulted in the loss of the embodied energy of the waste materials. The encapsulated plastic concrete blends utilised between 12.5 - 17% cement binder and 83 - 87.5% waste materials. The usage of waste materials may reduce the overall building and/or construction cost. The only notable cost associated with the use of the waste materials in the encapsulated plastic concrete technology is the cost of the cement binder (CEM IIB or PG), cost related with the recycling of waste and the transportation cost of the waste materials from the recycling plants to concrete production site. As such, the cost implication of the encapsulated plastic concrete is likely to be much lower when

compared to the concrete developed using natural aggregates. According to Speedbuild UK Limited, the current cost of the waste materials (PFA, FBA and waste plastics) is about £5 per tonne per material type, most of which relates to the collection and transportation of the materials. The cost of the river sand and 10mm limestone aggregates utilised in the current studies (as obtained from Jewson UK Limited) is currently £33 per tonne per aggregate.

Additional cost savings may also be made from utilising the waste plastics in construction rather than the land-filling or incinerating. The landfill or incineration taxes incurred by the polymer extrusion companies (according to Speedbuild UK Limited) for disposing the mechanically recycled waste plastic in landfills or incinerators currently stands at £115.00-£135.00 per tonne for land-filling or £80.00–£90.00 per tonne for incinerating. These costs will not be incurred if the waste materials are recycled and reused in construction.

The current work has shown that it is possible to immobilise waste plastics in cementitious materials using encapsulation technology. The encapsulated plastic concrete mixtures have shown that high volumes of waste plastics can be mechanically bounded into solid monoliths, which based on the physical, mechanical and durability properties investigated as part of this work may be suitable for use in civil engineering applications. The optimised encapsulated plastic concrete can be regarded as pervious-lightweight concrete with unconfined compressive strength ranging between 2.8 $N/mm^2$ – 17.4$N/mm^2$ after 28 days of curing. Like the concrete developed with natural aggregates, the encapsulated plastic concrete also exhibited good resistance to frost action, sulphate attack and tolerated temperature increments up to 150$^oC$.

The drawbacks of the encapsulated plastic concrete system include the low workability of most of the fresh mixtures observed during placement and compaction and, the low tensile strength of some of the concrete blends relative to the reference concrete. Low workability concrete according to the specification of BS EN 206 and BS 8500, may be suitable for use in kerb bedding and backing, wall/strip footings (house and garage floors), cast in-situ paving (drives and domestic parking) and sliding concrete formwork (ICF blocks) and compacted concrete blocks, which do not need workability. The low workability of the encapsulated plastic concrete may be eased through mechanical mixing, power vibration using poker vibrators, roller compactors, high-pressure concrete

pumps and/or compacting in thin layers, while the tensile strength may be improved using mesh or other reinforcements depending on the use of the concrete.

The lightweight property of the encapsulated plastic concrete makes it particularly suitable for off – site production. The planning, design, fabrication and assembly of building elements at a location other than their final location may support rapid and efficient construction of permanent structures, and reduce the cost of a construction project. In addition, the lightweight classification of the encapsulated plastic concrete mixtures based on the specifications of BS EN 206:2013+A1:2016 also makes them applicable in lightweight applications such as concrete fills, landscaping and structural formworks. The classification based on density, compressive strength and intended application distinguishes the encapsulated plastic concrete into low-density, moderate strength and structural lightweight concrete. Low density LWC has densities only occasionally exceeding 800 kg/m$^3$, compressive strength ranging between 0.69 – 6.89 N/mm$^2$ and are mainly used for insulating purposes. The encapsulated plastic concrete with such low levels of compressive strength may be useful as concrete fillers in applications such as sandwich concrete with an outer load bearing leaf of precast concrete and insulated concrete forms (ICF), with interlocking modular units that are dry stacked and filled with concrete.

Moderate strength LWC, has densities ranging between 800 -1400kg/m$^3$, requires a fair degree of compressive strength (6.89 – 17 N/mm$^2$) and its application includes concrete fills, landscape designs (for example curbing blocks), boundary and retention walls. Finally, structural lightweight concrete requires a minimum compressive strength of 17 N/mm$^2$ and density of 1400 – 2000kg/m$^3$ and can be used in load bearing construction works. As highlighted in the results and discussions, one of the CEM IIB-PFA encapsulated plastic concrete with PFA utilised as a micro-filler (mix CPP1$_f$) complies with the required compressive strength for structural lightweight concrete specified in BS EN 1992-1-1:2004+A1:2014. Although, fire safety measures such as safeguarding ignition sources, fire alarm, smoke alarms and sprinkler systems may have to be deployed due to the fire risk associated with the use of plastic materials in building construction. The encapsulated plastic concrete may be of particular benefit in low fire risk buildings such as sport centres and playgrounds, farmhouses, DIY outlets, outbuildings, storage units, garden centres among others.

The high porosity of the encapsulated plastic concrete may also distinguish them as pervious concrete. Pervious concrete (or permeable concrete) is a special type of concrete with networks of void spaces used in concrete flatwork applications such as driveways, sidewalks, parking lots, road drainage and other pavement works. Pervious concrete permits water from precipitations and other sources to flow through its void openings, thereby reducing surface runoffs and allowing groundwater recharge. Similarly, the high porosity of the concrete may also support its application in flood defence applications such as sustainable drainage systems for direct channelling of surface water through networks of pipes and sewers to nearby watercourses, flood embankment/slope design, levees and flood walls.

The high porosity of the encapsulated plastic concrete may also support its application in vegetation friendly concrete. That is, concrete that supports the growth of vegetation. In a separate work carried out at the University of South Wales, non-rigid waste plastics, similarly encapsulated with cement binder and organic fillers ( wood chippings and saw dust) supported the growth of vegetation during the entire observation period (about 12 months). Some of the test cubes from the investigation are shown in Figure 6.23. The concrete may be suitable for green walling, earth sheltered housing, playgrounds or other applications requiring vegetative aesthetics. Other possible applications of the encapsulated plastic concrete include low- energy and low-carbon construction, speedy construction and extreme weather construction.

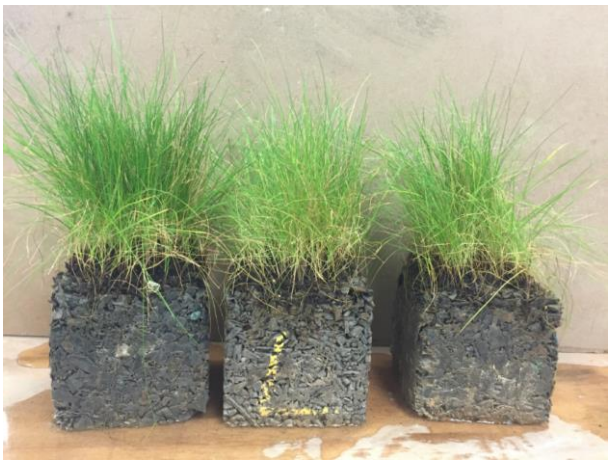

Figure 6.23: Some of the vegetation – friendly concrete developed at the University of South Wales

Reinforcements of the CEM IIB and PG-encapsulated plastic concrete mixtures (CP1-3 and PP1-3) with steel mesh or similar reinforcements may however be necessary in colder climate. The mixtures (CP1-3 and PP1-3), recorded mass and compressive strength losses due to the loss (chipping) of aggregates around the edges during the freezing and thawing cycles. Likewise, for the duration investigated (90 days), the encapsulated plastic mixtures (specifically those including PFA) showed some degradation (loss in mass and compressive strength) when subjected to harsh sulphate environment. Measures to help control sulphate attack such as the use of sulphate resisting cement, replacement of high carbon PFA with BS 450 compliant PFA or natural pozzolans such as burned clay or shale, adequate concrete thickness and, proper compaction and curing among others should be considered when using the encapsulated plastic concrete mixtures with PFA.

The leachate test simulated by immersing 50×50×50mm test cubes from each of the optimised encapsulated plastic blends (with or without PFA) in deionised water held in air tight glass cylinders recorded pH values between 8.9 - 9.5 after 360 immersion days. This suggest the leachate of alkaline (possibly $Ca(OH)_2$) from the encapsulated plastic test specimens. Water with high alkalinity does not pose a health risk, but may cause aesthetic problems such as scale build up in plumbing among others (EU council directive 98/93/EC, 2008).

# CHAPTER 7–CONCLUSIONS AND RECOMMENDATIONS FOR FUTURE WORKS

## 7.1 CONCLUSIONS

The results obtained from the current work suggest that, there is potential for the use of reclaimed waste plastics encapsulated in cementitious systems within the construction industry. This will contribute to current endeavours to finding sustainable means for managing waste arising from the use of plastic, a material of immense importance to modern living. It will also facilitate the reduction of the hefty carbon footprint associated with concrete. The following conclusion are therefore drawn from this research:

### 7.1.1 Encapsulation of waste in cementitious systems

As identified in literatures, plastic aggregates may be immobilised in cementitious materials using encapsulation technology. Some challenges associated with the disposal of plastic through this route, including easy dispersibility and mobility of the waste was nullified by minimising the aggregates to a manageable volume using correction factors. The presence of void volumes also recognised in literatures as a major influence on the performance of encapsulated waste-forms, was mitigated by the use of aggregate and micro filler (FBA and PFA). Subsequent experimental investigations also indicated that the encapsulated plastic waste forms demonstrated adequate physico-mechanical and durability properties suitable for some construction works. The major drawbacks of the concrete include low workability and low tensile strength, which can be mitigated by using mechanical mixing, power vibration using poker vibrators, roller compactors, high-pressure concrete pumps and/or compaction in thin layers (for improved workability) and, using reinforcements such as wire mesh to improve the tensile strength. As such, this study as shown that encapsulation technology may be a plausible route for managing waste plastics due to the economic and ecological advantages. The technology may help divert the significant quantities of waste plastics from landfill and help reduce the health and environmental concerns associated with the current disposal routes (landfill and incineration). It may also contribute to sustainable construction particularly in the areas social, environment and economic sustainability including cost, materials and energy efficiency.

### 7.1.2 Binding systems

The preliminary and optimised concrete blends made using CEM IIB Portland cement, showed high potential for encapsulated plastic concrete manufacture. In comparison to conventional and encapsulated plastic concrete developed using Pozament grout, the concrete made using CEM IIB cement demonstrated quicker setting times, better cohesiveness, compaction and better finishing. The CEM IIB concrete also demonstrated higher strength development and durability at the water/binder ratios investigated relative to the PG-concrete. Pozament grout due to its low water demand was at a disadvantage at the water/binder ratios (0.5 and 0.6) utilised in the concrete mix design. The low standard consistency of Pozament grout (0.17), suggest the concrete utilising it as the primary binder may benefit from reduction in mix water. As prescribed by the manufacturer the grout is capable of attaining very high compressive and ultimate tensile strength (90 $N/mm^2$ and 11 $N/mm^2$) after 90days at a water/binder ratio near the consistency.

The inclusion of PFA increased the water demand and reduced the flow of both the CEM IIB and PG-binders due to the high carbon content of the fly ash. Similarly, PFA retarded the hydration of the binders and increased the setting times. The increase in water demand of the binders incorporating PFA, may actually offer an advantage in the manufacture of the encapsulated plastic concrete, as it mitigated the problems of excess water observed with the concrete with CEM IIB and PG-binders used on their own. The impact of the increase water demand was mostly felt on the workability of the encapsulated plastic concrete, as both rheology and homogeneity increased with the inclusion of fly ash. These improvements translated to increased cohesion between the cement past and the aggregate and better compaction of the vibrated concrete which had some influence on the properties of the hydrated concrete.

Overall, the variation in binding systems highlight the importance of having control over the total mix water, in order to optimise the performance of the binding materials used for waste immobilisation in this study. The low water absorption capacity of some waste materials may increase the free water content (total water – unabsorbed water), hence increase porosity of the fresh and hydrated concrete.

### 7.1.3 Inferential statistical analysis

The inferential statistical analysis concluded that for the encapsulated plastic concrete made using CEM IIB, CEM IIB+PFA, PG and, PG+PFA-binders, relative to the equivalent conventional concrete, statistically significant reductions were observed in all the physical and mechanical properties investigated. Few exceptions were observed with the porosities of $CPP1_f$ and $CPP2_f$ and, PP3, $PPP1_f$ and $PPP2_f$ and, the tensile strength of tensile strength analyses for CPP1 and $CPP1_f$. The result of the statistical analysis highlights the influence of quantity and physical properties of the recycled aggregates on the physical and mechanical properties of concrete incorporating waste materials

### 7.1.4 Physical property of the fresh concrete mixtures

The encapsulated plastic concrete generally demonstrated low-range workability, which was mostly attributed to the water content and, the volume and physical properties of the recycled aggregates (FBA and 0-10 mm plastic aggregates). The optimum relative workability of the CEM IIB-encapsulated plastic concrete based on the compaction index was observed in the mix utilising water/binder ratio of 0.6 and aggregate/binder ratio of 5/1. In comparison to the reference mixtures (CEM IIB-concrete mixes C1-3), the encapsulated plastic concrete (with or without PFA) recorded lower range workability. The reference mixtures all achieved medium range workability. The optimum workability was also observed in the mix utilising higher water/binder (0.6) and lower aggregate to binder ratio (5/1). Reducing the water content or increasing the aggregate content decreased the workability of the concrete.

The inclusion of PFA in the encapsulated plastic concrete mixtures, improved the rheology and homogeneity of the mixtures. The spherical particles and the reduced water demand of the CEM IIB-PFA binder improved the particle size distribution and microstructure of the fresh encapsulated plastic mixes, thus reducing the segregation and increasing the workability. The CEM IIB-PFA encapsulated plastic concrete mixtures with PFA utilised as mineral admixtures (CPP1-3), all demonstrated low workability. The workability appears to increase with increased water content and decreased with increased aggregate/binder ratio. As with the encapsulated plastic concrete with CEM IIB-binder (CP1-3), the optimum workability was also observed at water/binder ratio and aggregate/binder ratio of 0.6 and 5/1 respectively.

Encapsulated plastic concrete mixtures with PFA utilised as mineral admixtures (CPP1-3) demonstrated lower workability relative to the encapsulated plastic concrete mixtures with PFA utilised as micro-filler ($CPP1_f$-$3_f$). This is thought to be due to the higher fine and coarse aggregate, and water content utilised when PFA was used as a mineral admixture. The mixtures utilising PFA as micro-filler demonstrated higher workability relative to the other encapsulated plastic concrete mixtures in the CEM IIB-concrete system. They were more cohesive and compacted better than any CEM IIB-based encapsulated plastic concrete. The variations in workability indicated that, the CEM IIB-PFA encapsulated plastic concrete mixtures with PFA micro-filler demonstrated medium – high range workability.

The utilisation of PG as the primary binder instead of CEM IIB mostly decreased the workability of the resulting composite mixture. The reduction in workability was mainly attributed to the increased segregation of the mixtures in the PG-concrete system due to the low water demand of the PG-binder. The PG-encapsulated plastic concrete (PP1-3) mostly demonstrated very low-low range workability. Under visual observation, the concrete was observed to leach out mix water and as such, the mixtures were highly segregated, dry and non-cohesive.

The inclusion of PFA in the PG-encapsulated plastic concrete slightly increased the workability. The mixtures were more cohesive and compacted with less difficulty. The mixtures utilising PFA as mineral admixtures (PPP1-3) due to the higher aggregate content recorded slightly lower workability relative to the mixtures utilising PFA as micro-filler ($PPP1_f$-$3_f$). The PG-PFA encapsulated plastic concrete mixtures (PPP1-3) recorded very low – low range workability, which increased with increased water content and decreased with increased aggregate/binder ratio. The maximum relative workability was obtained with the optimum mix utilising a water/binder ratio of 0.5 and lower aggregate to binder ratio of 5/1. The PG-PFA encapsulated plastic concrete mixtures utilising PFA as micro-filler ($PPP1_f$-$3_f$) were the most cohesive encapsulated plastic concrete from the PG-concrete system. The variations in workability obtained from the compaction index analyses, suggested that, the PG-PFA encapsulated plastic concrete mixtures with PFA as micro-filler demonstrated medium – high range apparent workability.

In comparison to the encapsulated plastic concrete (with PG or PG-PFA binder), the conventional PG-concrete mixtures (P1-3) recorded higher workability. They demonstrated low-medium range workability (slump). The slump values recorded by the mixtures were mostly lower than the target slump of 30-60 mm. The optimum workability (60 mm) was also observed in the mix utilising higher water/binder (0.6) and lower aggregate to binder ratio (5/1). As such as with the other concrete types investigated in the current work, the workability of the PG-concrete mixtures increased with increase in water content and decreased with increased aggregate/binder ratio.

The low range workability recorded by most of the encapsulated plastic concrete mixtures was the main drawback of the system. However, as mentioned in the discussion, there are many applications for low workability concrete such as kerb and culvert bedding and backing, wall/strip footings (house and garage floors), cast in-situ paving (drives and domestic parking), sliding concrete formwork (ICF blocks) and compacted concrete blocks, all which do not need high workability. In addition, the low workability can be remedied by utilising water reducers, mechanical mixers and high-pressure concrete pumps and/or, compacting in thin layers.

### 7.1.5 Properties of the hydrated concrete

a) Density

The CEM IIB-encapsulated plastic concrete is lightweight, with 28-days density values ranging between 1520 – 1600 kg/m$^3$. The low density may be attributed to the high void size and volume in the matrix of the test specimens. The test specimens from the hydrated mixtures were visually observed to be very open textured with high percentages of visible void spaces. The density result obtained for the CEM IIB-encapsulated plastic concrete, as with the density of all the other concrete types investigated decreased with increase in water/binder ratio and increase in aggregate/binder ratio.

When PFA was included in the CEM IIB-PFA encapsulated plastic concrete (with PFA used either as mineral admixture of micro-filler), the visible void spaces reduced drastically with the aggregates (FBA and 0-10 mm plastic aggregates) completely embedded in the encapsulating matrix (CEM IIB-binder). As a result, the densities of the CEM IIB-PFA encapsulated plastic concrete (with PFA used either as mineral admixture of micro-filler) marginally increased relative to the densities of the encapsulated plastic

concrete with CEM IIB used on its own (CP1-3). The CEM IIB-PFA encapsulated plastic concrete with PFA utilised either as a mineral admixture or as a micro-filler (CPP1-3 or CPP1$_f$-3$_f$) recorded density values ranging between 1570 -1640 kg/m$^3$. The range of density values recorded by the mixtures also designate them as lightweight concrete.

The CEM IIB-concrete mixtures recorded density values ranging from 2390 – 2440 kg/m$^3$, which are within the typical density range for conventional concrete. From the density values recorded by the CEM IIB-encapsulated plastic concrete mixtures (with or without PFA), the substitution of natural aggregates with recycled waste materials (FBA and 0-10 mm plastic aggregates) was shown to significantly decrease the density relative to the CEM IIB-concrete mixtures. In comparison to the conventional CEM IIB-concrete (C1-3), the densities recorded by the CEM IIB-encapsulated plastic concrete (with or without PFA) were lower by approximately 33 – 36%.

When the binding material Portland cement (CEM IIB) was replaced with Pozament grout (PG), the densities of the resulting concrete (conventional and encapsulated plastic concrete) decreased slightly, when compared to their equivalents from the CEM IIB-concrete system. As observed with workability, the high fluidity of the PG-binder further increased the entrapped water and hence increased the void percentages of the (conventional or encapsulated) PG-concrete system, relative to the equivalents from the CEM IIB-system. The conventional PG-concrete mixtures (P1-3) recorded density values ranging from 2360 – 2390 kg/m$^3$, while the all the mixtures from the PG-encapsulated plastic concrete (PP1-3) recorded density values ranging between 1420 – 1590 kg/m$^3$. The inclusion of PFA in the mixtures marginally increased the densities of the encapsulated plastic concrete. Encapsulated plastic concrete with PFA mineral admixture (PPP1-3) recorded density values ranging from 1560 -1590 kg/m$^3$, while the mixtures utilising PFA as micro-filler recorded densities within a wider range from 1550-1600 kg/m$^3$. In general, the density values recorded by the PG-encapsulated plastic concrete (with or without PFA) designate them as lightweight concrete.

Although the encapsulated plastic concrete recorded lower densities relative to the conventional concrete mixtures. The lightweight properties of the concrete make them particularly an attractive option in speedy construction particularly in off-site concrete production. They may also be suitable in concrete fills, landscaping and structural formworks.

b) porosity

The porosities of the CEM IIB-concrete system (convention or encapsulated plastic) generally increased with increase in water/binder and aggregate/binder ratios. The CEM IIB-concrete mixtures were the least porous of all the concrete types investigated. The mixtures recorded porosities within the range of 8.9-9.3%. Substituting the natural aggregates (river sand and 10 mm limestone aggregates) in the mixtures with recycled aggregates (FBA and 0-10 mm plastic aggregates) led to significant increase in porosity (about 66%). The high porosity values recorded by the CEM IIB-encapsulated plastic concrete were mostly attributed to initial amount of free water (total mix water – unabsorbed water) content and, the volume and physical properties of the recycled aggregates including particle size, shape, texture, specific gravity and water absorption.

When PFA was added to the encapsulated plastic concrete mixtures, the filler effect of the fly ash and improved microstructure of the concrete due to the likely formation of more C-S-H gel, combined to reduce the porosity of the concrete mixtures relative to the equivalent with CEM IIB-binder used on its own. In general, the CEM IIB-PFA encapsulated plastic concrete with PFA used as mineral admixtures (CPP1-3) recorded lower porosities relative to the CEM IIB-PFA encapsulated plastic concrete utilising PFA as micro-filler ($CPP1_f$-$3_f$). The former group of mixtures recorded porosity values between 18.1 -19.4 %, while the latter recorded porosities between 12.2 -15.1%.

When the binding material was switched from Portland cement (CEM IIB) to Pozament grout (PG), the porosities of the concrete mixtures (conventional and encapsulated plastic) with PG binder increased relative to the equivalents from the CEM IIB-system. The increased segregation observed with the fresh PG-concrete mixtures (conventional or encapsulated plastic) was also retained and observed in the hardened mixtures inform of increased porosity. The PG-concrete mixtures recorded the lowest porosities of all the mixtures from the PG-concrete system. The replacement of natural aggregates with recycled aggregates in the PG-encapsulated plastic concrete (as with the CEM IIB-equivalents) also dramatically increased the porosity of the resulting concrete mixtures.

The PG-encapsulated plastic concrete mixtures with PFA generally recorded lower porosities relative to the mixtures with PG-binder used on its own. The mixtures ((PPP1-3 and $PPP1_f$-$3_f$) recorded porosity values ranging between 13.0-21.5%. The mixtures

utilising PFA as mineral additive (PPP1-3) mostly recorded higher porosities, in comparison to the mixtures with PFA used as micro-filler ($PPP1_f$-$3_f$). The factors responsible for the variations in the porosity values observed in the CEM IIB-concrete systems were also responsible for the variations observed between the porosity of the mixtures from this PG-system.

The porosity played a major role in the physical (density), mechanical strength and durability performance of the concrete mixtures, particularly the encapsulated plastic concrete mixtures. The measured performance parameters may all be said to be inversely related to the porosity. The increase in porosity led to decrease in density, the most porous concrete types were shown to demonstrate the lowest densities, while the least porous mixtures/concrete types demonstrated the highest densities. As shown later in this chapter, increase in porosity also adversely affect the affected the strength development (compressive and tensile), as well as the durability performances of the different concrete types evaluated.

The high porosities of the CEM IIB or PG-encapsulated plastic concrete (with or without PFA) may however be of particular advantage flatwork applications such as driveways, sidewalks, parking lots, road drainage, pavement works and flood defence applications, where permeability is an important property. Due to the high porosity, plastic concrete system organic fillers such as saw dust and risk husks may also be useful in concrete capable of supporting growth of vegetation.

C) Water absorption

A linear relationship was observed between the porosity and water absorption of all the concrete types investigated in the current work. The water absorption of the test specimens from the mixtures in CEM IIB-concrete and PG-concrete systems increased with increase in porosity. The least porous of all the concrete types investigated in the current work (CEM IIB-concrete) also recorded the lowest water absorption (%). The replacement of natural aggregates (river sand and 10 mm limestone aggregates), with recycled aggregates (FBA and 0-10 mm plastic aggregates), due to the relative increase in porosity, also significantly led to increased water absorption (%) of the CEM IIB-encapsulated plastic concrete. The water absorption (%) of the encapsulated plastic concrete mixtures utilising CEM IIB binder on its own (CP1-3), were approximately 80%

higher than the water absorption (%) of the equivalents from the CEM IIB-concrete mixtures (C1-3).

When PFA was included in the CEM IIB-encapsulated plastic concrete, the water absorption (%) of the concrete decreased. The filler effect and the improved microstructure of the CEM IIB-PFA encapsulated plastic concrete significantly decreased the water absorption of the concrete mixtures relative to its equivalents with CEM IIB binder used on its own. Inherently, as observed with porosity, the water absorption (%) of the concrete mixtures from the CEM IIB-PFA encapsulated plastic concrete with PFA utilised as a mineral admixture (CPP1-3) were higher than the water absorption (%) of the equivalent from the CEM IIB-PFA encapsulated plastic concrete with PFA utilised as a micro-filler ($CPP1_f$-$3_f$).

When the CEM IIB was replaced with the PG as the binding material, the PG-encapsulated plastic concrete mixtures (PP1-3) recorded the highest water absorption percentages of all the concrete types investigated. These mixtures also recorded the highest porosities of all the concrete types investigated. The inclusion of PFA similarly reduced the water absorption (%) of the PG-encapsulated plastic concrete, with the mixtures utilising PFA as mineral additive (PPP1-3) recording higher water absorption than the mixtures with PFA used as micro-filler ($PPP1_f$-$3_f$). Overall, due to their relatively lower porosities, the conventional PG-concrete mixtures (P1-3) demonstrated the lowest water absorption (%) of all the concrete types investigated in the PG-concrete system.

In comparison with the equivalents from the CEM IIB-concrete system, the mixtures from the PG-concrete system recorded marginally higher water absorption (%). The variations observed between the water absorption (%) of the mixtures from the CEM IIB-concrete system and the PG-concrete system was attributed mainly to the increased segregation/porosity of the PG-concrete mixtures (conventional or encapsulated plastic).

d) Compressive strength

In general, the CEM IIB-concrete incorporating FBA and 0-10 mm plastic aggregates achieved lower compressive strength than the control CEM IIB-concrete mixtures (C1-3) for at all the curing ages investigated. The relatively high porosity of the CEM IIB-encapsulated plastic concrete mixtures (CP1-3) significantly decreased the compressive strength of the concrete mixtures relative to their equivalents from the other concrete

types in the CEM IIB-concrete system. For all curing ages, the maximum relative compressive strength of the CEM IIB-encapsulated plastic concrete was achieved by the mix with the lowest porosity (mix CP1). The mix utilised water/binder ratio of 0.5 and an aggregate/binder ratio of 5/1. Due to the increased porosity, increasing the water/binder ratio to 0.6 or aggregate/binder ratio to 6/1, both decreased the hydration of the CEM IIB-encapsulated plastic concrete.

The strength characteristics of the CEM IIB-encapsulated plastic concrete improved with the inclusion of PFA. The combined action of PFA with CEM IIB strongly bound the plastic aggregates. The strength-enhancing effect of PFA is thought to be due to pozzolanic reaction that resulted in the accumulation of additional C–S–H gel within the pore structure of the concrete. This reduced the porosity and increased the strength values obtained by the CEM IIB-PFA encapsulated plastic concrete (CPP1-3 and CPP$1_f$-$3_f$). The gel formation was further promoted by the incorporation of PFA as micro-filler rather than a mineral admixture. Relative to the CEM IIB-PFA encapsulated plastic concrete with PFA utilised as mineral admixtures (CPP1-3), the mixtures utilising PFA as micro-filler (CPP$1_f$-$3_f$) achieved higher strength values for all curing ages. The CEM IIB-PFA encapsulated plastic concrete with PFA micro-filler (CPP$1_f$) utilising the lower water/binder and aggregate to binder ratio (0.5 and 5/1, respectively), attained enough 28-day strength development for it to be regarded as structural lightweight concrete. The mix (CPP$1_f$) recorded the optimum compressive strength for all the ages investigated. The relatively high porosities of the other two mixtures making up the concrete type (CPP$2_f$ and $3_f$) consequently decreased their compressive strength.

For all the curing ages investigated, the equivalent mix in the CEM IIB-PFA encapsulated plastic concrete with PFA used as mineral admixtures, utilising the lower water/binder and aggregate to binder ratio (0.5 and 5/1, respectively) also demonstrated the highest relative compressive strength relative to the two other mixtures in the group. Its strength development for all curing ages were however lower than that required for classification as structural lightweight concrete. The increase in porosity also decreased the compressive strength of the subsequent mixes in this category (CPP2 and CPP3).

Overall, the control CEM IIB-concrete mixture (C1-3) achieved higher compressive strength at all curing ages, relative to the CEM IIB-encapsulated plastic concrete (with or without PFA). For all ages tested, the optimum compressive strength performance was

observed in the mix designed using the British mix design approach (mix C1). The mix achieved the target compressive strength of 49 N/mm$^2$ after curing for 28 days. Attempts at increasing the workability of the designed mix by increasing the water/binder ratio or making the mix leaner by increasing the aggregate/binder ratio, both decreased the compressive strength of the concrete. This was thought to be due to the relatively high porosities of both mixtures.

The utilisation of PG as the primary binder instead of CEM IIB mostly decreased the compressive strength of the resulting composite mixtures relative to their CEM IIB equivalents. The high porosity ascribed to the low water demand of the PG-binder was also accredited with the low compressive strength development of the PG-concrete mixtures. In hindsight, the PG-concrete mixtures (conventional and encapsulated plastic) should have utilised a lower water/binder ratio. The addition of water beyond standard consistency decreased the viscosity of the concrete and increased the porosity thus decreased the compressive strength of the concrete mixtures. The standard consistency of the PG-binder was 0.17, which was significantly lower than the 0.31 obtained for Portland cement. Hence, due to the high water/binder ratios utilised in the concrete work (0.5 and 0.6), the PG-concrete mixtures (conventional and encapsulated plastic concrete) were very fluid, highly segregated, thus demonstrated lower strength values relative to the CEM IIB-equivalent.

The PG-concrete mixtures (P1-3) due to their relatively lower porosities recorded the highest compressive strength values of all the concrete types in the PG-concrete system for all curing ages. The strength development of the PG-concrete mixtures was below the target compressive strength for convention concrete at 28 days. For all curing ages, the replacement of natural aggregates with recycled aggregates in the PG-encapsulated plastic concrete (PP1-3) resulted in the lowest strength development observed in any of the concrete types investigated in the research. The mixtures (PP1-3) as noted earlier also recorded the highest porosity values, compared to the other concrete types.

The inclusion of PFA both as micro-filler or mineral admixtures generally decreased the porosities and increased the compressive strength of the encapsulated plastic concrete. For all curing ages, the mixtures utilising PFA as micro-filler (PPP1$_f$-3$_f$) due to the lower amount of aggregate and decreased porosity maintained higher compressive strength values, relative to the mixtures utilising PFA as mineral admixtures. The influence of

PFA, due to the formation of more CSH gel, was more prevalent at 90 days. In general, the optimum compressive strength performances were observed in the first mix from each PG-concrete type. That is, the mixtures with the lower water/binder and aggregate/binder ratios.

e) Tensile strength

As observed with the compressive strength development, porosity also mainly accounted for the variations observed in the tensile strength development of the concrete types making up the CEM IIB-concrete system. The substitution of natural aggregates with recycled aggregates significantly reduced the tensile strength of the encapsulated plastic concrete equivalents, relative to the reference CEM IIB-concrete mixtures.

The CEM IIB-encapsulated plastic concrete mixtures (CP1-3) recorded tensile strength values within the range of 0.7 – 1.0 N/mm$^2$, which was about 70% lower than the equivalents in the CEM IIB-concrete mixtures (C1-3). The mix with the lowest porosity (CP1) recorded the highest tensile strength, while the concrete mix with the highest porosity (CP3) recorded the lowest tensile strength. The 28-days tensile strength of CP1-3 were observed to increase with increase in compressive strength.

When PFA was added to the encapsulated plastic concrete, first as a mineral admixture, then as a micro-filler, the tensile strength values achieved by the encapsulated plastic concrete improved relative to those recorded by the CEM IIB-encapsulated plastic concrete without PFA. The CEM IIB-PFA encapsulated plastic concrete mixtures with PFA utilised as mineral admixture (CPP1-3) recorded higher tensile strength values, relative to the equivalents in the CEM IIB-PFA encapsulated plastic concrete with PFA used as micro filler ($CPP1_f$-$3_f$).

The referenced CEM IIB-concrete mixtures (C1-3) recorded the highest 28–day tensile strength values of all the concrete mix types in the CEM IIB-concrete system. The concrete mix with the lowest porosity (C1) also recorded the highest tensile strength, while the concrete mix with the highest porosity (C3) recorded the lowest tensile strength. The 28–day tensile strength values of the mixtures (C1-3) increased with increase in compressive strength. It was also observed to be directly proportional to the product of the square root of its compressive strength and the coefficient derived from the regression analysis curves. That is, the power law is applicable to the CEM IIB-concrete mixtures.

When PG replaced the CEM IIB as the main binder, some of the mixtures from the PG concrete system (P1-3 and PP1) recorded slightly higher tensile strength values relative to the equivalents from the CEM IIB-concrete system, while the rest of the mixtures recorded slightly lower tensile strength values. The reasons for these variations cannot be ascertained but may be because of the low water demand of the PG-paste, the presence of mineral additives or the effect of PFA on the PG-binder. In general, the PG-concrete mixtures without plastics (P1-3) demonstrated the highest tensile strength of all the concrete types in the PG-system. The PG-encapsulated plastic demonstrated the lowest tensile strength, while as with the CEM IIB-equivalents, the PG-PFA encapsulated plastic concrete mixtures with PFA utilised as mineral admixture (PPP1-3) recorded higher tensile strength relative to the PG-PFA encapsulated plastic concrete with PFA used as micro filler ($PPP1_f$-$3_f$).

### 7.1.6 Durability properties of the hydrated concrete

a) Freeze-thaw resistance

In general, all the concrete types from the CEM IIB and PG concrete systems demonstrated good performance during the freeze-thaw analyses. Porosity again played a major role on the behaviour of the test specimens exposed to freeze-thaw conditions. The deterioration in weight and compressive strength after 20 freeze-thaw cycles was observed to increase with increase in porosity. The results of the investigation revealed that:

- The CEM IIB-encapsulated plastic concrete (CP1-3) recorded minor weight and compressive strength losses after 20 freeze-thaw cycles. They were also visually observed with minor chipping of aggregates around the edges. The reference conventional concrete mixtures (C1-3) demonstrated the lowest weight and compressive strength losses of all the concrete types investigated in the current research. The mixtures all recorded relatively lower deterioration in weight and compressive strength relative to the CEM IIB-encapsulated plastic concrete (with or without PFA). The concrete also maintained dimensional stability throughout the investigation
- The inclusion of PFA generally improved the resistance of the encapsulated plastic concrete to frost action. All the CEM IIB-encapsulated concrete mixtures

with PFA (CPP1-3 and CPP1$_f$-3$_f$) demonstrated lower weight and compressive strength losses relative to the CEM IIB-encapsulated plastic concrete without PFA (CP1-3). There was no chipping of aggregates as the entire test specimen maintained dimensional stability. The mixtures utilising PFA as mineral admixtures (CPP1-3) demonstrated higher weight and compressive strength losses relative to the mixture with PFA used as micro-filler (CPP1$_f$-3$_f$).

- When PG replaced CEM IIB as the primary binder, the weight and compressive strength losses demonstrated by the PG-encapsulated plastic concrete (PP1-3) were marginally higher than those recorded by the equivalents in the CEM IIB system (CP1-3). As with the CEM IIB-counterparts, aggregate chipping around the edges of the test specimens were also observed, the PG-encapsulated plastic concrete (PP1-3).
- The inclusion of PFA improved the resistance of the PG-concrete mixtures to frost actions. After 20 consecutive freezing and thawing cycles, the concrete mixtures (PPP1-3 and PPP1$_f$-3$_f$) also recorded minor weight and compressive strength losses. Relative to the equivalents from the CEM IIB-concrete system (CPP1-3 and CPP1$_f$-3f), the mixtures with PG-binder (PPP1-3 and PPP1f and 3f) recorded marginally higher weight and compressive strength losses. The mixtures utilising PFA as mineral admixtures (PPP1-3) again recorded slightly lower weight and strength losses relative to the mixtures with PFA used as micro-filler (PPP1$_f$-3$_f$).

b) Chemical resistance

The ability of the concrete mixtures to absorb and retain moisture played an important role in the sulphate resistance of the concrete. The deteriorations in weight and compressive strength of the test specimens from the conventional CEM IIB-concrete (C1-3) immersed in seawater were observed to increase with increase in water absorption (%). Nonetheless, all the mixtures demonstrated good durability performance in marine (seawater) conditions.

The CEM IIB-encapsulated plastic concrete mixtures (CP1-3), due to their relatively high-water absorption recorded the highest weight and compressive strength (%) losses when immersed in seawater for up to 90 days. The mixtures (CP1-3) all exhibited no changes in dimensions.

The inclusion of PFA in the CEM IIB-encapsulated plastic concrete mixtures (CPP1-3 and CPP1$_f$-3$_f$) improved the durability performance of the encapsulated plastic concrete under marine conditions, relative to the concrete mixtures utilising CEM IIB-binder on its own (CP1-3). The concrete mixtures (CPP1-3 and CPP1$_f$-3$_f$) also recorded minor weight and compressive strength losses. They recorded no changes in dimensions, but surface indentations were observed after 28 and 90 days immersion periods. The surface indentations were mostly thought of as 'gas holes' caused by entrapped air.

The encapsulated plastic concrete mixtures utilising PFA as mineral admixtures (CPP1-3) due to their higher water absorption also recorded higher (%) mass losses after exposure to marine condition, relative to the equivalents encapsulated plastic concrete mixtures with PFA micro filler (CPP1$_f$-3$_f$). The increase in water absorption due to differential effect of PFA, did not automatically translate to an increase in compressive strength losses. Mix CPP1, recorded higher water absorption, as such recorded marginally higher deterioration in weight and compressive strength relative to the equivalent with PFA used as micro-filler, CPP1$_f$. Mix CPP2 and CPP3 meanwhile, recorded slighter lower compressive strength losses relative to CPP2$_f$ and 3$_f$, even with the higher water absorption.

The CEM IIB-concrete (C1-3) experienced minor (%) weight and compressive strength losses but no major visible physical damage (that is, no aggregate chipping was observed), when subjected to marine condition. In comparison to the CEM IIB-encapsulated plastic concrete with or without PFA, the deterioration in mass and compressive strength observed with the CEM IIB-concrete mixtures was much lower.

The same behavioural patterns were observed in the concrete types from the PG-concrete system. The replacement of CEM IIB with PG generally decreased the resistance of the concrete mixtures to chemical attacks. The PG-encapsulated plastic concrete (PP1-3) due to their high-water absorption percentages demonstrated the highest deterioration in weight and compressive strength observed in any of the concrete type subjected to marine condition in this study.

As observed with the freeze-thaw resistance, the inclusion of PFA similar improvement in the resistance of the encapsulated concrete to chemical attack. The PG-PFA encapsulated plastic concrete with PFA utilised as a mineral admixture (PPP1-3), due to

the higher water absorption recorded higher mass loss percentages, relative to the PG-PFA encapsulated plastic concrete with PFA utilised as a micro-filler ($PPP1_f$-$3_f$). Also, due to the differential effect of the PFA on the concrete mixtures, some of the mixtures utilising PFA as mineral admixture (PPP2 and 3) were observed with higher water absorption (%) but marginally lower compressive strength loss percentages relative to their equivalents with PFA utilised as micro-filler (PPP2f and PPP3f). Mix PPP1, recorded higher water absorption (%), as such recorded marginally higher deterioration in weight and compressive strength relative to the equivalent with PFA used as micro-filler, $PPP1_f$.

The PG-concrete mixtures (P1-3) also experienced minor (%) weight and compressive strength losses but no major physical damages, when subjected to marine/seawater condition. The deterioration weight and compressive by these mixtures, were relatively lower than their equivalents from the PG-encapsulated plastic concrete with or without PFA.

In comparison to the equivalents from the CEM IIB-concrete system, the deterioration in weight and compressive strength demonstrated by the PG-concrete (conventional or encapsulated plastic) mixtures under marine conditions were marginally higher due to their relatively higher water absorption (%).

c) Thermal resistance

The result obtained from the thermal analysis carried out on the two most performing concrete mixtures from the reference concrete and the encapsulated plastic concrete (C1 and CPP1) suggest that, relative to the reference concrete, the encapsulated plastic concrete (CPP1) recorded higher deformation and property changes.

The CEM IIB-concrete suffered minor spalling around the edges, along with minimal weight and compressive strength (%) losses, during the thermal resistant investigation. This finding was attributed to the release of bound water from the cement paste and the occurrence of air voids in the concrete. The highest deterioration (weight compressive strength losses) occurred when the specimens were subjected to 200$^{o}$C. In general, the deterioration in weight and compressive strength of the CEM IIB-concrete test specimens was less than 2% for the observed temperature range (30 – 200$^{o}$C).

The encapsulated plastic concrete tolerated temperature increment up to 50$^{o}$C. At this temperature, the test specimens experienced minor (%) weight and compressive strength losses (less than 2%) but no major visible physical damage. The reduction in compressive strength and weight loss were slightly higher (3-4%), when the specimens were subjected to temperature range 100-150$^{o}$C. This result may be accredited to the loss water of water of crystallisation, in addition to the changes in the morphology of the plastic aggregates and the formation of micro-cracks and surface indentations. At 200$^{o}$C, the densification of the concrete by the molten plastic resulted in a slight increase in mass and compressive strength of the concrete, compared to the test specimen heated at 150$^{o}$C.

## 7.2 RECOMMENDATIONS FOR FUTHER WORK

As discussed in Chapter 6, the encapsulated plastic concrete mixtures developed in the current work have shown that, it is possible to immobilise high volumes of waste plastic in cementitious systems. They may also be suitable for use in some civil engineering construction applications, including concrete fills, load bearing structural concrete, vegetation friendly concrete and concrete requiring specific properties such as low-density concrete, pervious concrete and concrete for insulating purposes. There is however still a significant body of research work required in the field of encapsulating plastic or other solid waste forms in cementitious systems for application in civil engineering construction work. Thus, based on this current study, the following recommendations may be drawn for future and further work.

1) Life-cycle assessment analysis may be required to evaluate the environmental impacts associated with all the stages involved in the development of the encapsulated plastic concrete from raw material processing, through to use, repair, maintenance, and disposal or recycling of the concrete. That is, it may be necessary to account for the environmental effect of all the inputs and outputs throughout the life cycle of the encapsulated plastic concrete from cradle to grave.
2) Leachate analyses focused particularly on organic synthetic compound using toxicity characteristic leaching procedure (TCLP) is also highly recommended.
3) The low-workability of the encapsulated plastic concrete are likely to increase if;
    a) The distance between the blades in the grinding units of the mechanical recycling plant is varied (between 2-10 mm) rather than maintained at the 6 mm currently used in reducing bulk waste plastics into manageable size

volumes before land filling or incinerating. Varying the distance between the blades will yield plastic aggregates with dense gradation, which may mitigate, the effect of particle size distribution and non – uniform shaped (flaky and elongated) particles observed during the workability assessment.

b) Likewise, the encapsulated plastic concrete mixtures may also benefit from the use of water reducers. The low water absorption capacity of the plastic aggregates as observed during the workability assessment increased the segregation of the encapsulated plastic concrete and as such decreased the workability.

c) The particle size distribution of the filler material (Furnace bottom ash) may also be improved by either grinding the material into uniform shaped, fine-grained particles or sieving the material to remove the coarse-grained particles. This may also help achieve a dense gradation, which may help increase the workability of the encapsulated plastic concrete mixtures.

4) The dwindling availability of PFA due to the decline in coal burning at the power stations, may also affect the availability of FBA. Hence, the applicability of alternatives filler and micro-filler materials in the encapsulated plastic concrete system need to be evaluated. Materials such as waste sludge, biomass ash, rice husk ash, slags and other residue of refining or distillation, sediment run-offs, demolition wastes (wood, brick and concrete), natural pozzolans (sand, calcined clay, calcined shale or metakaolin), agricultural wastes and other non-hazardous solid industrial wastes may be considered.
5) The utilisation of some of the above listed materials may also be used to optimise the mass density of the encapsulated plastic concrete. This may also result in higher compressive strength development in the encapsulated plastic concrete
6) Higher strength values are also likely to be achieved by either chemically of mechanically increasing the abrasion on the surface of the plastic aggregates. Rougher surface texture are likely to generate stronger bond between the paste and aggregate creating higher strength.
7) Further research into studies on the durability of the encapsulated plastic concrete such as, abrasion and erosion resistance, efflorescence, acid attack and carbonations are also recommended.

8) Further research studies on the use of fire-retarding agents and fillers in the encapsulated plastic concrete are also recommended.
9) Market studies and economic business cases for widespread use of the encapsulated plastic concrete technology is necessary. This will add confidence to material manufacturer and enticing investment in the technology.
10) In addition, thorough studies of the existing business regulations may be necessary to identify any deterrent or logjams that may reduce the potential uptake of the technology for widespread applications in civil engineering construction works.

# REFERENCES


1) Abd-Elaziz, M.A., Faried A.S. and Kamel M.M.A. (2017): Influence of Silica Fume Incorporation on the Fresh, Thermal and Mechanical Properties of Expanded Polystyrene (EPS) Foamed Concrete. American Journal of Civil Engineering, Volume 5. Issue 3. Paper page 188.
2) ACI 213R-14: Guide for Structural Lightweight-Aggregate Concrete
3) ACI 201: Guide to durable concrete
4) ACI 318: the ACI building code and standard specification for structural concrete
5) Agrawal A., Goyal A., Waghmare K.D., Gupta R. and Goyal. R. (2017) Use of Plastic Waste in Manufacturing of Bricks. International Journal for Scientific Research & Development. Volume 5. Issue 01. Paper page 1216-1218.
6) Agarwal P., Aggarwal Y. and Gupta S.M. (2007): Effect of furnace bottom ash as replacement of fine aggregates in concrete. Asian journal of civil engineering (building and housing). Volume 8. Paper pages 49 - 62
7) Aikawa Y., Miyahara S. and Atarashi D. (2015). Theoretical analysis of the hydration of fly ash cement. Journal of the ceramic society of Japan. Volume 12. PP 1073-1079.
8) Akcaozoglu, S., Akcaozoglu, K. and Atiş, C. (2013). Thermal conductivity, compressive strength and ultrasonic wave velocity of cementitious composite containing waste PET lightweight aggregate (WPLA). Composites Part B: Engineering. Volume 45. Issue 1. Paper page 721-726.
9) Akcaozoglu, S. and Ulu, C., (2014): Recycling of waste PET granules as aggregate in alkaliactivated blast furnace slag/metakaolin blends. Constr. Build. Mater. 58, 31–37
10) Al-Barakah. F.N., Radwan, S.M.A., and Abdel-Aziz R.A. (2013): Using biotechnology in recycling agricultural waste for sustainable agriculture and environmental protection. Int.J.Curr.Microbiol.App.Science. Volume 2. Issue 12. Paper page 446-459

11) Al-Hadithi A.I. (2013). Improving impact and mechanical properties of gap graded concrete by adding waste plastic fibers. International Journal of Civil Engineering and Technology (IJCIET), 2(4), 118-131.
12) Al-Hadithi A.I. and Hilal N.J. (2016): The possibility of enhancing some properties of self-compacting concrete by adding waste plastic fibers. Journal of Building Engineering. Volume 8. Paper page 20-28.
13) Al-Manaseer A.A. and Dalal T.R. (1997). Concrete containing plastic aggregates. Concrete International Volume 19, number 8, pp 47-52.
14) Al-Saleem SM. (2009): Establishing an integrated databank for plastic manufacturers and converters in Kuwait. Waste Manag. Volume 29. Paper page 479–84.
15) Al-Salem S., Lettieri P. and Baeyens J. (2008): Recycling and recovery routes of plastic solid waste (PSW): a review. Waste Manage. Volume 29. Paper page 2625-2643
16) Al-Saleem S.M., Lettieri P. and Baeyens J. (2010): The valorization of plastic solid waste (PSW) by primary to quaternary routes: From re-use to energy and chemicals.
17) Albano C., Camacho N., Hernandez M., Matheus A., and Gutierrez A. (2009): Influence of content and particle size of waste pet bottles on concrete behaviour at different w/c ratios. Waste Manage. Issue 29. Paper page 2707-2716
18) Aldahdooh M.A.A., Jamrah A., Ali Alnuaimi, Martini M.I., Ahmed M.S.R and Ahmed A.S.R. (2017): Influence of various plastics-waste aggregates on properties of normal concrete. Journal of Building Engineering, Volume 17, Paper page 13-22
19) Alexander M. And Mindess S. (2005): Aggregates in concrete. Modern concrete technology. Taylor and Francis. London and New york.
20) Ali N., Din N., Khalid F.S., Shahidan S., Abdullah S.R., Samad A.A. and Mohamad N. (2017): Compressive strength and initial water absorption rate for cement brick containing high-density polyethylene (HDPE) as a substitutional material for sand. IOP Conf. Series: Materials Science and Engineering 271 012083 doi:10.1088/1757-899X/271/1/012083.

21) Alqahtani F., Khan M.I., Ghataora G and Dirar S. (2017): Production of Recycled Plastic Aggregates and its Utilization in Concrete. Journal of Materials in Civil Engineering, vol 29, no. 4,
22) Andrady A.L. and Neal, M.A. (2009). Applications and societal benefits of plastics, Philosophical Transactions. The Royal Society brochure 364, pp 1977-1984
23) Araghi J.H. Nikbin I.M., Reskati S.R., Rahmani E. and Allahyari H. (2015): An experimental investigation on the erosion resistance of concrete containing various PET particles percentages against sulfuric acid attack. Construction and Building Materials. Volume 77. Paper page 461-471
24) Arun W.S. (2004): Chemically bonded phosphate ceramics, twenty first century materials with diverse applications. Elsevier Ltd.
25) Arulrajah A., Yaghoubi E. and Wong Y.C. and Horpibulsuk S. (2017): Recycled plastic granules and demolition wastes as construction materials: Resilient moduli and strength characteristics. Construction and Building Materials. Volume 147, Paper pages 639-647
26) ASTM E1131 - Thermogravimetry thermal analysis (TGA) testing.
27) Atkins M. and Glasser F.P. (1992): Application of Portland cement-based materials to radioactive waste immobilization. Waste Manag. Volume 12.
28) Awang H., Ahmad M.H. and Al-Mulali (2015): Influence of kenaf and polypropylene fibres on the mechancail and durability properties of fibre reinforced lightweight concrete. Journal of Engineering Science and Technology. Vol. 10, No. 4. Paper page 496 - 508
29) Ay Lie, H., Gan B.S., Suryanto B. and Pariastiwi Y. (2017): Influence of the Stiffness Modulus and Volume Fraction of Inclusions on Compressive Strength of Concrete. Procedia Engineering. Volume 171. Paper page 760 -767
30) Ayub T., Shafiq N., Khan S. (2013): Durability of Concrete with Different Mineral Admixtures: A review. international journal of civil, environmental, structural, construction and architectural engineering. Volume 7, issue 8. Paper page 601 – 612
31) Azhdarpour A.M., Nikoudel M.R. and taheri M. (2016): The effect of using polyethylene terephthalate particles on physical and strength-related properties

of concrete; a laboratory evaluation. Construction and Building Materials. Volume 109. Paper pages 55-62.

32) Badache A., Benosman A.S., Senhadji Y. and Mouli M. (2018): Thermo-physical and mechanical characteristics of sand-based lightweight composite mortars with recycled high-density polyethylene (HDPE). Construction and Building Materials Volume 163. Paper pages 40-52

33) Bagherzadeh, R., Sadeghi, A.-H. and Latifi, M. (2011): Utilizing polypropylene fibers to improve physical and mechanical properties of concrete. Text. Res. J. http://dx.doi.org/10.1177/0040517511420767.

34) Bai Y., Ibrahim R, Basheer P.A.M. (2004): Properties of lightweight concrete manufactured with fly ash, bottom ash and lytag. International Workshop on Sustainable Development and Concrete Technology. Paper Page 77 – 88

35) Bai Y. and Basheer P.A.M. (2003): Influence of furnace bottom ash on properties of concrete. Proceedings of the Institution of Civil Engineers - Structures and Buildings. Volume 156 Issue 1. Paper Page 85-92

36) Bai Y. Collier N.C., Milestone N.B. and Yang C.H. (2011): The potential for using slags activated with near neutral salts as immobilisation matrices for nuclear wastes containing reactive metals. Journal of Nuclear Materials. Volume 413. Paper page 183–192.

37) Bailey C., & Khoury, G. A. (2011). Performance of Concrete Structures in Fire. Surrey: MPA – The Concrete Centre.

38) Barbhuiya S. and Kumala D. (2017): Behaviour of a Sustainable Concrete in Acidic Environment. Journal of sustainability Volume 9, 1556. Paper page 2 - 13

39) Baron Colbert W. and You Z.(2012): Properties of modified asphalt binders blended with electronic waste powders. Journal of Materials in Civil Engineering. Volume 24. Issue 10. Paper page 1261–1267.

40) Batayneh M. Marie I. and Asi I. (2007). Use of selected waste materials in concrete mixes. Journal of waste management. Volume 27 (12). PP 1870–1876.

41) Bayasi, Z. and Zeng, J. (1993). Properties of polypropylene fibre reinforced concrete. ACI materials journal. Volume 90 (6). PP 605–610.

42) Bennett D.G., Higgo, J.J.W. and Wickham, S.M. (2001): Review of Waste Immobilisation Matrices. Glason Science Limited Oakham UK.
43) Behfarnia K. and Rostami M. (2017): Mechanical Properties and Durability of Fiber Reinforced Alkali Activated Slag Concrete. Journal of Materials in Civil Engineering. Volume 29 Issue 12
44) Bensted J. (2002) Calcium aluminate cements, Structure and Performance of Cements, 2nd ed., (Edited by. Bensted J and Barnes P). Spon press London.
45) Bhogayata A.C., Arora A.C. and Narenda K. (2017): Fresh and strength properties of concrete reinforced with metalized plastic waste fibers. Construction and Building Materials. Volume 146. Paper pages 455-463.
46) Blott S. J. and Pye K. (2001). Grain size distribution and statistics package for the analysis of unconsolidated sediments. Earth surface processes and landforms. Volume 26. PP 1237–1248
47) Boccaccini A.R., Berthier T. and Seglem S. (2007): Encapsulated gadolinium zirconate pyrochlore particles in soda borosilicate glass as novel radioactive waste form. Ceramics International. Volume 33, Issue 7, Paper page 1231-1235.
48) Bolat H. and Erkus P. ( 2014): Use of polyvinyl chloride (PVC) powder and granules as aggregate replacement in concrete mixtures. Science and Engineering of Composite Materials. Volume 23. Issue 2
49) BS EN 1097-2:2010: Tests for mechanical and physical properties of aggregates. Methods for the determination of resistance to fragmentation.
50) BS EN 1097-3:1998: Tests for mechanical and physical properties of aggregates. Determination of loose bulk density and voids.
51) BS EN 1097-6:2013: Tests for mechanical and physical properties of aggregates. Determination of particle density and water absorption.
52) BS EN 12350-2:2009: Testing fresh concrete. Slump-test.
53) BS EN 12350 – 4: 2009: Testing fresh concrete. Degree of compactability.
54) BS EN 12390-2:2009: Testing hardened concrete. Making and curing specimens for strength tests
55) BS EN 12390-3:2009: Testing hardened concrete. Compressive strength of test specimens.

56) BS EN 12390-6: 2009: Testing hardened concrete. Tensile splitting strength of test specimens.
57) BS EN 12390-7:2009: Testing hardened concrete Part 7: Density of hardened concrete.
58) BS EN 13055-1:2002: Lightweight aggregates. Lightweight aggregates for concrete, mortar and grout.
59) BS EN 13139:2013: Aggregates for mortar.
60) BS EN 1504-3:2005: Products and systems for the protection and repair of concrete structures. Definitions, requirements, quality control and evaluation of conformity. Structural and non-structural repair.
61) BS EN 15169:2007: Characterization of waste. Determination of loss on ignition in waste, sludge and sediments
62) BS EN 15743:2010+A1:2015: Supersulfated cement. Composition, specifications and conformity criteria
63) BS 1881-122:2011: Testing concrete Part 122: Method for determination of water absorption.
64) BS EN 15304:2010: Determination of the freeze-thaw resistance of autoclaved aerated concrete.
65) BS EN 196-3:2005 + A1:2008: Methods of testing cement. Determination of setting times and soundness.
66) BS EN 196-8:2010: Methods of testing cement. Heat of hydration. Solution method
67) BS EN 197-1:2000: Cement. Composition, specifications and conformity criteria for common cements
68) BS EN 1992-1-1:2004+A1:2014: UK National Annex to Eurocode 2: Design of concrete structures. General rules and rules for buildings
69) EN 196-2:2005: Methods of testing cement — Part 2: Chemical analysis of cement
70) EN 196-7:2007: Methods of testing cement — Part 7: Methods of taking and preparing samples of cement
71) BS EN 206:2013+A1:2016: Concrete. Specification, performance, production and conformity.

72) BS EN 450-1:2012: Fly ash for concrete. Definition, specifications and conformity criteria.
73) BS 812-105-105.1:1989: Testing aggregates. Methods for determination of particle shape. Flakiness index.
74) BS 812-105.2:1990: Testing aggregates. Methods for determination of particle shape. Elongation index of coarse aggregate.
75) BS EN 932-1:1997: Tests for general properties of aggregates. Methods for samplin
76) BS EN 932-2:1999: Tests for general properties of aggregates. Methods for reducing laboratory samples
77) BS EN 932–5:2012: Tests for general properties of aggregates. Common equipment and calibration
78) BS EN 933-1: 2012: Tests for geometrical properties of aggregates. Determination of particle size distribution. Sieving method
79) Bui N., Satomi T. and Takahashi, H. (2018). Recycling woven plastic sack waste and PET bottle waste as fiber in recycled aggregate concrete: An experimental study. Waste Management. Volume 78. Paper page 79-93.
80) Bulut, H. and Şahin, R. (2017): A study on mechanical properties of polymer concrete containing electronic plastic waste. Composite Structures. Volume 178. Paper page.50-62.
81) Bye G.C. (1999): Portland cement: composition, production and properties (2nd edition) Thomas Telford Limited London.
82) CEA - French atomic energy commission (2009): Bulletine on nuclear waste conditioning (Paris, France)
83) Chaudhary, M., Srivastava, V., Agarwal, V. (2014); Effect of waste low-density polyethylene on mechanical properties of concrete. J. Acad. Ind. Res. (JAIR). Volume 3, 123.
84) Chen T., Zhang Z. and Yanjun Liu (2017): Durability of High-strength Concrete Made with High Belite Cement. 2nd International Conference on Architectural Engineering and New Materials (ICAENM).

85) Cheng F P, Kodur V K R and Wang T C., 2004. Stress-Strain Curves for High Strength Concrete at Elevated Temperatures. Journal of Materials in Civil Engineering 16(1) 84-90.

86) Choi Y. and Yuan R.L. (2005): Experimental relationship between splitting tensile strength and compressive strength of GFRC and PFRC. Cement and Concrete Research. Volume 35. Issue 8. Paper pages 1587-1591.

87) Choi Y., Moon, D., Kim, Y. and Lachemi, M. (2009). Characteristics of mortar and concrete containing fine aggregate manufactured from recycled waste polyethylene terephthalate bottles. Construction and Building Materials. Volume 23. Issue 8. Paper page 2829-2835.

88) Colangelo F., Cloffi R., Liguori B. and Lucolano F. (2016): Recycled polyolefins waste as aggregates for lightweight concrete. Composites Part B: Engineering. Volume 106. Paper page 234-241.

89) Collier N.C. and Milestone N.B. Encapsulation of $Mg(OH)_2$ sludge in composite cement. Cement and concrete research. Volume 40. Paper page 452-459

90) Collier N.C., Milestone N.B., Gordon L.E. and Ko C. (2014): The suitability of a supersulfated cement for nuclear waste immobilisation. Journal of Nuclear Materials. Volume 452, Issues 1–3, September 2014, Pages 457-464.

91) Colombo P., Brusatin G., Bernardo G. and Scarinci G. (2003): Inertization and reuse of waste materials by vitrification and fabrication of glass-based products. Current Opinion in Solid State and Materials Science. Volume 7, Issue 3. Paper pages 225-23.

92) Coppola B., Courard L., Michel F. Incarnato L. and Di Malo L. (2016): Investigation on the use of foamed plastic waste as natural aggregates replacement in lightweight mortar. Composites Part B: Engineering. Volume 99. Paper page 75-83

93) Corinaldesi, V., Mazzoli, A. and Moriconi, G. (2011). Mechanical Behaviour and Thermal Conductivity of Mortars with Waste Plastic Particles. Key Engineering Materials. Volume 466. Paper page 115-120.

94) Corinaldesi, V., Donnini, J. and Nardinocchi, A. (2015). Lightweight plasters containing plastic waste for sustainable and energy-efficient building. Construction and Building Materials. Volume 94. Paper page 337-345.

95) Cornelis G., Johnson C.A., Van Gerven, T. and Vandecasteele, C. (2008): Leaching mechanisms of oxyanionic metalloid and metal species in alkaline solid wastes: A review. Applied geochemistry. Volume 23. Issue 5. Paper page 955-976.

96) Correia A.U., Lima J.S., De-Brito J. (2014): Post fire mechanical performance of concrete made with selected plastic waste aggregates. Cement and concrete composites. Volume 53. Paper page 187-199.

97) Dalhat, M. and Al-Abdul Wahhab. H., (2017): Properties of Recycled Polystyrene and Polypropylene Bounded Concretes Compared to Conventional Concretes. Journal of Materials in Civil Engineering. Volume 29. Issue 9. P04017120.

98) Daud, M., Selamat, M. and Rivai, A. (2013). Effect pf Thermoplastic Polymer Waste (PET) in Lightweight Concrete. Advanced Materials Research, 795, pp.324-328.

99) De Oliveira, L.A.P.; and Castro-Gomes, J.P. (2011): Physical and mechanical behavior of recycled PET fiber reinforced mortar. Construction and Building Materials. Volume 25. Issue 4. Paper page 1712-1717.

100) Department for Environment, Food & Rural Affairs, DEFRA. (2015): Carrier bag charges: retailers' responsibilities. Charges for single-use plastic carrier bags and Waste and recycling. available online at https://www.gov.uk/guidance/carrier-bag-charges-retailers-responsibilities accessed 21/07/16.

101) Department of trade and industry, DTI (1999): Project Summary of the effect of coal type and burner aerodynamics on NOx emission and carbon burnout in PF flames. DTI/Pub URN 00/513, London, UK, Department of Trade and Industry, Paper page 2.

102) Donald I.W. (2010): Waste immobilization in glass and ceramic based hosts: Radioactive, toxic and hazardous waste. Wiley & sons, UK

103) Divsholi B.S., Darren Lim T.Y. and Teng S. (2014): durability properties and microstructure of ground granulated blast furnace slag cement concrete.

104) Dwaikat M. B. and Kodur V. K. R. (2010): "Fire induced spalling in high strength concrete beams," Fire Technology, vol. 46, no. 1, pp. 251–274, 2010

105) Ede N.A., Aleguino, V., Awoyera P.O. (2014): Use of Advanced Plastic Materials in Nigeria: Performance Assessment of Expanded Polystyrene Building Technology System. American Journal of Engineering Research (AJER). Volume -03, Issue 04. Paper Page 301-308.

106) Elbusaefi A. (2012): Corrosion of reinforcement steel embedded in concrete manufactured with various cement replacement materials and their gas permeability. Proceeding of the 9th international PhD symposium in Civil engineering. Karlsruhe institute of technology (KIT). Germany.

107) EU infographic with facts and figures on plastic waste (2015) available online http://ec.europa.eu/environment/waste/plastic_waste.htm ( assessed 10/10/17)

108) Ferreira J.A., Bila D.M., Ritter E., Braga A.C. (2012a) Chemical healthcare waste management in small Brazilian municipalities. Waste Management and Research. Volume 30. Issue 12. Paper page 1306-1311.

109) Ferreira L., de Brito J. and Saikia N. (2012b): Influence of curing conditions on the mechanical performance of concrete containing recycled plastic aggregate. Constr. Build. Mater. Volume 36. Paper page 196–204

110) Fraj B. A., Kismi M. and Mounanga P. (2010): Valorization of coarse rigid polyurethane foam waste in lightweight aggregate concrete. Construction and Building Materials. Volume 24. Issue 6. Paper page 1069-1077

111) Fraternali, F.; Ciancia, V.; Chechile, R.; Rizzano, G.; Feo, L.; and Incarnato, L. (2011): Experimental study of the thermo-mechanical properties of recycled PET fiber-reinforced concrete. Composite Structures. Volume 93, Issue 9. Paper page 2368-2374

112) Frigione, M., (2010); Recycling of PET bottles as fine aggregate in concrete. Waste Manage. Volume 30. Paper page 1101–1106

113) Galvao J.C.A., Portella K.F., Joukoski A., Mendes R. and Ferreira E.S. (2011): Use of waste polymers in concrete for repair of dam hydraulic surfaces. Constr. Build. Mater. Volume 25. Paper page 1049-1055.

114) Gawandea A., Zamarea G., Renge V.C., Taydea S. and Bharsakale G. (2012): An overview on waste plastic utilisation in asphalting of roads. Journal of engineering research and studies. Volume III, issue II. Paper page 01-05.

115) Gavela, S., Ntziouni, A., Rakanta, E., Kouloumbi, N. and Kasselouri-Rigopoulou, V. (2013). Corrosion behaviour of steel rebars in reinforced concrete containing thermoplastic wastes as aggregates. Construction and Building Materials. Volume 41. Paper page 419-426.

116) Ghernouti Y., Rabehi B., Safi B. and Chaid R. (2010): Use of recycled plastic bag waste in concrete. Journal of International Scientific Publications: Materials, Methods and Technologies. Volume 8, ISSN 1314-7269 (Online), Published at: http://www.scientific-publications.net.

117) Glasser F. P. (1997): Fundamental aspects of cement solidification and stabilisation, Journal of hazardous materials, Vol. 52 (2-3). PP 151-170.

118) Glasser F. P. (2004): Coal combustion wastes: characterization, reuse and disposal. Geological Society, London, Special Publications, 236, 211-222.

119) Gu L. and Ozbakkaloglu T. (2016): Use of recycled plastics in concrete: A critical review. Waste Management, Issue 51. Paper page 19–42.

120) Guo Z., Lim C.W., Sun Moon K. and Manos G.C. (2016): Belite Cement Prepared from High Carbon-Content Fly Ash. Materials Science Forum. Volume 866. Paper page 20-24

121) Haghighatnejad N., Mousavi S.Y., Khaleghi J.S., Tabarsa, A., Yousefi S. (2016): Properties of recycled PVC aggregate concrete under different curing conditions. Construction and Building Materials. Volume 126. Paper page 943-95

122) Halden R. U. (2010). Plastics and health risk. Annual review of public health. Volume 31. PP 179 -194.

123) Hannawi K and Prince-Agbodjan W. (2014): Transfer behavior and durability of cementitious mortars containing polycarbonate plastic wastes.

European Journal of Environmental and Civil Engineering. Volume 19. Issue 4. Paper pages 467-481

124) Helene P., Carvalho M. and Pacheco J. (2017): Engineering field tests for alkali-aggregate reaction. Structural Concrete. Volume 18, Issue 2. Paper pages 349–355

125) Herki A., Khatib, J. and Negim, E. (2013). Lightweight concrete made from waste polystyrene and fly ash. World Appl. Sci. J. 21, 1356–1360.

126) Higgins D. (2006). Concrete for a sustainable future (sustainable concrete - how can additions contribute). Technical paper presented at the institute of concrete technology annual technical symposium.

127) Hirai H., Takada H., Ogata Y., Yamashita R., Mizukawa, K., Saha M., Kwan C., Moore C., Gray H., Laursen D., Zettler E.R., Farrington J.W., Reddy C.M., Peacock E.E. and Ward M.W. (2011). Organic micropollutants in marine plastic debris from the open ocean and remote and urban beaches. Marine Pollution Bulletin. Volume 62. PP 1683–1692.

128) Hsie, M., Tu, C. and Song, P. (2008): Mechanical properties of polypropylene hybrid fiber reinforced concrete. Mater. Sci. Eng.: Volume A. 494. Paper page 153–157.

129) Ibrahim, H. (2017). Mechanical Behavior of Recycled Self-Compacting Concrete Reinforced with Polypropylene Fibres. Journal of Architectural Engineering Technology. Volume 06(02).

130) International Atomic Energy Agency, IAEA (1993a): Improved cement solidification of low and intermediate level radioactive wastes. IAEA Technical Report Series No. 350.

131) International Atomic Energy Agency, IAEA (1993b): Bituminization processes to condition radioactive wastes. IAEA Technical Report Series No. 352.

132) International Atomic Energy Agency, IAEA (2003). Radioactive waste management glossary. Available online at http://www-pub.iaea.org/mtcd/publications/pdf/pub1155_web.pdf (assessed 07/01/16)

133) Irwan J.K., Awang M., Annas M.M.K., Boon K.H., Othman N., Kadir A.A., Roslan M.A. and Khalid, F.S. (2013): Relationship between compressive,

splitting tensile and flexural strength of concrete containing granulated waste Polyethylene Terephthalate (PET) bottles as fine aggregate. Adv. Mater. Res. Volume 795. Paper page 356–359.

134) Islam M.D., Rakinul Islam A. K. M., Meherier S. (2015): An Investigation on Fresh and Hardened Properties of Concrete while Using Polyethylene Terephthalate (PET) as Aggregate. World Academy of Science, Engineering and Technology. International Journal of Civil and Environmental Engineering. Volume 9. No:5. Paper page 558 – 561

135) Ismail Z.Z. and Al-Hashmi E.A. (2008): Use of waste plastic in concrete mixture as aggregate replacement. Journal of waste management, Issue 28. Paper page 2041 -2047

136) Jiang C., Li R., Mo J. and Zhong D. (2011): Effect of fiber surface treatment on interfacial mechano-electric properties of carbon fiber reinforced concrete Adv. Mater. Res. Volume 211–212. Paper page 1087-1090.

137) Jamshidi A., Kurumisawa K., Nawa T. and Hamzah M.O. (2014): Analysis of structural performance of airport concrete pavement incorporating blast furnace slag. Journal of cleaner production. Volume 90. PP 1 -16.

138) Jordan C. (2009). Midway message from the Gyre. The New York review. Available online at www.nybooks.com/daily/2009/11/11/chris-jordan: (assessed 07/01/16).

139) Johnson, O.A., Madzlan, N. Kamaruddin, I. (2015). Encapsulation of petroleum sludge in building blocks, Construction and Building Materials, Volume 78, 1 March 2015. PP 281–288.

140) Juki, M.I., Awang, M., Annas, M.M.K., Boon, K.H., Othman, N., Kadir, A.A., Roslan, M.A. and Khalid, F.S. (2013): Relationship between compressive, splitting tensile and flexural strength of concrete containing granulated waste Polyethylene Terephthalate (PET) bottles as fine aggregate. Adv. Mater. Res. Volume 795. Paper page 356–359.

141) Kakooei S., Akil, H.M., Jamshidi, M., Rouhi, J., 2012. The effects of polypropylene fibers on the properties of reinforced concrete structures. Constr. Build. Mater. Volume 27. Paper page 73–77.

142) Kamaruddin M.A., Abdullah M.M.A., Zawawi M. H., and Zainol M.R.R.A. (2017): Potential use of plastic waste as construction materials: recent progress and future prospect. IOP Conf. Ser.: Mater. Sci. Eng. Volume 267.

143) Katayama T. (2010): The so-called alkali-carbonate reaction (ACR) — Its mineralogical and geochemical details, with special reference to ASR. Cement and Concrete Research. Volume 40, issue 4. Paper pages 643-675

144) Kan A. and Demirboga R. (2009). A novel material for lightweight concrete production Journal of cement and concrete composites. Volume 31. PP 489–495.

145) Karahan, O. and Atis, C.D., 2011. The durability properties of polypropylene fiber reinforced fly ash concrete. Mater. Des. Vol 32. Paper page 1044–1049.

146) Kartalis C.N., Papaspyrides C.D., Pfaendner R., Hoffmann, K. and Herbst. H. (2000): Mechanical recycling of post-used HDPE crates using the restabilization technique. II: influence of artificial weathering. J Appl Polymer Science. Volume 77. Paper page 1118–27.

147) Khalid F.S., Azmi N.B., Mazenan P.N., Anak Guntor N.A., (2018): Self-consolidating concretes containing waste PET bottles as sand replacement. Conference: Conference: International conference on engineering and technology (IntCET 2017)

148) Kim S.B., Yi N.H., Kim H.Y., Kim J.H.J and Song. Y.C. (2010). Material and structural performance evaluation of recycled PET fibre reinforced concrete. Journal of cement and concrete composite. Volume 32. PP 232–240.

149) Koch H. M. and Calafat A. (2009) Human body burdens of chemicals used in plastic manufacture. Philosophical transactions of the royal society (B) biological Sciences. Volume 364. PP 2063–2078.

150) Kotatkova J., Zatloukal, J., Reitrman P., Kolar, K. (2017): Concrete and cement composites used for radioactive waste. Journal of Environmental Radioactivity. Volume 178-179. Paper page 147-155.

**151)** Kou S. C. and Poon C. S. (2009). Properties of concrete prepared with crushed fine stone, furnace bottom ash and recycled aggregate as fine aggregates. Construction and Building materials. Volume 23 (8). PP 2877-2886.

**152)** Kou S.C., Lee G., Poon C.S. and Lai W.L. (2009). Properties of lightweight aggregate concrete prepared with PVC granules derived from scraped. Journal of waste management. Volume 29. PP 621–628.

153) Kodur V. (2014): Properties of Concrete at Elevated Temperatures. Hindawi Publishing Corporation. ISRN Civil Engineering. Volume 2014, Article ID 468510, 15 pages available online http://dx.doi.org/10.1155/2014/468510

154) Kodur, V. And Franssen, J. (2010). Structures in fire. Lancaster: Destech Publications.

155) Kodur V. K. R. and Phan L (2007): Critical factors governing the fire performance of high strength concrete systems. Fire Safety Journal, vol. 42, no. 6-7, Paper page 482–488.

156) Kuenzel C., Neville T.P., Omakowskie, T., Vandeperre L., Boccaccini A.R., Bensted J., Simons S.J.R. and Cheeseman C.R. (2014): Encapsulation of aluminium in geopolymers produced from metakaolin. Journal of Nuclear materials. Volume 447, Issue 1-3. Paper page 208 -214.

157) Kumar K.S. and Baskar K. (2015a): Recycling of E-plastic waste as a construction material in developing countries. J Mater Cycles Waste Manag. Volume 17: Issue 4. Paper page 718 – 724

158) Kumar S. K., Gandhimathi, R. and Baskar, K. (2016). Assessment of Heavy Metals in Leachate of Concrete Made With E-Waste Plastic. Advances in Civil Engineering Materials, 5(1), p.20160003.

159) Kumar K.S. and Baskar K. (2015b): Development of Ecofriendly Concrete Incorporating Recycled High-Impact Polystyrene from Hazardous Electronic Waste. Journal of Hazardous, Toxic, and Radioactive Waste. Vol 19. Issue 3

160) Kumar K.S. and Baskar K. (2015c): Briefing: Shear strength of concrete with E-waste plastic. Proceedings of the Institution of Civil Engineers - Construction Materials. Volume 168. Issue 2. Paper page 53-56.

161) Kumar S.K., Premalatha P., Baskar, K., Sankaran Pillai, G., and Shahul Hameed, P. (2018): Assessment of Radioactivity in Concrete Made with e-

Waste Plastic. Journal of Testing and Evaluation, Vol. 46, No. 2. Paper page 574-579

162) Kumari V.K. and Kanmani S. (2011). A study of polypropylene encapsulation and solidification of textile sludge. J Environ Sci Eng. 53(4): PP 403-408.

163) Kupwade-Patil K., Erez N. Allouche, M. D., Rashedul I and Gunasekaran A. (2014) Encapsulation of Solid Waste Incinerator Ash in Geopolymer Concretes and Its Applications. Materials Journal. Volume 111, Issue 6. Paper page 691 – 700.

164) Lakshmi R. and Nagan S. (2011); Utilization of waste E-plastic particles in cementitious mixtures. Journal of Structural Engineering (Madras) (SERC Chennai). Volume 38. Issue 1. Paper page 26–35

165) Lamond J.F. and Pielert J.H. (2006). Significance of tests and properties of concrete and concrete-making materials symposium papers, issue 169, part 4. ASTM International.

166) Lasco D.J.D., Madlangbayan M.S., Sundo M.B. (2017): Compressive Strength and Bulk Density of Concrete Hollow Blocks (CHB) with Polypropylene (PP) Pellets as Partial Replacement for Sand. Civil engineering journal. Vol. 3. Paper pages 821 – 830

167) Latroch N., Benosman A.S., Bouhamou N., Senhadji Y. and Mouli M. (2018): Physico-mechanical and thermal properties of composite mortars containing lightweight aggregates of expanded polyvinyl chloride. Construction and Building Materials Volume 175. Paper page 77-87

168) Lavanya G. and Jegan J. (2015): Evaluation of relationship between split tensile strength and compressive strength for geopolymer concrete of varying grades and molarity. International Journal of Applied Engineering Research. Volume 10, Number 15. Paper page 23-27.

169) Lima, P.R.L., Leite, M.B. and Santiago, E.Q.R., (2010): Recycled lightweight concrete made from footwear industry waste and CDW. Waste Manage. Volume 30. Paper page 1107–1113.

170) Liu Y. W., Tsong Y., Hsu, Tsao-Hua (2006): Abrasion erosion of concrete by water-borne sand. Cement and Concrete Research. Volume 36, issue 10. Paper pages 1814-1820.

171) Lo Monte, F., Bamonte, P. and Gambarova, P. (2014). Physical and mechanical properties of heat-damaged structural concrete containing expanded polystyrene syntherized particles. Fire and Materials, 39(1), pp.58-71.

172) Lucolano, F., Liguori, B., Caputo, D., Colangelo, F. and Cioffi, R. (2013): Recycled plastic aggregate in mortars composition: Effect on physical and mechanical properties. Materials & Design (1980-2015), 52, pp.916-922.

173) Madandoust R., Ranjbar M.M. and Mousavi S.Y. (2011): An investigation on the fresh properties of self-compacted lightweight concrete containing expanded polystyrene. Construction and Building Materials. Volume 25. Issue 9. Paper page 3721-373

174) Malkapur S.M., Divakar L., Mattur C., Narasimhan B., Narayana B., Karkera B., Goverdhan P., Sathian V., Prasad N.K., (2017): Fresh and hardened properties of polymer incorporated self-compacting concrete mixes for neutron radiation shielding. Construction and Building Materials, Volume 157, Paper page 917-929.

175) Manjunath A. B. T. (2016): Partial replacement of E-plastic Waste as Coarse-aggregate in Concrete. Procedia Environmental Sciences. Issue 35. Paper page 731 – 739.

176) Masaki K and Maki I., 2002. Effect of prolonged heating at elevated temperatures on the phase composition and textures of portland cement clinker. Cement Concrete Res., 32 (2002), pp. 931–934

177) Mastali, M., Dalvand, A. and Sattarifard, A. (2016). The impact resistance and mechanical properties of reinforced self-compacting concrete with recycled glass fibre reinforced polymers. Journal of Cleaner Production, Volume 124. Paper page 312-324.

178) Mazaheripour H., Ghanbarpour, S., Mirmoradi, S. and Hosseinpour, I., (2011): The effect of polypropylene fibers on the properties of fresh and hardened lightweight self-compacting concrete. Constr. Build. Mater. Volume 25. Paper page 351–358.

179) Mello, E.; Ribellato, C.; and Mohamedelhassan, E. (2014): Improving concrete properties with fibers addition. World academy of science, engineering and technology. International Journal of Civil, Environmental, Structural, Construction and Architectural Engineering. Volume 8. Issue 3. Paper page 249-254.

180) Mee A., Rideout B.A., Hamber J.A., Todd J.N., Austin G., Clark M. and Wallace M.P. (2007) Junk ingestion and nestling mortality in a reintroduced population of California condors gymnogyps californianus. Bird conservation Int. Volume 17. Paper page 119-130.

181) Meegoda J.N., Ezeldin A.S., Hsai-Yang Fang and Inyang H.I. (2003). Waste immobilization technologies: Practice periodical of hazardous, toxic, and radioactive waste management. Volume 7 (1). PP 46-58.

182) Mermerdas K., Nassani D.E. and Sakin M. (2017): Fresh, Mechanical and Absorption Characteristics of Self-Consolidating Concretes Including Low Volume Waste PET Granules. Civil Engineering Journal. Volume 3, No 10. Paper pages 809-820

183) Metha J.K. and Monteiro P.J.M. (2006): Concrete microstructures properties and materials 3rd edition. McGraw –Hill.

184) McCarthy M. J., Dhir R.K, Halliday J.E and Wibowo A (2006): Role of PFA quality and conditioning in minimising alkali–silica reaction in concrete. Magazine of Concrete Research. Volume 58, issue 1. Paper page 49-61.

185) Milestone, N. B., (2006), Reactions in cement encapsulated nuclear wastes: need for toolbox of different cement types, Advances in Applied Ceramics, Vol. 105 (1). PP. 13-20.

186) Mindess S., Young, J.F., Darwin, D. (2003): Concrete, 2nd Edition. Pearson

187) Miranda V. J., Narváez Hernández, L., Tapia López, J., Martínez Flores, E. and Hernández, L. (2014). Polymer mortars prepared using a polymeric resin and particles obtained from waste pet bottle. Construction and Building Materials, 65, pp.376-383.

188) Monteiro P. J. M. (2006): Scaling and saturation laws for the expansion of concrete exposed to sulphate attack. Proceedings of the National Academy

of Sciences of the United States of America. Volume 103, issue 31. Paper page 1467-11472

189) Mukesh K., Singh K.S and Singh N. P. (2012): Heat evolution during the hydration of Portland cement in the presence of fly ash, calcium hydroxide and super plasticizer. Thermochimica Acta. Volume 548. Paper page 27– 32.

190) Naik T.R., Kraus R.N., Ramme B.W., Chun Y.M., and Kumar R. (2006). High-carbon fly ash in manufacturing of conductive controlled low strength materials (CLSM) and concrete. Journal of materials in civil engineering. Volume 18 Issue 6. Paper page 743–746.

191) Naka K. (2015): Inorganic polymers: Overview. Encyclopedia of Polymeric Nanomaterials. Paper page 1-6

192) Navrro-Blasco I., Sirera r., Perez-Nicholas M., Duran A., Fernandez J.M. and Alvarez J.J. (2015): Calcium aluminate cement as an effective matrix for the encapsulation of hazardous materials. 14th international conference on chemistry of cement.

193) Nibudey, R.N., Nagarnaik, P.B., Parbat, D.K. and Pande, A.M. (2013): Strength and fracture properties of post consumed waste plastic fiber reinforced concrete. International Journal of Civil, Structural, Environmental and Infrastructure Engineering Research and Development. Volume 3. Issue 2. Paper page 9-16.

194) Nielsen, P., Nicolai S., Darimont A. and Kestemont X. (2014): Influence of cement and aggregate type on thaumasite formation in concrete. Cement and Concrete Composites. Volume 53. Paper pages 115-126

195) Nili M. and Afroughsabet, V. (2010): The effects of silica fume and polypropylene fibers on the impact resistance and mechanical properties of concrete. Constr. Build. Mater. Volume 24. Paper page 927–933.

196) Neville A. M. (2012). Properties of concrete. Pearson Prentice Hall. London.

197) Newman, j., & Choo, b. S. (2003). Advanced concrete technology. United Kingdom-Amsterdam: A Butterworth-Heinemann.

198) North E.M. and Halden R.U. (2013). Plastics and environmental health - the road ahead, Reviews on Environmental Health. Volume 28. PP 1-8

199) Novak J. and Kohoutkova A. (2018): Mechanical properties of concrete composites subject to elevated temperature. Fire Safety Journal. Volume 95. Paper page 66-76

200) Nursyamsi Z., Berkat W.S., Tim B.E., Ueda T.C. and Mueller H.S. (2017): The influence of PET plastic waste gradation as coarse aggregate towards compressive strength of light concrete. Procedia Engineering. Volume 171. Paper page 614-619

201) Ochs M., Mallants D. and Wang L. Radionuclide and Metal Sorption on Cement and Concrete. Springer Verlag. DE.

202) Ojovan M.I., (2011): Handbook of advanced radioactive waste conditioning technologies

203) Ojovan M.I. and Batyukhnova O.G (2007): Glasses for nuclear waste immobilisation. Presentation at the waste management conference. tuscon, AZ

204) Okamura, H.M. and Ouchi, M. (2003): Self-compacting concrete. J. Adv. Concr. Technol. Volume 1. Issue 1. Paper page 5-15.

205) Oti J.E., Kinuthia J.M., Robinson, R. and Davies, P. (2015): Heating and Cooling Scenario of Blended Concrete Subjected to 780 Degrees Celsius. World Academy of Science, Engineering and Technology International Journal of Civil, Structural, Construction and Architectural Engineering Vol:9, No:4, 2015

206) Oti J., Kinuthia J., Bai J. (2010): Freeze and thaw of stabilised clay bricks. Jonathan E. Oti. Proceedings of the Institution of Civil Engineers Waste and Resource Management Volume 163. Issue 3. Paper pages 129 – 135. Available from: https://www.researchgate.net/publication/279917752_Freeze-thaw_of_stabilised_clay_brick [accessed Sep 26, 2017].

207) Pacheco-Torgal, F., Ding, Y. and Jalali, S., (2012). Properties and durability of concrete containing polymeric wastes (tyre rubber and polyethylene terephthalate bottles): an overview. Constr. Build. Mater. Volume 30. Paper page 714–724.

208) Paliwal A.U., Marua G. and Savita T.I. (2017): Effect of fly ash and plastic waste on the mechanical and durability properties of concrete. Advances in concrete construction. Volume 5. Issue 6. Paper page 575-586

209) Pandya J.M. and Purohit. B.M. (2014): Experimental study on the mechanical properties of concrete incorporating PET fibers. IJSRD - Int. J. Sci. Res. Dev. Volume 2. Issue 9. Paper page 20-27.

210) Paprec (2017). Sorting plastic waste. Available online at https://www.paprec.com/en/understanding-recycling/recycling-plastic/sorting-plastic-waste . Viewed 12/07/2017.

211) Park J.M., Kim K.G., Jang J.H., Wang Z., Hwang B.S. and DeVries K.L. (2008): Interfacial evaluation and durability of modified Jute fibers/polypropylene (PP) composites using micromechanical test and acoustic emission. Compos. Part B, 39 Paper page 1042-1061.

212) Pastor J.M., Garcia D.I., Quintana S. and Pefia J. (2014): Glass reinforced concrete panels containing recycled tyres: Evaluation of the acoustic properties of for their use as sound barriers. Construction and Building Materials. Volume 54. Paper page 541-549.

213) Patel H., and Pandey S., (2012). Evaluation of physical stability and leachability of Portland pozzolana cement solidified chemical sludge generated from textile wastewater treatment plants. Journal Hazardous Materials. 207-208: PP 56-64.

214) Patil S.S., Sajane A.S, Ladage R.B. (2017): Effect of packing density of aggregate on characteristics of self-compacting concrete. International Research Journal of Engineering and Technology (IRJET). Volume 4, Issue 5. Paper page 2113 -2121.

215) Pathak K.A., Pandey V., Murari K. and Singh J.P. (2014): Soil stabilisation using ground granulated blast furnace slag. Int. Journal of Engineering Research and Applications. Volume 4. Issue 5 (Version 2). Paper page 164-171

216) Parfitt J. (200) Analysis of household waste composition and factors driving waste increases, WRAP for strategy unit. London, U.K: Government Cabinet Office;

217) Pelisser, F., Montedo, O.R.K., Gleize, P.J.P. and Roman, H.R. (2012): Mechanical properties of recycled PET fibers in concrete. Mater. Res. Volume 15. Paper page 679–686.

218) Pirzada R.A., Kalra T. and Laherwal F.A. (2018): Experimental Study on Use of Waste Plastic as Coarse Aggregate in Concrete with Admixture Superplasticizer Polycarboxylate Ether. International Research Journal of Engineering and Technology (IRJET). Volume: 05 Issue: 03. Paper page 558-563

219) http://www.pozament.co.uk/products/high-performance-repair-mortar/

220) http://www.pozament.co.uk/wp-content/uploads/2013/02/2232_Web-Version.pdf

221) http://www.pozament.co.uk/wp-content/uploads/2013/02/Ultra-High-Strength-Construction-Grout-Technical-Datasheet-July-16.pdf

222) http://www.pozament.co.uk/wp-content/uploads/2016/05/SDS-06.01-Tunnelling-Grouts-Caulking-V5-August-2016.pdf

223) PlasticEurope (2015). The facts about plastics, analysis of plastics production, demand and waste data. Available online at http://www.plasticseurope.org/documents/document/20150227150049-final_plastics_the_facts_2014_2015_260215.pdf (assessed 15/03/2016).

224) Poshadri A. and Aparna K. (2010): Microencapsulation technology. A review. Journal of research ANGRAU. Volume 38. Paper page 86-102.

225) Prakash K. and Sridharan A. (2009): Beneficial Properties of Coal Ashes and Effective Solid Waste Management. Practice Periodical of Hazardous, Toxic, and Radioactive Waste Management 13(4), p. 239-248.

226) Prahallada M.C. and Prakash K.B. (2013a): Effect of different aspect ratios of waste plastic fibres on the properties of fibre reinforced concrete-an experimental investigation. International Journal of Advanced Research in IT and Engineering. Volume 2. Number 2.

227) Purnomo H., Pamudji G. and Satim M. (2017): Influence of uncoated and coated plastic waste coarse aggregates to concrete compressive strength. MATEC Web of Conferences

228) Radioactive waste management (2015) Geological Disposal Guidance on the production of encapsulated waste-forms –. WPSGD no. WPS/502/01. Available online, https://www.gov.uk/government/uploads/system/uploads/attachment_data/file/

492588/WPS_502_01_-_Guidance_on_the_production_of_encapsulated_wasteforms.pdf. accessed Sep: 2017)

229) Radioactive waste management appendix (2015), Geological Disposal Guidance on the production of encapsulated waste forms. WPSGD no. WPS/502/01. Available online at: file:///E:/WPS_502_01_-_Guidance_on_the_production_of_encapsulated_wasteforms.pdf (accessed Sep 2017).

230) Rai B., Rushad S.T., Kr, B. and Duggal S., (2012): Study of Waste Plastic Mix Concrete with Plasticizer. International Scholarly Research Notices.

231) Raja A.H. and Ramakrishnan A. (2017): Experimental Investigation on Steel Fibre Reinforced Concrete Made Pet Waste Pet Waste with Partial Replacement of Coarse Aggregate. International Journal of Engineering Research and, Volume 6. Issue 06.

232) Raji J.R. and Kanmani, S. (2008): A study of polyethylene micro-encapsulation of textile sludge. Journal for scientific and industrial research. Volume 67. Paper page 319-323.

233) Rahmani, E.; Dehestani, M.; Beygi, M.H.A.; Allahyari, H.; and Nikbin, I.M. (2013): On the mechanical properties of concrete containing waste PET particles. Construction and Building Materials, 47, 1302-1308.

234) Ramadevi, K.and Manju, R. (2012). Experimental investigation on the properties of concrete with plastic PET (bottle) fibres as fine aggregates. Int. J. Emerg. Technol. Adv. Eng. Volume 2. Paper page 42–46.

235) Rao S.M., Mamatha P., Shanta R.P. and Venkatarama Reddy B.V. (2007) Encapsulation of fluoride sludge in stabilised mud blocks. Proceedings of the Institution of Civil Engineers Waste and Resource Management, Issue WR4: PP 167–174.

236) Randall, P.M., Chattopadhyay S. and Condit W.E. (2002): Technical Report Advances in Encapsulation Technologies for the Management of Mercury-Contaminated Hazardous Wastes, report submitted to U.S. Environmental Protection Agency National Risk Management Research Laboratory.

237) Rathod S.T., Bankar L.R., Hakepatil U.R. and Vhanamane M.M (2017): Utilization of bottle caps in concrete. International Journal of Engineering Research & Science. Volume 3. Issue 6. Paper page 29-32.

238) Rice G., Miles N. and Farris S. (2007): Approaches to control the quality of cementitious PFA grouts for nuclear waste encapsulation. Power technology. Volume 174. Paper page 56-59.

239) Richardson I. and Taylor H.F.W (2017): Cement Chemistry, 3rd edition, published by Thomas Telford services limited, London UK

240) Rooses A. Steins, P., Dannoux-Papin A., Lambertin D., Poulesquen A., Frizon F. (2013): Encapsulation of Mg–Zr alloy in metakaolin-based geopolymer. Applied clay science. Volume 73. Paper page 86-92.

241) Ruiz-Herrero J.L., Nieto D.V., Lopez-Gil A., Arranz A., Fernandez A., Lorenza A., Merino S., De Saja J.A. and Rodriguez-Perez M.A. (2016): Mechanical and thermal performance of concrete and mortar cellular materials containing plastic waste. Construction and Building Materials. Volume 104. Paper page 298-310

242) Rumsys D., Bačinskas D., Spudulis E. and Meškėnas A., (2017): Comparison of material properties of lightweight concrete with recycled polyethylene and expanded clay aggregates. Modern Building Materials, Structures and Techniques, MBMST 2016. Procedia Engineering Volume 172. Paper pages 937 – 944

243) Safi, B., Saidi, M., Aboutaleb, D. and Maallem, M. (2013). The use of plastic waste as fine aggregate in the self-compacting mortars: Effect on physical and mechanical properties. Construction and Building Materials, 43, pp.436-442.

244) Saikia N. and de Brito J. (2012). Use of plastic waste aggregate in concrete: A review. Journal for construction and building materials. Volume 34. PP 85–401.

245) Saikia, N. and de Brito J. (2014): Mechanical properties and abrasion behavior of concrete containing shredded PET bottle waste as a partial substitution of natural aggregate. Construction and building materials. Volume 52. Paper page 236-244.

246) Sanchez L.F.M., Fournier B., Jolin m., Mitchell d. and Bastie J., (2017): Overall assessment of Alkali-Aggregate Reaction (AAR) in concretes presenting different strengths and incorporating a wide range of reactive aggregate types and natures. Cement and Concrete Research. Volume 93. Paper pages 17-31

247) Sayadi A., Tapia J., Neitzert T. and Clifton, G. (2016). Effects of expanded polystyrene (EPS) particles on fire resistance, thermal conductivity and compressive strength of foamed concrete. Construction and Building Materials, 112, pp.716-724.

248) Schaefer, C., Kupwade-Patil, K., Ortega, M., Soriano, C., Büyüköztürk, O., White, A. and Short, M. (2018). Irradiated recycled plastic as a concrete additive for improved chemo-mechanical properties and lower carbon footprint. Waste Management, 71, pp.426-439.

249) Schallhorn K. (2015). You should know - the great pacific garbage patch available online at http://wastelessthinking.com/you-should-know-great-pacific-garbage-patch/ (assessed 30/03/2016)

250) Sharp, J. H. Hill, J. Milestone, N.B. and Miller, E.W. (2003) Cementitious Systems for the encapsulation of intermediate level waste, the 9th International Conference on Radioactive Waste Management and Environmental Remediation, Proceedings of ICEM '03: icem03-4554.

251) Senhadji Y., Escadeillas G., Benosman A.S., Mouli M., Khelafi H. and Kaci O.S (2015): Effect of incorporating PVC waste as aggregate on the physical, mechanical, and chloride-ion-penetration behaviour of concrete. Journal of Adhesion Science and Technology. Volume 29. Paper page 625-640

252) Shaikh, F., Kerai, S. and Kerai, S. (2015). Effect of micro-silica on mechanical and durability properties of high volume fly ash recycled aggregate concretes (HVFA-RAC). Advances in concrete construction, 3(4), pp.317-331.

253) Shamsaei M., Aghayan I., Kazemi K.A.(2017): Experimental investigation of using cross-linked polyethylene waste as aggregate in roller compacted concrete pavement. Journal of Cleaner Production Volume 165, Paper pages 290-29

254) Shanmugapriya, M. and Santhi H.(2017): Strength and Chloride Permeable Properties of Concrete with High Density Polyethylene Wastes. International Journal of Chemical Sciences. Volume 15 Issue 1.

255) Shi C. and Stegemann J.A. Acid corrosion resistance of different cementing materials. Cem. Concr. Res. Volume 30. Paper page 803–808.

256) Singh N., Hui D., Singh R., Ahuja I.P.S., Feo L and Fraternali F. (2017): Recycling of plastic solid waste: A state of art review and future applications. Composites Part B: Engineering. Volume 115. Issue 15. Paper pages 409-422

257) Silva, R., De Brito, J., Saikia, N., 2013. Influence of curing conditions on the durability-related performance of concrete made with selected plastic waste aggregates. Cement Concr. Compos.Volume 35. Paper page 23–31.

258) Skripkiunas G., Nagrokiene D., Girskas G., Vaiciene M. And Baranauskaite E. (2013): The Cement Type Effect on Freeze – Thaw and Deicing Salt Resistance of Concrete. Procedia engineering. Volume 57. Paper page 1045-1051

259) Snelson D.G., Kinuthia, J.M., Davies P.A. and Chang S.-R. (2009): Sustainable construction: Composite use of tyres and ash in concrete. Waste management. Volume 29. Paper page 360 - 367

260) Stukovnik, P., Marinšek M., Mirtič B., Bokan Bosiljkov V. (2015): Influence of alkali carbonate reaction on compressive strength of mortars with air lime binder. Construction and Building Materials. Volume 75. Paper page 247-254

261) Subramanian, M.N. (2013): Plastics Additives and Testing. Copyright © 2013 Scrivener Publishing LLC. Beverly, USA.

262) Sugaya A., Tanaka A. and Akutsu S. (2011): Cement Based Encapsulation Experiments for Low-Radioactive Liquid Waste at Tokai Reprocessing Plant – 11078. WM2011 Conference, February 27-March 3, 2011, Phoenix, AZ

263) Svenson A., Sjöholm S., Allard A.S. and Kaj L. (2009). Antiestrogenicity and estrogenicity in leachates from solid waste deposits. Environmental toxicology. Volume 26. PP 233–239.

264) Swami V., Patil, K., Patil S., Patil sushil and Salokhe K., (2012). The use of waste plastic in construction of bituminous road. International Journal of Engineering Science and Technology (IJEST). Volume 4. PP 2351 – 2355.

265) Swift P.D. (2013). The development of calcium aluminate phosphate cement for radioactive waste encapsulation. Unpublished PhD thesis, University of Sheffield; available online; http://etheses.whiterose.ac.uk/ assessed 20.02.2015.

266) Swift P., Collier N. C., Kinoshita H. and Utton C. (2013). Phosphate modified calcium aluminate cement for radioactive waste encapsulation. Advances in applied ceramics. Volume 112(1). PP 1-8.

267) Thokchom S.I., Ghosh, P. and Ghosh S. (2009). Effect of water absorption, porosity and sorptivity on durability of geopolymer mortars. Journal of engineering and applied sciences. Volume 4 (7). PP 28 – 32.

268) Thorneycroft J., Savoikar P., Orr J. and Ball R (2018): performance of structural concrete with recycled plastic waste as a partial replacement for sand. Construction and building materials. Volume 161.

269) The UK National Planning Policy Framework and relevant planning practice guidance (2016) available online at https://www.gov.uk/government/collections/planning-practice-guidance accessed 21/07/2017.

270) Thomas, M.D.A. and Folliard, K.J. (2007): Concrete aggregates and the durability of concrete. Durability of Concrete and Cement Composites. A volume in Woodhead Publishing Series in Civil and Structural Engineering. Paper page 247–281

271) Thompson, R.C., Swan S.H., Moore, C.H. and Saal F.V. (2009a): Our plastic age. Philosophical Transaction Royal Society B. Volume 364. Paper page 1973-1976

272) Thompson, R.C., Swan S.H., Moore, C.H. and Saal F.V. (2009b) Plastics, the environment and human health: current consensus and future trends. Philosophical Transaction Royal Society B. Volume 364. PP 2153-2166.

273) Toutanji H., Xu., B Gilbert J. and lavin T. (2010): Properties of poly(vinyl alcohol) fiber reinforced high-performance organic aggregate

cementitious material: Converting brittle to plastic. Construction and Building Materials. Volume 24, Issue 1. Paper page 1-10.

274) Tsuchida, D.; Kajihara, Y.; Shimidzu, N.; Hamamura, K.; Nagase, M. Hydrogen (2011). Sulfide production by sulfate-reducing bacteria utilizing additives eluted from plastic resins. Waste Manag. Res., 29, 594–601

275) United Nation Environmental Program, UNEP (2014). Emerging issues update. Plastic debris in the ocean. Available online at http://www.unep.org/yearbook/2014/PDF/chapt8.pdf (assessed 30/03/2016).

276) U.S food and drug administration, USFDA (2011): Bisphenol A (BPA): Use in Food Contact Application

277) Vasudevan R., Sekar R.C., Sundarakannan B. and Velkennedy R. (2011). A technique to dispose waste plastics in an eco-efficient way – application in construction of flexible pavements Construction and Building Materials Journal, vol. 28, Issue 7, 2011, pp. 311-320

278) Verdolotti L., Iucolano F., Capasso L., Lavorgna M., Lannace S. and Liquori B. (2014): Recycling and recovery of PE-PP-PET-based fiber polymeric wastes as aggregate replacement in lightweight mortar: Evaluation of environmental friendly application. Environmental progress and sustainable energy. Volume 33. Issue 4. Paper page 1445-1451

279) Verma S.K., Bhadauria S.S. and Akhtar S. (2013): Evaluating effect of chloride attack and concrete cover on the probability of corrosion. Frontiers of Structural and Civil Engineering. Volume 7, Issue 4. Paper pages 379–390.

280) Wang W.C. (2014): Effects of fly ash and lithium compounds on the water-soluble alkali and lithium content of cement specimens. Construction and Building Materials. Volume 50, Paper pages 727-735

281) Wang Z., Wang L. and Yang Y. (2014): Effect of moisture content on freeze and thaw behaviour of cement paste by electrical resistance measurements. Material Science Volume 49. Paper pages 4305–4314

282) Wang R. and Meyer C. (2012): Performance of cement mortar made with recycled high impact polystyrene. Cement Concr. Compos. Volume 34, Paper page 975–981

283) Waste & Resources Action Programme. WRAP (2006). Environmental benefits of recycling: An international review of life cycle assessment comparisons for key materials in the UK recycling sector.

284) Waste & Resources Action Programme. WRAP (2014). Using recycled polymer in new products: a business opportunity available at http://wrap.org.uk\content\cases-study\-using-recycled-content-plastics-packaging-benefits (assessed 30/03/2016).

285) Webb, H.K., Arnott, J., Crawford R.J. and Ivanova E.P. (2013). Plastic degradation and its environmental implications with special reference to polyethylene terephthalate. Polymer science journal. Volume 5 (1). PP 1-18.

286) Wegian F.M. (2010): Effect of seawater for mixing and curing on structural concrete. The IES Journal Part A: Civil & Structural Engineering. Volume 3: Issue 4: Paper Page 235-243.

287) Wuttig, M. and Raoux, S. (2012): The Science and Technology of Phase Change Materials. Z. anorg. allg. Chem., 638: 2455–2465.

288) Wentworth C.K. (1922): A scale of grade and class terms for clastic sediments. Journal of geology. Volume 30: PP 377–392.

289) Won J. P., Jang C. I., Lee S. W., Lee S. J. and Kim H. Y. (2009): Long-term performance of recycled PET fibre-reinforced cement composites. Construction and Building Materials. Volume 24. Paper page 660-665. http://dx.doi.org/10.1016/j. conbuildmat.2009.11.003

290) Wong L.L., Asrah H., Rahman M.E. and Mannam M.A. (2013): Effects of Aggressive Ammonium Nitrate on Durability Properties of Concrete using Sandstone and Granite Aggregates. World Academy of Science, Engineering and Technology. International Journal of Civil and Environmental Engineering. Vol:7, No:1. Paper pages 49 -53

291) Wu Z (2002): NOx control for pulverised coal fired power stations. CCC/69, London, UK, IEA Clean Coal Centre

292) Xiao C., Laurence, A., Biddle, M.B. (1999). Electrostatic separation and recovery of mixed plastics. In: SPE annual recycling conference (ARC), Dearborn, Michigan (US).

293) Xuan W., Wu Y., Chen Y. (2017) Experimental research on compressive properties of concrete with different plastics content. 3rd International Forum on Energy, Environment Science and Materials.

294) Yang S., Wue X., Liu X. and Tong Y. (2015): Properties of self-compacting lightweight concrete containing recycled plastic particles. Construction and Building Materials. Volume 84. Paper page 444-453.

295) Yarsley V. E. and Couzens, E. G. (1945): Plastics. Penguin books limited, Middlesex, UK.

296) Yasuhara A, Kalami T, Shibamoto T. (2005): Dioxin formation during combustion of nonchloride plastics, polystyrene and its products. Bulletin of environmental contamination and toxicology. Volume 74 (5). PP 899 -903

297) Yesilata, B., Isıker, Y., Turgut, P., 2009. Thermal insulation enhancement in concretes by adding waste PET and rubber pieces. Constr. Build. Mater. Volume 23. Paper page 1878–1882.

298) Yilmaz A.B., Dehri I., Erbil M. (2002): Effects of ammonium chloride salt added to mixing water on concrete and reinforced concrete subject to atmospheric corrosion. Cement and Concrete Research. Volume 32, Issue 1. Paper pages 91-95

299) Yin S., Tuladhar R., Riella J., Chung D., Collister T., Combe M. and Sivakugan N. (2016): Comparative evaluation of virgin and recycled polypropylene fibre reinforced concrete. Construction and Building Materials. Volume 114. Paper page134–14

300) Zaleska M., Pokorny J., Pavlíkova M. and Pavlík Z. (2017): Thermal properties of lightweight concrete with waste polypropylene aggregate. AIP Conference Proceedings 1866

301) Zhang B. and Poon C.S. (2015): Use of Furnace Bottom Ash for producing lightweight aggregate concrete with thermal insulation properties. Journal of cleaner production. Volume 99. Paper page 94-100

302) Zhang S.P. and Zong I. (2014): Evaluation of relationship between water absorption and durability of concrete materials. Advances in Materials Science and Engineering. Volume 2014. Available from:

https://www.hindawi.com/journals/amse/2014/650373/ [accessed Sep 26, 2017].

303) Zhou Q., Milestone N.B. and Hayes M. (2006): An alternative to Portland Cement for waste encapsulation—The calcium sulfoaluminate cement system. Journal of Hazardous Materials. Volume 136. Paper page 120–129

# APPENDIX 1.0

## 1.1 Phase characterisation of the different binding materials

### *1.1.1 Thermogravimetric analysis of CEM IIB-binder*

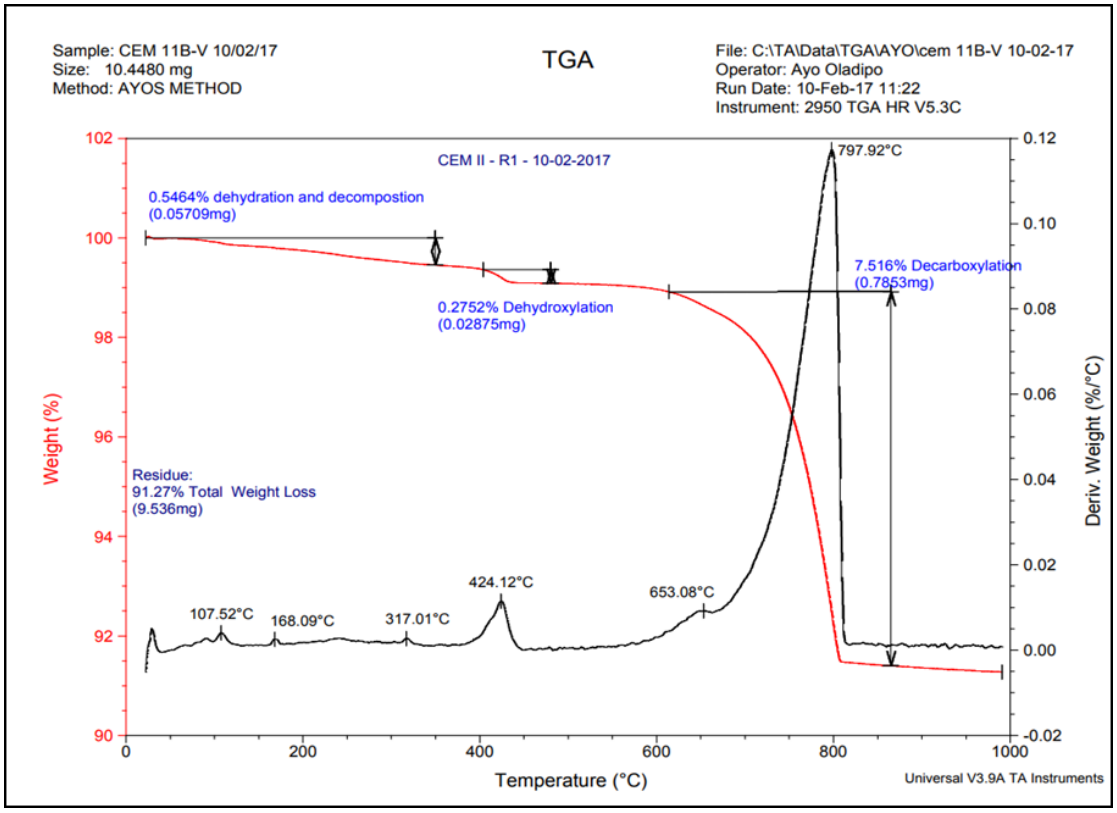


TG/DTG curves of unhydrated Portland cement

### 1.1.2 Thermogravimetric analysis of PG-binder

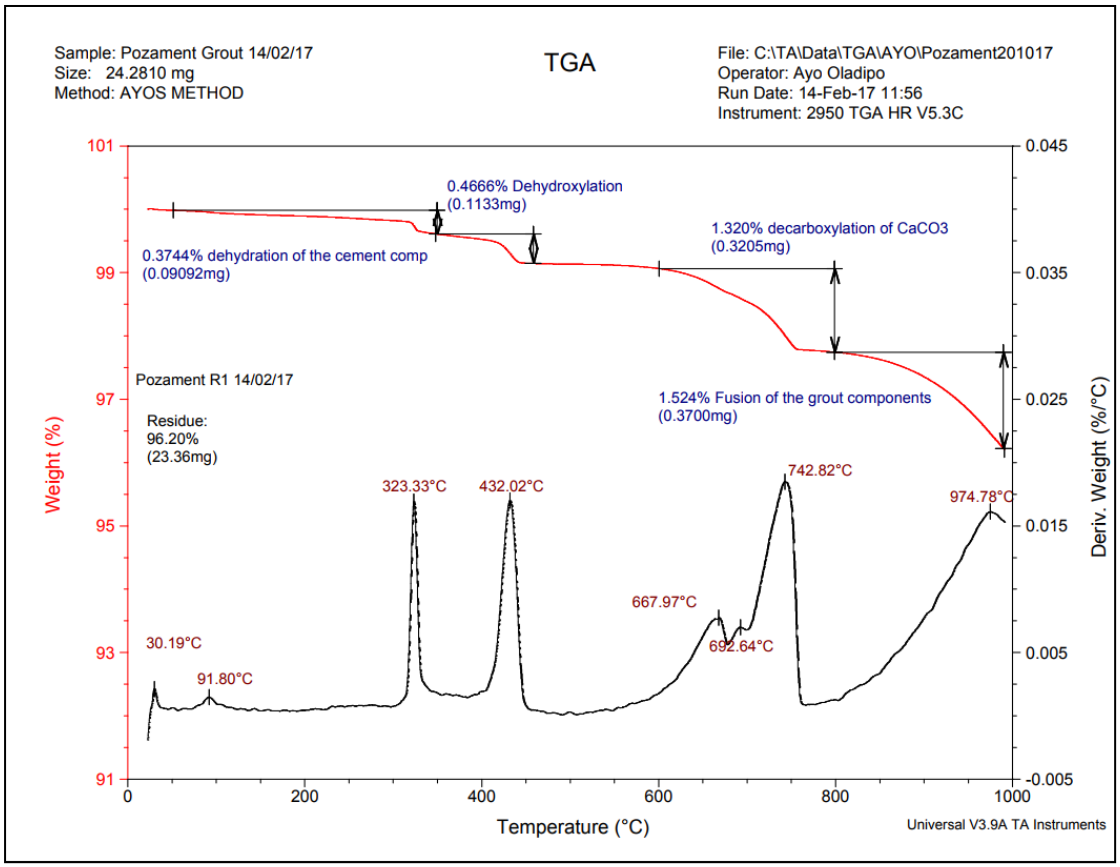


TG/DTG curves of unhydrated Pozament ultra high strength grout

### 1.1.3 Thermogravimetric analysis of CEM IIB – PFA binding system

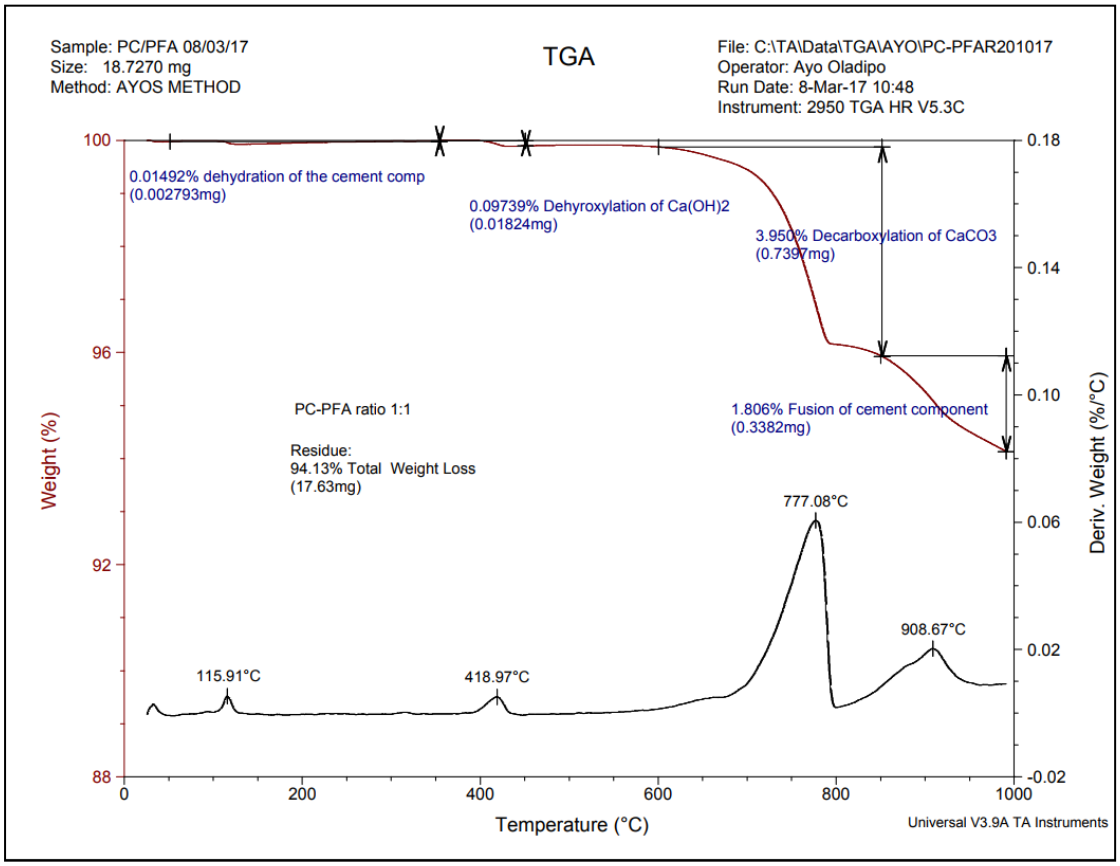


TG/DTG curves of unhydrated Portland cement – pulverised fly ash binding system

**1.2 Particle size distribution curve of the coarse aggregates used in the ongoing work (Sample 2)**

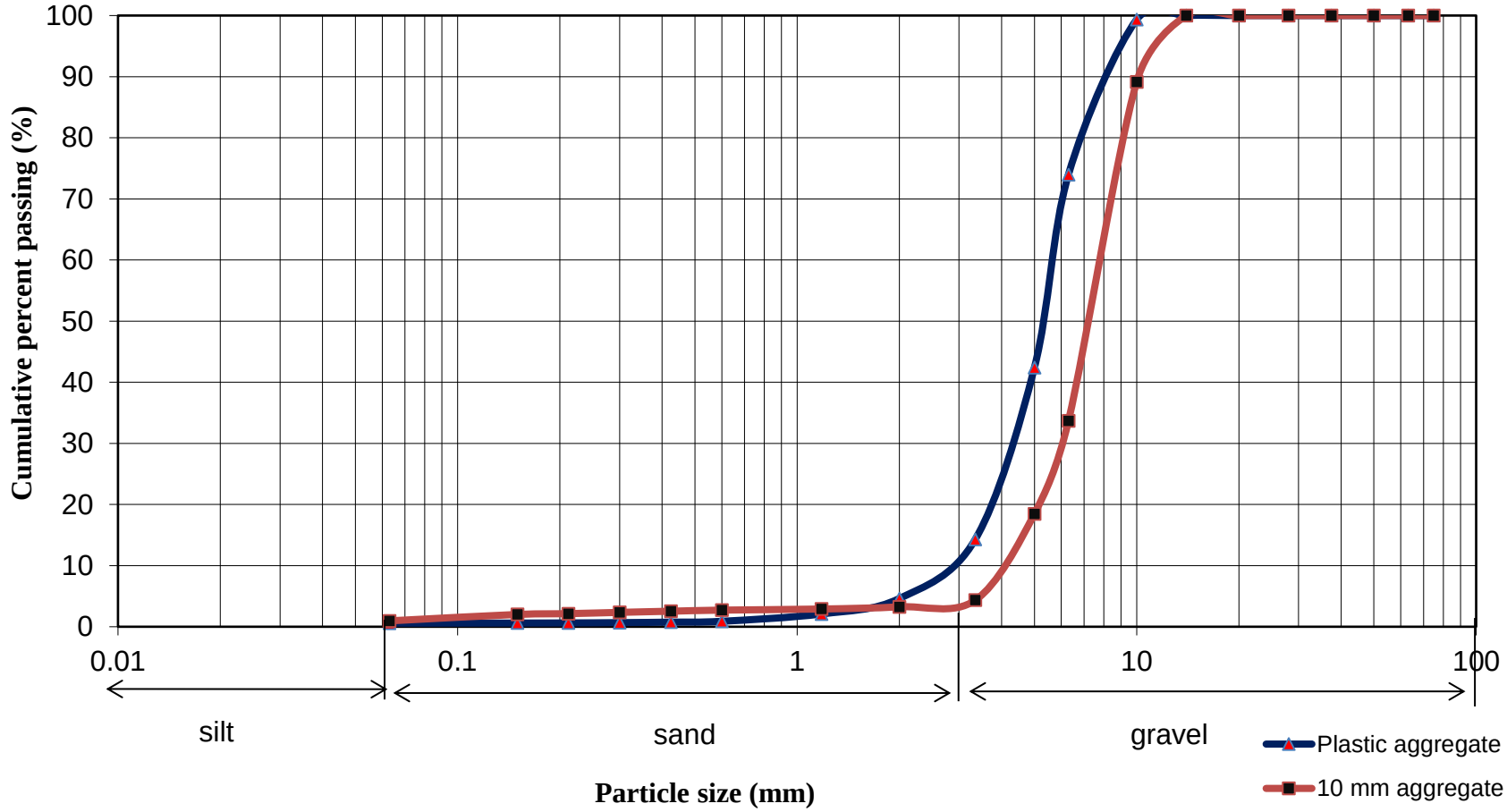


Particle size distribution curve of the coarse aggregates used in the ongoing work (Sample 2)

**1.3 Particle size distribution curve of the coarse aggregates used in the ongoing work (Sample 2)**

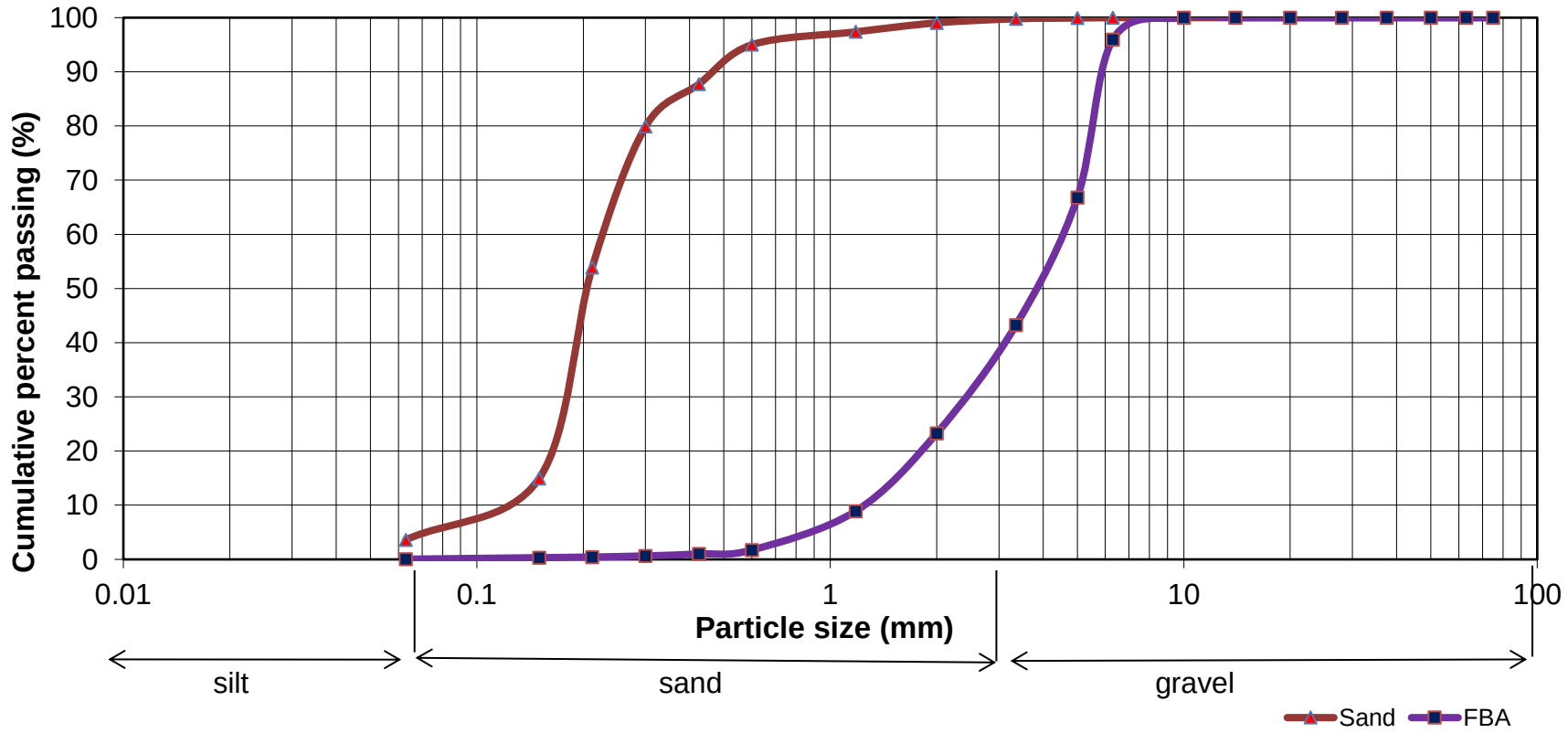


The distribution curve for the fine aggregates used in the ongoing work (Sample 2)

## 1.4 Statistical interpretation of the particle size distribution curves

Statistical distribution of the fine and coarse aggregates used in the ongoing work

| ***Statistical parameters*** | ***Plastic aggregate*** | ***10 mm aggregates*** | ***Furnace bottom ash*** | ***River sand*** |
|---|---|---|---|---|
| **Mode** | 5 mm | 6.3 mm | 5 mm | 212 µm |
| **Median** | 5 mm | 5.6 mm | 3.9 mm | 0.2 mm |
| **Effective size ($D_{10}$)** | 3 mm | 4 mm | 1. 3 | 0.13 |
| **$D_{30}$** | 4.1 | 6 | 2.4 | 0.19 |
| **$D_{60}$** | 5.5 | 7 | 4.5 | 0.23 |
| **Coefficient of uniformity ($C_u$) $D_{60}/D_{10}$** | 1.83 | 1.75 | 3.46 | 1.77 |
| **Coefficient of curvature ($C_c$) $D_{30}/(D_{10}\times D_{60})$** | 1.02 | 1.29 | 0.98 | 1.21 |

- Mode – the most common particle size
- Median ($D_{50}$) - median is the point on the particle size distribution curve where 50% of the particles have lower or higher particle size
- Effective size ($D_{10}$) - is the maximum particle size of the smallest 10% of the aggregates (sieve opening with 10% finer aggregate).
- The coefficients of uniformity and curvature both gives an indication of the grading of the aggregates, when $C_u$ is greater than 4 and $C_c$ is between 1 and 3, the aggregates are well graded, but when the $C_u$ is less than 4, they are considered to be poorly graded or uniformly graded (unified soil classification grading criteria). $Cu = D_{60}/D_{10}$. $C_C = D_{30}/(D_{10}\times D_{60})$.

# APPENDIX 2.0

**Data for:** mass in water, mass in air, density and compressive strength

| Mix ref. | Mix composition | Age in days | Mass in water (grams) | Mass in air (grams) | Density | Load (kN) | Stress ($N/mm^2$) |
|---|---|---|---|---|---|---|---|
| C1 | 1:2:3 | 7 | 1430 | 2446 | 2400 | 285.0 | 28.50 |
| C1 | 1:2:3 | 7 | 1427 | 2442 | 2400 | 253.38 | 25.34 |
| C1 | 1:2:3 | 7 | 1426 | 2456 | 2400 | 239.94 | 24.00 |
| C2 | 1:2:3 | 7 | 1380 | 2440 | 2360 | 292.27 | 29.27 |
| C2 | 1:2:3 | 7 | 1382 | 2445 | 2410 | 284.5 | 28.48 |
| C2 | 1:2:3 | 7 | 1378 | 2440 | 2390 | 236.1 | 23.61 |
| C3 | 1:2:4 | 7 | 1517 | 2556 | 2460 | 244.09 | 24.04 |
| C3 | 1:2:4 | 7 | 1457 | 2476 | 2420 | 220.06 | 22.01 |
| C3 | 1:2:4 | 7 | 1446 | 2456 | 2430 | 231.04 | 23.10 |
| | | | | | | | |
| C1 | 1:2:3 | 28 | 1399 | 2471 | 2380 | 494.05 | 49.4 |
| C1 | 1:2:3 | 28 | 1454 | 2467 | 2470 | 410.02 | 41.00 |
| C1 | 1:2:3 | 28 | 1430 | 2456 | 2460 | 490.00 | 49.00 |
| C2 | 1:2:3 | 28 | 1430 | 2450 | 2400 | 435.47 | 43.55 |
| C2 | 1:2:3 | 28 | 1450 | 2440 | 2410 | 447.11 | 44.71 |
| C2 | 1:2:3 | 28 | 1440 | 2420 | 2430 | 454.07 | 45.41 |
| C3 | 1:2:4 | 28 | 1499 | 2512 | 2380 | 421.35 | 42.14 |
| C3 | 1:2:4 | 28 | 1465 | 2472 | 2390 | 441.32 | 44.13 |
| C3 | 1:2:4 | 28 | 1457 | 2512 | 2390 | 435.97 | 43.6 |
| C1 | 1:2:3 | 90 | 1451 | 2462 | 2430 | 607.807 | 60.8 |
| C1 | 1:2:3 | 90 | 1445 | 2461 | 2420 | 641.83 | 64.18 |
| C1 | 1:2:3 | 90 | 1454 | 2467 | 2430 | 607.62 | 60,8 |
| C2 | 1:2:3 | 90 | 1420 | 2440 | 2380 | 555.8 | 55.6 |
| C2 | 1:2:3 | 90 | 1437 | 2440 | 2380 | 552.04 | 55.2 |

| | | | | | | | |
|---|---|---|---|---|---|---|---|
| C2 | 1:2:3 | 90 | 1444 | 2440 | 2390 | 558.90 | 55.9 |
| C3 | 1:2:4 | 90 | 1466 | 2462 | 2420 | 538.8 | 53.9 |
| C3 | 1:2:4 | 90 | 1445 | 2461 | 2460 | 520.24 | 52.0 |
| C3 | 1:2:4 | 90 | 1465 | 2472 | 2450 | 521.39 | 52.1 |
| Mix ref. | Mix composition | Age in days | Mass in water (grams) | Mass in air (grams) | Density | Load (kN) | Stress ($N/mm^2$) |
| CP1 | 1:2:3 | 7 | 461 | 1375 | 1600 | 39.9 | 4.0 |
| CP1 | 1:2:3 | 7 | 597 | 1426 | 1600 | 54.81 | 5.5 |
| CP1 | 1:2:3 | 7 | 506 | 1458 | 1520 | 54.53 | 5.51 |
| CP2 | 1:2:3 | 7 | 710 | 1890 | 1600 | 48.31 | 4.8 |
| CP2 | 1:2:3 | 7 | 640 | 1880 | 1590 | 51.80 | 5.2 |
| CP2 | 1:2:3 | 7 | 600 | 1770 | 1570 | 48.88 | 4.9 |
| CP3 | 1:2:4 | 7 | 4242 | 1347 | 1560 | 24.99 | 2.5 |
| CP3 | 1:2:4 | 7 | 422 | 1323 | 1500 | 30.61 | 3.1 |
| CP3 | 1:2:4 | 7 | 427 | 1316 | 1480 | 23.93 | 2.4 |
| CP1 | 1:2:3 | 28 | 506 | 1477 | 1600 | 75.23 | 7.52 |
| CP1 | 1:2:3 | 28 | 506 | 1456 | 1600 | 83.90 | 8.39 |
| CP1 | 1:2:3 | 28 | 497 | 1477 | 1600 | 79.65 | 7.97 |
| CP2 | 1:2:3 | 28 | 629 | 1665 | 1580 | 77.21 | 7.7 |
| CP2 | 1:2:3 | 28 | 617 | 1656 | 1570 | 78.40 | 7.8 |
| CP2 | 1:2:3 | 28 | 625 | 1656 | 1600 | 76.12 | 7.6 |
| CP3c | 1:2:4 | 28 | 462 | 1406 | 1540 | 46.32 | 4.6 |
| CP3 | 1:2:4 | 28 | 460 | 1365 | 1500 | 50.0 | 5.0 |
| CP3 | 1:2:4 | 28 | 460 | 1406 | 1525 | 48.32 | 4.8 |
| CP1 | 1:2:3 | 90 | 514 | 1449 | 1590 | 85.23 | 8.5 |
| CP1 | 1:2:3 | 90 | 525 | 1580 | 1580 | 96.01 | 9.6 |
| CP1 | 1:2:3 | 90 | 525 | 1590 | 1600 | 96.24 | 9.6 |
| CP2 | 1:2:3 | 90 | 640 | 1660 | 1590 | 89.32 | 8.9 |
| CP2 | 1:2:3 | 90 | 610 | 1770 | 1590 | 89.76 | 9.0 |
| CP2 | 1:2:3 | 90 | 620 | 1665 | 1590 | 92.01 | 9.2 |
| CP3 | 1:2:4 | 90 | 505 | 1443 | 1540 | 55.55 | 5.6 |
| CP3 | 1:2:4 | 90 | 463 | 1388 | 1500 | 54.55 | 5.5 |

| | | | | | | | |
|---|---|---|---|---|---|---|---|
| CP3 | 1:2:4 | 90 | 462 | 1476 | 1540 | 56.52 | 5.6 |

| Mix ref. | Mix composition | Age in days | Mass in water (grams) | Mass in air (grams) | Density | Load (kN) | Stress ($N/mm^2$) |
|---|---|---|---|---|---|---|---|
| CPP1 | 1:1:4:6 | 7 | 640 | 1660 | 1630 | 79.07 | 7.9 |
| CPP1 | 1:1:4:6 | 7 | 647 | 1647 | 1630 | 79.54 | 8.0 |
| CPP1 | 1:1:4:6 | 7 | 646 | 1669 | 1630 | 82.45 | 8.2 |
| CPP2 | 1:1:4:6 | 7 | 571 | 1672 | 1600 | 71.3 | 7.1 |
| CPP2 | 1:1:4:6 | 7 | 597 | 1582 | 1590 | 68.58 | 6.8 |
| CPP2 | 1:1:4:6 | 7 | 606 | 1598 | 1560 | 73.10 | 7.3 |
| CPP3 | 1:1:4:8 | 7 | 620 | 1624 | 1600 | 67.4 | 6.7 |
| CPP3 | 1:1:4:8 | 7 | 606 | 1647 | 1590 | 67.14 | 6.7 |
| CPP3 | 1:1:4:8 | 7 | 646 | 1630 | 1600 | 67.21 | 6.7 |
| CPP1 | 1:1:4:6 | 28 | 609 | 1614 | 1630 | 123.86 | 12.4 |
| CPP1 | 1:1:4:6 | 28 | 645 | 1671 | 1660 | 114.4 | 11.4 |
| CPP1 | 1:1:4:6 | 28 | 613 | 1626 | 1600 | 121.80 | 12.2 |
| CPP2 | 1:1:4:6 | 28 | 643 | 1663 | 1600 | 117.37 | 11.7 |
| CPP2 | 1:1:4:6 | 28 | 659 | 1686 | 1600 | 119.0 | 11.9 |
| CPP2 | 1:1:4:6 | 28 | 660 | 1690 | 1600 | 117.4 | 11.7 |
| CPP3 | 1:1:4:8 | 28 | 583 | 1592 | 1580 | 113.21 | 11.3 |
| CPP3 | 1:1:4:8 | 28 | 569 | 1586 | 1600 | 116.87 | 11.7 |
| CPP3 | 1:1:4:8 | 28 | 583 | 1586 | 1620 | 118.03 | 11.8 |
| CPP1 | 1:1:4:6 | 90 | 636 | 1636 | 1630 | 153.40 | 15.3 |
| CPP1 | 1:1:4:6 | 90 | 660 | 1626 | 1630 | 166.78 | 16.7 |
| CPP1 | 1:1:4:6 | 90 | 650 | 1643 | 1630 | 133.94 | 13.39 |
| CPP2 | 1:1:4:6 | 90 | 662 | 1706 | 1600 | 148.34 | 14.83 |
| CPP2 | 1:1:4:6 | 90 | 658 | 1690 | 1590 | 144.04 | 14.4 |
| CPP2 | 1:1:4:6 | 90 | 670 | 1680 | 1600 | 140.13 | 14.0 |
| CPP3 | 1:1:4:8 | 90 | 556 | 1578 | 1590 | 138.09 | 13.8 |
| CPP3 | 1:1:4:8 | 90 | 561 | 1578 | 1600 | 139.01 | 13.9 |
| CPP3 | 1:1:4:8 | 90 | 561 | 1592 | 1600 | 137.12 | 13.7 |

| Mix ref. | Mix composition | Age in days | Mass in water (grams) | Mass in air (grams) | Density | Load (kN) | Stress ($N/mm^2$) |
|---|---|---|---|---|---|---|---|
| $CPP1_f$ | 1:2:3 | 7 | 625 | 1637 | 1640 | 111.173 | 11.2 |
| $CPP1_f$ | 1:2:3 | 7 | 630 | 1646 | 1610 | 111.817 | 11.2 |
| $CPP1_f$ | 1:2:3 | 7 | 618 | 1641 | 1620 | 110.71 | 11.2 |
| $CPP2_f$ | 1:2:3 | 7 | 590 | 1599 | 1580 | 67.492 | 6.7 |
| $CPP2_f$ | 1:2:3 | 7 | 590 | 1599 | 1580 | 66.48 | 6.6 |
| $CPP2_f$ | 1:2:3 | 7 | 580 | 1598 | 1580 | 66.78 | 6.7 |
| $CPP3_f$ | 1:2:4 | 7 | 574 | 1570 | 1540 | 73.517 | 7.35 |
| $CPP3_f$ | 1:2:4 | 7 | 546 | 1540 | 1570 | 65.007 | 6.5 |
| $CPP3_f$ | 1:2:4 | 7 | 550 | 1560 | 1590 | 65.132 | 6.5 |
| $CPP1_f$ | 1:2:3 | 28 | 638 | 1656 | 1640 | 160.558 | 16.01 |
| $CPP1_f$ | 1:2:3 | 28 | 638 | 1684 | 1630 | 174.334 | 17.4 |
| $CPP1_f$ | 1:2:3 | 28 | 647 | 1672 | 1640 | 174.84 | 17.5 |
| $CPP2_f$ | 1:2:3 | 28 | 590 | 1607 | 1580 | 105.937 | 10.6 |
| $CPP2_f$ | 1:2:3 | 28 | 595 | 1593 | 1590 | 114.720 | 11.47 |
| $CPP2_f$ | 1:2:3 | 28 | 610 | 1599 | 1610 | 131.109 | 13.11 |
| $CPP3_f$ | 1:2:4 | 28 | 590 | 1607 | 1560 | 106.126 | 10.61 |
| $CPP3_f$ | 1:2:4 | 28 | 587 | 1597 | 1580 | 113.625 | 11.36 |
| $CPP3_f$ | 1:2:4 | 28 | 566 | 1573 | 1580 | 114.72 | 11.4 |
| $CPP1_f$ | 1:2:3 | 90 | 643 | 1654 | 1640 | 230.958 | 23.1 |
| $CPP1_f$ | 1:2:3 | 90 | 642 | 1649 | 1630 | 236.995 | 23.70 |
| $CPP1_f$ | 1:2:3 | 90 | 645 | 1672 | 1640 | 234.129 | 23.4 |
| $CPP2_f$ | 1:2:3 | 90 | 599 | 1590 | 1600 | 181.304 | 18.1 |
| $CPP2_f$ | 1:2:3 | 90 | 609 | 1619 | 1590 | 172.099 | 17.66 |
| $CPP2_f$ | 1:2:3 | 90 | 600 | 1620 | 1590 | 176.667 | 17.67 |
| $CPP3_f$ | 1:2:4 | 90 | 594 | 1574 | 1570 | 155.506 | 15.55 |
| $CPP3_f$ | 1:2:4 | 90 | 591 | 1594 | 1590 | 176.575 | 17.66 |
| $CPP3_f$ | 1:2:4 | 90 | 572 | 1580 | 1560 | 166.607 | 16.66 |

| Mix ref. | Mix composition | Age in days | Mass in water (grams) | Mass in air (grams) | Density | Load (kN) | Stress ($N/mm^2$) |
|---|---|---|---|---|---|---|---|
| P1 | 1:2:3 | 7 | 1467 | 2418 | 2390 | 316.078 | 31.60 |
| P1 | 1:2:3 | 7 | 1464 | 2421 | 2380 | 305.143 | 30.514 |
| P1 | 1:2:3 | 7 | 1465 | 2420 | 2370 | 310.323 | 31.03 |
| P2 | 1:2:3 | 7 | 1369 | 2385 | 2340 | 207.566 | 20.08 |
| P2 | 1:2:3 | 7 | 1385 | 2383 | 2380 | 218.882 | 21.90 |
| P2 | 1:2:3 | 7 | 1366 | 2385 | 2340 | 220.723 | 22.07 |
| P3 | 1:2:4 | 7 | 1387 | 2400 | 2360 | 242.020 | 24.20 |
| P3 | 1:2:4 | 7 | 1426 | 2398 | 2410 | 203.977 | 20.40 |
| P3 | 1:2:4 | 7 | 1390 | 2400 | 2360 | 223.098 | 22.31 |
| P1 | 1:2:3 | 28 | 1407 | 2415 | 2370 | 435.241 | 43.05 |
| P1 | 1:2:3 | 28 | 1398 | 2419 | 2370 | 456.933 | 45.7 |
| P1 | 1:2:3 | 28 | 1400 | 2404 | 2370 | 440.26 | 44.03 |
| P2 | 1:2:3 | 28 | 1366 | 2371 | 2350 | 252.407 | 25.2 |
| P2 | 1:2:3 | 28 | 1348 | 2323 | 2380 | 265.82 | 26.6 |
| P2 | 1:2:3 | 28 | 1382 | 2384 | 2350 | 222.490 | 22.25 |
| P3 | 1:2:4 | 28 | 1382 | 2438 | 2390 | 259.71 | 25.97 |
| P3 | 1:2:4 | 28 | 1420 | 2343 | 2390 | 235.158 | 23.52 |
| P3 | 1:2:4 | 28 | 1360 | 2415 | 2390 | 246.711 | 24.74 |
| P1 | 1:2:3 | 90 | 1301 | 2254 | 2360 | 467.885 | 46.79 |
| P1 | 1:2:3 | 90 | 1423 | 2435 | 2370 | 433.499 | 43.35 |
| P1 | 1:2:3 | 90 | 1321 | 2303 | 2380 | 332.267 | 33.223 |
| P2 | 1:2:3 | 90 | 1380 | 2382 | 2370 | 291.167 | 29.12 |
| P2 | 1:2:3 | 90 | 1391 | 2386 | 2390 | 309.956 | 31.00 |
| P2 | 1:2:3 | 90 | 1379 | 2368 | 2390 | 309.787 | 31.00 |
| P3 | 1:2:4 | 90 | 1384 | 2371 | 2400 | 310.667 | 31.00 |
| P3 | 1:2:4 | 90 | 1435 | 2449 | 2410 | 288.718 | 28.87 |
| P3 | 1:2:4 | 90 | 1402 | 2393 | 2410 | 303.116 | 30.31 |

| Mix ref. | Mix composition | Age in days | Mass in water (grams) | Mass in air (grams) | Density | Load (kN) | Stress ($N/mm^2$) |
|---|---|---|---|---|---|---|---|
| PP1 | 1:2:3 | 7 | 483 | 1395 | 1430 | 54.036 | 5.4 |
| PP1 | 1:2:3 | 7 | 471 | 1395 | 1410 | 39.06 | 3.91 |
| PP1 | 1:2:3 | 7 | 470 | 1395 | 1430 | 42.57 | 4.57 |
| PP2 | 1:2:3 | 7 | 399 | 1281 | 1450 | 20.222 | 2.02 |
| PP2 | 1:2:3 | 7 | 381 | 1302 | 1410 | 16.936 | 1.69 |
| PP2 | 1:2:3 | 7 | 390 | 1300 | 1450 | 20.410 | 2.04 |
| PP3 | 1:2:4 | 7 | 422 | 1307 | 1490 | 17.02 | 1.70 |
| PP3 | 1:2:4 | 7 | 319 | 1319 | 1460 | 16.768 | 1.68 |
| PP3 | 1:2:4 | 7 | 420 | 1310 | 1460 | 17.14 | 1.71 |
| PP1 | 1:2:3 | 28 | 307 | 1055 | 1410 | 78.36 | 7.8 |
| PP1 | 1:2:3 | 28 | 298 | 997 | 1440 | 71.20 | 7.1 |
| PP1 | 1:2:3 | 28 | 313 | 1101 | 1400 | 74.18 | 7.4 |
| PP2 | 1:2:3 | 28 | 463 | 1392 | 1500 | 43.31 | 4.33 |
| PP2 | 1:2:3 | 28 | 442 | 1333 | 1490 | 35.31 | 3.53 |
| PP2 | 1:2:3 | 28 | 430 | 1350 | 1490 | 38.89 | 3.89 |
| PP3 | 1:2:4 | 28 | 439 | 1400 | 1450 | 34.04 | 3.4 |
| PP3 | 1:2:4 | 28 | 435 | 1331 | 1480 | 24.09 | 2.4 |
| PP3 | 1:2:4 | 28 | 436 | 1380 | 1460 | 27.08 | 2.7 |
| PP1 | 1:2:3 | 90 | 490 | 1441 | 1510 | 65.15 | 6.515 |
| PP1 | 1:2:3 | 90 | 458 | 1386 | 1490 | 51.85 | 5.185 |
| PP1 | 1:2:3 | 90 | 465 | 1377 | 1520 | 82.65 | 8.2 |
| PP2 | 1:2:3 | 90 | 322 | 1078 | 1490 | 42.553 | 4.26 |
| PP2 | 1:2:3 | 90 | 321 | 1082 | 1440 | 46.620 | 4.70 |
| PP2 | 1:2:3 | 90 | 318 | 1082 | 1420 | 46.340 | 4.63 |
| PP3 | 1:2:4 | 90 | 321 | 1082 | 1420 | 42.836 | 4.28 |
| PP3 | 1:2:4 | 90 | 320 | 1078 | 1460 | 42.601 | 4.26 |
| PP3 | 1:2:4 | 90 | 319 | 1084 | 1460 | 43.111 | 4.3 |

| Mix ref. | Mix composition | Age in days | Mass in water (grams) | Mass in air (grams) | Density | Load (kN) | Stress ($N/mm^2$) |
|---|---|---|---|---|---|---|---|
| PPP1 | 1:1:4:6 | 7 | 618 | 1647 | 1590 | 43.201 | 4.3 |
| PPP1 | 1:1:4:6 | 7 | 620 | 1624 | 1570 | 42.907 | 4.3 |
| PPP1 | 1:1:4:6 | 7 | 582 | 1643 | 1610 | 41.447 | 4.1 |
| PPP2 | 1:1:4:6 | 7 | 574 | 1566 | 1580 | 37.211 | 3.7 |
| PPP2 | 1:1:4:6 | 7 | 570 | 1568 | 1580 | 35.081 | 3.5 |
| PPP2 | 1:1:4:6 | 7 | 588 | 1590 | 1570 | 38.64 | 3.9 |
| PPP3 | 1:1:4:8 | 7 | 562 | 1562 | 1560 | 34.120 | 3.4 |
| PPP3 | 1:1:4:8 | 7 | 568 | 1565 | 1540 | 35.476 | 3.5 |
| PPP3 | 1:1:4:8 | 7 | 595 | 1565 | 1550 | 33.112 | 3.3 |
| PPP1 | 1:1:4:6 | 28 | 640 | 1643 | 1590 | 77.414 | 7.74 |
| PPP1 | 1:1:4:6 | 28 | 620 | 1630 | 1590 | 73.543 | 7.4 |
| PPP1 | 1:1:4:6 | 28 | 595 | 1609 | 1600 | 80.812 | 8.08 |
| PPP2 | 1:1:4:6 | 28 | 603 | 1587 | 1580 | 51.873 | 5.2 |
| PPP2 | 1:1:4:6 | 28 | 575 | 1586 | 1580 | 49.73 | 5.0 |
| PPP2 | 1:1:4:6 | 28 | 568 | 1568 | 1580 | 53.501 | 5.4 |
| PPP3 | 1:1:4:8 | 28 | 538 | 1518 | 1560 | 49.006 | 4.9 |
| PPP3 | 1:1:4:8 | 28 | 582 | 1599 | 1560 | 48.730 | 4.9 |
| PPP3 | 1:1:4:8 | 28 | 540 | 1531 | 1560 | 30.901 | 3.1 |
| PPP1 | 1:1:4:6 | 90 | 557 | 1582 | 1590 | 110.543 | 11.1 |
| PPP1 | 1:1:4:6 | 90 | 566 | 1633 | 1580 | 115.213 | 11.5 |
| PPP1 | 1:1:4:6 | 90 | 615 | 1628 | 1580 | 100.43 | 10.43 |
| PPP2 | 1:1:4:6 | 90 | 540 | 1551 | 1570 | 82.100 | 8.2 |
| PPP2 | 1:1:4:6 | 90 | 557 | 1554 | 1580 | 82.217 | 8.2 |
| PPP2 | 1:1:4:6 | 90 | 566 | 1548 | 1580 | 68.173 | 6.8 |
| PPP3 | 1:1:4:8 | 90 | 542 | 1518 | 1560 | 71.004 | 7.1 |
| PPP3 | 1:1:4:8 | 90 | 549 | 1530 | 1560 | 68.621 | 6.9 |
| PPP3 | 1:1:4:8 | 90 | 540 | 1574 | 1570 | 73.104 | 7.3 |

| Mix ref. | Mix composition | Age in days | Mass in water (grams) | Mass in air (grams) | Density | Load (kN) | Stress ($N/mm^2$) |
|---|---|---|---|---|---|---|---|
| $PPP1_f$ | 1:2:3 | 7 | 614 | 1659 | 1580 | 72.25 | 7.23 |
| $PPP1_f$ | 1:2:3 | 7 | 619 | 1647 | 1600 | 42.89 | 4.29 |
| $PPP1_f$ | 1:2:3 | 7 | 615 | 1651 | 1590 | 30.36 | 3.04 |
| $PPP2_f$ | 1:2:3 | 7 | 607 | 1615 | 1590 | 38.63 | 3.0 |
| $PPP2_f$ | 1:2:3 | 7 | 581 | 1605 | 1590 | 35.98 | 4.9 |
| $PPP3_f$ | 1:2:3 | 7 | 597 | 1627 | 1570 | 34.9 | 3.49 |
| $PPP3_f$ | 1:2:4 | 7 | 545 | 1551 | 1540 | 36.82 | 3.68 |
| $PPP3_f$ | 1:2:4 | 7 | 547 | 1554 | 1540 | 21.276 | 2.13 |
| $PPP3_f$ | 1:2:4 | 7 | 547 | 1548 | 1540 | 32.819 | 3.28 |
| $PPP1_f$ | 1:2:3 | 28 | 596 | 1600 | 1600 | 94.16 | 9.416 |
| $PPP1_f$ | 1:2:3 | 28 | 588 | 1561 | 1600 | 96.60 | 9.66 |
| $PPP1_f$ | 1:2:3 | 28 | 614 | 1634 | 1600 | 95.04 | 9.50 |
| $PPP2_f$ | 1:2:3 | 28 | 599 | 1607 | 1590 | 61.34 | 6.13 |
| $PPP2_f$ | 1:2:3 | 28 | 613 | 1587 | 1590 | 54.66 | 5.5 |
| $PPP3_f$ | 1:2:3 | 28 | 557 | 1529 | 1590 | 56.29 | 5.6 |
| $PPP3_f$ | 1:2:4 | 28 | 552 | 1570 | 1540 | 53.8 | 5.4 |
| $PPP3_f$ | 1:2:4 | 28 | 565 | 1580 | 1550 | 52.199 | 5.2 |
| $PPP3_f$ | 1:2:4 | 28 | 555 | 1540 | 1560 | 47.40 | 4.7 |
| $PPP1_f$ | 1:2:3 | 90 | 627 | 1647 | 1610 | 124.84 | 12.48 |
| $PPP1_f$ | 1:2:3 | 90 | 624 | 1637 | 1600 | 131.57 | 13.16 |
| $PPP1_f$ | 1:2:3 | 90 | | | | | |
| $PPP2_f$ | 1:2:3 | 90 | 578 | 1552 | 1590 | 81.74 | 8.17 |
| $PPP2_f$ | 1:2:3 | 90 | 605 | 1599 | 1590 | 91.919 | 9.19 |
| $PPP3_f$ | 1:2:3 | 90 | | | | | |
| $PPP3_f$ | 1:2:4 | 90 | 566 | 1563 | 1560 | 74.818 | 7.18 |
| $PPP3_f$ | 1:2:4 | 90 | 565 | 1565 | 1560 | 80.687 | 8.07 |
| $PPP3_f$ | 1:2:4 | 90 | | | | | |

# APPENDIX 3.0

Data for: water absorption and porosity

| Mix ref. | Mix composition | Age in days | Mass in water (grams) | Mass in air (grams) | Dry weight |
|---|---|---|---|---|---|
| C1 | 1:2:3 | 28 | 1381 | 2302 | 2220 |
| C1 | 1:2:3 | 28 | 1437 | 2392 | 2307 |
| C1 | 1:2:3 | 28 | 1475 | 2462 | 2374 |
| C2 | 1:2:3 | 28 | 1523 | 2511 | 2422 |
| C2 | 1:2:3 | 28 | 1487 | 2476 | 2388 |
| C2 | 1:2:3 | 28 | 1528 | 2517 | 2428 |
| C3 | 1:2:4 | 28 | 1543 | 2543 | 2450 |
| C3 | 1:2:4 | 28 | 1534 | 2533 | 2440 |
| C3 | 1:2:4 | 28 | 1532 | 2530 | 2437 |
| CP1 | 1:2:3 | 28 | 493 | 1485 | 1227 |
| CP1 | 1:2:3 | 28 | 478 | 1440 | 1190 |
| CP1 | 1:2:3 | 28 | 491 | 1476 | 1220 |
| CP2 | 1:2:3 | 28 | 455 | 1373 | 1128 |
| CP2 | 1:2:3 | 28 | 461 | 1390 | 1142 |
| CP2 | 1:2:3 | 28 | 476 | 1431 | 1176 |
| CP3 | 1:2:4 | 28 | 420 | 1261 | 1034 |
| CP3 | 1:2:4 | 28 | 437 | 1315 | 1078 |
| CP3 | 1:2:4 | 28 | 408 | 1227 | 1006 |
| CPP1 | 1:1:4:6 | 90 | 660 | 1670 | 1487 |
| CPP1 | 1:1:4:6 | 90 | 653 | 1680 | 1494 |
| CPP1 | 1:1:4:6 | 90 | 649 | 1673 | 1488 |
| CPP2 | 1:1:4:6 | 90 | 610 | 1588 | 1408 |
| CPP2 | 1:1:4:6 | 90 | 603 | 1590 | 1408 |
| CPP2 | 1:1:4:6 | 90 | 617 | 1633 | 1446 |
| CPP3 | 1:1:4:8 | 90 | 587 | 1648 | 1442 |
| CPP3 | 1:1:4:8 | 90 | 619 | 1676 | 1471 |
| CPP3 | 1:1:4:8 | 90 | 602 | 1665 | 1459 |

| Mix ref. | Mix composition | Age in days | Mass in water (grams) | Mass in air (grams) | Dry mass (grams) |
|---|---|---|---|---|---|
| $CPP1_f$ | 1:2:3 | 28 | 640 | 1643 | 1521 |
| $CPP1_f$ | 1:2:3 | 28 | 620 | 1609 | 1488 |
| $CPP1_f$ | 1:2:3 | 28 | 595 | 1630 | 1504 |
| $CPP2_f$ | 1:2:3 | 28 | 603 | 1643 | 1486 |
| $CPP2_f$ | 1:2:3 | 28 | 575 | 1609 | 1453 |
| $CPP2_f$ | 1:2:3 | 28 | 568 | 1596 | 1441 |
| $CPP3_f$ | 1:2:4 | 28 | 575 | 1582 | 1443 |
| $CPP3_f$ | 1:2:4 | 28 | 538 | 1568 | 1426 |
| $CPP3_f$ | 1:2:4 | 28 | 528 | 1518 | 1381 |
| P1 | 1:2:3 | 28 | 1414 | 2414 | 2297 |
| P1 | 1:2:3 | 28 | 1406 | 2406 | 2289 |
| P1 | 1:2:3 | 28 | 1409 | 2418 | 2300 |
| P2 | 1:2:3 | 28 | 1369 | 2369 | 2230 |
| P2 | 1:2:3 | 28 | 1353 | 2339 | 2202 |
| P2 | 1:2:3 | 28 | 1431 | 2474 | 2329 |
| P3 | 1:2:4 | 28 | 1258 | 2464 | 2300 |
| P3 | 1:2:4 | 28 | 1211 | 2365 | 2208 |
| P3 | 1:2:4 | 28 | 1204 | 2358 | 2201 |
| PP1 | 1:2:3 | 28 | 548 | 1367 | 1128 |
| PP1 | 1:2:3 | 28 | 541 | 1350 | 1114 |
| PP1 | 1:2:3 | 28 | 561 | 1369 | 1133 |
| PP2 | 1:2:3 | 28 | 543 | 1315 | 1078 |
| PP2 | 1:2:3 | 28 | 553 | 1338 | 1097 |
| PP2 | 1:2:3 | 28 | 555 | 1347 | 1104 |
| PP3 | 1:2:4 | 28 | 514 | 1393 | 1123 |
| PP3 | 1:2:4 | 28 | 582 | 1503 | 1212 |
| PP3 | 1:2:4 | 28 | 530 | 1365 | 1101 |

| Mix ref. | Mix composition | Age in days | Mass in water (grams) | Mass in air (grams) | Dry mass |
|---|---|---|---|---|---|
| PPP1 | 1:1:4:6 | 28 | 641 | 1615 | 1427 |
| PPP1 | 1:1:4:6 | 28 | 634 | 1601 | 1414 |
| PPP1 | 1:1:4:6 | 28 | 640 | 1607 | 1420 |
| PPP2 | 1:1:4:6 | 28 | 626 | 1585 | 1398 |
| PPP2 | 1:1:4:6 | 28 | 614 | 1558 | 1374 |
| PPP2 | 1:1:4:6 | 28 | 624 | 1578 | 1392 |
| PPP3 | 1:1:4:8 | 28 | 608 | 1610 | 1409 |
| PPP3 | 1:1:4:8 | 28 | 615 | 1625 | 1422 |
| PPP3 | 1:1:4:8 | 28 | 614 | 1619 | 1417 |
| $PPP1_f$ | 1:2:3 | 28 | 584 | 1630 | 1494 |
| $PPP1_f$ | 1:2:3 | 28 | 581 | 1612 | 1478 |
| $PPP1_f$ | 1:2:3 | 28 | 576 | 1599 | 1466 |
| $PPP2_f$ | 1:2:3 | 28 | 580 | 1597 | 1437 |
| $PPP2_f$ | 1:2:3 | 28 | 578 | 1591 | 1432 |
| $PPP3_f$ | 1:2:3 | 28 | 572 | 1592 | 1441 |
| $PPP3_f$ | 1:2:4 | 28 | 639 | 1680 | 1456 |
| $PPP3_f$ | 1:2:4 | 28 | 625 | 1648 | 1428 |
| $PPP3_f$ | 1:2:4 | 28 | 627 | 1654 | 1433 |

# APPENDIX 4.0

Data for: Freeze-thaw analysis (CEM IIB-concrete system)

| *Mix reference* | $M_{id,n}^{m}$ $(g)$ | $M_{id,0}^{m}(g)$ | $f_{ci,n}^{m}$ $(N/mm^2)$ | $f_{cr,n}^{m}$ $(N/mm^2)$ |
|---|---|---|---|---|
| C1 | 2434 | 2440 | 45.34 | 45.46 |
| | 2424 | 2433 | 45.38 | 45.44 |
| | 2432 | 2438 | 45.30 | 45.39 |
| C2 | 2198 | 2207 | 39.61 | 39.66 |
| | 2197 | 2205 | 39.49 | 39.57 |
| | 2199 | 2209 | 39.40 | 39.60 |
| C3 | 2157 | 2175 | 39.24 | 37.44 |
| | 2157 | 2165 | 39.20 | 41.40 |
| | 2013 | 2032 | 39.27 | 36.10 |
| CP1 | 1179 | 1189 | 7.15 | 7.3 |
| | 1182 | 1191 | 7.20 | 7.3 |
| | 1176 | 1193 | 7.10 | 7.2 |
| CP2 | 1307 | 1320 | 6.92 | 7.0 |
| | 1301 | 1325 | 6.80 | 6.4 |
| | 1313 | 1227 | 6.65 | 7.6 |
| CP3 | 1237 | 1250 | 4.57 | 4.6 |
| | 1238 | 1258 | 4.43 | 4.7 |
| | 1233 | 1257 | 4.50 | 4.5 |
| CPP1 | 1078 | 1079 | 11.19 | 11.28 |
| | 1069 | 1080 | 11.18 | 11.32 |
| | 1072 | 1075 | 11.2 | 11.24 |
| CPP2 | 1525 | 1536 | 10.42 | 10.50 |
| | 1526 | 1530 | 10.44 | 1.40 |
| | 1524 | 1542 | 10.40 | 10.60 |
| CPP3 | 1274 | 1282 | 9.68 | 9.73 |
| | 1262 | 1280 | 9.60 | 9.70 |
| | 1283 | 1281 | 7.12 | 9.84 |
| $CPP1_f$ | 1426 | 1429 | 15.80 | 15.90 |

| | | | | |
|---|---|---|---|---|
| | 1426 | 1426 | 15.75 | 16.00 |
| | 1417 | 1433 | 15.85 | 15.80 |
| $CPP2_f$ | 1313 | 1326 | 13.90 | 14.03 |
| | 1318 | 1323 | 13.87 | 14.50 |
| | 1323 | 1329 | 13.94 | 13.56 |
| $CPP3_f$ | 1338 | 1347 | 11.04 | 11.26 |
| | 1336 | 1341 | 11.34 | 11.21 |
| | 1342 | 1353 | 11.16 | 11.31 |

Data for: Freeze-thaw analysis (PG-system)

| *Mix reference* | $M_{id,n}^{m}\ (g)$ | $M_{id,0}^{m}(g)$ | $f_{ci,n}^{m}$ *(N/mm²)* | $f_{cr,n}^{m}$ *(N/mm²)* |
|---|---|---|---|---|
| P1 | 2276 | 2344 | 39.18 | 39.34 |
| | 2274 | 2344 | 39.16 | 39.34 |
| | 2283 | 2345 | 39.11 | 39.35 |
| P2 | 2156 | 2254 | 24.38 | 24.58 |
| | 2150 | 2249 | 24.14 | 24.45 |
| | 2159 | 2250 | 24.24 | 24.68 |
| P3 | 2192 | 2274 | 21.33 | 21.5 |
| | 2198 | 2273 | 21.31 | 22.0 |
| | 2195 | 2278 | 21.32 | 21.1 |
| PP1 | 963 | 1102 | 6.58 | 6.76 |
| | 966 | 1100 | 6.49 | 6.68 |
| | 957 | 1105 | 6.64 | 6.87 |
| PP2 | 1018 | 1217 | 3.42 | 3.6 |
| | 1014 | 1219 | 3.49 | 3.3 |
| | 1022 | 1214 | 3.56 | 3.9 |
| PP3 | 982 | 1118 | 2.80 | 2.90 |
| | 990 | 1127 | 2.61 | 2.80 |
| | 1007 | 1121 | 2.56 | 2.90 |
| PPP1 | 1283 | 1470 | 5.98 | 5.87 |
| | 1287 | 1470 | 5.91 | 6.22 |
| | 1279 | 1468 | 6.06 | 6.05 |
| PPP2 | 1197 | 1337 | 4.25 | 4.29 |
| | 1201 | 1331 | 4.20 | 4.30 |
| | 1186 | 1343 | 4.27 | 4.26 |
| PPP3 | 1353 | 1599 | 3.53 | 3.58 |
| | 1357 | 1600 | 3.52 | 3.60 |
| | 1358 | 1604 | 2.01 | 2.91 |

| | | | | |
|---|---|---|---|---|
| $PPP1_f$ | 1311 | 1471 | 8.68 | 8.79 |
| | 1307 | 1464 | 8.28 | 8.75 |
| | 1315 | 1469 | 5.3 | 5.44 |
| $PPP2_f$ | 1212 | 1372 | 5.50 | 5.16 |
| | 1217 | 1358 | 5.20 | 5.54 |
| | 1215 | 1286 | 5.92 | 5.98 |
| $PPP3_f$ | 1284 | 1425 | 4.72 | 4.8 |
| | 1287 | 1439 | 4.71 | 4.7 |
| | 1281 | 1411 | 4.73 | 5.0 |

## APPENDIX 5.0

Data for: Sulphate resistance (mass loss (%) of the CEM IIB-concrete system)

| *Mix reference* | *7 days* | | *28 days* | | *90 days* | |
|---|---|---|---|---|---|---|
| | *Mass of reference specimen* | *Mass of main specimen* | *Mass of reference specimen* | *Mass of main specimen* | *Mass of reference specimen* | *Mass of main specimen* |
| C1 | 2446 | 2443 | 2471 | 2470 | 2494 | 2458 |
| | 2440 | 2445 | 2471 | 2469 | 2450 | 2450 |
| | 2452 | 2447 | 2470 | 2470 | 2642 | 2466 |
| C2 | 2443 | 2441 | 2398 | 2384 | 2440 | 2441 |
| | 2439 | 2440 | 2388 | 2392 | 2453 | 2442 |
| | 2444 | 2441 | 2390 | 2394 | 2442 | 2437 |
| C3 | 2457 | 2457 | 2472 | 2470 | 2473 | 2467 |
| | 2458 | 2453 | 2471 | 2472 | 2470 | 2464 |
| | 2455 | 2452 | 2470 | 2468 | 2475 | 2469 |
| CP1 | 1376 | 1374 | 1476 | 1474 | 1550 | 1543 |
| | 1378 | 1378 | 1478 | 1474 | 1552 | 1543 |
| | 1371 | 1370 | 1480 | 1475 | 1548 | 1544 |
| CP2 | 1347 | 1345 | 1669 | 1663 | 1657 | 1649 |
| | 1346 | 1345 | 1671 | 1669 | 1655 | 1650 |
| | 1348 | 1345 | 1667 | 1665 | 1668 | 1650 |
| CP3 | 1296 | 1294 | 1406 | 1398 | 1541 | 1529 |
| | 1293 | 1288 | 1404 | 1405 | 1535 | 1529 |
| | 1302 | 1300 | 1408 | 1403 | 1544 | 1528 |
| CPP1 | 1660 | 1659 | 1663 | 1661 | 1601 | 1595 |
| | 1661 | 1661 | 1660 | 1651 | 1597 | 1592 |
| | 1659 | 1657 | 1666 | 1671 | 1602 | 1598 |
| CPP2 | 1618 | 1619 | 1632 | 1630 | 1630 | 1623 |
| | 1621 | 1619 | 1630 | 1629 | 1630 | 1625 |

| | | | | | | |
|---|---|---|---|---|---|---|
| | 1621 | 1618 | 1634 | 1630 | 1630 | 1622 |
| CPP3 | 1645 | 1644 | 1671 | 1669 | 1674 | 1663 |
| | 1646 | 1643 | 1670 | 1667 | 1667 | 1666 |
| | 1649 | 1644 | 1673 | 1665 | 1669 | 1660 |
| $CPP1_f$ | 1641 | 1639 | 1650 | 1617 | 1656 | 1652 |
| | 1636 | 1643 | 1650 | 1620 | 1654 | 1650 |
| | 1643 | 1635 | 1656 | 1614 | 1655 | 1654 |
| $CPP2_f$ | 1580 | 1579 | 1612 | 1610 | 1618 | 1615 |
| | 1590 | 1575 | 1617 | 1606 | 1606 | 1606 |
| | 1570 | 1583 | 1608 | 1597 | 1633 | 1618 |
| $CPP3_f$ | 1568 | 1573 | 1599 | 1514 | 1597 | 15990 |
| | 1571 | 1558 | 1590 | 1509 | 1585 | 1579 |
| | 1571 | 1570 | 1610 | 1519 | 1601 | 1594 |

Data for: Sulphate resistance (Compressive strength loss (%) of the CEM IIB-concrete system)

| *Mix ref.* | *7 days* | | *28 days* | | *90 days* | |
|---|---|---|---|---|---|---|
| | *Comp. strength of reference specimen* | *Comp. strength of main specimen* | *Comp. strength of reference specimen* | *Comp. strength of main specimen* | *Comp. strength of reference specimen* | *Comp. strength of main specimen* |
| C1 | 28.89 | 28.76 | 52.28 | 52.29 | 60.8 | 59.9 |
| | 28.52 | 28.64 | 52.35 | 52.08 | 59.9 | 60.2 |
| | 28.99 | 28.85 | 52.42 | 52.44 | 61.4 | 61.4 |
| C2 | 31.62 | 31.28 | 46.14 | 46.28 | 56.1 | 55.68 |
| | 31.78 | 31.90 | 46.46 | 46.06 | 55.92 | 56.04 |
| | 31.76 | 31.83 | 46.42 | 46.36 | 56.28 | 56.11 |
| C3 | 31.72 | 31.68 | 44.22 | 44.35 | 51.49 | 51.30 |
| | 31.50 | 31.52 | 44.51 | 44.37 | 51.37 | 51.34 |
| | 31.88 | 31.66 | 44.45 | 44.15 | 51.64 | 51.35 |
| CP1 | 6.41 | 6.17 | 7.90 | 8.05 | 9.55 | 9.57 |
| | 6.30 | 6.46 | 8.08 | 8.09 | 10.00 | 9.97 |
| | 4.49 | 6.48 | 8.07 | 8.01 | 10.15 | 9.88 |
| CP2 | 5.21 | 5.03 | 8.8 | 7.91 | 9.18 | 9.18 |
| | 4.82 | 5.07 | 8.12 | 7.96 | 9.37 | 9.20 |
| | 5.19 | 5.05 | 7.80 | 7.89 | 9.35 | 9.10 |
| CP3 | 3.40 | 3.46 | 5.10 | 5.17 | 5.61 | 5.69 |
| | 3.56 | 3.30 | 5.10 | 4.69 | 5.95 | 5.70 |
| | 3.24 | 3.36 | 4.02 | 5.23 | 5.84 | 5.68 |
| CPP1 | 9.70 | 7.97 | 12.89 | 12.75 | 15.60 | 15.35 |
| | 7.83 | 7.99 | 12.52 | 12.74 | 15.33 | 15.18 |
| | 8.00 | 7.96 | 12.99 | 12.75 | 15.57 | 15.48 |

| | | | | | | |
|---|---|---|---|---|---|---|
| CPP2 | 6.97 | 6.87 | 12.10 | 12.28 | 14.99 | 14.28 |
| | 6.93 | 6.65 | 12.35 | 12.33 | 14.70 | 14.90 |
| | 6.80 | 7.09 | 12.45 | 12.08 | 15.01 | 14.86 |
| CPP3 | 6.90 | 6.88 | 12.14 | 11.95 | 14.24 | 13.74 |
| | 6.76 | 6.68 | 12.01 | 11.82 | 14.02 | 13.99 |
| | 7.04 | 6.93 | 12.25 | 11.93 | 14.04 | 13.98 |
| $CPP1_f$ | 11.49 | 11.90 | 18.60 | 18.55 | 24.14 | 23.68 |
| | 11.92 | 11.57 | 18.54 | 18.56 | 23.60 | 24.09 |
| | 11.99 | 11.84 | 18.66 | 18.54 | 24.26 | 23.99 |
| $CPP2_f$ | 6.70 | 7.07 | 12.5 | 12.44 | 17.78 | 17.79 |
| | 6.52 | 6.32 | 12.97 | 12.00 | 16.72 | 17.33 |
| | 7.22 | 6.89 | 12.03 | 12.82 | 17.20 | 16.06 |
| $CPP3_f$ | 6.3 | 6. 90 | 12. 77 | 11.86 | 17.67 | 16. 24 |
| | 5.82 | 5.21 | 11.10 | 11.81 | 17.20 | 16.67 |
| | 6.78 | 6.52 | 12.43 | 11.91 | 17.90 | 17.10 |

## APPENDIX 6.0

Data for: Sulphate resistance (mass loss (%) of the PG concrete system)

| *Mix reference* | *7 days* | | *28 days* | | *90 days* | |
|---|---|---|---|---|---|---|
| | *Mass of reference specimen* | *Mass of main specimen* | *Mass of reference specimen* | *Mass of main specimen* | *Mass of reference specimen* | *Mass of main specimen* |
| P1 | 2325 | 2419 | 2419 | 2420 | 2437 | 2430 |
| | 2532 | 2425 | 2420 | 2414 | 2431 | 2427 |
| | 2411 | 2422 | 2419 | 2418 | 2438 | 2434 |
| P2 | 2371 | 2386 | 2384 | 2382 | 2386 | 2379 |
| | 2389 | 2386 | 2380 | 2379 | 2382 | 2379 |
| | 2395 | 2385 | 2388 | 2383 | 2390 | 2378 |
| P3 | 2434 | 2431 | 2434 | 2434 | 2373 | 2361 |
| | 2433 | 2430 | 2434 | 2434 | 2364 | 2355 |
| | 2438 | 2434 | 2446 | 2435 | 2376 | 2370 |
| PP1 | 1330 | 1329 | 1351 | 1344 | 1385 | 1376 |
| | 1330 | 1333 | 1350 | 1352 | 1391 | 1382 |
| | 1331 | 1324 | 1352 | 1349 | 1382 | 1380 |
| PP2 | 1300 | 1302 | 1340 | 1342 | 1380 | 1367 |
| | 1300 | 1293 | 1345 | 1340 | 1366 | 1365 |
| | 1300 | 1300 | 1344 | 1337 | 1382 | 1373 |
| PP3 | 1322 | 1306 | 1384 | 1365 | 1380 | 1370 |
| | 1281 | 1308 | 1356 | 1381 | 1371 | 1370 |
| | 1327 | 1303 | 1400 | 1380 | 1399 | 1369 |
| PPP1 | 1641 | 1640 | 1644 | 1642 | 1641 | 1635 |
| | 1625 | 1623 | 1640 | 1642 | 1644 | 1634 |
| | 1660 | 1659 | 1648 | 1641 | 1637 | 1635 |
| PPP2 | 1605 | 1614 | 1642 | 1638 | 1642 | 1630 |
| | 1611 | 1609 | 1653 | 1645 | 1637 | 1637 |
| | 1614 | 1603 | 1637 | 1642 | 1641 | 1637 |
| PPP3 | 1573 | 1561 | 1578 | 1582 | 1587 | 1572 |
| | 1570 | 1575 | 1584 | 1583 | 1580 | 1581 |

| | | | | | | |
|---|---|---|---|---|---|---|
| | 1576 | 1574 | 1590 | 1577 | 1588 | 1576 |
| $PPP1_f$ | 1625 | 1635 | 1626 | 1622 | 1632 | 1631 |
| | 1633 | 1632 | 1636 | 1643 | 1649 | 1642 |
| | 1632 | 1621 | 1642 | 1633 | 1645 | 1643 |
| $PPP2_f$ | 1596 | 1593 | 1608 | 1601 | 1599 | 1599 |
| | 1600 | 1595 | 1610 | 1609 | 1598 | 1593 |
| | 1589 | 1593 | 1605 | 1606 | 1600 | 1587 |
| $PPP3_f$ | 1555 | 1552 | 1562 | 1569 | 1569 | 1561 |
| | 1558 | 1547 | 1573 | 1566 | 1560 | 1562 |
| | 1550 | 1556 | 1575 | 1568 | 1563 | 1549 |

Date for: Sulphate resistance (compressive strength (%) of the PG-concrete system)

| *Mix ref.* | *7 days* | | *28 days* | | *90 days* | |
|---|---|---|---|---|---|---|
| | *Comp. strength of reference specimen* | *Comp. strength of main specimen* | *Comp. strength of reference specimen* | *Comp. strength of main specimen* | *Comp. strength of reference specimen* | *Comp. strength of main specimen* |
| P1 | 37. 42 | 36.30 | 44.36 | 44. 69 | 45.16 | 45.59 |
| | 36.66 | 37.95 | 44.03 | 43.21 | 45.77 | 45.71 |
| | 37.04 | 36.60 | 44.60 | 44. 85 | 45.48 | 45.10 |
| P2 | 22.65 | 21.91 | 26.47 | 26.64 | 31.32 | 30.49 |
| | 21.69 | 21.55 | 26.53 | 24.40 | 31.79 | 30.47 |
| | 22.11 | 22.48 | 26.41 | 25.88 | 30.85 | 31.98 |
| P3 | 22.00 | 22.57 | 26.89 | 25.03 | 31.70 | 30.26 |
| | 23.77 | 22.49 | 25.51 | 24.42 | 29.87 | 30.80 |
| | 22.03 | 22.33 | 25.00 | 26.54 | 30.53 | 29.72 |
| PP1 | 5.37 | 5.49 | 7.20 | 7.85 | 8.53 | 8.00 |
| | 5.43 | 5.17 | 7.93 | 8.84 | 7.33 | 8.35 |
| | 5.10 | 5.21 | 7.67 | 6.86 | 9.13 | 8.55 |
| PP2 | 2.13 | 2.41 | 4.05 | 3.44 | 4.21 | 4.36 |
| | 2.46 | 2.72 | 4.80 | 4.50 | 5.77 | 4.62 |

| | | | | | | |
|---|---|---|---|---|---|---|
| | 2.50 | 2.31 | 3.15 | 3.97 | 4.15 | 4.92 |
| PP3 | 1.48 | 1.91 | 3.28 | 3.35 | 4.14 | 4.45 |
| | 1.96 | 2.37 | 2.60 | 2.92 | 4.57 | 4.08 |
| | 2.47 | 1.54 | 2.72 | 3.18 | 4.91 | 4.82 |
| PPP1 | 4.74 | 4.13 | 8.20 | 8.18 | 11.31 | 11.56 |
| | 4.88 | 4.93 | 8.42 | 7.88 | 11.13 | 11.18 |
| | 4.78 | 4.58 | 8.01 | 8.88 | 11.49 | 11.04 |
| PPP2 | 4.40 | 4.29 | 6.20 | 6.00 | 8.48 | 8.44 |
| | 4.02 | 3.37 | 5.98 | 6.09 | 8.13 | 8.04 |
| | 3.58 | 3.98 | 6.12 | 6.12 | 8.23 | 8.24 |
| PPP3 | 3.70 | 3.24 | 5.25 | 5.20 | 7.28 | 7.04 |
| | 2.85 | 3.62 | 5.17 | 5.46 | 7.04 | 7.12 |
| | 4.55 | 4.18 | 5.48 | 5.12 | 7.10 | 7.08 |
| $PPP1_f$ | 4.80 | 5.29 | 9.09 | 10.51 | 12.85 | 12.95 |
| | 5.29 | 5.10 | 10.52 | 9.50 | 12.90 | 12.85 |
| | 5.51 | 5.21 | 10.39 | 9.90 | 12.65 | 12.45 |
| $PPP2_f$ | 4.62 | 4.20 | 5.18 | 6.00 | 8.79 | 8.67 |
| | 4.08 | 4.22 | 6.29 | 5.45 | 9.61 | 8.55 |
| | 4.20 | 4.36 | 5.36 | 5.80 | 7.70 | 8.68 |
| $PPP3_f$ | 4.34 | 4.24 | 5.50 | 5.60 | 7.81 | 7.27 |
| | 4.16 | 4.28 | 5.88 | 5.75 | 7.69 | 7.61 |
| | 4.40 | 4.10 | 5.72 | 5.55 | 7.90 | 7.53 |

# APPENDIX 7.0

Particle shape index

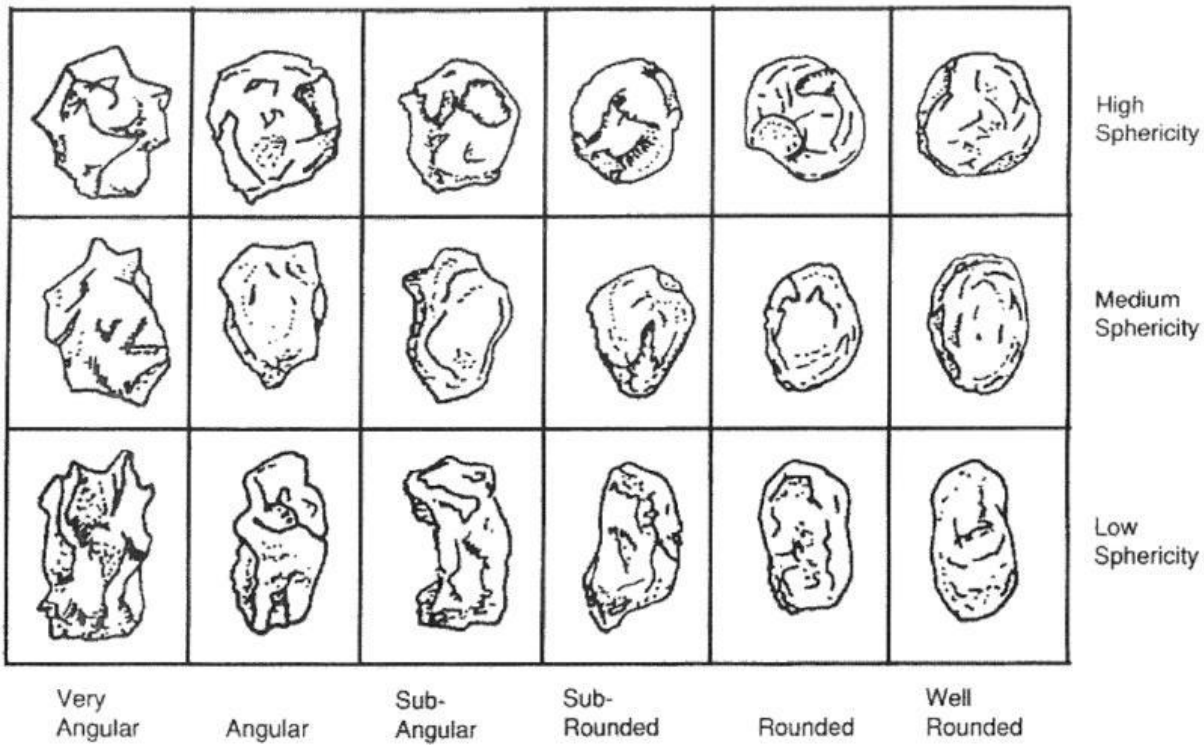

# APPENDIX 8.0

Statistical analysis

## DENSITY

**Paired Samples Statistics**

| | | Mean | N | Std. Deviation | Std. Error Mean |
|---|---|---|---|---|---|
| Pair 1 | DensityC1 | 2436.6667 | 3 | 49.32883 | 28.48001 |
| | DensityCP1 | 1600.0000 | 3 | .00000 | .00000 |
| Pair 2 | DensityC1 | 2436.6667 | 3 | 49.32883 | 28.48001 |
| | DenistyCPP1 | 1630.0000 | 3 | 30.00000 | 17.32051 |
| Pair 3 | DensityC1 | 2436.6667 | 3 | 49.32883 | 28.48001 |
| | DensityCPP1f | 1636.6667 | 3 | 5.77350 | 3.33333 |

**Paired Samples Correlations**

| | | N | Correlation | Sig. |
|---|---|---|---|---|
| Pair 1 | DensityC1 & DensityCP1 | 3 | . | . |
| Pair 2 | DensityC1 & DenistyCPP1 | 3 | .101 | .935 |
| Pair 3 | DensityC1 & DensityCPP1f | 3 | -.585 | .602 |

**Paired Samples Test**

| | | Paired Differences | | | | | t | df | Sig. (2-tailed) |
|---|---|---|---|---|---|---|---|---|---|
| | | Mean | Std. Deviation | Std. Error Mean | 95% Confidence Interval of the Difference Lower | Upper | | | |
| Pair 1 | DensityC1 - DensityCP1 | 836.66667 | 49.32883 | 28.48001 | 714.12706 | 959.20627 | 29.377 | 2 | .001 |
| Pair 2 | DensityC1 - DenistyCPP1 | 806.66667 | 55.07571 | 31.79797 | 669.85103 | 943.48230 | 25.368 | 2 | .002 |
| Pair 3 | DensityC1 - DensityCPP1f | 800.00000 | 52.91503 | 30.55050 | 668.55179 | 931.44821 | 26.186 | 2 | .001 |

**Paired Samples Statistics**

| | | Mean | N | Std. Deviation | Std. Error Mean |
|---|---|---|---|---|---|
| Pair 1 | DensityC2 | 2413.3333 | 3 | 15.27525 | 8.81917 |
| | DensityCP2 | 1583.3333 | 3 | 15.27525 | 8.81917 |
| Pair 2 | DensityC2 | 2413.3333 | 3 | 15.27525 | 8.81917 |
| | DenistyCPP2 | 1600.0000 | 3 | 50.00000 | 28.86751 |
| Pair 3 | DensityC2 | 2413.3333 | 3 | 15.27525 | 8.81917 |
| | DensityCPP2f | 1593.3333 | 3 | 17.55942 | 10.13794 |

**Paired Samples Correlations**

| | | N | Correlation | Sig. |
|---|---|---|---|---|
| Pair 1 | DensityC2 & DensityCP2 | 3 | .786 | .425 |
| Pair 2 | DensityC2 & DenistyCPP2 | 3 | -.655 | .546 |
| Pair 3 | DensityC2 & DensityCPP2f | 3 | .963 | .173 |

**Paired Samples Test**

| | | Paired Differences | | | | | t | df | Sig. (2-tailed) |
|---|---|---|---|---|---|---|---|---|---|
| | | Mean | Std. Deviation | Std. Error Mean | 95% Confidence Interval of the Difference Lower | Upper | | | |

| | | | | | | | | | |
|---|---|---|---|---|---|---|---|---|---|
| Pair 1 | DensityC2 - DensityCP2 | 830.00000 | 10.00000 | 5.77350 | 805.15862 | 854.84138 | 143.760 | 2 | .001 |
| Pair 2 | DensityC2 - DenistyCPP2 | 813.33333 | 61.10101 | 35.27668 | 661.55001 | 965.11665 | 23.056 | 2 | .002 |
| Pair 3 | DensityC2 - DensityCPP2f | 820.00000 | 5.00000 | 2.88675 | 807.57931 | 832.42069 | 284.056 | 2 | .001 |

**Paired Samples Statistics**

| | | Mean | N | Std. Deviation | Std. Error Mean |
|---|---|---|---|---|---|
| Pair 1 | DensityC3 | 2386.6667 | 3 | 5.77350 | 3.33333 |
| | DensityCP3 | 1521.6667 | 3 | 20.20726 | 11.66667 |
| Pair 2 | DensityC3 | 2386.6667 | 3 | 5.77350 | 3.33333 |
| | DenistyCPP3 | 1600.0000 | 3 | 20.00000 | 11.54701 |
| Pair 3 | DensityC3 | 2386.6667 | 3 | 5.77350 | 3.33333 |
| | DensityCPP3f | 1573.3333 | 3 | 11.54701 | 6.66667 |

**Paired Samples Correlations**

| | | N | Correlation | Sig. |
|---|---|---|---|---|
| Pair 1 | DensityC3 & DensityCP3 | 3 | -.786 | .425 |
| Pair 2 | DensityC3 & DenistyCPP3 | 3 | .866 | .333 |
| Pair 3 | DensityC3 & DensityCPP3f | 3 | 1.000 | .000 |

**Paired Samples Test**

| | | Paired Differences | | | | | t | df |
|---|---|---|---|---|---|---|---|---|
| | | Mean | Std. Deviation | Std. Error Mean | 95% Confidence Interval of the Difference Lower | Upper | | |
| Pair 1 | DensityC3 - DensityCP3 | 865.00000 | 25.00000 | 14.43376 | 802.89656 | 927.10344 | 59.929 | 2 |
| Pair 2 | DensityC3 - DenistyCPP3 | 786.66667 | 15.27525 | 8.81917 | 748.72084 | 824.61250 | 89.200 | 2 |
| Pair 3 | DensityC3 - DensityCPP3f | 813.33333 | 5.77350 | 3.33333 | 798.99116 | 827.67551 | 244.000 | 2 |

# POROSITY

**Paired Samples Statistics**

| | | Mean | N | Std. Deviation | Std. Error Mean |
|---|---|---|---|---|---|
| Pair 1 | PorosityC1 | 8.9000 | 3 | 1.50000 | .86603 |
| | PorosityCP1 | 26.0000 | 3 | 2.40000 | 1.38564 |
| Pair 2 | PorosityC1 | 8.9000 | 3 | 1.50000 | .86603 |
| | PorosityCPP1 | 18.1000 | 3 | 1.90000 | 1.09697 |
| Pair 3 | PorosityC1 | 8.9000 | 3 | 1.50000 | .86603 |
| | PorosityCPP1f | 12.2000 | 3 | 1.90000 | 1.09697 |

**Paired Samples Correlations**

| | | N | Correlation | Sig. |
|---|---|---|---|---|
| Pair 1 | PorosityC1 & PorosityCP1 | 3 | -1.000 | .000 |
| Pair 2 | PorosityC1 & PorosityCPP1 | 3 | 1.000 | .000 |
| Pair 3 | PorosityC1 & PorosityCPP1f | 3 | -1.000 | .000 |

**Paired Samples Test**

| | | Paired Differences | | | | | t | df |
|---|---|---|---|---|---|---|---|---|
| | | | | | 95% Confidence Interval of the Difference | | | |
| | | Mean | Std. Deviation | Std. Error Mean | Lower | Upper | | |
| Pair 1 | PorosityC1 - PorosityCP1 | -17.10000 | 3.90000 | 2.25167 | -26.78814 | -7.41186 | -7.594 | 2 |
| Pair 2 | PorosityC1 - PorosityCPP1 | -9.20000 | .40000 | .23094 | -10.19366 | -8.20634 | -39.837 | 2 |
| Pair 3 | PorosityC1 - PorosityCPP1f | -3.30000 | 3.40000 | 1.96299 | -11.74607 | 5.14607 | -1.681 | 2 |

**Paired Samples Statistics**

| | | Mean | N | Std. Deviation | Std. Error Mean |
|---|---|---|---|---|---|
| Pair 1 | PorosityC2 | 9.0000 | 3 | .80000 | .46188 |
| | PorosityCP2 | 26.7000 | 3 | 2.60000 | 1.50111 |
| Pair 2 | PorosityC2 | 9.0000 | 3 | .80000 | .46188 |
| | PorosityCPP2 | 18.4000 | 3 | 2.10000 | 1.21244 |
| Pair 3 | PorosityC2 | 9.0000 | 3 | .80000 | .46188 |
| | PorosityCPP2f | 13.8000 | 3 | 3.80000 | 2.19393 |

**Paired Samples Correlations**

| | | N | Correlation | Sig. |
|---|---|---|---|---|
| Pair 1 | PorosityC2 & PorosityCP2 | 3 | 1.000 | .000 |
| Pair 2 | PorosityC2 & PorosityCPP2 | 3 | -1.000 | .000 |
| Pair 3 | PorosityC2 & PorosityCPP2f | 3 | 1.000 | .000 |

**Paired Samples Test**

| | | Paired Differences | | | | | | |
|---|---|---|---|---|---|---|---|---|
| | | | | | 95% Confidence Interval of the Difference | | | |
| | | Mean | Std. Deviation | Std. Error Mean | Lower | Upper | t | df |
| Pair 1 | PorosityC2 - PorosityCP2 | -17.70000 | 1.80000 | 1.03923 | -22.17145 | -13.22855 | -17.032 | 2 |
| Pair 2 | PorosityC2 - PorosityCPP2 | -9.40000 | 2.90000 | 1.67432 | -16.60400 | -2.19600 | -5.614 | 2 |
| Pair 3 | PorosityC2 - PorosityCPP2f | -4.80000 | 3.00000 | 1.73205 | -12.25241 | 2.65241 | -2.771 | 2 |

**Paired Samples Statistics**

| | | Mean | N | Std. Deviation | Std. Error Mean |
|---|---|---|---|---|---|
| Pair 1 | PorosityC3 | 9.3000 | 3 | .60000 | .34641 |
| | PorosityCP3 | 27.0000 | 3 | 3.00000 | 1.73205 |
| Pair 2 | PorosityC3 | 9.3000 | 3 | .60000 | .34641 |
| | PorosityCPP3 | 19.4000 | 3 | 1.40000 | .80829 |

| | | | | | |
|---|---|---|---|---|---|
| Pair 3 | PorosityC3 | 9.3000 | 3 | .60000 | .34641 |
| | PorosityCPP3f | 15.1000 | 3 | 1.30000 | .75056 |

**Paired Samples Correlations**

| | | N | Correlation | Sig. |
|---|---|---|---|---|
| Pair 1 | PorosityC3 & PorosityCP3 | 3 | -1.000 | .000 |
| Pair 2 | PorosityC3 & PorosityCPP3 | 3 | -1.000 | .000 |
| Pair 3 | PorosityC3 & PorosityCPP3f | 3 | -1.000 | .000 |

**Paired Samples Test**

| | | Paired Differences | | | | | t | df |
|---|---|---|---|---|---|---|---|---|
| | | | | | 95% Confidence Interval of the Difference | | | |
| | | Mean | Std. Deviation | Std. Error Mean | Lower | Upper | | |
| Pair 1 | PorosityC3 - PorosityCP3 | -17.70000 | 3.60000 | 2.07846 | -26.64290 | -8.75710 | -8.516 | 2 |
| Pair 2 | PorosityC3 - PorosityCPP3 | -10.10000 | 2.00000 | 1.15470 | -15.06828 | -5.13172 | -8.747 | 2 |
| Pair 3 | PorosityC3 - PorosityCPP3f | -5.80000 | 1.90000 | 1.09697 | -10.51986 | -1.08014 | -5.287 | 2 |

# WATER ABSORPTION

**Paired Samples Statistics**

| | | Mean | N | Std. Deviation | Std. Error Mean |
|---|---|---|---|---|---|
| Pair 1 | WAC1 | 3.7000 | 3 | .70000 | .40415 |
| | WACP1 | 21.0000 | 3 | 1.30000 | .75056 |
| Pair 2 | WAC1 | 3.7000 | 3 | .70000 | .40415 |
| | WACPP2 | 12.5000 | 3 | 1.40000 | .80829 |
| Pair 3 | WAC1 | 3.7000 | 3 | .70000 | .40415 |
| | WACPP1f | 8.0400 | 3 | .96000 | .55426 |

**Paired Samples Correlations**

| | | N | Correlation | Sig. |
|---|---|---|---|---|
| Pair 1 | WAC1 – WACP1 | 3 | -1.000 | .000 |
| Pair 2 | WAC1 - WACPP2 | 3 | -1.000 | .000 |
| Pair 3 | WAC1 - WACPP1f | 3 | 1.000 | .000 |

**Paired Samples Test**

| | Paired Differences | | | | | | |
|---|---|---|---|---|---|---|---|
| | | | | 95% Confidence Interval of the Difference | | | |
| | Mean | Std. Deviation | Std. Error Mean | Lower | Upper | t | df |

| | | | | | | | | | |
|---|---|---|---|---|---|---|---|---|---|
| Pair 1 | WAC1 – WACP1 | -17.30000 | 2.00000 | 1.15470 | -22.26828 | -12.33172 | -14.982 | 2 | .004 |
| Pair 2 | WAC1 - WACPP2 | -8.80000 | 2.10000 | 1.21244 | -14.01669 | -3.58331 | -7.258 | 2 | .018 |
| Pair 3 | WAC1 - WACPP1f | -4.34000 | .26000 | .15011 | -4.98588 | -3.69412 | -28.912 | 2 | .001 |

**Paired Samples Statistics**

| | | Mean | N | Std. Deviation | Std. Error Mean |
|---|---|---|---|---|---|
| Pair 1 | WAC2 | 3.7000 | 3 | .10000 | .05774 |
| | WACP2 | 21.7000 | 3 | .60000 | .34641 |
| Pair 2 | WAC2 | 3.7000 | 3 | .10000 | .05774 |
| | WACPP2 | 12.8000 | 3 | .40000 | .23094 |
| Pair 3 | WAC2 | 3.7000 | 3 | .10000 | .05774 |
| | WACPP2f | 9.6700 | 3 | .57000 | .32909 |

**Paired Samples Correlations**

| | | N | Correlation | Sig. |
|---|---|---|---|---|
| Pair 1 | WAC2 & WACP2 | 3 | 1.000 | .000 |
| Pair 2 | WAC2 & WACPP2 | 3 | 1.000 | .000 |
| Pair 3 | WAC2 & WACPP2f | 3 | -1.000 | .000 |

**Paired Samples Test**

| Paired Differences | t | df | Sig. ( |
|---|---|---|---|

| | | Mean | Std. Deviation | Std. Error Mean | 95% Confidence Interval of the Difference | | | | |
|---|---|---|---|---|---|---|---|---|---|
| | | | | | Lower | Upper | | | |
| Pair 1 | WAC2 - WACP2 | -18.00000 | .50000 | .28868 | -19.24207 | -16.75793 | -62.354 | 2 | .000 |
| Pair 2 | WAC2 - WACPP2 | -9.10000 | .30000 | .17321 | -9.84524 | -8.35476 | -52.539 | 2 | .000 |
| Pair 3 | WAC2 - WACPP2f | -5.97000 | .67000 | .38682 | -7.63437 | -4.30563 | -15.433 | 2 | .004 |

**Paired Samples Statistics**

| | | Mean | N | Std. Deviation | Std. Error Mean |
|---|---|---|---|---|---|
| Pair 1 | WAC3 | 3.8000 | 3 | .40000 | .23094 |
| | WACP3 | 22.0000 | 3 | 2.80000 | 1.61658 |
| Pair 2 | WAC3 | 3.8000 | 3 | .40000 | .23094 |
| | WACPP3 | 13.9000 | 3 | 1.00000 | .57735 |
| Pair 3 | WAC3 | 3.8000 | 3 | .40000 | .23094 |
| | WACPP3f | 11.3000 | 3 | .80000 | .46188 |

**Paired Samples Correlations**

| | | N | Correlation | Sig. |
|---|---|---|---|---|
| Pair 1 | WAC3 & WACP3 | 3 | -1.000 | .000 |
| Pair 2 | WAC3 & WACPP3 | 3 | -1.000 | .000 |
| Pair 3 | WAC3 & WACPP3f | 3 | -1.000 | .000 |

**Paired Samples Test**

| | | Paired Differences | | | | | t | df | Sig. (2-tailed) |
|---|---|---|---|---|---|---|---|---|---|
| | | | | | 95% Confidence Interval of the Difference | | | | |
| | | Mean | Std. Deviation | Std. Error Mean | Lower | Upper | | | |
| Pair 1 | WAC3 - WACP3 | -18.20000 | 3.20000 | 1.84752 | -26.14924 | -10.25076 | -9.851 | 2 | .010 |
| Pair 2 | WAC3 - WACPP3 | -10.10000 | 1.40000 | .80829 | -13.57779 | -6.62221 | -12.496 | 2 | .006 |
| Pair 3 | WAC3 - WACPP3f | -7.50000 | 1.20000 | .69282 | -10.48097 | -4.51903 | -10.825 | 2 | .008 |

## COMPRESSIVE STRENGTH

**Paired Samples Statistics**

| | | Mean | N | Std. Deviation | Std. Error Mean |
|---|---|---|---|---|---|
| Pair 1 | CompressiveC1 | 25.9467 | 3 | 2.31053 | 1.33398 |
| | CompCP1 | 5.0033 | 3 | .86893 | .50167 |
| Pair 2 | CompressiveC1 | 25.9467 | 3 | 2.31053 | 1.33398 |
| | CompCPP1 | 8.0333 | 3 | .15275 | .08819 |
| Pair 3 | CompressiveC1 | 25.9467 | 3 | 2.31053 | 1.33398 |
| | COMPCPP1f | 11.2000 | 3 | .30000 | .17321 |

**Paired Samples Correlations**

| | | N | Correlation | Sig. |
|---|---|---|---|---|
| Pair 1 | CompressiveC1 & CompCP1 | 3 | -.959 | .184 |
| Pair 2 | CompressiveC1 & CompCPP1 | 3 | -.913 | .267 |

| | | | | |
|---|---|---|---|---|
| Pair 3 | CompressiveC1 & COMPCPP1f | 3 | .290 | .813 |

**Paired Samples Test**

| | | Paired Differences | | | | | t | df | Sig. (2-tailed) |
|---|---|---|---|---|---|---|---|---|---|
| | | Mean | Std. Deviation | Std. Error Mean | 95% Confidence Interval of the Difference Lower | Upper | | | |
| Pair 1 | CompC1 - CompCP1 | 20.94333 | 3.15326 | 1.82053 | 13.11021 | 28.77646 | 11.504 | 2 | .007 |
| Pair 2 | CompC1 - CompCPP1 | 17.91333 | 2.45082 | 1.41498 | 11.82515 | 24.00152 | 12.660 | 2 | .006 |
| Pair 3 | CompC1 - COMPCPP1f | 14.74667 | 2.24199 | 1.29442 | 9.17725 | 20.31609 | 11.393 | 2 | .008 |

**Paired Samples Statistics**

| | | Mean | N | Std. Deviation | Std. Error Mean |
|---|---|---|---|---|---|
| Pair 1 | CompC2 | 27.1200 | 3 | 3.06531 | 1.76976 |
| | CompCP2 | 4.9667 | 3 | .20817 | .12019 |
| Pair 2 | CompC2 | 27.1200 | 3 | 3.06531 | 1.76976 |
| | CompCPP2 | 7.0667 | 3 | .25166 | .14530 |
| Pair 3 | CompC2 | 27.1200 | 3 | 3.06531 | 1.76976 |
| | COMPCPP2f | 6.6667 | 3 | .05774 | .03333 |
| Pair 4 | COMPC3 | 23.0500 | 3 | 1.01592 | .58654 |
| | COMPCP3 | 2.6667 | 3 | .37859 | .21858 |
| Pair 5 | COMPC3 | 23.0500 | 3 | 1.01592 | .58654 |
| | COMPCPP3 | 6.7000 | 3 | .00000 | .00000 |
| Pair 6 | COMPC3 | 23.0500 | 3 | 1.01592 | .58654 |
| | COMPCPP3F | 6.7833 | 3 | .49075 | .28333 |

**Paired Samples Correlations**

| | | N | Correlation | Sig. |
|---|---|---|---|---|
| Pair 1 | CompC2 & CompCP2 | 3 | .151 | .903 |
| Pair 2 | CompC2 & CompCPP2 | 3 | -.719 | .489 |
| Pair 3 | CompC2 & COMPCPP2f | 3 | -.384 | .749 |
| Pair 4 | COMPC3 & COMPCP3 | 3 | -.818 | .391 |
| Pair 5 | COMPC3 & COMPCPP3 | 3 | . | . |
| Pair 6 | COMPC3 & COMPCPP3F | 3 | .844 | .360 |

**Paired Samples Test**

| | | Paired Differences | | | | | t | df | Sig. (2-tailed) |
|---|---|---|---|---|---|---|---|---|---|
| | | Mean | Std. Deviation | Std. Error Mean | 95% Confidence Interval of the Difference Lower | Upper | | | |
| Pair 1 | CompC2 - CompCP2 | 22.15333 | 3.04079 | 1.75560 | 14.59958 | 29.70709 | 12.619 | 2 | . 006 |
| Pair 2 | CompC2 - CompCPP2 | 20.05333 | 3.25107 | 1.87700 | 11.97724 | 28.12943 | 10.684 | 2 | .009 |
| Pair 3 | CompC2 - COMPCPP2f | 20.45333 | 3.08795 | 1.78283 | 12.78244 | 28.12423 | 11.472 | 2 | .008 |
| Pair 4 | COMPC3 - COMPCP3 | 20.38333 | 1.34329 | .77555 | 17.04641 | 23.72026 | 26.282 | 2 | .001 |
| Pair 5 | COMPC3 - COMPCPP3 | 16.35000 | 1.01592 | .58654 | 13.82631 | 18.87369 | 27.875 | 2 | .001 |
| Pair 6 | COMPC3 - COMPCPP3F | 16.26667 | .65684 | .37922 | 14.63500 | 17.89834 | 42.895 | 2 | .001 |

**28-DAYS**

**Paired Samples Statistics**

| | Mean | N | Std. Deviation | Std. Error Mean |
|---|---|---|---|---|

| | | | | | |
|---|---|---|---|---|---|
| Pair 1 | CompC1 | 46.4667 | 3 | 4.73849 | 2.73577 |
| | CompCP1 | 7.9600 | 3 | .43509 | .25120 |
| Pair 2 | CompC1 | 46.4667 | 3 | 4.73849 | 2.73577 |
| | CompCPP1 | 12.0000 | 3 | .52915 | .30551 |
| Pair 3 | CompC1 | 46.4667 | 3 | 4.73849 | 2.73577 |
| | COMPCPP1f | 16.9700 | 3 | .83289 | .48087 |
| Pair 4 | COMPC2 | 44.5567 | 3 | .93943 | .54238 |
| | COMPCP2 | 7.7000 | 3 | .10000 | .05774 |
| Pair 5 | COMPC2 | 44.5567 | 3 | .93943 | .54238 |
| | COMPCPP2 | 11.7667 | 3 | .11547 | .06667 |
| Pair 6 | COMPC2 | 44.5567 | 3 | .93943 | .54238 |
| | COMPCPP2f | 11.7267 | 3 | 1.27453 | .73585 |
| Pair 7 | COMPC3 | 43.2900 | 3 | 1.03058 | .59501 |
| | COMPCP3 | 4.8000 | 3 | .20000 | .11547 |
| Pair 8 | COMPC3 | 43.2900 | 3 | 1.03058 | .59501 |
| | COMPCPP3 | 11.6000 | 3 | .26458 | .15275 |
| Pair 9 | COMPC3 | 43.2900 | 3 | 1.03058 | .59501 |
| | COMPCPP3F | 11.1233 | 3 | .44501 | .25693 |

**Paired Samples Correlations**

| | | N | Correlation | Sig. |
|---|---|---|---|---|
| Pair 1 | CompC1 & CompCP1 | 3 | -.877 | .319 |
| Pair 2 | CompC1 & CompCPP1 | 3 | .989 | .094 |
| Pair 3 | CompC1 & COMPCPP1f | 3 | -.484 | .678 |
| Pair 4 | COMPC2 & COMPCP2 | 3 | -.373 | .757 |
| Pair 5 | COMPC2 & COMPCPP2 | 3 | .141 | .910 |

| | | | | |
|---|---|---|---|---|
| Pair 6 | COMPC2 & COMPCPP2f | 3 | .950 | .202 |
| Pair 7 | COMPC3 & COMPCP3 | 3 | .965 | .168 |
| Pair 8 | COMPC3 & COMPCPP3 | 3 | .900 | .287 |
| Pair 9 | COMPC3 & COMPCPP3F | 3 | .954 | .194 |

**Paired Samples Test**

| | | Paired Differences | | | | | | | |
|---|---|---|---|---|---|---|---|---|---|
| | | | | | 95% Confidence Interval of the Difference | | | | |
| | | Mean | Std. Deviation | Std. Error Mean | Lower | Upper | t | df | Sig. (2-tailed) |
| Pair 1 | CompC1 - CompCP1 | 38.50667 | 5.12432 | 2.95853 | 25.77716 | 51.23618 | 13.015 | 2 | .006 |
| Pair 2 | CompC1 - CompCPP1 | 34.46667 | 4.21584 | 2.43402 | 23.99393 | 44.93940 | 14.160 | 2 | .005 |
| Pair 3 | CompC1 - COMPCPP1f | 29.49667 | 5.19336 | 2.99839 | 16.59563 | 42.39770 | 9.838 | 2 | .010 |
| Pair 4 | COMPC2 - COMPCP2 | 36.85667 | .98109 | .56643 | 34.41951 | 39.29382 | 65.068 | 2 | .000 |
| Pair 5 | COMPC2 - COMPCPP2 | 32.79000 | .93016 | .53703 | 30.47935 | 35.10065 | 61.058 | 2 | .000 |
| Pair 6 | COMPC2 - COMPCPP2f | 32.83000 | .48135 | .27791 | 31.63425 | 34.02575 | 118.132 | 2 | .000 |
| Pair 7 | COMPC3 - COMPCP3 | 38.49000 | .83911 | .48446 | 36.40554 | 40.57446 | 79.450 | 2 | .000 |
| Pair 8 | COMPC3 - COMPCPP3 | 31.69000 | .80069 | .46228 | 29.70098 | 33.67902 | 68.552 | 2 | .000 |
| Pair 9 | COMPC3 - COMPCPP3F | 32.16667 | .62067 | .35834 | 30.62483 | 33.70850 | 89.765 | 2 | .000 |

**90 DAYS**

**Paired Samples Statistics**

| | | Mean | N | Std. Deviation | Std. Error Mean |
|---|---|---|---|---|---|
| Pair 1 | CompC1 | 61.9267 | 3 | 1.95144 | 1.12667 |
| | CompCP1 | 9.2333 | 3 | .63509 | .36667 |
| Pair 2 | CompC1 | 61.9267 | 3 | 1.95144 | 1.12667 |
| | CompCPP1 | 15.1300 | 3 | 1.66154 | .95929 |
| Pair 3 | CompC1 | 61.9267 | 3 | 1.95144 | 1.12667 |
| | COMPCPP1f | 23.4000 | 3 | .30000 | .17321 |
| Pair 4 | COMPC2 | 55.5667 | 3 | .35119 | .20276 |
| | COMPCP2 | 9.0333 | 3 | .15275 | .08819 |
| Pair 5 | COMPC2 | 55.5667 | 3 | .35119 | .20276 |
| | COMPCPP2 | 14.4100 | 3 | .41509 | .23965 |
| Pair 6 | COMPC2 | 55.5667 | 3 | .35119 | .20276 |
| | COMPCPP2f | 17.8100 | 3 | .25120 | .14503 |
| Pair 7 | COMPC3 | 52.6667 | 3 | 1.06927 | .61734 |
| | COMPCP3 | 5.5667 | 3 | .05774 | .03333 |
| Pair 8 | COMPC3 | 52.6667 | 3 | 1.06927 | .61734 |
| | COMPCPP3 | 13.8000 | 3 | .10000 | .05774 |
| Pair 9 | COMPC3 | 52.6667 | 3 | 1.06927 | .61734 |
| | COMPCPP3F | 16.6233 | 3 | 1.05548 | .60938 |

**Paired Samples Test**

| | | Paired Differences | | | | | t | df | Sig. (2-tailed) |
|---|---|---|---|---|---|---|---|---|---|
| | | Mean | Std. Deviation | Std. Error Mean | 95% Confidence Interval of the Difference Lower | Upper | | | |
| Pair 1 | CompC1 - CompCP1 | 52.69333 | 1.72399 | .99534 | 48.41071 | 56.97596 | 52.940 | 2 | .000 |
| Pair 2 | CompC1 - CompCPP1 | 46.79667 | 1.12349 | .64865 | 44.00576 | 49.58757 | 72.145 | 2 | .000 |
| Pair 3 | CompC1 - COMPCPP1f | 38.52667 | 1.69827 | .98050 | 34.30792 | 42.74541 | 39.293 | 2 | .001 |
| Pair 4 | COMPC2 - COMPCP2 | 46.53333 | .28868 | .16667 | 45.81622 | 47.25044 | 279.200 | 2 | .000 |
| Pair 5 | COMPC2 - COMPCPP2 | 41.15667 | .64392 | .37177 | 39.55708 | 42.75625 | 110.705 | 2 | .000 |
| Pair 6 | COMPC2 - COMPCPP2f | 37.75667 | .41041 | .23695 | 36.73716 | 38.77617 | 159.346 | 2 | .000 |
| Pair 7 | COMPC3 - COMPCP3 | 47.10000 | 1.03923 | .60000 | 44.51841 | 49.68159 | 78.500 | 2 | .000 |
| Pair 8 | COMPC3 - COMPCPP3 | 38.86667 | 1.07858 | .62272 | 36.18733 | 41.54601 | 62.415 | 2 | .000 |
| Pair 9 | COMPC3 - COMPCPP3F | 36.04333 | 2.07196 | 1.19625 | 30.89629 | 41.19038 | 30.130 | 2 | .001 |

## TENSILE STRENGTH

**Paired Samples Statistics**

| | | Mean | N | Std. Deviation | Std. Error Mean |
|---|---|---|---|---|---|
| Pair 1 | TensileC1 | 3.2000 | 3 | .30000 | .17321 |
| | TensileCP1 | 1.0000 | 3 | .26458 | .15275 |
| Pair 2 | TensileC1 | 3.2000 | 3 | .30000 | .17321 |
| | TensileCPP1 | 2.1000 | 3 | .17321 | .10000 |

| | | | | | |
|---|---|---|---|---|---|
| Pair 3 | TensileC1 | 3.2000 | 3 | .30000 | .17321 |
| | TensileCPP1f | 1.6500 | 3 | .25000 | .14434 |
| Pair 4 | TensileC2 | 3.1000 | 3 | .10000 | .05774 |
| | TensileCP2 | .9000 | 3 | .20000 | .11547 |
| Pair 5 | TensileC2 | 3.1000 | 3 | .10000 | .05774 |
| | TensileCPP2 | 1.7000 | 3 | .35000 | .20207 |
| Pair 6 | TensileC2 | 3.1000 | 3 | .10000 | .05774 |
| | TensileCPP2f | 1.0100 | 3 | .29000 | .16743 |
| Pair 7 | TensileC3 | 3.0000 | 3 | .20000 | .11547 |
| | TensileCP3 | .7000 | 3 | .40000 | .23094 |
| Pair 8 | TensileC3 | 3.0000 | 3 | .20000 | .11547 |
| | TensileCPP3 | 1.4000 | 3 | .30000 | .17321 |
| Pair 9 | TensileC3 | 3.0000 | 3 | .20000 | .11547 |
| | TensileCPP3F | .9200 | 3 | .06000 | .03464 |

**Paired Samples Correlations**

| | | N | Correlation | Sig. |
|---|---|---|---|---|
| Pair 1 | TensileC1 & TensileCP1 | 3 | .945 | .212 |
| Pair 2 | TensileC1 & TensileCPP1 | 3 | -.866 | .333 |
| Pair 3 | TensileC1 & TensileCPP1f | 3 | -1.000 | .000 |
| Pair 4 | TensileC2 & TensileCP2 | 3 | -.500 | .667 |
| Pair 5 | TensileC2 & TensileCPP2 | 3 | -.500 | .667 |
| Pair 6 | TensileC2 & TensileCPP2f | 3 | -.500 | .667 |
| Pair 7 | TensileC3 & TensileCP3 | 3 | 1.000 | .000 |
| Pair 8 | TensileC3 & TensileCPP3 | 3 | -1.000 | .000 |
| Pair 9 | TensileC3 & TensileCPP3F | 3 | -1.000 | .000 |

**Paired Samples Test**

| | | Paired Differences | | | | | t | df | Sig. (2-tailed) |
|---|---|---|---|---|---|---|---|---|---|
| | | Mean | Std. Deviation | Std. Error Mean | 95% Confidence Interval of the Difference Lower | Upper | | | |
| Pair 1 | TensileC1 - TensileCP1 | 2.20000 | .10000 | .05774 | 1.95159 | 2.44841 | 38.105 | 2 | .001 |
| Pair 2 | TensileC1 - TensileCPP1 | 1.10000 | .45826 | .26458 | -.03837 | 2.23837 | 4.158 | 2 | .053 |
| Pair 3 | TensileC1 - TensileCPP1f | 1.55000 | .55000 | .31754 | .18372 | 2.91628 | 4.881 | 2 | .040 |
| Pair 4 | TensileC2 - TensileCP2 | 2.20000 | .26458 | .15275 | 1.54276 | 2.85724 | 14.402 | 2 | .005 |
| Pair 5 | TensileC2 - TensileCPP2 | 1.40000 | .40927 | .23629 | .38332 | 2.41668 | 5.925 | 2 | .027 |
| Pair 6 | TensileC2 - TensileCPP2f | 2.09000 | .35086 | .20257 | 1.21843 | 2.96157 | 10.318 | 2 | .009 |
| Pair 7 | TensileC3 - TensileCP3 | 2.30000 | .20000 | .11547 | 1.80317 | 2.79683 | 19.919 | 2 | .003 |
| Pair 8 | TensileC3 - TensileCPP3 | 1.60000 | .50000 | .28868 | .35793 | 2.84207 | 5.543 | 2 | .031 |
| Pair 9 | TensileC3 - TensileCPP3F | 2.08000 | .26000 | .15011 | 1.43412 | 2.72588 | 13.856 | 2 | .005 |

**POZAMENTT GROUT -CONCRETE**

**DENSITY**

**Paired Samples Statistics**

| | | Mean | N | Std. Deviation | Std. Error Mean |
|---|---|---|---|---|---|
| Pair 1 | DensityP1 | 2390.0000 | 3 | 10.00000 | 5.77350 |
| | DensityPP1 | 1493.3333 | 3 | 5.77350 | 3.33333 |
| Pair 2 | DensityP1 | 2390.0000 | 3 | 10.00000 | 5.77350 |
| | DensityPPP1 | 1593.3333 | 3 | 5.77350 | 3.33333 |
| Pair 3 | DensityP1 | 2390.0000 | 3 | 10.00000 | 5.77350 |
| | DensityPPP1f | 1600.0000 | 3 | 52.91503 | 30.55050 |
| Pair 4 | DensityP2 | 2366.6667 | 3 | 5.77350 | 3.33333 |
| | DensityPP2 | 1463.3333 | 3 | 15.27525 | 8.81917 |
| Pair 5 | DensityP2 | 2366.6667 | 3 | 5.77350 | 3.33333 |
| | DensityPPP2 | 1580.0000 | 3 | .00000 | .00000 |
| Pair 6 | DensityP2 | 2366.6667 | 3 | 5.77350 | 3.33333 |
| | DensityPPP2f | 1590.0000 | 3 | 20.00000 | 11.54701 |
| Pair 7 | DensityP3 | 2360.0000 | 3 | 17.32051 | 10.00000 |
| | DensityPP3 | 1416.6667 | 3 | 20.81666 | 12.01850 |
| Pair 8 | DensityP3 | 2360.0000 | 3 | 17.32051 | 10.00000 |
| | DensityPPP3 | 1560.0000 | 3 | .00000 | .00000 |
| Pair 9 | DensityP3 | 2360.0000 | 3 | 17.32051 | 10.00000 |
| | DensityPPP3f | 1550.0000 | 3 | 10.00000 | 5.77350 |

**Paired Samples Correlations**

| | | N | Correlation | Sig. |
|---|---|---|---|---|
| Pair 1 | DensityP1 & DensityPP1 | 3 | .866 | .333 |
| Pair 2 | DensityP1 & DensityPPP1 | 3 | -.866 | .333 |
| Pair 3 | DensityP1 & DensityPPP1f | 3 | .756 | .454 |
| Pair 4 | DensityP2 & DensityPP2 | 3 | .756 | .454 |
| Pair 5 | DensityP2 & DensityPPP2 | 3 | . | . |
| Pair 6 | DensityP2 & DensityPPP2f | 3 | .000 | 1.000 |
| Pair 7 | DensityP3 & DensityPP3 | 3 | .971 | .154 |
| Pair 8 | DensityP3 & DensityPPP3 | 3 | . | . |
| Pair 9 | DensityP3 & DensityPPP3f | 3 | .000 | 1.000 |

**Paired Samples Test**

| | | Paired Differences | | | | | t | df | Sig tail |
|---|---|---|---|---|---|---|---|---|---|
| | | Mean | Std. Deviation | Std. Error Mean | 95% Confidence Interval of the Difference Lower | Upper | | | |
| Pair 1 | DensityP1 - DensityPP1 | 896.66667 | 5.77350 | 3.33333 | 882.32449 | 911.00884 | 269.000 | 2 | .00 |
| Pair 2 | DensityP1 - DensityPPP1 | 796.66667 | 15.27525 | 8.81917 | 758.72084 | 834.61250 | 90.334 | 2 | .00 |
| Pair 3 | DensityP1 - DensityPPP1f | 790.00000 | 45.82576 | 26.45751 | 676.16251 | 903.83749 | 29.859 | 2 | .00 |
| Pair 4 | DensityP2 - DensityPP2 | 903.33333 | 11.54701 | 6.66667 | 874.64898 | 932.01768 | 135.500 | 2 | .00 |
| Pair 5 | DensityP2 - DensityPPP2 | 786.66667 | 5.77350 | 3.33333 | 772.32449 | 801.00884 | 236.000 | 2 | .00 |
| Pair 6 | DensityP2 - DensityPPP2f | 776.66667 | 20.81666 | 12.01850 | 724.95522 | 828.37812 | 64.623 | 2 | .00 |
| Pair 7 | DensityP3 - DensityPP3 | 943.33333 | 5.77350 | 3.33333 | 928.99116 | 957.67551 | 283.000 | 2 | .00 |
| Pair 8 | DensityP3 - DensityPPP3 | 800.00000 | 17.32051 | 10.00000 | 756.97347 | 843.02653 | 80.000 | 2 | .00 |

| | | | | | | | | | |
|---|---|---|---|---|---|---|---|---|---|
| Pair 9 | DensityP3 - DensityPPP3f | 810.00000 | 20.00000 | 11.54701 | 760.31725 | 859.68275 | 70.148 | 2 | .001 |

**POROSITY**

**Paired Samples Statistics**

| | | Mean | N | Std. Deviation | Std. Error Mean |
|---|---|---|---|---|---|
| Pair 1 | PorosityP1 | 11.7000 | 3 | 1.70000 | .98150 |
| | PorosityPP1 | 29.2000 | 3 | .60000 | .34641 |
| Pair 2 | PorosityP1 | 11.7000 | 3 | 1.70000 | .98150 |
| | PorosityPPP1 | 19.3000 | 3 | 2.10000 | 1.21244 |
| Pair 3 | PorosityP1 | 11.7000 | 3 | 1.70000 | .98150 |
| | PorosityPPP1f | 13.0000 | 3 | 1.00000 | .57735 |
| Pair 4 | PorosityP2 | 13.6000 | 3 | 1.40000 | .80829 |
| | PorosityPP2 | 30.7000 | 3 | 1.10000 | .63509 |
| Pair 5 | PorosityP2 | 13.6000 | 3 | 1.40000 | .80829 |
| | PorosityPPP2 | 19.5000 | 3 | .50000 | .28868 |
| Pair 6 | PorosityP2 | 13.6000 | 3 | 1.40000 | .80829 |
| | PorosityPPP2f | 15.7000 | 3 | .80000 | .46188 |
| Pair 7 | PorosityP3 | 13.9000 | 3 | 2.10000 | 1.21244 |
| | PorosityPP3 | 19.3000 | 3 | 1.70000 | .98150 |
| Pair 8 | PorosityP3 | 13.9000 | 3 | 2.10000 | 1.21244 |
| | PorosityPPP3 | 20.1000 | 3 | 1.20000 | .69282 |

| | | | | | |
|---|---|---|---|---|---|
| Pair 9 | PorosityP3 | 13.9000 | 3 | 2.10000 | 1.21244 |
| | PorosityPPP3f | 21.2000 | 3 | .80000 | .46188 |

**Paired Samples Correlations**

| | | N | Correlation | Sig. |
|---|---|---|---|---|
| Pair 1 | PorosityP1 & PorosityPP1 | 3 | -1.000 | .000 |
| Pair 2 | PorosityP1 & PorosityPPP1 | 3 | -1.000 | .000 |
| Pair 3 | PorosityP1 & PorosityPPP1f | 3 | 1.000 | .000 |
| Pair 4 | PorosityP2 & PorosityPP2 | 3 | 1.000 | .000 |
| Pair 5 | PorosityP2 & PorosityPPP2 | 3 | 1.000 | .000 |
| Pair 6 | PorosityP2 & PorosityPPP2f | 3 | 1.000 | .000 |
| Pair 7 | PorosityP3 & PorosityPP3 | 3 | -1.000 | .000 |
| Pair 8 | PorosityP3 & PorosityPPP3 | 3 | -1.000 | .000 |
| Pair 9 | PorosityP3 & PorosityPPP3f | 3 | -1.000 | .000 |

**Paired Samples Test**

| | | Paired Differences | | | | | | | |
|---|---|---|---|---|---|---|---|---|---|
| | | | | | 95% Confidence Interval of the Difference | | | | |
| | | Mean | Std. Deviation | Std. Error Mean | Lower | Upper | t | df | Sig tail |
| Pair 1 | PorosityP1 - PorosityPP1 | -17.50000 | 2.30000 | 1.32791 | -23.21352 | -11.78648 | -13.179 | 2 | .00 |

| | | | | | | | | | |
|---|---|---|---|---|---|---|---|---|---|
| Pair 2 | PorosityP1 - PorosityPPP1 | -7.60000 | 3.80000 | 2.19393 | -17.03972 | 1.83972 | -3.464 | 2 | .074 |
| Pair 3 | PorosityP1 - PorosityPPP1f | -1.30000 | .70000 | .40415 | -3.03890 | .43890 | -3.217 | 2 | .085 |
| Pair 4 | PorosityP2 - PorosityPP2 | -17.10000 | .30000 | .17321 | -17.84524 | -16.35476 | -98.727 | 2 | .000 |
| Pair 5 | PorosityP2 - PorosityPPP2 | -5.90000 | .90000 | .51962 | -8.13572 | -3.66428 | -11.355 | 2 | .008 |
| Pair 6 | PorosityP2 - PorosityPPP2f | -2.10000 | .60000 | .34641 | -3.59048 | -.60952 | -6.062 | 2 | .026 |
| Pair 7 | PorosityP3 - PorosityPP3 | -5.40000 | 3.80000 | 2.19393 | -14.83972 | 4.03972 | -2.461 | 2 | .133 |
| Pair 8 | PorosityP3 - PorosityPPP3 | -6.20000 | 3.30000 | 1.90526 | -14.39765 | 1.99765 | -3.254 | 2 | .083 |
| Pair 9 | PorosityP3 - PorosityPPP3f | -7.30000 | 2.90000 | 1.67432 | -14.50400 | -.09600 | -4.360 | 2 | .049 |

**WATER ABSORPTION**

**Paired Samples Statistics**

| | | Mean | N | Std. Deviation | Std. Error Mean |
|---|---|---|---|---|---|
| Pair 1 | WAP1 | 5.1000 | 3 | .30000 | .17321 |
| | WAPP1 | 21.1667 | 3 | 2.15019 | 1.24141 |
| Pair 2 | WAP1 | 5.1000 | 3 | .30000 | .17321 |
| | WAPPP1 | 22.0000 | 3 | 2.20000 | 1.27017 |
| Pair 3 | WAP1 | 5.1000 | 3 | .30000 | .17321 |
| | WAPPP1F | 24.0000 | 3 | 3.50000 | 2.02073 |
| Pair 4 | WAP2 | 6.2000 | 3 | .20000 | .11547 |
| | WAPP2 | 13.2000 | 3 | .60000 | .34641 |
| Pair 5 | WAP2 | 6.2000 | 3 | .20000 | .11547 |
| | WAPPP2 | 13.4000 | 3 | 3.20000 | 1.84752 |
| Pair 6 | WAP2 | 6.2000 | 3 | .20000 | .11547 |
| | WAPPP2F | 14.3000 | 3 | .30000 | .17321 |

| | | | | | |
|---|---|---|---|---|---|
| Pair 7 | WAP3 | 7.1000 | 3 | .70000 | .40415 |
| | WAPP3 | 9.1000 | 3 | 1.20000 | .69282 |
| Pair 8 | WAP3 | 7.1000 | 3 | .70000 | .40415 |
| | WAPPP3 | 11.1000 | 3 | 1.50000 | .86603 |
| Pair 9 | WAP3 | 7.1000 | 3 | .70000 | .40415 |
| | WAPPP3F | 15.4000 | 3 | 1.60000 | .92376 |

**Paired Samples Correlations**

| | | N | Correlation | Sig. |
|---|---|---|---|---|
| Pair 1 | WAP1 & WAPP1 | 3 | 1.000 | .009 |
| Pair 2 | WAP1 & WAPPP1 | 3 | -1.000 | .000 |
| Pair 3 | WAP1 & WAPPP1F | 3 | -1.000 | .000 |
| Pair 4 | WAP2 & WAPP2 | 3 | 1.000 | .000 |
| Pair 5 | WAP2 & WAPPP2 | 3 | 1.000 | .000 |
| Pair 6 | WAP2 & WAPPP2F | 3 | 1.000 | .000 |
| Pair 7 | WAP3 & WAPP3 | 3 | -1.000 | .000 |
| Pair 8 | WAP3 & WAPPP3 | 3 | -1.000 | .000 |
| Pair 9 | WAP3 & WAPPP3F | 3 | -1.000 | .000 |

**Paired Samples Test**

| | Paired Differences | t | df | Sig. |
|---|---|---|---|---|

| | | Mean | Std. Deviation | Std. Error Mean | 95% Confidence Interval of the Difference | | | | |
|---|---|---|---|---|---|---|---|---|---|
| | | | | | Lower | Upper | | | |
| Pair 1 | WAP1 - WAPP1 | -16.06667 | 1.85023 | 1.06823 | -20.66288 | -11.47045 | -15.040 | 2 | .004 |
| Pair 2 | WAP1 - WAPPP1 | -16.90000 | 2.50000 | 1.44338 | -23.11034 | -10.68966 | -11.709 | 2 | .007 |
| Pair 3 | WAP1 - WAPPP1F | -18.90000 | 3.80000 | 2.19393 | -28.33972 | -9.46028 | -8.615 | 2 | .013 |
| Pair 4 | WAP2 - WAPP2 | -7.00000 | .40000 | .23094 | -7.99366 | -6.00634 | -30.311 | 2 | .001 |
| Pair 5 | WAP2 - WAPPP2 | -7.20000 | 3.00000 | 1.73205 | -14.65241 | .25241 | -4.157 | 2 | .053 |
| Pair 6 | WAP2 - WAPPP2F | -8.10000 | .10000 | .05774 | -8.34841 | -7.85159 | -140.296 | 2 | .000 |
| Pair 7 | WAP3 - WAPP3 | -2.00000 | 1.90000 | 1.09697 | -6.71986 | 2.71986 | -1.823 | 2 | .210 |
| Pair 8 | WAP3 - WAPPP3 | -4.00000 | 2.20000 | 1.27017 | -9.46510 | 1.46510 | -3.149 | 2 | .088 |
| Pair 9 | WAP3 - WAPPP3F | -8.30000 | 2.30000 | 1.32791 | -14.01352 | -2.58648 | -6.250 | 2 | .025 |

**COMPRESSIVE STRENGTH**

7-DAYS

**Paired Samples Statistics**

| | | Mean | N | Std. Deviation | Std. Error Mean |
|---|---|---|---|---|---|
| Pair 1 | COMP1 | 31.0480 | 3 | .54322 | .31363 |
| | COMPP1 | 4.6267 | 3 | .74661 | .43106 |
| Pair 2 | COMP1 | 31.0480 | 3 | .54322 | .31363 |
| | COMPPP1 | 4.2333 | 3 | .11547 | .06667 |
| Pair 3 | COMP1 | 31.0480 | 3 | .54322 | .31363 |

| | | | | | |
|---|---|---|---|---|---|
| | COMPPP1F | 4.8533 | 3 | 2.15105 | 1.24191 |
| Pair 4 | COMP2 | 21.3500 | 3 | 1.10313 | .63689 |
| | COMPP2 | 1.9167 | 3 | .19655 | .11348 |
| Pair 5 | COMP2 | 21.3500 | 3 | 1.10313 | .63689 |
| | COMPPP2 | 3.7000 | 3 | .20000 | .11547 |
| Pair 6 | COMP2 | 21.3500 | 3 | 1.10313 | .63689 |
| | COMPPP2F | 3.7967 | 3 | .98642 | .56951 |
| Pair 7 | COMP3 | 22.3033 | 3 | 1.90001 | 1.09697 |
| | COMPP3 | 1.6967 | 3 | .01528 | .00882 |
| Pair 8 | COMP3 | 22.3033 | 3 | 1.90001 | 1.09697 |
| | COMPPP3 | 3.4000 | 3 | .10000 | .05774 |
| Pair 9 | COMP3 | 22.3033 | 3 | 1.90001 | 1.09697 |
| | COMPPP3F | 3.0300 | 3 | .80467 | .46458 |

**Paired Samples Correlations**

| | | N | Correlation | Sig. |
|---|---|---|---|---|
| Pair 1 | COMP1 & COMPP1 | 3 | .999 | .024 |
| Pair 2 | COMP1 & COMPPP1 | 3 | .029 | .982 |
| Pair 3 | COMP1 & COMPPP1F | 3 | .704 | .503 |
| Pair 4 | COMP2 & COMPP2 | 3 | -.385 | .748 |
| Pair 5 | COMP2 & COMPPP2 | 3 | .077 | .951 |
| Pair 6 | COMP2 & COMPPP2F | 3 | .642 | .556 |
| Pair 7 | COMP3 & COMPP3 | 3 | .657 | .544 |

| | | | | |
|---|---|---|---|---|
| Pair 8 | COMP3 & COMPPP3 | 3 | -.503 | .665 |
| Pair 9 | COMP3 & COMPPP3F | 3 | .964 | .171 |

**Paired Samples Test**

| | | Paired Differences | | | | | t | df | Sig. (2-tailed) |
|---|---|---|---|---|---|---|---|---|---|
| | | Mean | Std. Deviation | Std. Error Mean | 95% Confidence Interval of the Difference Lower | Upper | | | |
| Pair 1 | COMP1 - COMPP1 | 26.42133 | .20476 | .11822 | 25.91269 | 26.92998 | 223.500 | 2 | .002 |
| Pair 2 | COMP1 - COMPPP1 | 26.81467 | .55211 | .31876 | 25.44315 | 28.18618 | 84.122 | 2 | .001 |
| Pair 3 | COMP1 - COMPPP1F | 26.19467 | 1.81018 | 1.04511 | 21.69793 | 30.69140 | 25.064 | 2 | .002 |
| Pair 4 | COMP2 - COMPP2 | 19.43333 | 1.19274 | .68863 | 16.47040 | 22.39627 | 28.220 | 2 | .001 |
| Pair 5 | COMP2 - COMPPP2 | 17.65000 | 1.10585 | .63846 | 14.90292 | 20.39708 | 27.645 | 2 | .001 |
| Pair 6 | COMP2 - COMPPP2F | 17.55333 | .89002 | .51385 | 15.34240 | 19.76426 | 34.160 | 2 | .001 |
| Pair 7 | COMP3 - COMPP3 | 20.60667 | 1.89001 | 1.09120 | 15.91162 | 25.30171 | 18.884 | 2 | .003 |
| Pair 8 | COMP3 - COMPPP3 | 18.90333 | 1.95219 | 1.12710 | 14.05383 | 23.75283 | 16.772 | 2 | .004 |
| Pair 9 | COMP3 - COMPPP3F | 19.27333 | 1.14457 | .66082 | 16.43007 | 22.11660 | 29.166 | 2 | .001 |

**Compressive strength 28-days**

**Paired Samples Statistics**

| | | Mean | N | Std. Deviation | Std. Error Mean |
|---|---|---|---|---|---|
| Pair 1 | COMP1 | 44.2600 | 3 | 1.33989 | .77358 |
| | COMPP1 | 7.4333 | 3 | .35119 | .20276 |
| Pair 2 | COMP1 | 44.2600 | 3 | 1.33989 | .77358 |
| | COMPPP1 | 7.7400 | 3 | .34000 | .19630 |
| Pair 3 | COMP1 | 44.2600 | 3 | 1.33989 | .77358 |
| | COMPPP1F | 9.5253 | 3 | .12396 | .07157 |
| Pair 4 | COMP2 | 24.6833 | 3 | 2.22055 | 1.28203 |
| | COMPP2 | 3.9167 | 3 | .40067 | .23132 |
| Pair 5 | COMP2 | 24.6833 | 3 | 2.22055 | 1.28203 |
| | COMPPP2 | 5.2000 | 3 | .20000 | .11547 |
| Pair 6 | COMP2 | 24.6833 | 3 | 2.22055 | 1.28203 |
| | COMPPP2F | 5.7433 | 3 | .33858 | .19548 |
| Pair 7 | COMP3 | 24.7433 | 3 | 1.22500 | .70726 |
| | COMPP3 | 2.8333 | 3 | .51316 | .29627 |
| Pair 8 | COMP3 | 24.7433 | 3 | 1.22500 | .70726 |
| | COMPPP3 | 4.3000 | 3 | 1.03923 | .60000 |
| Pair 9 | COMP3 | 24.7433 | 3 | 1.22500 | .70726 |
| | COMPPP3F | 5.1000 | 3 | .36056 | .20817 |

**Paired Samples Correlations**

| | | N | Correlation | Sig. |
|---|---|---|---|---|
| Pair 1 | COMP1 & COMPP1 | 3 | -.973 | .147 |
| Pair 2 | COMP1 & COMPPP1 | 3 | -.623 | .572 |
| Pair 3 | COMP1 & COMPPP1F | 3 | 1.000 | .018 |
| Pair 4 | COMP2 & COMPP2 | 3 | -.260 | .833 |
| Pair 5 | COMP2 & COMPPP2 | 3 | -.979 | .129 |
| Pair 6 | COMP2 & COMPPP2F | 3 | .055 | .965 |
| Pair 7 | COMP3 & COMPP3 | 3 | .975 | .143 |
| Pair 8 | COMP3 & COMPPP3 | 3 | .002 | .998 |
| Pair 9 | COMP3 & COMPPP3F | 3 | .280 | .820 |

**Paired Samples Test**

| | | Paired Differences | | | | | t | df | Sig. (2-tailed) |
|---|---|---|---|---|---|---|---|---|---|
| | | Mean | Std. Deviation | Std. Error Mean | 95% Confidence Interval of the Difference Lower | Upper | | | |
| Pair 1 | COMP1 - COMPP1 | 36.82667 | 1.68364 | .97205 | 32.64428 | 41.00905 | 37.886 | 2 | .001 |
| Pair 2 | COMP1 - COMPPP1 | 36.52000 | 1.57439 | .90897 | 32.60900 | 40.43100 | 40.177 | 2 | .001 |
| Pair 3 | COMP1 - COMPPP1F | 34.73467 | 1.21599 | .70205 | 31.71399 | 37.75535 | 49.476 | 2 | .000 |
| Pair 4 | COMP2 - COMPP2 | 20.76667 | 2.35670 | 1.36064 | 14.91230 | 26.62103 | 15.262 | 2 | .004 |
| Pair 5 | COMP2 - COMPPP2 | 19.48333 | 2.41678 | 1.39533 | 13.47972 | 25.48695 | 13.963 | 2 | .005 |
| Pair 6 | COMP2 - COMPPP2F | 18.94000 | 2.22785 | 1.28625 | 13.40572 | 24.47428 | 14.725 | 2 | .005 |
| Pair 7 | COMP3 - COMPP3 | 21.91000 | .73369 | .42360 | 20.08741 | 23.73259 | 51.724 | 2 | .000 |
| Pair 8 | COMP3 - COMPPP3 | 20.44333 | 1.60457 | .92640 | 16.45737 | 24.42930 | 22.068 | 2 | .002 |
| Pair 9 | COMP3 - COMPPP3F | 19.64333 | 1.17628 | .67913 | 16.72129 | 22.56537 | 28.924 | 2 | .001 |

**90-Days**

**Paired Samples Statistics**

| | | Mean | N | Std. Deviation | Std. Error Mean |
|---|---|---|---|---|---|
| Pair 1 | COMP1 | 41.1210 | 3 | 7.05282 | 4.07194 |
| | COMPP1 | 6.6333 | 3 | 1.51098 | .87236 |
| Pair 2 | COMP1 | 41.1210 | 3 | 7.05282 | 4.07194 |
| | COMPPP1 | 11.0100 | 3 | .54065 | .31214 |
| Pair 3 | COMP1 | 41.1210 | 3 | 7.05282 | 4.07194 |
| | COMPPP1F | 12.9167 | 3 | .37899 | .21881 |
| Pair 4 | COMP2 | 30.3733 | 3 | 1.08542 | .62667 |
| | COMPP2 | 4.5300 | 3 | .23643 | .13650 |
| Pair 5 | COMP2 | 30.3733 | 3 | 1.08542 | .62667 |
| | COMPPP2 | 7.1000 | 3 | .20000 | .11547 |
| Pair 6 | COMP2 | 30.3733 | 3 | 1.08542 | .62667 |
| | COMPPP2F | 7.7867 | 3 | .52577 | .30355 |
| Pair 7 | COMP3 | 30.0600 | 3 | 1.08678 | .62746 |
| | COMPP3 | 4.2800 | 3 | .02000 | .01155 |
| Pair 8 | COMP3 | 30.0600 | 3 | 1.08678 | .62746 |
| | COMPPP3 | 7.7333 | 3 | .80829 | .46667 |
| Pair 9 | COMP3 | 30.0600 | 3 | 1.08678 | .62746 |
| | COMPPP3F | 8.5033 | 3 | .59475 | .34338 |

**Paired Samples Correlations**

| | | N | Correlation | Sig. |
|---|---|---|---|---|
| Pair 1 | COMP1 & COMPP1 | 3 | -.763 | .447 |
| Pair 2 | COMP1 & COMPPP1 | 3 | .811 | .398 |
| Pair 3 | COMP1 & COMPPP1F | 3 | -.647 | .552 |
| Pair 4 | COMP2 & COMPP2 | 3 | .989 | .095 |
| Pair 5 | COMP2 & COMPPP2 | 3 | .000 | 1.000 |
| Pair 6 | COMP2 & COMPPP2F | 3 | .999 | .024 |
| Pair 7 | COMP3 & COMPP3 | 3 | .663 | .539 |
| Pair 8 | COMP3 & COMPPP3 | 3 | -.199 | .872 |
| Pair 9 | COMP3 & COMPPP3F | 3 | -.943 | .216 |

**Paired Samples Test**

| | | Paired Differences | | | | | t | df | Sig. (2-tailed) |
|---|---|---|---|---|---|---|---|---|---|
| | | Mean | Std. Deviation | Std. Error Mean | 95% Confidence Interval of the Difference Lower | Upper | | | |
| Pair 1 | COMP1 - COMPP1 | 34.48767 | 8.26426 | 4.77137 | 13.95811 | 55.01722 | 7.228 | 2 | .019 |
| Pair 2 | COMP1 - COMPPP1 | 30.11100 | 6.62203 | 3.82323 | 13.66097 | 46.56103 | 7.876 | 2 | .016 |
| Pair 3 | COMP1 - COMPPP1F | 28.20433 | 7.30382 | 4.21687 | 10.06063 | 46.34804 | 6.688 | 2 | .022 |
| Pair 4 | COMP2 - COMPP2 | 25.84333 | .85231 | .49208 | 23.72608 | 27.96059 | 52.518 | 2 | .000 |
| Pair 5 | COMP2 - COMPPP2 | 23.27333 | 1.10369 | .63722 | 20.53161 | 26.01505 | 36.523 | 2 | .001 |

| | | | | | | | | | |
|---|---|---|---|---|---|---|---|---|---|
| Pair 6 | COMP2 - COMPPP2F | 22.58667 | .56039 | .32354 | 21.19459 | 23.97874 | 69.811 | 2 | .000 |
| Pair 7 | COMP3 - COMPP3 | 25.78000 | 1.07364 | .61987 | 23.11293 | 28.44707 | 41.590 | 2 | .001 |
| Pair 8 | COMP3 - COMPPP3 | 22.32667 | 1.47798 | .85331 | 18.65515 | 25.99818 | 26.165 | 2 | .001 |
| Pair 9 | COMP3 - COMPPP3F | 21.55667 | 1.65941 | .95806 | 17.43447 | 25.67886 | 22.500 | 2 | .002 |

**28- DAYS TENSILE STRENGTH**

**Paired Samples Statistics**

| | | Mean | N | Std. Deviation | Std. Error Mean |
|---|---|---|---|---|---|
| Pair 1 | TENSP1 | 3.6300 | 3 | .18000 | .10392 |
| | TENSPP1 | 1.1500 | 3 | .15000 | .08660 |
| Pair 2 | TENSP1 | 3.6300 | 3 | .18000 | .10392 |
| | TENSPPP1 | 1.6000 | 3 | .10000 | .05774 |
| Pair 3 | TENSP1 | 3.6300 | 3 | .18000 | .10392 |
| | TENSPPP1F | 1.1800 | 3 | .08000 | .04619 |
| Pair 4 | TENSP2 | 3.5000 | 3 | .30000 | .17321 |
| | TENSPP2 | .6400 | 3 | .06000 | .03464 |
| Pair 5 | TENSP2 | 3.5000 | 3 | .30000 | .17321 |
| | TENSPPP2 | 1.2000 | 3 | .06000 | .03464 |
| Pair 6 | TENSP2 | 3.5000 | 3 | .30000 | .17321 |

| | | | | | |
|---|---|---|---|---|---|
| | TENSPPP2F | .7800 | 3 | .14000 | .08083 |
| Pair 7 | TENSP3 | 2.7333 | 3 | .15275 | .08819 |
| | TENSPP3 | .7800 | 3 | .18000 | .10392 |
| Pair 8 | TENSP3 | 2.7333 | 3 | .15275 | .08819 |
| | TENSPPP3 | .9000 | 3 | .15000 | .08660 |
| Pair 9 | TENSP3 | 2.7333 | 3 | .15275 | .08819 |
| | TENSPPP3F | .7500 | 3 | .13000 | .07506 |

**Paired Samples Correlations**

| | | N | Correlation | Sig. |
|---|---|---|---|---|
| Pair 1 | TENSP1 & TENSPP1 | 3 | 1.000 | .000 |
| Pair 2 | TENSP1 & TENSPPP1 | 3 | -1.000 | .000 |
| Pair 3 | TENSP1 & TENSPPP1F | 3 | -1.000 | .000 |
| Pair 4 | TENSP2 & TENSPP2 | 3 | -1.000 | .000 |
| Pair 5 | TENSP2 & TENSPPP2 | 3 | -1.000 | .000 |
| Pair 6 | TENSP2 & TENSPPP2F | 3 | 1.000 | .000 |
| Pair 7 | TENSP3 & TENSPP3 | 3 | -.982 | .121 |
| Pair 8 | TENSP3 & TENSPPP3 | 3 | .982 | .121 |
| Pair 9 | TENSP3 & TENSPPP3F | 3 | -.982 | .121 |

**Paired Samples Test**

| | | Paired Differences | | | | | t | df | Sig. (2-tailed) |
|---|---|---|---|---|---|---|---|---|---|
| | | Mean | Std. Deviation | Std. Error Mean | 95% Confidence Interval of the Difference Lower | Upper | | | |
| Pair 1 | TENSP1 - TENSPP1 | 2.48000 | .03000 | .01732 | 2.40548 | 2.55452 | 143.183 | 2 | .000 |
| Pair 2 | TENSP1 - TENSPPP1 | 2.03000 | .28000 | .16166 | 1.33444 | 2.72556 | 12.557 | 2 | .006 |
| Pair 3 | TENSP1 - TENSPPP1F | 2.45000 | .26000 | .15011 | 1.80412 | 3.09588 | 16.321 | 2 | .004 |
| Pair 4 | TENSP2 - TENSPP2 | 2.86000 | .36000 | .20785 | 1.96571 | 3.75429 | 13.760 | 2 | .005 |
| Pair 5 | TENSP2 - TENSPPP2 | 2.30000 | .36000 | .20785 | 1.40571 | 3.19429 | 11.066 | 2 | .008 |
| Pair 6 | TENSP2 - TENSPPP2F | 2.72000 | .16000 | .09238 | 2.32254 | 3.11746 | 29.445 | 2 | .001 |
| Pair 7 | TENSP3 - TENSPP3 | 1.95333 | .33126 | .19125 | 1.13044 | 2.77623 | 10.213 | 2 | .009 |
| Pair 8 | TENSP3 - TENSPPP3 | 1.83333 | .02887 | .01667 | 1.76162 | 1.90504 | 110.000 | 2 | .000 |
| Pair 9 | TENSP3 - TENSPPP3F | 1.98333 | .28148 | .16251 | 1.28409 | 2.68258 | 12.204 | 2 | .007 |